Characterization of Distinct Populations of Histone H3 Phosphorylated in Response to Mitogen Stimulation Before and After Oncogene-Mediated Cellular Transformation

By

Katherine Leslie Ruth Dunn

A Thesis Submitted to the Faculty of Graduate Studies in Partial Fulfillment of the requirements for the Degree of Doctor of Philosophy.

Department of Biochemistry and Medical Genetics

University of Manitoba

September 2006©

Characterization of Distinct Populations of Histone H3 Phosphorylated in Response to Mitogen Stimulation Before and After Oncogene-Mediated Cellular Transformation

BY

Katherine Leslie Ruth Dunn

A Thesis/Practicum submitted to the Faculty of Graduate Studies of The University of Manitoba in partial fulfillment of the requirement of the degree

Of

Doctor of Philosophy

Abstract

Approximately 30% of human cancers contain a mutation to one of the *ras* oncogenes. Stimulation of the Ras-mitogen activated protein kinase (Ras-MAPK) pathway leads to rapid phosphorylation of histone H3 at serines 10 and 28, phosphorylation of the structural chromatin protein HMGN1 at serines 6, 20 and 24, and expression of immediate-early genes. H3 phosphoacetylated at serine 10 lysine 14 has been found associated with immediate-early genes following stimulation of the Ras-MAPK pathway. *Ras*-transformed cells contain higher levels of H3 phosphorylated at serine 10 and display a less condensed chromatin structure. We hypothesize that phosphorylation of H3 at serine 28 contributes to chromatin remodelling and immediate early gene activity.

Following mitogen stimulation, H3 phosphorylation at serine 28 follows the same temporal induction pattern as that at serine 10. We illustrate that both modifications are excluded from regions of highly condensed chromatin, take place on the same H3 variants, occur in regions of chromatin undergoing dynamic acetylation, and are present in increased amounts in *ras*-transformed cells. In addition, we found that levels of phosphorylation on the structural chromatin protein HMGN1 are elevated in *ras*-transformed cells. We also found that despite constitutive activation of the Ras-MAPK pathway, many characteristics of mitogen-induced H3 phosphorylation are unchanged in *ras*-transformed cells.

We have also determined that these two mitogen-induced modifications, once thought to act as a combination, occur for the most part on different pools of chromatin. Further, although mitogen-induced H3 phosphorylated at serine 10 or at serine 28 is dynamically acetylated, phosphorylation of H3 at serine 28 tends to occur on tails with a higher steady state level of acetylation. Stimulation of serum-starved mouse fibroblasts results in the appearance of numerous small foci of H3 phosphorylated at serine 10 and H3 phosphorylated at serine 28. We determined that a number of foci containing mitogen-induced serine 28-phosphorylated H3 colocalized with foci of RNA polymerase II phosphorylated at serine 5, providing evidence that mitogen induced H3 phosphorylation at serine 28 occurs at sites of transcriptional activity. These results suggest that phosphorylation of H3 at serine 28 promotes transcription independently of phosphorylation at serine 10. Further, foci of mitogen-induced serine 28-phosphorylated H3 did not colocalize with foci of mitogen-induced serine 6-phosphorylated HMGN1, a finding that adheres to a model in which HMGN1 phosphorylation results in its dissociation from chromatin to facilitate H3 phosphorylation and encourage transcription.

Acknowledgements

I shall first acknowledge my advisor, Dr. James Davie. His guidance, scientific excellence and direction made this project, and my time in graduate school, a success.

I would like to thank Drs. Janice Dodd, Spencer Gibson, and Gilbert Arthur, the members of my graduate committee, for their input throughout my program. A special thanks to Dr. Raj Bhullar for stepping in to review my thesis, and to Dr. Juan Ausio for agreeing to be my external examiner.

I thank Dr. David Eisenstat and Dr. Janice Richman-Eisenstat for career advice and Dr. Spencer Gibson for making me see the "big picture". I also thank Drs. Spencer Gibson and David Eisenstat for the many letters of reference they provided on my behalf.

I would like to acknowledge the many people who made life in graduate school enjoyable, especially Kendra Cann, Jeanne Fourie, Warren Law, James Paul, Cielo Monterrosa, Francisco Mendoza, Greg Smith and Kofi Chapman. Many members of the Davie lab, both past and present, provided advice and friendship over the years. For this I thank Mariko Moniwa, Laura Hart, Simy Buckwold, Helen Zhao, Anoushe Sekhavat, Dr. Soma Mandal, Dr. Shihua He, and Dr. Jenny Yu and Lin Li.

I thank my parents for providing me the opportunity to achieve higher education, and my Grandparents for their constant encouragement.

I must not forget the ever-supportive Tuntun Sarkar, Dr. Steve Pind, Jan Middleton, Lil Cameron and Gerhard Dyck from Biochemistry, who always made things less complicated.

This research was supported by the National Cancer Institute of Canada, the Canadian Institutes of Health Research, the K.M. Hunter Charitable Foundation, and the CancerCare Manitoba Foundation.

Table of Contents

Chapter Two: Materials and Methodology

Chapter Three: Results

Chapter Four

List of Figures

List of Tables

List of Abbreviations

aa	amino acid
ADP	adenosine di-phosphate
AGC	PKA, PKG, PKC
ASK1	apoptosis signal-regulating kinase 1
Akt	(protein kinase B)
AMPK	AMP-activated protein kinase
ANS	8-anilino-1-naphthalene-sulfonic acid
AP-1	activator protein 1
APP	amyloid β-protein precursor
APS	ammonium persulfate
ATF	activating transcription factor
ATPase	adenosine tri-phosphatase
AU	acid-urea
AUT	acid-urea-triton
BEAF	boundary element associated factor
BORIS	brother of the regulator of imprinted sites
BSA	bovine serum albumin
C3	ciras-3
Caf1	chromatin assembly factor 1
CBP	CREB binding protein
CENP-A	centromere protein A
ChIP	chromatin immunoprecipitation
CK2	casein kinase II
CREB	cyclic AMP-responsive element binding protein
CTCF	CCCTC-binding factor
CTD	C-terminal domain
C-terminus	carboxyl-terminus
CTF-1	CCAAT-binding transcription factor 1
DAPI	4`, 6-diamidino-2-phenylindole

dCTCF	*drosophila* CTCF
ddH_20	double distilled water
DLK	dual leucine zipper-bearing kinase
Dlk/ZIP	death-associated protein-like kinase
DMEM	dulbecco's modified eagle medium
DMSO	dimethylsulfoxide
DOT	disruptor of telomeric silencing
DOT1L	disruptor of telomeric silencing 1-like
DNA	deoxyribonucleic acid
4E-BP1	eIF4E-binding protein 1
ECL	enhanced chemiluminescence
EGF	epidermal growth factor
ER	estrogen receptor
ER81	ets-related protein
ERK	extracellular regulated kinase
FACS	fluorescence activated cell sorting
FBS	fetal bovine serum
FITC	fluorescein isothiocyanate
FSH	follicle stimulating hormone
GAP	GTPase activating protein
GDP	guanine nucleotide di-phosphate
GRF	guanine nucleotide releasing factor
GRP	guanine nucleotide-releasing protein
GTP	guanine nucleotide tri-phosphate
h	hours
HAT	histone acetyltransferase
HBO1	histone acetyltransferase bound to ORC1
HDAC	histone deacetylase
HIRA	histone regulatory homolog A
HMGN1	high mobility group N protein 1
HP1	heterochromatin protein 1

HRP	horse radish peroxidase
hsp	heat shock protein
hTERT	human telomerase reverse transcriptase
ICR	imprinted control region
IF	indirect immunofluorescence
Igf2	insulin-like growth factor 2
IgG	immunoglobulin
IKK	IκB kinase
IL-6	interleukin-6
INO80	inositol requiring protein 80
ISWI	imitation switch
JNK/SAPK	c-jun amino-terminal kinase/stress-activated protein kinase
LCR	locus control region
LDL	low-density lipoprotein
MAPK	mitogen activated protein kinase
MAPKAP-K1b	MAPK-activated protein kinase 1b
MEK	MAPK kinase kinase
MEKK	mitogen-activated protein kinase/extracellular signal-regulated kinase kinase kinase-1
α-MEM	minimum essential alpha medium
min	minute
MLTKα	mixed lineage triple kinase alpha
MLK	mixed lineage kinase
MOZ	monocytic leukemia zinc finger protein
mRNA	messenger RNA
MSK1/2	mitogen and stress activated kinase 1 and 2
NFκB	nuclear factor kappa B
NPC	nuclear pore complex
N-terminus	amino-terminus
NuRD	nucleosome remodelling and histone deacetylation
PAK-1	p21-activated kinase-1

PARP-1	poly(ADP-ribose) polymerase
PBS	phosphate buffered saline
PBST	phosphate buffered saline containing 0.5% tween 20
PIC	pre-initiation complex
pS6 HMGN1	high mobility group protein N1 phosphorylated at serine 6
pS10AcK14 H3	H3 phosphorylated at serine 10 and acetylated at lysine 14
pS10 H3	H3 phosphorylated at serine 10
pS28 H3	H3 phosphorylated at serine 28
PI3K	phosphatidylinosytol-3-OH kinase
PKA	cAMP dependent protein kinase
PKC	protein kinase C
PKG	protein kinase G
PMA	phorbol 12-myristate 13-acetate
PMSF	phenylmethanesulfonyl fluoride
POZ	pox virus and zinc finger
PRMT1	protein arginine *N*-methyltransferase
PVDF	polyvinylidine fluoride
RNA	ribonucleic acid
RNA pol II	RNA polymerase II
ROCK-II	rho-dependent protein kinase II (ROKα or Rho kinase)
RSK2	ribosomal S6 kinase 2
S6K1	p70 ribosomal protein S6 kinase
SAP	SRF accessory protein
SATB1	special AT-rich binding protein 1
SDS-PAGE	sodium-dodecyl-sulfate polyacrylamide gel electrophoresis
SET	suppressor of variegation, enhancer of zest and trithorax
SMP	skim milk powder
Sos	son of sevenless
S phase	synthesis phase
STAT	signal transducer and activator of transcription
Su(Hw)	suppressor of hairy wing

SWI/SNF	switch/sucrose non-fermentable
SWRI	Swi2/Snf2-related adenosine triphosphate complex
T3	triiodothyronine
Tip60	HIV tat-interacting protein
TNF	tumour necrosis factor
Topors	topoisomerase I-interacting arginine/serine rich
TPA	12-0-tetradeconylphorbol-13-acetate
TR	texas red
TSA	trichostatin A
UPA	urokinase plasminogen activator
USF	upstream stimulatory factor
UV	ultraviolet
V	volts
WB	Western blotting
XIST	X-inactive specific transcript
YB-1	Y-box DNA/RNA-binding factor

List of Copyrighted Material for which Permission was Obtained

Chapter One: Introduction

I. *Cell Cycle Regulation and Cancer*

The conversion of a normal cell into a cancer cell is referred to as malignant transformation. Once transformed, cells are immortal, growing and dividing indefinitely and often excessively. This can lead to the invasion of surrounding tissues and metastasis. Transformed cells do not exhibit the normal phenomenons of contact inhibition or adherence, the latter meaning that they do not require attachment to solid surfaces in order to grow and divide. These cells are characterized by genetic abnormalities that prevent normal regulation of the cell cycle. Most malignant tumours arise from a single cell of origin, having undergone multiple DNA-damaging, transforming events that led to the malignant phenotype.

The cell cycle is made up of four phases: gap 1 (G1), synthesis (S), gap 2 (G2), and mitosis (M). Progression from one phase to another is governed by checkpoints. From start to finish the length of the cell cycle varies among different cell types, the average being approximately 20 hours. Two gap phases are interspersed between the phases of synthesis and mitosis. Cells in G1 are metabolically active but do not replicate their DNA. This phase lasts for a varying length of time before cells progress into S phase, when DNA synthesis takes place such that 2N cells become 4N. Following DNA synthesis is the second gap phase, G2, after which cells undergo mitosis and the cell divides into two daughter cells.

Oncogenes and Tumour Suppressor Genes: Abnormalities affecting the genes responsible for regulating cell growth and division often result in the deregulated cell division that marks cancer cells. Some of these, termed oncogenes, code for protein products that are excessively active and contribute to the transformation of a normal cell

into a cancer cell. Oncogenes have benign counterparts, termed proto-oncogenes that can become oncogenes when mutated. Tumour suppressor genes also tend to be involved in the regulation of cell growth and act to prevent cellular transformation. A mutation resulting in the loss of function of a tumour suppressor protein may contribute to cellular transformation and the formation of cancer.

II. *The Nucleus*

The nucleus is a dynamic organelle surrounded by plasma membranes. Nuclear pores connect the cytosol and nucleoplasm and allow for transport of proteins and nucleic acids into and out of the nucleus. Many pathways relay information from the cells exterior into the nucleus leading to detailed responses. Various subnuclear structures exist including chromatin, nucleoli, the nuclear matrix, and several types of nuclear bodies.

The Nuclear Matrix: The nuclear matrix is a dynamic, fibrous structure consisting of protein and RNA present throughout the nucleoplasm [2]. Experiments indicate that the nuclear matrix is involved in transcription, DNA replication and RNA processing [2-4]. Chromatin is attached to the nuclear matrix via sequences of DNA termed matrix attachment regions or MARs.

The nuclear matrix is the structure remaining after interphase nuclei are digested with nucleases and treated under high salt conditions [5,6]. It is composed of residual nucleoli, nuclear pore lamina and a network of ribonucleoproteins [7,8]. An internal network of interwoven fibers made up of smaller, 10 nm filaments is connected to the nuclear lamina [9,10]. Transcriptionally active genes are enriched in the nuclear matrix

[11-15]. Various proteins involved in transcriptional regulation, such as transcription factors, co-activators and co-repressors associate with the nuclear matrix, providing further evidence that this structure is of functional significance. These include chromatin modifying enzymes such as histone deacetylases (HDACs), histone acetyltransferases and chromatin remodellers [11,16,17]. In addition, RNA polymerase II is also associated with the nuclear matrix [13,18].

It has been postulated that the loops created by MAR attachment serve not only to spatially organize chromatin but also to create functional domains in which genes are regulated together. Loop domains created by association of DNA with the nuclear matrix are between 5 and 200 kb long and have an average length of 70 -100 kb [19]. A gene positioned close to a MAR will be in close proximity to factors involved in transcription. Furthermore, some genes appear to be targeted to the nuclear matrix in response to specific cellular signals. For example, the estrogen receptor alpha (ERα) interacts with target DNA sequences and tightly associates with the nuclear matrix once it is bound to estrogen [20].

III. *Chromatin*

Serving not only to compact DNA, this protein-nucleic acid complex is highly organized such that the processes of transcription, replication, DNA repair and cell division take place in a regulated fashion. Positioning of chromosomes in the nucleus is not random; they are organized into discrete chromosome territories [21]. At physiological ionic strength chromatin exists as a 30 nm fiber and higher order structures [19] formed by long range interactions [22]. Within this structure, an already compact 30 nm fiber

consists of linker histones bound to a folded 10 nm fiber (Figure 1-1). Short range intra- and internucleosomal interactions condense the 10 nm fiber from its form as an unfolded, extended chromatin fiber comprised of DNA packaged into the nucleosomes.

The Nucleosome: The basic repeating unit of chromatin is the nucleosome [23-25]. Nucleosomes, which measure 110 Å diameter and 57 Å high [23], are made up of approximately 146 base pairs of DNA wrapped around a histone octamer core (Figure 1-2). Within the core, two H2A-H2B dimers interact with a $(H3\text{-}H4)_2$ tetramer to form a disc-like structure. Approximately two turns of the DNA double helix wraps around this core in 1.8 negative superhelical turns [26]. The amino-terminal tails of the four core histones protrude from the nucleosome such that they can interact with linker DNA and nucleoproteins [27].

The Core Histones: All of the core histones are basic in charge, providing high affinity for the negatively charged DNA. H2A, H2B, H3 and H4 have a similar structure with a globular center surrounded by C-terminal and N-terminal regions [28]. Approximately 90 base pairs in the center of nucleosomal DNA interact with the H3-H4 tetramer; the ~30 base pairs of DNA flanking this region bind H2A/H2B dimers [28]. A histone fold domain found within the globular center of all core histones is crucial to histone octamer formation and nucleosome folding [29]. This domain is organized into three α-helices connected through two loops and is involved in histone-DNA interactions [27,30]. Furthermore, it serves as the binding site for other histone fold motifs [27]. The H2A/H2B interface in H2A-H2B dimers is very stable, as is the sum of interactions holding the H3-H4 tetramer together [22]. Electrostatic bonds holding the H2A-H2B dimers in contact with the H3-H4 tetramer create a much less stable interaction [31].

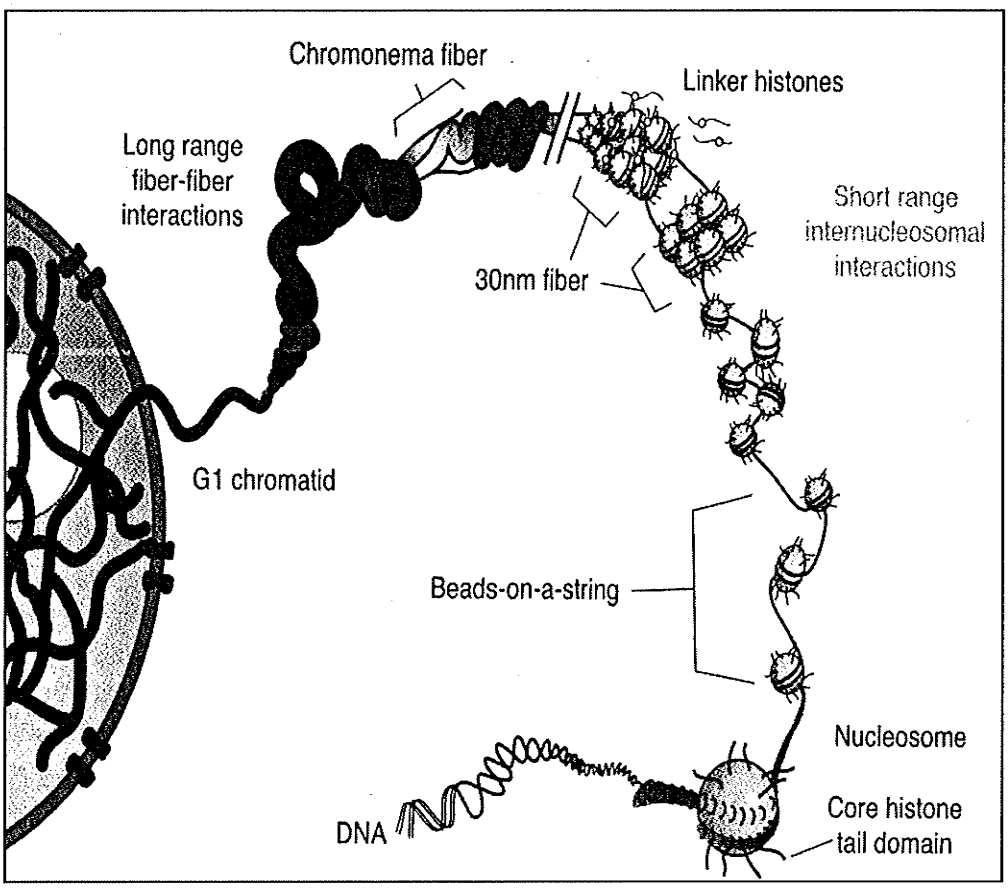

Figure 1-1. Higher order chromatin structure. The folding of higher order chromatin conformations involving long and short range interactions are depicted. Reprinted, with permission, from the *Annual Review of Biophysics and Biomolecular Structure, volume 31* © 2002 by Annual Reviews.

A

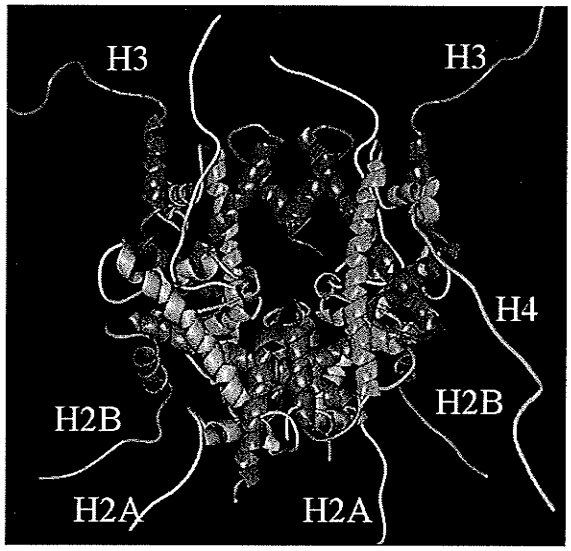

B

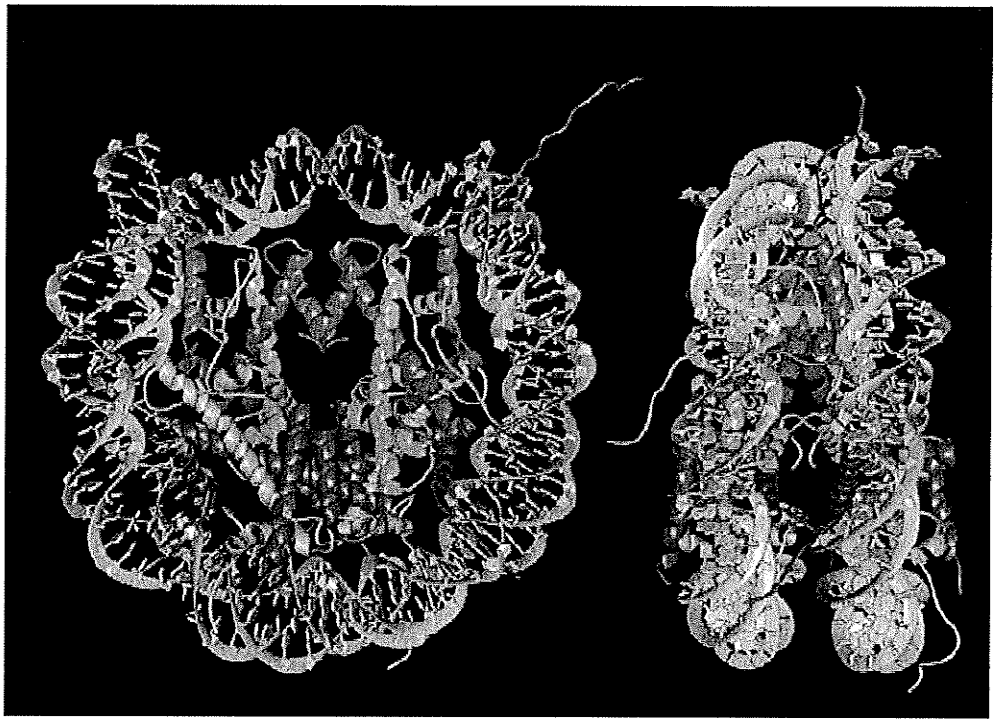

Figure 1-2. The nucleosome. A) The histone octamer. B) The nucleosome. Ribbon traces portray the phosphodiester backbone of DNA; histones are as in (A). Reprinted, with permission, from *Nature volume 389:251-260* © 1997 by Nature Publishing Group .

Linker Histone H1: Nucleosomes are attached together through linker DNA. Linker histone H1 plays a crucial role in chromatin compaction, binding linker DNA as it enters and exits nucleosomes and nucleosomal DNA near the dyad axis of symmetry shown in Figure 1-2 B [29,32]. H1 is comprised of a globular domain flanked by N- and C-terminal tails. Binding of H1 to DNA is dynamic, it remains bound to one site for only a short time before it dissociates [33,34]. Phosphorylation of H1 diminishes its binding to DNA [34-36], implying that this modification is an important player in the regulation of chromatin structure.

Stabilization of Higher Order Chromatin Structure: Higher order chromatin structures are stabilized by the amino-terminal tails of the core histones and the linker histone H1. The amino-terminal regions of all four core histones protrude from the nucleosome such that they are easily accessible to other molecules in the nucleoplasm. Higher order chromatin structure can be stabilized or destabilized by specific modifications to the amino-terminal tails and to histone H1 [37]. The amino-terminus of histone H3 is the longest at 44 amino acids, and protrudes the farthest from the nucleosome. Crystalographic evidence indicates that this region is in position to make several contacts with linker DNA [24,38,39].

Modification of Histones

The amino- and carboxyl-terminal tails of histones are subject to post-translational modifications such as acetylation, phosphorylation, ubiquitination, sumoylation, biotinylation, methylation, citrullination and ribosylation [40-42]. A diagrammatic representation of the core histones and their modification sites is shown in Figure 1-3. Many histone modifications are associated with specific chromatin states or functions including transcription, silencing and DNA repair. Methylation, for example, can take place on at least one residue of each of the four core histones and is associated with both silencing and transcriptional activity. Hyperacetylation of histones H3 and H4 is also associated with transcriptional activity while hypoacetylation of these histones is not. Although it has historically been thought that post-translational modifications to histones were restricted to the amino- and carboxyl-termini, it was recently discovered that several residues within the histone fold are modified by acetylation and methylation [43,44]. Modifications are mediated by various enzymes and are dynamic.

The biological relevance of each modification is influenced by the chromatin structure surrounding it. Overall level of compaction, non-histone chromatin proteins and the presence of other histone modifications can have significantly impact. Thus although the functional relevance of certain modifications has been elucidated, the full extent and purpose of most remains unknown.

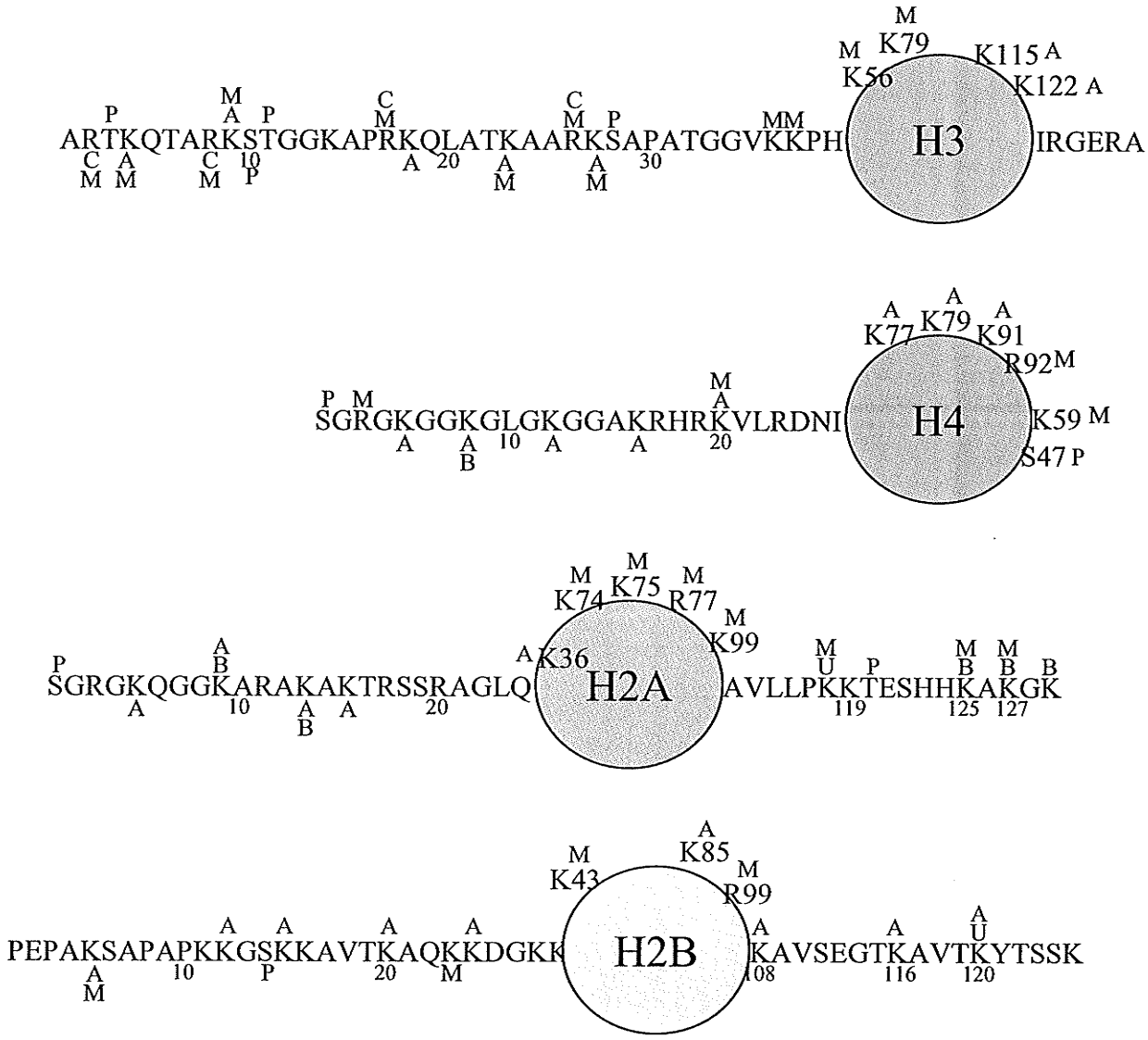

Figure 1-3. Post-translational modification of the four core histones. Sites of post-translational modification by acetylation (A), phosphorylation (P), methylation (M), ubiquitination (U), biotinylation (B) and citrullination (C) are shown.

Acetylation: The acetylation reaction on core histones is shown in Figure 1-4. All four core histones can be acetylated at the ε-amino group of specific lysine residues. Steady-state levels of this charge-altering modification are balanced by the action of histone acetyltransferases (HATs) and histone deacetylases (HDACs). Hyperacetylation of the amino-termini of histones H3 and H4 has long been associated with transcriptional activity [11,45-47]. In addition, many activators of transcription associate with HATs, and many repressors with HDACs. In this manner HATs and HDACs can be recruited to specific loci to modulate chromatin structure.

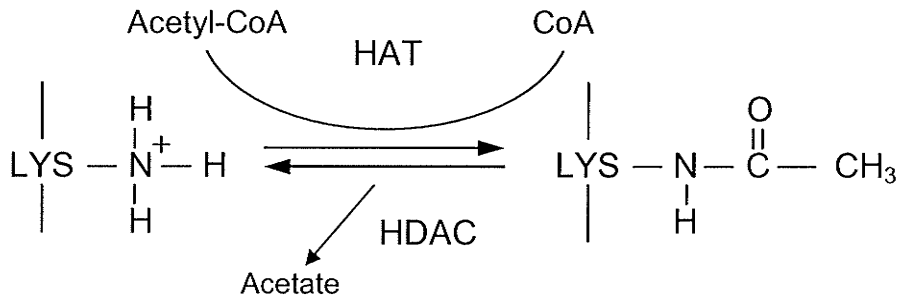

Figure 1-4. Acetylation of histones. Histones can be acetylated by histone acetyltransferases (HATs) on the epsilon amino group of lysine residues. The steady state level of this modification is determined by the action of HATs and HDACs.

Histone Acetyltransferases: HATs acetylate histones in a specific manner, can be recruited to genomic loci and act as transcriptional co-activators [48]. These enzymes tend to be found in large protein complexes whose components then determine the HAT substrate specificity [29,49]. Five main families of HATs exist: the Gcn5-related N-

acetyltransferase (GNAT), MYST (MOZ, Ybf2/Sas3, Sas2 and Tip60), p300/CBP (CBP: CREB binding protein), p160 and $TAF_{II}250$ families.

Members of the GNAT family are involved in transcriptional initiation (Gcn5 and PCAF: p300/CBP associated factor) and elongation (Elp3), and can be recruited to DNA by several transcription factors [48]. GNAT family members contain bromodomains that recognize and bind acetyl-lysine [50,51]. CBP and p300 are highly related proteins that function to regulate transcription in combination with many transcription factors including Fos-Jun (AP-1) and CREB (cAMP-response element binding protein) [52]. Like members of the GNAT family, CBP and p300 each have a bromodomain in addition to other motifs to modulate protein-protein interactions [52]. The MYST family of HATs consists of MOZ (monocytic leukemia zinc finger), Ybf2/Sas3, Sas2, Tip60 (HIV Tat-interacting protein), Esa1 and HBO1 (histone acetyltransferase bound to ORC1). Members of this family appear to function in DNA replication as well as transcriptional initiation and elongation [53,54]. Subunits of the TFIID transcription factor complex are HATs belonging to the $TAF_{II}250$ family. As was described above for members of the GNAT and p300/CBP families, $TAF_{II}250$ HATs have a bromodomain [52]. The p160 family of HATs act as co-activators of nuclear receptors and interact with CBP [55].

Phosphorylation: Histones H1, H2A, H3 and H4 have serine and/or threonine residues subject to phosphorylation. This modification lowers the net positive charge of the histone and is involved in several cellular functions such as transcription, mitosis, DNA damage repair, and apoptosis [56]. Phosphorylation, represented in Figure 1-5, is mediated by several different enzymes.

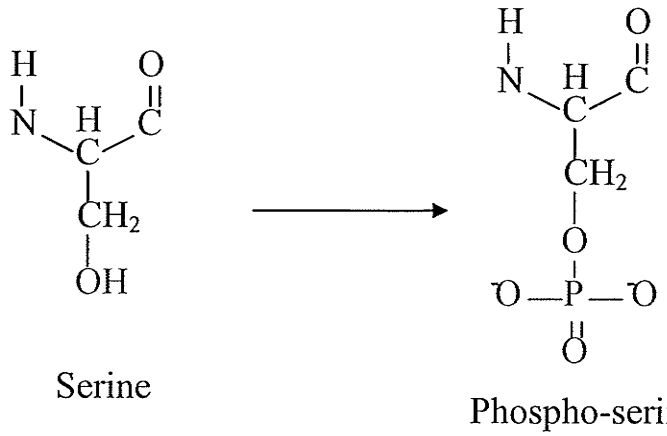

Figure 1-5. Phosphorylation of serine. Histones are phosphorylated at serine or threonine residues. Phosphorylation of serine results in the incorporation of negative charge into the histone molecule.

Methylation: Certain arginine and lysine residues can be mono-, di- or tri-methylated. Arginine methylation can be symmetric or asymmetric; dimethylated arginine is symmetric if it contains one methyl group on each terminal nitrogen and asymmetric if both methyl groups are on the same terminal nitrogen. Methylation is catalyzed by members of several different protein families including DOT1/DOT1L (disruptor of telomeric silencing 1 and disruptor of telomeric silencing 1-like), the PRMT1 (protein arginine *N*-methyltransferase) family, and the family of SET (suppressor of variegation, enhancer of zest and trithorax) domain containing proteins [57].

This modification, which unlike acetylation and phosphorylation is not charge-altering, can act as a signal for activation or repression of transcription, depending on the particular residue methylated and the number of methyl groups added. H3 tri-methylated at lysine 9 tends to be within heterochromatin, while H3 mono- or di-methylated at lysine

9 is more likely to be in euchromatic regions [58,59]. Methylation of H3 can also take place on several other lysine and arginine residues including lysine 27 which has also been linked to transcriptional silencing [60]. Sites of methylation associated with transcriptional activity include lysines 4, 36 and 79 [57]. It appears as though histone methylation acts to create binding sites for nuclear factors that upon binding contribute specifically to active or inactive chromatin states. Protein domains that interact specifically with methylated lysine residues include the chromodomain, the WD40-repeat domain and the Tudor domain [61-65].

High Mobility Group Proteins

Many proteins are bound to or become associated with chromatin. High mobility group proteins (HMGs) are non-histone structural chromatin proteins that bind select nucleosomes. Five HMG subtypes, HMGN1, HMGN2, HMGN3, HMGN4 and NBP-45 (nucleosome binding protein 45) exist [66-69]. Of these, the best studied are HMGN1 and HMGN2, which have similar structures and generate matching footprints on nucleosomal DNA [70]. HMGN1 and HMGN2 interact with nucleosomal DNA near the entry/exit points of the histone core and in the major grooves surrounding the dyad axis (refer to Figure 1-6) [71]. Evidence suggests that HMGN1 and HMGN2 are involved in transcription [72]. HMGN1 and HMGN2 compete for chromatin binding sites with histone H1 [73]. In addition to interacting with nucleosomal DNA, the amino-terminus of HMGN1 interacts with H2B, while the C-terminal region of HMGN1 interacts with the amino-tail of histone H3 [1]. Binding of HMGN1 reduces chromatin compaction; the loss of this protein at transcribed genes decreases their accessibility to nucleases [74].

It is thought that this protein modulates histone modifications as well as the accessibility of DNA for protein interactions. Experiments have shown that a loss or decrease of HMGN1 alters the expression of various genes, including N-cadherin [75], and Sox9 respectively [76]. HMGN1 is also linked to DNA damage repair. HMGN1-/- cells are more sensitive to ionizing radiation and do not require adherence to proliferate [77]. Moreover, mice of this nature develop more tumours [77] and exhibit a slower rate of photoproduct removal [74]. It has been postulated that the decrease in chromatin compaction upon HMGN1 binding to nucleosomes facilitates access to sites of DNA damage in order to speed up the repair process [74].

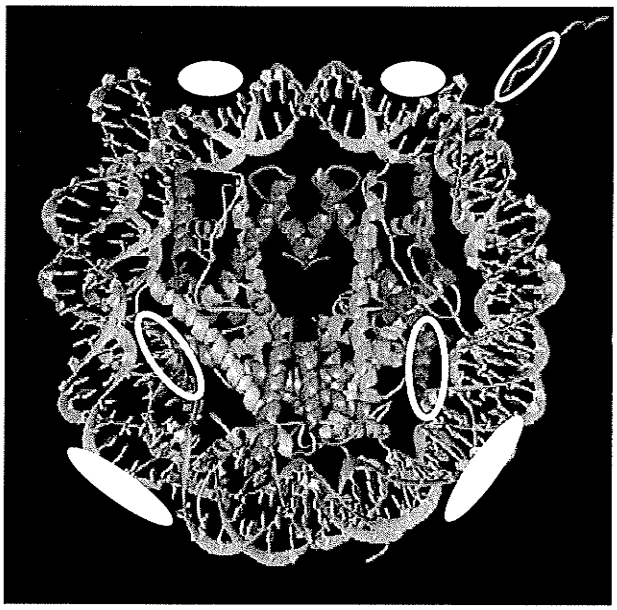

Figure 1-6. Model of HMGN binding to nucleosomes. Ribbon traces represent the core histones and nucleosomal DNA. Solid white symbols are located in the major grooves in areas protected from hydroxyl radical cleavage by HMGN1/2. Photocrosslinking experiments indicate that the region surrounding amino acid 88 in the C-terminal region of HMGN1 targets the amino-terminal tail of H3 (see open oval), and that the region surrounding amino acid 8 in the amino-terminus of HMGN1 targets H2B (see open oval). H3 is shown in blue; H2B is shown in red. Reprinted, with permission, from *Nature volume 389:251-260* © 1997 by Nature Publishing Group.

Histone Variants

Histone variants are implicated in specialized roles such as transcription, DNA repair, and nucleosome stability. Variants are encoded by separate genes and may or may not be expressed in a manner dependent upon DNA replication. Those that are expressed throughout the cell cycle and can be incorporated into chromatin in a manner that is independent of DNA replication have the potential to mark specific domains of chromatin, possibly for particular cellular activities, in between cycles of cell division. Variants of H1, H2A, H2B and H3 have been identified.

H2A and H2B: Several variants of H2A and H2B exist including H2A.X, macroH2A, H2A.Z, H2A-Bbd, H2A.1, H2A.2, H2B.1 and H2B.2. Phosphorylated H2A.X (referred to as γ-H2A.X) is present at sites of double stranded DNA breaks [78-80] and appears to facilitate the repair process [81]. This could occur through a mechanism in which γ-H2A.X serves as a signal to recruit DNA repair factors in conjunction with chromatin remodellers to assist repair [81]. Evidence indicates that macroH2A, occurring at a ratio of 1 to 30 nucleosomes in rat liver, is involved in X-chromosome inactivation through interactions with XIST (X-inactive specific transcript) RNA [82-84]. The function of H2A.Z is still being deciphered. This variant is proposed to stabilize chromatin and has been associated with both transcriptionally active and repressed regions [85]. Recent reports concur that this variant is able to stabilize chromatin and that acetylation influences its chromatin-stabilizing properties and separates H2A.Z in regions of active transcription from H2A.Z that is outside these regions [86,87]. H2A-Bbd has been linked to transcription and may be enriched in actively transcribing chromatin [88]. The functions of the other H2A variants, H2A.1 and H2A.2, remain a mystery. Variants of

H2B have also been discovered. The function of H2B.1 and H2B.2 has yet to be elucidated, but studies suggest a role in stabilizing the interaction of the H2A-H2B dimer with the nucleosome [89]. Levels of these variants change with the development of malignant Friend tumour cells [90].

Variants of H3: To date 5 variants of H3 have been discovered in mammals: H3.1, H3.2, H3.3, testis-specific H3.1t and centromeric CENP-A. The N-terminal of CENP-A is unique among H3 variants while its histone fold domain, 60% identical to other H3 variants, is positioned within its C-terminus [91]. H3.1, H3.2 and H3.3 are shown in Table 1; they differ only by a few amino acids [92] yet appear to function in the cell in very different ways. H3.2 differs from H3.1 at residue 96, where a serine is substituted for a cysteine. H3.3 varies at 4 additional residues: alanine 31 of H3.1 is replaced with a serine in H3.3, serine 87 with alanine, valine 89 with isoleucine, and methionine 90 with glycine. Of these, only H3.3 can undergo replication-independent incorporation into chromatin and is basally expressed [93]. This could result in an enrichment of H3.3 at transcriptionally active genes. This variant appears to be involved in transcription; it is present in transcriptionally active regions of chromatin [93-96] and is enriched in modifications associated with transcriptional activity, such as hyperacetylation and di-methylation at lysine 36 and lysine 79 [97]. Expression of H3.1 and H3.2 is restricted to S-phase and their incorporation into chromatin is in a DNA-replication-dependent basis. While modifications associated with silencing such as di- and tri-methylation of lysine 27 are enriched on H3.2, H3.1 is enriched in K14 acetylation, which can be used as an indicator of transcriptional activity, and silencing-associated lysine 9 di-methylation [97]. Further, modifications to variant-specific residues, as is seen during mitosis when H3.3

becomes phosphorylated at serine 31, also indicate unique functions for histone variants [98].

The mechanism by which histone variants are incorporated into chromatin outside of DNA replication is still being deciphered. In *Drosophila*, which has only two H3 variants, H3 and H3.3, replication-coupled incorporation appears to involve the histone chaperone chromatin assembly factor 1 (Caf1) while replication-independent incorporation of H3.3 may be associated with an alternate histone chaperone, HIRA (histone regulatory homolog A) [99]. H3 variants may be brought in through contacts between Caf1 and proteins present at replication forks, while HIRA may mediate H3.3 deposition by interacting with components of the RNA pol II complex [99,100].

Residue	H3.1	H3.2	H3.3
31	alanine	alanine	serine
87	serine	serine	alanine
89	valine	valine	isoleucine
90	methionine	methionine	glycine
96	cysteine	serine	serine

Table 1.1. Non-centromeric variants of mammanlian histone H3. Differences in amino acid sequence between murine H3.1, H3.2 and H3.3 are shown.

Euchromatin, Heterochromatin and Position Effects

Euchromatin and heterochromatin differ from each other structurally and biochemically. Euchromatin, with its relatively decondensed structure, irregularly spaced nucleosomes, sensitivity to nucleases, and enrichment in histone modifications such as trimethylation of H3 at lysine 4, dimethylation of H3 at arginine 17, and acetylation of H4 at lysine 16, is the place of transcriptionally active genes [101,102].

The term heterochromatin once referred only to the portion of chromatin remaining condensed following the completion of mitosis. Currently, the definition includes any condensed chromatin in which transcription does not take place. Subtypes of heterochromatin exist; facultative heterochromatin is that which can move between euchromatic and heterochromatic states, whereas constitutive heterochromatin, including pericentromeric heterochromatin, remains condensed and silent [103]. Heterochromatin contains regularly spaced nucleosomes, has a high content of methylated DNA, is not sensitive to nucleases, and is enriched in a specific set of modified histones such as H3 di- or tri-methylated at lysine 9 [104-107]. Proteins complexed with DNA in heterochromatin confer its unique characteristics. This includes heterochromatin protein 1 (HP1), which contains a chromodomain that allows it to recognize H3 methylated at lysine 9 [61,108] . Although highly compacted, regions of condensed chromatin are accessible to macromolecules [109,110]. Components undergo turnover at a significant rate, although much slower than what is seen in euchromatin, with that of HP1 being 1 minute [111,112]. Heterochromatin is self-propagating, spreading from one or more sites of nucleation at silencers as well as protosilencers, which enhance silencer activity [113,114]. The self-propagating nature of heterochromatin explains the phenomenon of

position effect variegation wherein expression of a transgene is silenced due to its incorporation into a region of heterochromatin [115].

Chromatin Remodellers

Nucleosomes are stable, restrict access to DNA, and have limited mobility. Chromatin remodellers are protein complexes that use ATP to work in conjunction with chromatin modifying proteins to mediate nucleosome stability and mobility to facilitate access to nucleosomal DNA during replication, transcription, and repair. Eukaryotes contain several families of chromatin remodellers including SWI/SNF (switch/sucrose nonfermentable), NURD/Mi-2/CHD (NURD: nucleosome remodelling and deacetylase repressor), ISWI (imitation switch), INO80 (inositol 80-containing complex) and SWRI (Swi2/Snf2-related adenosine triphosphate complex). ATPase subunits are conserved within families, and there is considerable similarity between ATPase domains in the ISWI and SWI/SNF families, suggesting that ATP use by chromatin remodellers is through a common mechanism [116].

ISWI complexes function in chromatin assembly following DNA replication, while SWI/SNF complexes do not [117]. ISWI remodellers also organize nucleosomes in such a way as to promote repression [118,119], and at certain loci promote transcriptional elongation, suggesting that the function of chromatin remodellers varies with chromatin context [116,120]. Like ISWI, various reports indicate that SWI/SNF remodellers contribute to or repress transcription; SWI/SNF can reorganize nucleosome positioning to facilitate the binding of transcription factors and transcription [121] or promote binding of repressor proteins [122].

IV. *Transcription*

Transcription of genes to messenger RNA (mRNA) is mediated by RNA polymerase II (RNA pol II). This process requires the general transcription factors TFIIB, TFIID, TFIIF, TFIIE, TFIIH, and TFIIA. First, TFIID, containing the TATA-binding protein, binds to the TATA element. Transcription can be stimulated by interactions between TFIID and activating proteins bound to promoters/enhancers.

The C-terminal domain (CTD) of the largest subunit of RNA pol II is made up of tandem repeats of the highly conserved heptapeptide YSPTSPS and undergoes a series of phosphorylation and dephosphorylation events throughout the process of transcription. Following assembly of RNA pol II with the general transcription factors, Ser-5 in the CTD of RNA pol II is phosphorylated. This phosphorylation is mediated by the general transcription factor TFIIH.

Nucleosomes act as barriers to RNA-pol II-mediated transcription [89] and thus must be overcome. Electron spectroscopic imaging has revealed that these nucleosomes have taken on an unfolded, extended "U" shape [123], suggesting that the basic repeating structural unit of chromatin is disrupted by the passage of the RNA pol II complex. Cysteine thiol groups in H3 buried near the dyad axis of symmetry in transcriptionally silent chromatin are exposed during transcription [124], and a number of studies have found decreased amounts of histones present at transcriptionally active loci [125]. Furthermore, transcription through an *in vitro* mononucleosomal template results in the formation of a hexamer containing an H3-H4 tetramer and one H2A-H2B dimer [126].

The Progressive Displacement Model of Transcription: In this model of gene transcription histone octamers are progressively displaced from the DNA as RNA pol II

passes [127]; re-binding of the octamer takes place with low efficiency, making the transcribed sequence deplete in nucleosomes and more easily transcribed.

An approaching RNA pol II complex prompts the release of the proximal H2A-H2B dimer, possibly through the induction of positive superhelicity [127] or factors associated with the RNA pol II complex [126]. This dissociation facilitates the entry of RNA pol II into the nucleosome, and may result in a competition between the hexamer and RNA pol II for DNA binding. In addition, it could alter higher order chromatin structure and provide an opportunity for other nuclear factors, such as chromatin remodellers and histone modifying enzymes, to bind the somewhat exposed chromatin [128,129]. Loss of the proximal H2A-H2B dimer may also destabilize the central part of the nucleosome and aid in dissociation of DNA from the proximal H3-H4 pair once it is approached by RNA pol II. This, combined with the fact that DNA near the dyad axis of symmetry has already been released, permits RNA pol II to transcribe past the dyad region. Procession of RNA pol II displaces DNA from the distal H3-H4 pair of the $(H3\text{-}H4)_2$ tetramer. The proximal H3-H4 dimer then rebinds DNA, and at some point the released proximal H2A-H2B dimer also re-associates. As RNA pol II progresses, the distal H2A-H2B dimer is displaced such that all of the nucleosomal DNA is transcribed [127]. Re-association of the distal H2A-H2B dimer takes place following the passage of RNA pol II [127].

V. *Regulation of Transcription*

Levels of transcription of any particular gene can be influenced by several factors. Cells contain signalling pathways that influence and regulate gene expression. Stimulation results in the activation/repression of specific sets of genes in a transcriptional program

that leads to a particular cellular event, such as growth or apoptosis. Signalling pathways can pick up intra- or extracellular signals that are then relayed to the nucleus. These include the mitogen activated protein kinase pathway (MAPK) that will be described in further detail in a later section. Many signalling pathways alter the activity of transcription factors, which are proteins that bind to specific sequences of DNA at what are termed regulatory elements. These sites may be in promoters, enhancers, locus control regions, silencers, or insulators. Transcription factors tend to have inactive and active states, often marked by post-translational modifications or conformational changes brought on by protein-protein interactions.

Once bound, transcription factors play an important role in transcription. Activators may enhance or initiate transcription by promoting the binding of RNA pol II and the general transcription factors. Those factors that, upon binding, function to silence or repress transcription are termed repressors. Many transcription factors associate with chromatin modifying enzymes such as histone acetyltransferases (co-activators) and histone deacetylases (co-repressors), resulting in the alteration of chromatin structure.

Locus Control Regions, Enhancers and Silencers: Locus control regions (LCRs) were functionally defined in transgenic mice to be sequences required and sufficient for position-independent expression of a transgene [114]. As implicated by their name, enhancers function to enhance transcription. Enhancers may be located up to 1 megabase away from their target promoter, and studies have shown that most are not specific, meaning they are capable of enhancing transcription at many genes [130,131]. Enhancers act through one of two mechanisms. The first involves direct contact between the enhancer and promoter in which factors bound to the enhancer are thought to allow for

easier formation of the RNA pol II complex at the promoter of the target gene. Intrachromosomal loops can juxtapose enhancers with upstream promoters to increase transcription [132-134]. The second does not involve direct contact and instead relies upon the propagation of a signal that travels down the strand of DNA from enhancer to promoter.

Silencers and protosilencers are involved in the formation of transcriptionally repressed states of chromatin. Protosilencers are defined functionally as elements able to enhance the activity of a silencer without acting as a silencer independently. The assembly of heterochromatin begins at one or more focal points (silencers or protosilencers) [135,136] and propagates down the chromatin fiber [137]. This mechanism of spreading would suggest that all chromatin from point A to point B is affected, and in effect, silenced. However, several studies indicate that this is not the case, that in fact unaffected domains of euchromatin undergo a "looping out" mechanism in which they are separated from the heterochromatin around them [135,137].

Insulators: Insulators protect genes from activation by inappropriate enhancers or silencing as the result of the spread of heterochromatin. Promoter activity is not compromised; transcription can be activated by suitable stimuli. Insulators are located on DNA interspersed between the protected promoter and heterologous enhancer or heterochromatin. Several insulators are associated with the nuclear matrix (MARs).

VI. *Phosphorylation of Histone H3*

H3 phosphorylation appears to have two very different functions in the cell. This modification occurs during interphase and mitosis, and is best known to occur at serines 10 and 28. During interphase H3 phosphorylation occurs on a small subset of genes as the result of stimulation of the mitogen activated protein kinase pathways and is associated with the resulting gene expression. Phosphorylation of H3 during mitosis is widespread and thought to contribute to the proper condensation and segregation of chromosomes.

Chromosome Condensation-Related Phosphorylation of H3 during Mitosis

Phosphorylation of histone H3 at serine 10 was originally associated with mitosis [138,139]. It is required for the initiation of chromosome condensation in mammalian cells [140] and in *T. thermophila* cells [138]. This modification is not required for cell cycle progression in yeast, although another modification, phosphorylation of H2B, may take its place [141]. More recently, phosphorylation has also been shown to occur at serine 28 [142] and at threonine 11 [143]. Appearing in G2 phase, phosphorylation begins in the highly condensed pericentromeric heterochromatin and then spreads, along with chromosome condensation, to other regions of the genome [144]. The exact timing of the onset of H3 phosphorylation during mitosis may be variable for different cell types and lines. In one study of Chinese Hamster Ovary cells, phosphorylation was found to start in prophase, reach a maximal amount in metaphase and begin to disappear in the transition to telophase [139]. Similar timing was also observed during meiosis in

Tetrahymena thermophila [138,145]. In any case, phosphorylation of H3 reaches a maximum and dissipates before the end of mitosis.

Aurora B: The mitosis-specific H3 kinase was first identified in mammals as a novel kinase causing arrest of growth in yeast upon overexpression [146]. Aurora B, called AIM 1 in mouse, mediates phosphorylation of H3 at serine 10 and at serine 28 during mitosis [147-149] . This kinase is part of the well-conserved IpI1 kinase family, showing homology to IpI1, the only aurora kinase in yeast. *Drosophila* contains two aurora kinases, while mammals have three, now called Aurora A, B and C. Phosphorylation of H3 by Aurora B during mitosis is counteracted by protein phosphatase 1 (PP1) [150,151]. It is believed that the balance between the activities of Aurora B and PP1 regulates levels of H3 phosphorylation [152].

The amount of Aurora B present in cells varies through the cell cycle, reaching a maximum in G2/M phase [153]. Levels drop significantly following telophase [154]. Aurora B is a chromosomal passenger protein, meaning that it adheres to specific areas of localization throughout mitosis [155]. Chromosomal passenger proteins are nuclear in G2 phase and associate with the length of chromosomes during prophase. During prometaphase and metaphase these proteins localize to inner centromeres, and at the beginning of anaphase localization shifts to the central spindle before dissociation from the chromosomes into the midbody for cytokinesis. The localization of Aurora B to centromeres during prometaphase is dynamic and is not microtubule-dependent [155].

In mammalian cells, Aurora B functions in a complex with survivin and INCENP (inner centromeric protein). Studies suggest that the enzymatic activity of Aurora B is regulated by these proteins [153-156]. The H3-kinase activity of Aurora B is associated with

condensin recruitment and proper assembly of the mitotic spindle [149]. Loss of Aurora B function results in a loss of H3 phosphorylation, defects in chromosome alignment on the mitotic spindle, and failure in cytokinesis [153]. In addition to histone H3, Aurora B phosphorylates several other proteins including survivin, the myosin II regulatory light chain, INCENP, topoisomerase II alpha, vimentin, desmin, MgcRac1GAP, and CENP-A at serine 7 [155].

Changes to Chromatin during Mitosis: Chromatin becomes visibly altered by condensation in prophase. Later, chromosomes align upon a bipolar spindle, separate, and cytokinesis occurs. The events surrounding chromatin structural changes and spindle activity during mitosis are coordinated by a select group of kinases in the Aurora, cycling-dependent kinase, Polo and NIMA/Nek families including several that mediate phosphorylation of chromatin proteins [157]. Histone H1, histone H3 and HMGN1 are altered by post-translational modifications in the course of mitosis.

Phosphorylation of H3 at serine 10 and serine 28 mediated by Aurora B begins in late G2 phase before the onset of chromosome condensation. Phosphorylation of H3 at threonine 3, mediated by haspin, occurs before any condensation is visible on regions of chromatin that differ from those undergoing late G2 phase phosphorylation of H3 at serine 10, and appears to diminish substantially during anaphase [157]. These two modifications display distinct distributions on chromatin throughout mitosis. Though not a chromosomal passenger protein haspin associates with chromatin and components of the spindle, and there is evidence to suggest that it also targets spindle proteins for mitotic

phosphorylation. Haspin is necessary for proper chromosome alignment but is not required for general chromosome condensation [157,158].

H3 bearing a phosphorylated threonine 11 occurs during mitosis in a temporal pattern similar to that of H3 phosphorylation at serine 10, serine 28 and threonine 3 [143]. This modification is enriched in centromeres at a time when death-associated protein-like (Dlk/ZIP) kinase, which phosphorylates H3, H4 and H2A *in vitro* [159], localizes to centromeres [143]. Dlk/ZIP is an important factor in cell death induced by interferon γ and TNFα/fas [160-162] and is known to interact with transcription factors and a splicing factor [163-165]. Coincidental association of Dlk/ZIP with centromeres enriched in phospho-H3 (threonine 11) during mitosis indicates that it is likely the kinase responsible for this phosphorylation and further implies its involvement in multiple cellular processes [143].

Histones H4, H1, H2A, the centromeric H3 variant CENP-A and structural chromatin protein HMGN1 are also phosphorylated during mitosis [166,167]. H3 variant CENP-A is phosphorylated at serine 7 by Aurora A during prophase, followed by Aurora B-mediated phosphorylation. Blocking CENP-A phosphorylation with RNA interference leads to defects in kinetochore attachment and chromosome alignment [168]. Serine 1 of both H3 and H1 is phosphorylated from prophase to anaphase [169]. Hyperphosphorylated histone H1 is present from late G2 phase until telophase; this may serve to decrease its affinity for DNA as phosphorylated H1 binds DNA less tightly than hypophosphorylated H1 [170]. Phosphorylation in the nucleosomal binding domain of the structural chromatin protein HMGN1 during mitosis leads to its dissociation from

chromosomes and prevents the re-entry of HMGN1 into the re-formed nucleus in telophase [166,167].

Phosphorylation of Histone H3 Induced by Stimulation of the MAPK Pathway

Extracellular signals such as growth factors, stresses and cytokines are relayed into the nuclear interior through the mitogen activated protein kinase (MAPK) pathways. Stimulation of MAPK pathways results in the activation of distinct sets of kinases, phosphorylation of transcription factors, modification of chromatin structure and the activation of a programmed transcriptional response. Those genes whose transcription is activated by the MAPK pathway within 15 minutes of stimulation and requires no new protein synthesis are referred to as immediate-early genes. These genes tend to be directly or indirectly involved in cell cycle progression. While genes such as *c-fos, Jun B,* and *MAP kinase phosphatase-1* become activated within 15 minutes of stimulation, other targets are transcribed later [171]. Serum-stimulation of quiescent human fibroblasts leads to the induction of genes whose products are involved in wound repair hours after serum addition [171].

Mammalian cells contain at least four arms of this pathway, the extracellular signal-regulated kinase/mitogen-activated protein kinase (ERK) pathway, the p38 pathway, the c-Jun amino-terminal kinase/stress-activated protein kinase (JNK/SAPK) pathway, and the recently identified ERK5 pathway. Each leads to specific changes in cellular processes such as transcription, metabolism, protein stability and enzyme activity and has its own set of MAPK kinase kinases (MAPKKKs), MAPK kinases (MAPKKs), and MAPKs. Many stimuli act through more than one arm of the MAPK pathway. For

example, growth factors such as epidermal growth factor primarily stimulate the Ras-MAPK pathway, but also weakly activate the p38 arm. As well, some proteins are linked to more than one arm of the pathway. As indicated by name, the mitogen and stress activated protein kinases (MSKs) become phosphorylated following mitogen or stress stimulation. They can be activated by kinases of the p38 MAPK or the Ras-ERK MAPK pathways, however in each case the cellular response is unique and tailored to respond to individual stimuli.

The p38 Pathway: The p38 MAPK pathway regulates immune and inflammatory responses [172]. It is activated by inflammatory cytokines and environmental stresses; most stimuli that activate this pathway also activate the JNK/SAPK pathway. Some mitogens, including epidermal growth factor, weakly stimulate the p38 pathway [172]. The series of kinases activated following p38 pathway stimulation include the MAPKKKs MEKKs 1 to 4 (mitogen-activated protein kinase/extracellular signal-regulated kinase kinase kinase 1-4), DLK (dual leucine zipper-bearing kinase), ASK1 (apoptosis signal-regulating kinase 1), Tpl2, Tak1 and MLK2 and 3 (mixed lineage kinase 2 and 3); the MAPKKs MEK3 and MEK6 (MAP kinase kinase 3 and 6) and the MAPKs p38 α, β, δ, and γ (refer to Figure 1-7). p38 activates MSK1 and MSK2, which selectively phosphorylate histone H3, and several other kinases such as Mnk1/2 and PRAK (p38 regulated/activated protein kinase) [173]. Several transcription factors including Elk, SAP-1/2 (SRF accessory protein 1/2), and ATF-2 (activating transcription factor 2) are regulated by the p38 pathway [173].

The JNK/SAPK Pathway: This pathway responds to cellular stresses such as inhibition of protein synthesis, heat shock, exposure to ultraviolet radiation, and inflammatory cytokines [174]. MAPKKKs of the JNK/SAPK pathway are MEKK1-4, Tpl-2, MLK2/3, DLK (dual leucine zipper bearing kinase), Tak1 and ASK1/2 (Apoptosis signal-regulating kinase 1/2); MAPKs MKK4 and 7, and MAPKs are JNK1,2 and 3, which are also known as SAPKγ, SAPKα and SAPKβ respectively [172]. Activated JNKs catalyze phosphorylation of transcription factors such as ATF-2, Elk1 and STAT-3 [173].

The Ras-ERK MAPK Pathway: The Ras-MAPK pathway is activated by growth factors and phorbol esters such as 12-0-tetradecanoylphorbol-13-acetate (TPA). To a lesser extent, it is stimulated by cytokines, osmotic stress, and ligands that bind heterotrimeric G-protein coupled receptors [172]. While growth factors act through receptor tyrosine kinases, TPA activates the Ras-MAPK pathway through protein kinase C (PKC) and/or RasGRP (guanyl nucleotide-releasing protein) [175-177]. Exposure to growth factors or phorbol esters activates Ras at the plasma membrane, which leads to the activation of a series of kinases and transcription factors and a specific program of gene expression that promotes cell division. Shown in Figure 1-7, the ERK pathway includes MAPKKKs A-Raf, B-Raf and Raf-1, MAPKKs MEK1 and MEK2, and MAPKs ERK1 and ERK2. In addition, MEKK1/2/3 and c-Mos kinases also act as MAPKKKs of the ERK pathway. ERK1 and ERK2 share a high degree of amino acid identity. Once activated ERKs regulate several kinases and transcription factors including Elk1, SAP-1/2, ATF2, ribosomal S6 kinase 2 (RSK2) [173] and MSKs [173,178,179]. In mouse fibroblasts

MSK1 and MSK2 phosphorylate histone H3 at serine 10 and at serine 28, HMGN1 at serines 6, 20, and 24 [180] as well as several non-chromatin targets.

Interphase H3 Kinases

Several kinases are implicated in H3 phosphorylation following mitogen and/or stress stimulation. Phosphorylation at serine 10 is associated with MSK1/2, PKC, PKA, p90 RSK2, IκB kinase α (IKKα), mixed-lineage triple kinase alpha (MLTK-α), p21-activated kinase-1 (PAK-1) and Fyn [181]. Current evidence indicates that MSK1/2, JNK1, and MLTKα are involved in mediating mitogen or stress-induced phosphorylation of H3 at serine 28 [181]. Kinase activity towards H3 at any particular loci is cell-type and stimulus-specific.

Protein Kinase C: The protein kinase C family is activated by many stimuli, including TPA, and participates in a variety of cellular responses. Stimulation of human hepatoma HepG2 cells with TPA induces H3 phosphorylation at serine 10 and transcription of the low-density lipoprotein (LDL) receptor gene. In this case TPA-induced phosphorylation of H3 at serine 10 is PKC-dependent and does not require the ERK MAPK, p38 MAPK, RSK, or MSK-1 cascades [189]. Active PKCβ and PKCε can phosphorylate H3 *in vitro*, however an *in vivo* association between PKC and H3 could not be detected, suggesting that the effects of PKC on H3 phosphorylation are mediated through another kinase [181,189].

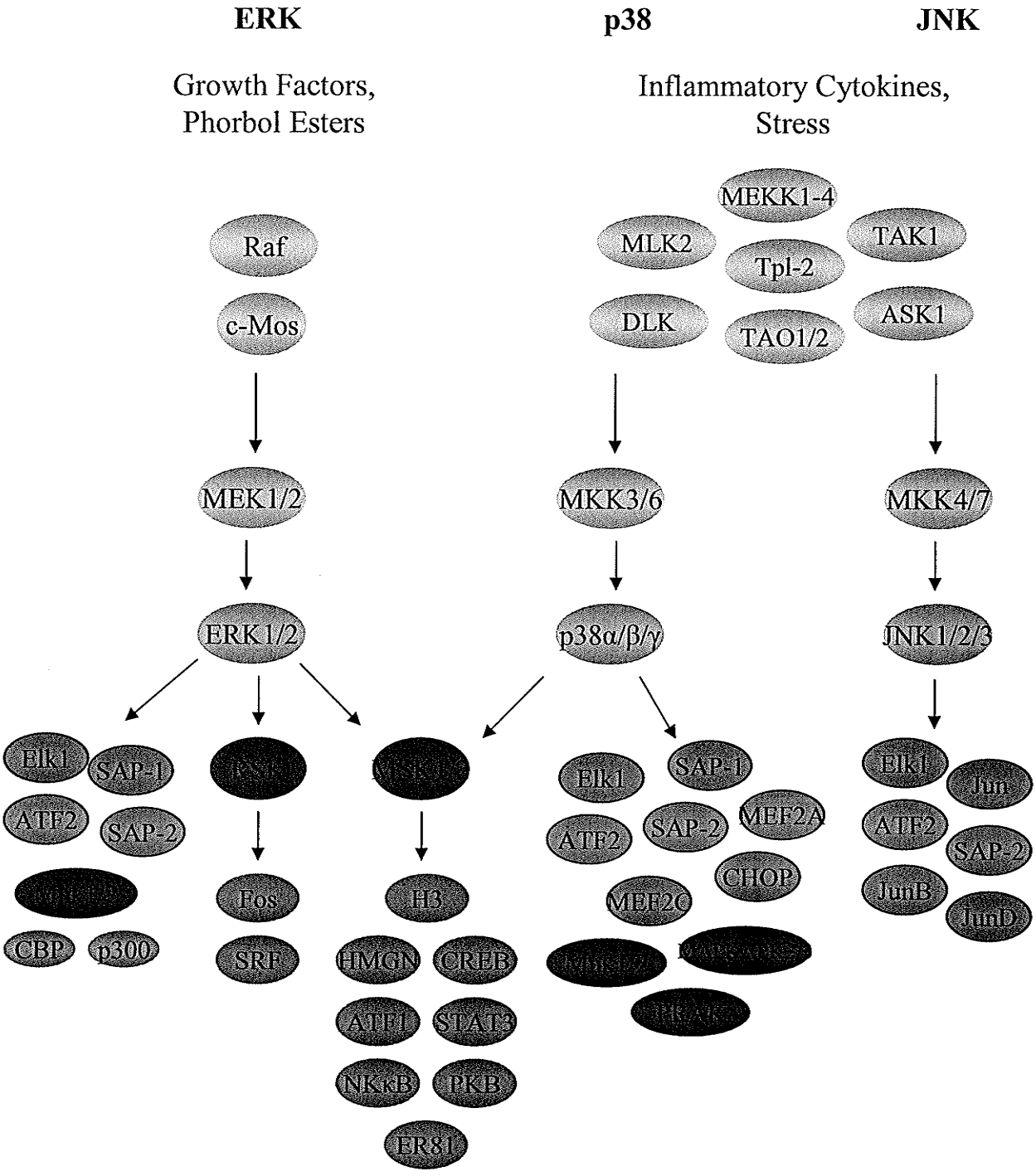

Figure 1-7. The mammalian MAPK pathway. Three arms of the mammalian MAPK pathway, the ERK, JNK, and p38 pathways are shown. The MAP kinases (ERK, p38, JNK) each phosphorylate several substrates. MSKs are activated by the ERK pathway and the p38 stress kinase pathway. Downstream kinases are shown in red. Targets for MSK1/2 mediated phosphorylation are shown in purple.

MLTKα: This stress-activated MAP kinase kinase kinase has been implicated as the mediator of EGF- and UVB-induced H3 phosphorylation at serine 28 in JB6 C141 epidermal keratinocyte cells [182,183]. EGF and UVB both activate the ERK and p38 MAPK pathways to differing extents. Upon EGF- or UVB-treatment MLTKα accumulates in the nucleus. *In vitro* assays indicate that MLTKα is capable of phosphorylating H3 at serine 28, but not at serine 10. EGF- and UVB-induced H3 phosphorylation at serine 28 in JB6 C141 cells was not prevented by treatment with pharmacological agents to inhibit MEK and p38 kinase, but was blocked by small interfering RNA (siRNA) to MLTKα [183]. While overexpression of MLTKα in JB6 cells enhances EGF- and UVB-induced phosphorylation of MSK1, siRNA to MLTKα lowered the level of EGF- and UVB-induced MSK1 phosphorylation. Thus MLTKα appears to be an H3 kinase that acts upstream of ERK1/2 and p38 kinase that can also phosphorylate H3 independently of the ERK and p38 MAPK pathways [183].

IKKα: NF-κB accumulates in the nucleus of cells treated with inflammatory cytokines such as tumour necrosis factor (TNF). This is preceded by activation of the IκB kinase (IKK) complex, consisting of IKKα and IKKβ, which phosphorylates IκB proteins and prompts their degradation, freeing NF-κB to relocate to the nucleus. IKKα, which is able to phosphorylate H3 *in vitro*, also accumulates in the nucleus following cytokine treatment, where it associates with NF-κB-responsive genes after TNF-α stimulation [184-186]. Cytokine-induced expression of NF-κB-responsive genes is severely impaired in MEFs lacking IKKα (IKKα -/-). Further, cytokine-induced H3

phosphorylation (serine 10) is diminished at NF-κB–responsive genes in IKKα -/- MEFs, demonstrating that this enzyme may be responsible for cytokine-induced H3 phosphorylation at NF-κB–responsive genes [184,185].

IKKα has also been implicated in EGF-induced H3 phosphorylation in mouse embryonic fibroblasts. EGF did not activate the classical NFκB pathway, but resulted in recruitment of IKKα to the *c-fos* gene promoter [184]. IKKα -/- MEFs exhibit significantly reduced c-fos gene expression following EGF-stimulation. In addition, EGF-induced H3 phosphorylation at serine 10 could not be detected at the c-fos gene in IKKα -/- cells, implying that IKKα-mediated H3 phosphorylation is a crucial factor in the expression of this immediate-early gene [184].

Fyn: Fyn kinase is part of the Src family of non-receptor protein–tyrosine kinases. It is activated after UVB exposure and is involved in UVB-induced H3 phosphorylation at serine 10. Several Src family members are known to interact with components of the MAPK pathway. Expression of a dominant negative Fyn in JB6 cells prevented UVB-induced H3 phosphorylation at serine 10 and decreased UVB-induced activation of ERK and Akt (protein kinase B), suggesting that Fyn plays a role in H3 phosphorylation by regulating Akt and ERKs [187]. Fyn relocates to the nucleus of HaCaT cells once activated following UVB exposure. Furthermore, in an *in vitro* kinase assay activated Fyn was able to phosphorylate H3 at serine 10, suggesting that this kinase not only acts to

regulate H3 phosphorylation through ERKs and Akt but also phosphorylates H3 directly *in vivo* [187].

Akt: Akt has *in vitro* H3 kinase activity and is implicated as an H3 kinase (serine 10) following UVB and arsenite exposure [181]. Treatment of cells with the tumour promoter arsenite induces H3 phosphorylation and increases activity of Akt [188]. Arsenite-induced H3 phosphorylation at serine 10 does not occur in RSK2 deficient cells, and in JB6 C141 cells arsenite-induced phosphorylation of H3 at serine 10 was preventable by expression of dominant negative Akt. In addition, most arsenite-induced H3 phosphorylation could be blocked by expressing dominant negative ERK2 or treating cells with the MEK inhibitor PD 98059, but expression of C- or N-terminal mutant MSK1 had little effect [188]. Thus Akt, along with ERK2 and RSK2, is likely a mediator of arsenite-induced H3 phosphorylation at serine 10 [188].

Protein Kinase A: Stimulation of rodent granulosa cells with follicle stimulating hormone (FSH) induces H3 phosphorylation at serine 10 and activation of PKA, ERKs, and RSK2 [190,191]. PKA activity is required for this H3 phosphorylation; pharmacological inhibitors of PKA decreased H3 phosphorylation at serine 10 induced by FSH. In a separate study, it was found that the catalytic subunit of PKA phosphorylates H3 *in vitro [192]*, indicating that FSH-induced phosphorylation of H3 in granulosa cells may be mediated by PKA in a mechanism that does not involve ERKs or RSK2 [191].

Tissue Transglutaminase 2: Most recently, tissue transglutaminase was identified as a kinase capable of phosphorylating H3 *in vitro* [193]. This ubiquitously expressed trans-amidating acyltransferase has intrinsic kinase activity [194], interacts with histones, and is proposed to phosphorylate H3 at serines 10 and 28 *in vivo* [193]. Association of tissue transglutaminase 2 with chromatin in MCF7 breast cancer cells increased in response to TPA-stimulation, but not estradiol-treatment [193].

MSKs and RSK2: Ribosomal S6 kinase 2 (RSK2), part of the $p90^{RSK}$ family of serine/threonine kinases, is activated by ERKs. MSK1 and MSK2 are activated by ERKs as well as p38 kinase. Both MSK1and RSK2 can phosphorylate nucleosomal histone H3 [195], however although MSKs and RSK2 are both activated by ERKs, these kinases respond differently to cellular stimuli. For example, following exposure of JB6 C141 cells to arsenite, H3 is phosphorylated at serine 10 in a mechanism that includes RSK2 but not MSK1 [188].

Patients with Coffin Lowery Syndrome (CSL) have missense, nonsense and deletion mutations to the *rsk2* gene [196]. RSK2 phosphorylates histone H3 *in vitro* [195]. In 1999, it was reported that cells taken from CSL patients did not exhibit mitogen (EGF)-induced H3 phosphorylation, and that disrupting the *rsk2* gene stops H3 phosphorylation induced by EGF in mouse stem cells [197]. Mouse embryonic fibroblasts devoid of MSK1 and or MSK2 (MSK1-/-, MSK2-/-, or MSK1/2-/-) display a dramatic reduction in TPA- (Ras-MAPK) and anisomycin- (p38-MAPK) induced H3 phosphorylation at serines 10 and 28 [180]. Phosphorylation of HMGN1 at serine 6 and histone H3 at serines 10 and 28 is abolished in these cells. Interestingly, knocking out either MSK1 or

MSK2 affected the phosphorylation of both H3 residues, with the MSK2 knockout cells displaying a more severe effect [180]. The activity of RSK2 is normal in these cells [179], thus this study is in direct contrast with that finding RSK2 to be the mitogen-induced H3 kinase. The results identifying RSK2 as the H3 kinase have also been contradicted by a subsequent study of RSK2-deficient CLS cells that found no lack of mitogen-induced H3 phosphorylation [180]. It is possible that this discrepancy is due to the differing stimuli; later studies employed TPA and anisomycin, while those experiments implicating RSK2 were performed with EGF. It may also be that different cells types employ signalling pathways differently.

Studies of TPA- and EGF-treated mouse 10T1/2 fibroblasts indicate that MSKs are responsible for induced H3 phosphorylation in these cells and in *ras*-transformed Ciras-3 mouse fibroblasts [198]. Inclusion of RO 318220, an inhibitor of both MSKs and RSK2, at a concentration of 5 nM did not prevent TPA- or EGF-induced H3 phosphorylation in these cells. This result by itself would indicate that neither MSKs nor RSK2 act as the H3 kinase, but mitogen-induced H3 phosphorylation was prevented by the MSK inhibitor H89. An *in vitro* kinase assay of RSK2 with core histones was included in this study and produced little, if any, phosphorylated H3 [198]. Furthermore, the median inhibitory concentration of RO 318220 is 3 nM for RSK2 and 8 nM for MSK1, thus the above result in consistent with MSK acting as the mitogen-induced H3 kinase [199].

There is also strong evidence indicating MSK1 as the H3 kinase phosphorylating H3 at serine 28 in response to UVB exposure. UVB stimulation results in activation of ERKs, MSKs, RSK2, p38 and JNKs and results in phosphorylation of H3 at serines 10 and 28 [200]. The MSK inhibitor H89 prevents UVB-induced H3 phosphorylation at serine 28

in JB6 C141 cells but does not stop activation of ERKs, RSK2, p38 or JNKs. Further, expression of N- or C-terminal MSK1 mutants also inhibits UVB-induced H3 phosphorylation at serine 28 [200].

The MAPK Pathway is Linked to Chromatin Structure and Transcription of Immediate-Early Genes

Levels of H3 phosphorylated at serines 10 and 28 increase dramatically upon stimulation of the Ras- or p38-MAPK pathway [180,200-203]. Likewise, HMGN1 becomes phosphorylated at serines 6, 20 and 24 [195,204]. Once activated, chromatin associated with specific genes is selectively modified. The mechanism by which this occurs is unclear. Phosphorylation of H3 at serine 10 following stimulation of the Ras-MAPK or p38-MAPK pathway is targeted to immediate early genes. As demonstrated by chromatin immunoprecipitation assays, regions within the promoter and coding regions of c-myc, c-fos, c-jun and the heat shock genes become phosphorylated on H3 at serine 10 following stimulation of the MAPK pathway in mouse fibroblasts [205-209]. Stimulation of the Ras-MAPK pathway in serum-starved mouse fibroblasts results in the appearance of numerous small foci of H3 phosphorylated at serine 10 [209]. These foci are excluded from regions of condensed chromatin and may mark sites for transcriptional activity [210]. Phosphorylation of H3 at immediate early genes is a crucial step in their activation. Impeding mitogen-induced phosphorylation of H3 in mouse fibroblasts with MSK inhibitors impairs the expression of immediate-early genes [198]. Furthermore, MSK-/- MEFs, in which mitogen-induced H3 phosphorylation is all but abolished,

display dramatically reduced levels of immediate-early gene expression following appropriate stimulation [180].

Levels of histone acetylation also increase at immediate-early genes following stimulation of the MAPK pathway. Histone modifications in combination with chromatin remodeling complexes likely facilitate their expression (Figure 1-8 and 1-9). Chromatin immunoprecipitation studies have detected increases in the steady-state level of acetylation of histone H3 in the transcribed regions of c-jun and c-fos following stimulation of the MAPK pathway [205,208]. Early studies of this relationship suggested that acetylated H3 became phosphorylated but also indicated that acetylation did not predispose H3 to further modification by phosphorylation [211]. Later analysis with antibodies recognizing di-modified H3 suggested the two modification were coupled; H3 phosphoacetylated at serine 10 lysine 9 and serine 10 lysine 14 was present at immediate early genes post-stimulation of the MAPK pathway [205,208]. However, an increase in H3 acetylation at immediate-early genes after mitogen stimulation is also detectable in MSK1/2 knockout cells [180], indicating that phosphorylation and acetylation occur independently. Furthermore, treating cells with inhibitors that prevent H3 phosphorylation does not prevent the increase in the steady-state level of acetylation at immediate-early genes [205].

Modifications to chromatin following stimulation of the MAPK pathway are gene specific. Although both acetylation and phosphorylation of histone H3 has been detected at several immediate-early genes, this combination is not present at the heat shock Hsp70 gene. Following appropriate stimulation, chromatin associated with the Hsp70 gene

becomes phosphorylated on histone H3 at serine 10, however there is no increase in the steady-state level of acetylation [206].

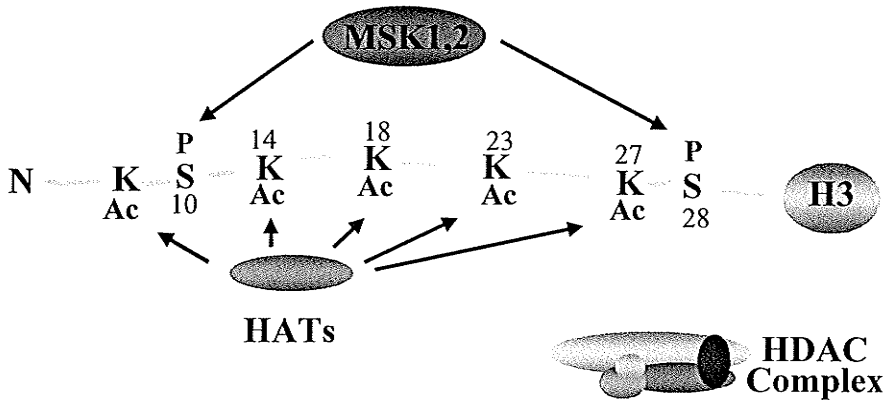

Figure 1-8. Phosphoacetylation of histone H3. Mitogen-induced phosphorylation of histone H3 is mediated by MSK1/2 on serine 10 and serine 28. Dynamic acetylation of the amino-terminal tail of H3 mediated by HATs takes place on lysines 9, 14, 18, 23, and 27. Acetylation is removed by the action of HDAC-containing complexes.

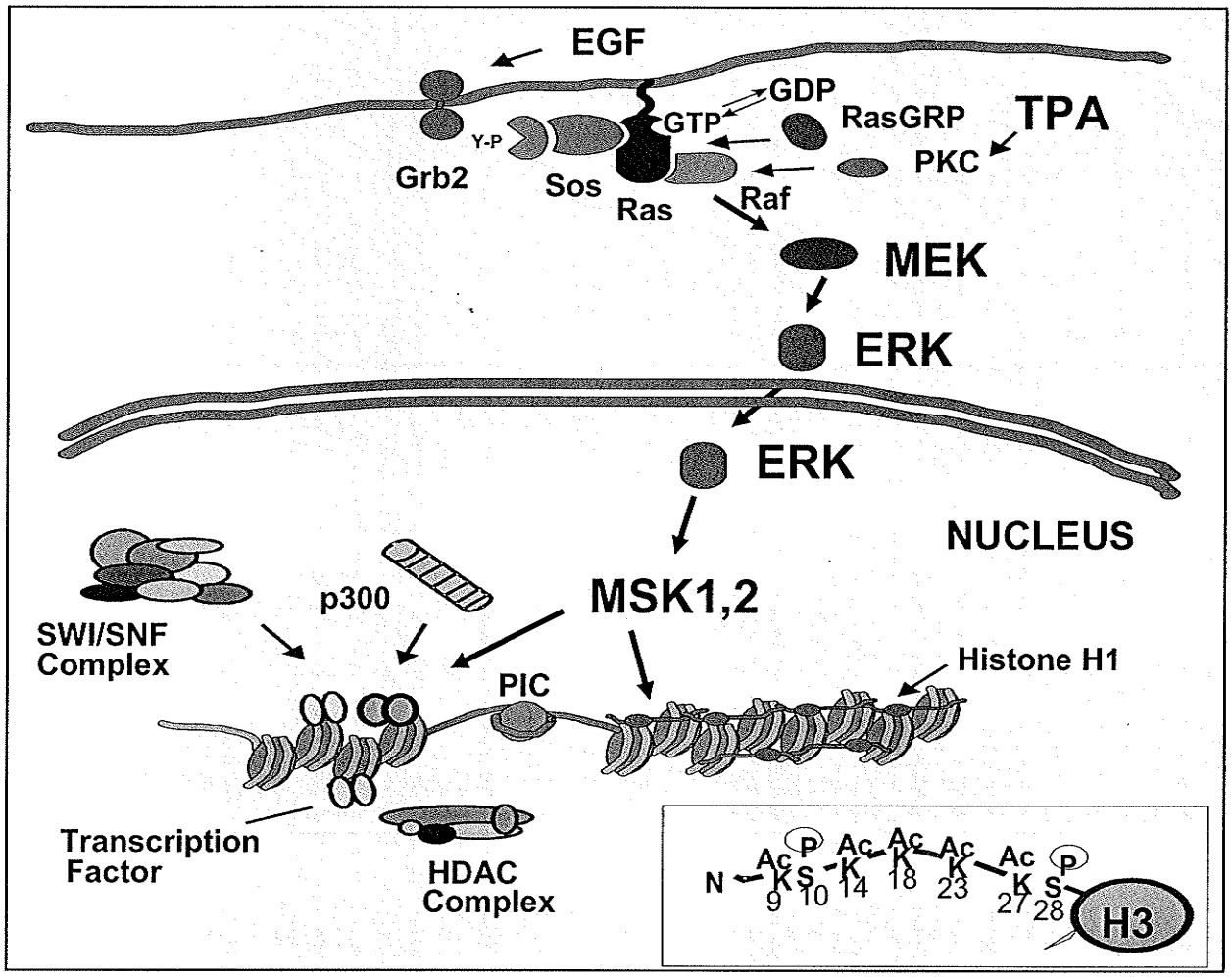

Figure 1-9. The Ras-mitogen activated protein kinase pathway. The Ras-MAPK pathway can be activated by EGF or TPA. Stimulation activates a series of kinases including the chromatin modifying enzymes MSK1 and MSK2. MSK1/2 phosphorylate histone H3 at serines 10 and 28. Phosphorylation of serine 10 occurs on chromatin associated with immediate-early genes. This chromatin is undergoing dynamic acetylation by HATs and HDACs. The SWI/SNF chromatin remodelling complex works in conjunction with histone modifications to facilitate transcription.

MSK1 and MSK2

MSKs are well conserved, primarily nuclear proteins. Human MSK1 and MSK2 are 802 and 705 amino acids, respectively. Mouse MSK1 and MSK2 are 863 and 773 amino acids long, respectively. Human and mouse MSK2 are 90% identical in amino acid sequence. Furthermore, human MSK1 and MSK2 are 75% identical.

The MSKs are widely expressed proteins present in the liver, kidney, heart, brain, pancreas, lung and placenta [212]. MSK1 and MSK2 are part of the AGC (protein kinase A, protein kinase G, and protein kinase C) kinase family along with the p70 and p90 ribosomal S6 kinases, protein kinase B, protein kinase C-related protein and serum and glucocorticoid-inducible kinase. Two kinase domains are found within one polypeptide in members of this family (Figure 1-10). A C-terminal kinase domain functions to initiate the activation of the N-terminal kinase domain [213,214].

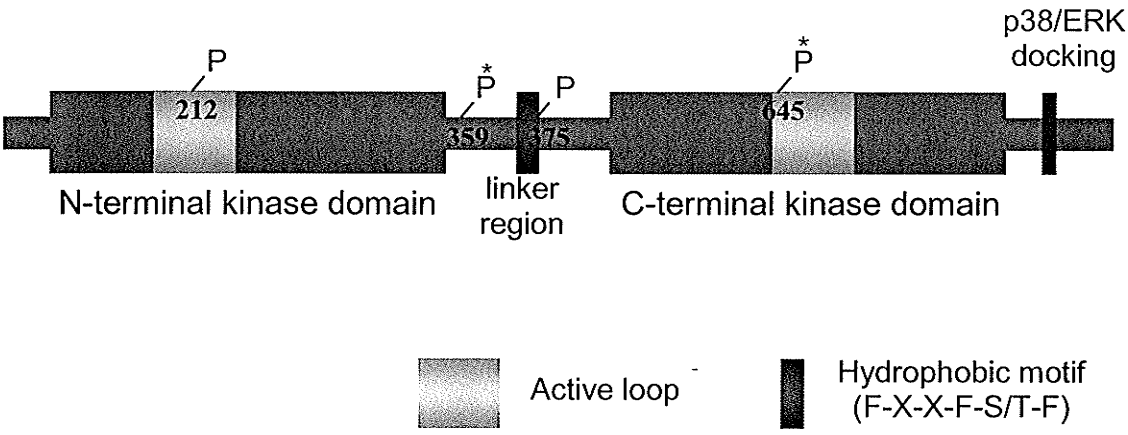

Figure 1-10. Schematic diagram of murine MSK1. MSK1 contains two kinase domains, each with an active loop, and a linker region containing a hydrophobic motif. Phosphorylation sites shown are at Thr 645, Ser 375, Ser 359 and Ser 212. Active ERK or p38 phosphorylates MSK1 at Thr 654 and Ser 359.

Active p38 or ERK phosphorylates MSK1 at Thr 645 in the activation loop of the C-terminal kinase domain and at serine 359 in the linker region. Autophosphorylation, mediated by the C-terminal kinase domain, then takes place at serine 375 in the hydrophobic motif. This promotes phosphorylation of a serine in the N-terminal kinase domain, leading to full activation of MSK1 [179]. Although the exact steps leading to the activation of MSK2 are not clear, one would predict that it is a sequence of events very similar to what occurs for MSK1. Several other phosphorylation sites have been identified on MSK1 and appear to contribute to its activity [215]. This study, done on human embryonic kidney 293 cells, found that MSK1 autophosphorylates serine residues 212, 376, 381, 750, 752 and 758. Phosphorylation of serine 212 in the N-terminal portion, mediated by the C-terminal kinase domain, is essential for catalytic activity of the N-terminal kinase domain of MSK1 [215]. As well, mutation of serine 381 decreases MSK1 activity, indicating that it too is an important MSK1 regulator [215].

MSK Substrates: In addition to histone H3 and HMGN1, transcription factors are also MSK substrates. This modification may alter the ability of these factors to interact with other proteins and DNA. Mitogen or stress induction leads to the MSK-mediated phosphorylation of cyclic AMP-responsive element binding protein (CREB) at serine 133 and activating transcription factor 1 (ATF1) at serine 63. Stress-induced phosphorylation of CREB and ATF1 is abolished in MSK knockouts [180]. Although mitogen-induced phosphorylation of these factors is also reduced in the knockout cells, a significant amount of CREB and ATF1 phosphorylation at serine 133 and serine 63 respectively

takes place following exposure to mitogens. This phosphorylation can be prevented by the MEK inhibitor PD-184352, which suggests that another ERK-activated kinase is involved [179,216].

MSK1 has also been shown to be involved in the phosphorylation of Akt (PKB), signal transducer and activator of transcription (STAT3), Bad, ets-related protein (ER81) and the p65 subunit of nuclear factor kappa B (NFκB). TNF activation results in MSK-mediated phosphorylation of serine 276 in the p65 subunit of NFκB [217]. MSK1 also phosphorylates the tumorigenesis-associated transcription factor ER81 at serines 191 and 216 [217]. UV-irradiation induces MSK1 activation and phosphorylation of Akt at threonine 308 and serine 473, STAT3 at serine 727 and Bad at serine 112 [218-220]. MSK1 is also involved in erythropoietin-induced phosphorylation of STAT3 through the Ras-MAPK pathway [221]. Cells containing N- or C-terminal kinase dead mutants of MSK1 exhibit reduced levels of stress-induced Akt, STAT3 and Bad phosphorylation. In addition, the kinase inhibitor H89, used under conditions to specifically inhibit MSK activity, prevents STAT3 phosphorylation [220].

In the cytoplasm, MSK1 phosphorylates serine 64 of eIF-4E-binding protein 1 (4E-BP1) in response to stimulants that activate the p38 MAPK pathway [222]. 4E-BP1 impedes the initiation of translation by binding to eIF-4E on the mRNA cap. Phosphorylation by MSK causes 4E-BP1 to release eIF-4F, releasing the block in translation. It has also been suggested that interplay between 4E-BP1 and MSKs contributes to UV-induced tumorigenesis [222].

The Nucleosomal Response

The term nucleosomal response refers to the rapid phosphorylation of histone H3 at serine 10 and of HMGN1 at serine 6 following stimulation of the MAPK pathway [223]. This process is thought to lead to the activation of immediate early gene transcription. As an architectural chromatin protein, HMGN1 binds nucleosomes to decrease the compaction of chromatin and influences transcription by several means. It is thought to regulate transcription factor binding to specific DNA sequences by altering accessibility, and regulates the post-translational modification of histone H3.

Phosphorylation of HMGN1 weakens its interaction with the nucleosome. This makes the tails of histone H3 more accessible for phosphorylation [195]. In accordance with this, phosphorylation of histone H3 at serine 10 is more rapid in HMGN1 -/- cells, and the presence of HMGN1 decreases MSK-mediated phosphorylation of H3 in nucleosome core particles at serines 10 and 28 [195,224]. These findings have led to a model of the nucleosomal response wherein mitogen-induced phosphorylation of HMGN1 causes its dissociation from chromatin, facilitating H3 phosphorylation by giving kinases better access to the amino-terminal tails of H3. In addition, acetylation of histone H3 at lysine 14, a modification known to be present in chromatin associated with immediate-early genes during mitogen and stress-induced transcription, is increased in HMGN1+/+ cells as compared to HMGN1 knockout cells [225]. HMGN1 and HMGN2 regulate H3 modifications differently. HMGN2 enhances acetylation of H3 at lysine 14 more robustly than HMGN1, and unlike HMGN1, HMGN2 does not impede MSK-mediated H3 phosphorylation [224].

Modification of proteins within or closely associated with nucleosomes may impact the stability of nucleosomal contacts and function. Nucleosome stability, placement and function is the basis for the "regulated nucleosome mobility model" of transcription [226]. In this model the stability of nucleosome placement is altered by histone modifications, particularly in those regions making contacts with DNA. The histone fold is the most important of those regions, providing the contact interphase with DNA within the nucleosome.

H3 Phosphatases

The steady state level of H3 phosphorylation at any genomic loci is governed by the balance of H3 kinases and H3 phosphatases. Two protein phosphatases, namely protein phosphatase 1 (PP1) and protein phosphatase 2A (PP2A) are implicated in the removal of phosphate groups from histone H3. PP1 and PP2A can be distinguished by their sensitivities to okadaic acid; 10 – 15 nM okadaic acid produces 50% inhibition of PP1, while PP2A is completely inhibited by 1 nM. PP1 was identified as the major H3 phosphatase in mouse 10T1/2 fibroblasts by using cellular extracts to dephosphorylate histones *in vitro* with various concentrations of okadaic acid. Dephosphorylation was not observed with a high concentration of okadaic acid (100 nM), while 2 nM okadaic acid only partially inhibited dephosphorylation [209].

More recent experiments link PP2A to the dephosphorylation of H3. For example, treatments of human hepatoma (HepG2) cells leading to increases in the concentration of intracellular calcium led to dephosphorylation of histone H3; this dephosphorylation could be prevented by inhibiting PP2A [227]. PP2A has also been associated with

widespread dephosphorylation of H3 during heat shock in drosophila [228]. Heat shock dramatically shifts the transcriptional program, and in drosophila this shift correlates with a shift in the location of phosphorylated H3. Heat shock induces a small percentage of genes in drosophila; these genes undergo increased H3 phosphorylation, while widespread dephosphorylation takes place at those genes that are no longer transcriptionally active. Inhibition of PP2A prevents the widespread dephosphorylation of formerly active genes, and PP2A mutants also display reduced heat-shock related dephosphorylation [228].

The Histone Code

It has been proposed that the numerous and highly variable patterns of histone modifications present at various nuclear loci form a system, a 'histone code', that is interpreted by the cell to specify future events [229]. Modifications may create or remove binding sites, for example bromodomains interact with acetylated histones while chromodomains interact with H3 methylated at lysine 9 [230]. Domains such as these may serve to target chromatin remodellers, histone modifying enzymes, and transcription factors to particular sites. For example, the heterochromatin component HP1, which aids in the spread of condensed chromatin structure, contains a chromodomain. Further, the ATPase subunit of chromatin remodeller SWI/SNF contains a bromodomain, and various chromodomains are found within other subunits of this complex [231,232]. Modification of a residue may also act simply to prevent future modification of that residue. For example, methylation of histone H3 at lysine 9 is thought to contribute to transcriptional repression by preventing the acetylation of that same residue [230].

H3 Phosphorylation in Contrasting Roles: Transcription and Chromosome Condensation

The association of H3 phosphorylation at serines 10 and 28 with condensed chromosomes during mitosis is an apparent contradiction to its proposed role following MAPK pathway stimulation. If the phosphorylation of H3 following MAPK pathway activation results in a chromatin structure that is less condensed and more compatible with transcription, how can it also be an important event correlating with mitotic chromosome condensation? There are two possible answers. First, the combination of modifications present on H3 during mitosis differ from those present following MAPK pathway activation [229]. For example, phosphorylation of H3 at serine 10 in combination with threonine 11, which is also phosphorylated during mitosis, could bind proteins unlike those that bind if phosphorylation is not present at threonine 11. In the second possibility, there is no apparent contradiction in the immediate function of H3 phosphorylation. In this scenario, mitotic H3 phosphorylation also results in a more open chromatin conformation, which in turn allows the factors associated with mitosis and condensed chromosomes to bind [229].

VII. *The MAPK Pathway is Involved in Cancer*

A mutation to one of the *ras* oncogenes causing the resultant protein to be constitutively active is found in approximately 30% of all human cancers [233]. Defects to all three Ras molecules have been detected, with Kirsten *ras* being mutated the most frequently [233-235]. Abnormalities are also present in other members of the MAPK pathway. Members of the epidermal growth factor family are upregulated in several cancers [236]. EGF is a tumour promoter; EGF-treatment of JB6 C141 epidermal cells can induce

transformation. Mutatating serine 10 of H3 to alanine suppresses EGF-induced neoplastic transformation, suggesting that the phosphorylation of H3 at serine 10 plays a crucial role in EGF-induced neoplastic transformation [237]. EGF can also induce HaCaT cell transformation to anchorage independent growth. This transformation was reduced by inhibitors of MEK and JNK, but increased upon inhibition of p38, implying that ERKs, JNKs and p38 have varying roles in EGF-induced transformation [238]. High levels of activated ERKs have been detected in tumor cell lines [239]. The BRAF gene, coding for a MAP kinase kinase kinase, is frequently mutated in cutaneous melanoma [240]. Constitutive activation of the MEK/ERK pathway is observed in cell lines containing a V599E mutation in BRAF irrespective of *ras*. The rate of proliferation of these cells, as well as their ability to grow in an anchorage-independent manner, decreases with reduced B-RAF activity [240]. Furthermore, in a study of low grade dysplastic adenomas of the colon, the rho GDP dissociation factor, which is involved in Ras activity, was upregulated along with proliferation-associated genes such as p21 and p38α [241]. Judged according to the "adenoma-carcinoma sequence" of carcinogenesis [242], deregulation of the MAPK pathway occurs near the beginning of colonic carcinogenesis [241].

The Ras Oncogene

Ras is part of a protein superfamily that takes part in a variety of cellular processes. Proteins in this family bind GTP and are characterized by low molecular weight. Functions include the generation of oxidases (Rac, Rap), roles in the cytoskeleton (Rho, Rac), intracellular vesicular trafficking (Rab, Arf) and proliferation (Ras, Rap).

Ras is a 21 kDa protein that associates with the plasma membrane through a 15-carbon isoprenyl group. This post-translational modification of Ras, mediated by farnesyltransferase, is required to maintain the transformational capabilities of oncogenic Ras [243-246]. The farnesyltransferase responsible for modifying Ras has thus been a target for cancer therapies. Unfortunately, to date the expected potential of these drugs appears to have been overestimated.

The Ras protein exists in inactive and active states. While inactive, Ras is bound to guanine nucleotide di-phosphate (GDP). Activation occurs as GDP is exchanged for guanine nucleotide tri-phosphate (GTP). This process is promoted by guanine nucleotide releasing factors (GRFs) that associate with Ras. Son of sevenless (Sos) also acts to promote formation of the active complex by inducing loading of GTP. Intrinsic Ras GTPase activity hydrolyzes GTP to GDP, resulting in the formation of an inactive complex. This activity is enhanced by GTPase activating proteins (GAPs).

Three *ras* oncogenes, Harvey-*ras* (*Ha-ras*), Neuroblastoma-*ras* (*N-ras*), and Kirsten-*ras* (*K-ras*) have been identified in human malignancies. These genes code for proteins that are constitutively active and may result in constitutive activation of the Ras-MAPK pathway. Missense mutations in codons 12, 13, 59 and 61 result in a constitutively active protein by abrogating the intrinsic GTPase activity of Ras. Residues 12 and 13, both glycines in the wild type protein, are most frequently mutated in human malignancies [247]. Each ras gene has been connected to specific forms of cancer [247]. K-ras is often affected in lung, colorectal, and pancreatic cancers while N-ras is commonly mutated in hepatocellular carcinoma, melanoma and hematological cancers. Point mutations resulting in constitutively active Ha-ras are associated with malignant tumours of the

bladder, thyroid, and kidneys [247]. The Canadian Cancer Society estimates that 2006 will see approximately 14 400 Canadians diagnosed with malignancies of the thyroid, bladder or kidney and 3400 Canadians die of one of these types of cancer.

Structural Changes in the Nucleus of Ras-Transformed Cells

Abnormal nuclear morphology can be used to diagnose cancer [248]. Studies have found that cellular transformation mediated by oncogenes leads to structural changes in the nucleus. *v-fes, v-mos, v-src, v-raf* and *H-ras* transformed cells contain nuclei that are misshapen, having a more spherical, rigid shape [249]. Further, the extent of changes to nuclear morphology correlates with the metastatic potential of transformed cells [249]. Components of the nuclear matrix are also altered in oncogene-transformed cells [250]. A study of *ras*- and kinase-transformed cells found similar nuclear matrix profiles for highly metastatic lines, suggesting that nuclear matrix proteins change with each stage of malignancy [7,250].

The mechanism of Ras-induced malignant progression in not fully understood. Resistance to this phenomenon has been described in several cell lines [251-256]. This may be due in part to variations in gene expression, as a single study comparing a resistant line with a susceptible line found significant differences in the expression of several genes including major excreted protein, *jun* and tissue inhibitor metalloproteinases [257].

Chromatin structure is also altered in oncogene-transformed cells. Oncogene-transformed cells display an increase in the nucleosome repeat length and altered levels

of histone variant $H1^0$ [258]. Micrococcal nuclease (MNase), which preferentially digests DNA outside of nucleosomes, can be used as a probe to measure chromatin compaction. Studies of bulk chromatin digested with this enzyme established that chromatin in *ras*-transformed cells is more susceptible to digestion than that in parental cells, indicating that the conformation of chromatin in *ras*-transformed cells is somewhat relaxed [258]. Furthermore, the DNA at the immediate-early genes ornithine decarboxylase and c-myc were also more susceptible to nuclease activity [258]. A later study determined that levels of DNA methylation were similar in parental and *ras*-transformed cells, excluding hypomethylation of DNA as the cause of this relaxation [259].

Other abnormalities of chromatin structure in *ras*-transformed cells include modifications to histones. Increased levels of phosphorylated H1 and H3 phosphorylated at serine 10 have been detected in mouse fibroblasts transformed with constitutively active components of the MAPK pathway, including MEK and Ras [260,261]. Levels of activated ERKs and H3 kinase activity are elevated in *ras*-transformed cells, indicating that these defects may be a direct result of a constitutively active Ras-MAPK pathway [262]. In addition, amounts of phosphorylated $H1^S$-3, a variant of H1, are elevated in cells transformed with oncogenes such as *ras*, *raf*, *fes*, *mos* and *myc* [260]. Similarly greater amounts of $H1^S$-3 phosphorylation are seen in MEK-transformed cells containing elevated levels of activated ERK1 and ERK2 [260]. This modification is unique; it requires ongoing transcription or DNA replication [263]. The accessibility of $H1^S$-3 to cyclin E-Cdk2 may be limited in the absence of these processes, resulting in lower levels of phosphorylation [263].

Human fibroblasts lacking the tumour suppressor *Rb* also display a "relaxed" chromatin structure and greater quantities of phosphorylated H1 [264]. Cyclin E-Cdk2 kinase activity is directly involved in elevating levels of phosphorylated H1 in these cells. High cyclin E-Cdk2 activity due to persistent activation of the Ras-MAPK pathway is also responsible for increased quantities of phosphorylated H1 in oncogene-transformed fibroblasts [265]. Detection of similar aberrations to chromatin structure in oncogene-transformed and tumour suppressor-deficient cells suggests that these proteins act to regulate transformation through a common mechanism [264].

Modification of H1 by phosphorylation results in a weaker interaction with chromatin and increased mobility of the histone [33,266]. Dephosphorylated, but not phosphorylated H1 inhibits chromatin remodeling by the SWI/SNF complex [267], suggesting that the lessened affinity phosphorylated H1 has for chromatin may also make chromatin more easily remodeled. These studies strongly suggest that phosphorylation of histone H1 destabilizes chromatin structure [268-270].

Immediate-early genes are known to be the targets for histone H3 phosphorylation at serine 10 following stimulation of the MAPK pathway [205,207,208]. Knockouts of the H3 kinases MSK1 and MSK2 are deficient in mitogen-induced H3 phosphorylation and immediate-early gene transcription [180]. This direct link between gene transcription, chromatin structure and the MAPK pathway suggests that deregulation of the Ras-MAPK pathway leads to abnormal chromatin structure and aberrant gene expression in transformed cells [271].

Rational and Hypothesis

Stimulation of the Ras-mitogen activated protein kinase pathway activates a series of kinases, leading to a programmed transcriptional response. At the end of this pathway, histone H3 is rapidly and transiently phosphorylated at serines 10 and 28 in a pattern that parallels that of immediate-early gene expression. Immediate-early genes are the known targets for phosphorylation at serine 10. Knocking out the MAPK pathway induced H3 kinases, MSK1 and MKS2, in mouse fibroblasts causes a dramatic reduction in mitogen-induced H3 phosphorylation and severely impairs mitogen-induced expression of immediate-early genes. Serine 10 and serine 28 of H3 are phosphorylated by the same enzymes, MSK1 and MKS2, in response to stimuli such as growth factors and phorbol esters. Further, the temporal induction pattern of phosphorylation at these two residues is very similar, thus it appears that phosphorylation at serine 28 works in conjunction with phosphorylation at serine 10 to promote the mitogen-induced expression of immediate-early genes.

Approximately 30% of all human cancers contain an activating mutation to one of the *ras* oncogenes. *Ras*-transformation is also associated with abnormal nuclear morphology, altered nuclear matrix profiles, aberrant gene expression, and a relatively relaxed chromatin structure. Cells containing a constitutively active Ras have also been found to have increased levels of phosphorylated histone H1 and histone H3 phosphorylated at serine 10. The direct link between gene transcription, chromatin structure and the MAPK pathway suggests that deregulation of the Ras-MAPK pathway leads to the abnormal chromatin structure and aberrant gene expression in transformed cells [271].

We hypothesized that:

Phosphorylation of histone H3 at serine 28 following stimulation of the Ras-MAPK pathway contributes to immediate early gene activation by occurring concomitantly with phosphorylation at serine 10. Aspects of this phosphorylation are altered in *ras*-transformed cells and contribute to their abnormal chromatin structure and aberrant gene expression.

The objectives of this study were to:

1. Characterize H3 phosphorylation at serine 28 with respect to that at serine 10.
2. Determine if mitogen stimulation induces the phosphorylation of serine 10 and serine 28 on the same molecules of H3, and if these two modifications work in conjunction with each other.
3. Contribute to our understanding of the mechanism by which the transcription of immediate-early genes is activated following mitogen stimulation.
4. Compare the timing, location and level of H3 phosphorylation in parental and *ras*-transformed cells, and to identify any abnormalities occurring in *ras*-transformed cells.
5. Identify the H3 variants targeted for mitogen-induced and mitosis-specific H3 phosphorylation and determine if any variant is preferentially phosphorylated.

Chapter Two: Materials and Methodology

Cell lines and Tissue Culture

Parental 10T1/2 mouse fibroblasts were originally obtained from the American Type Culture Collection (ATCC) (Rockville, MD). Ciras-3 (C3) mouse fibroblasts were derived from 10T1/2 cells by transfection with the T24 *H-ras* oncogene [272], in which glycine 12 is replaced with valine, and constitutively overexpress the T24 *Ha-ras* oncogene [272]. Cells were cultured in a humidified environment, at 37°C with 5% CO_2 in plastic tissue culture flasks or plates (Nunc, VWR International, Mississauga, ON). 10T1/2 and C3 mouse fibroblasts were cultured in α-MEM (Invitrogen Corporation) containing 10% (v/v) fetal bovine serum (FBS) (CanSera,Ontario,Canada), 100 U/ml penicillin G sodium, 100 μg/ml streptomycin sulfate and 0.25 μg/ml amphoteracin B (Invitrogen Corporation).

Medium was prepared as per manufacturers instructions. Powdered medium was added to a volume of ddH_2O measuring 5% less than the required final volume of media with gentle stirring. To this, 2.2g of sodium bicarbonate ($NaHCO_3$) was added per liter of media. The media was then diluted to its final volume and stirred gently until all particulates were fully dissolved. The pH was adjusted to 7.3 with 1N HCl or 1N NaOH and the media sterilized by filtration (Corning bottle top filter, 0.22 μm, Corning, NY). Media was stored at 4°C for no longer than two weeks before use. Supplements of FBS, penicillin, streptomycin, and amphoteracin B were added immediately before use.

Seeding Cells

Cells were allowed to reach approximately 70% confluence before re-seeding. Medium was aspirated and the cells washed with PBS, pH 7.5, before the addition of a small amount (1-2 ml) of 0.25X trypsin. Following a 3 – 5 min incubation at 37°C 5 – 10 ml complete medium was added to stop the reaction and the cells were distributed to new plates/flasks at a ratio of approximately 1 trypsinized plate to 5 new plates.

Harvesting Cells

10T1/2 and C3 cells were harvested from 140 mm plates in the following manner. Media was aspirated and 10 ml of cold PBS added to each plate. The plate was then tilted in several directions so that cells were washed with PBS, the PBS aspirated and replaced with another 10 ml PBS, and the cells washed a second time. After washing 2 ml PBS was added to each plate and the cells scraped. Cell suspensions, kept on ice, were then spun in 15 ml Falcon tubes at 1000 rpm for 2 minutes to pellet cells. Cell pellets were washed with 10 ml PBS, and cells spun down again. After aspirating the final wash, cell pellets were stored at -80°C.

Preparing Cells for Storage in Liquid Nitrogen, Starting up Frozen Cells

The medium on logarithmically growing cells was aspirated and the cells washed once with PBS, pH 7.5. Cells were trypsinized as described above, after which the resulting cell suspension was centrifuged to pellet cells. Cells were then washed with PBS, pH 7.5, and spun down again. The pellet was resuspended in a solution containing 900 µl

FBS (CanSera, Ontario, Canada) and 100 µl dimethylsulfoxide (DMSO) (Fisher Biotech). The cell suspension was placed in a Cryotube (Corning) and kept on ice for transport to liquid nitrogen tank.

Cells frozen in the liquid nitrogen tank were periodically started up. Before removing a vial of cells from the liquid nitrogen tank, complete media was warmed to 37°C and placed in small flasks prepared to receive the cells. A cryovial was then removed from the tank and rapidly warmed up to 37°C in the water bath, with agitation. Warm cells were added to the prepared flasks and placed in the incubator (37°C, 5% CO_2) overnight. The next day cells were observed with a light microscope and the media replaced.

Antibodies

Various antibodies to H3, modified H3, HMGN1, RNA pol II, MSK1 and MSK2 were obtained from commercially available sources including Sigma Chemical Company (Saint Louis, MO, USA), Cell Signaling Technology (New England Biolabs Ltd.) (Pickering, Ontario, Canada), Santa Cruz Biotechnology (Santa Cruz, CA, USA), Upstate Biotechnology (Lake Placid, NY, USA), Abcam (Cambridge, MA, USA) and Zymed (San Francisco, CA, USA) (Table 2.1). Secondary antibodies, conjugated to horse radish peroxidase (HRP) or fluorescein isothiocyanate (FITC), Cy3, or Texas Red were purchased from Sigma Chemical Company (Saint Louis, MO, USA), Jackson ImmunoResearch Laboratories (Hornby, ON, Canada) and BIO-RAD (Hercules, CA, USA). Primary antibodies used for Western blotting (WB) and indirect immunofluorescence (IF) are listed in Table 2.1. Secondary antibodies are listed in Table 2.2.

Type	Epitope Recognition	Application	Company
Rat monoclonal	pS28 H3	WB, IF	Sigma Chemical Company
Rabbit polyclonal	pS28 H3	WB	Upstate Biotechnology
Rabbit polyclonal	pS10 H3	WB	Cell Signaling Technology
Rabbit polyclonal	pS10 H3	IF	Santa Cruz Biotechnology
Rabbit polyclonal	pS10AcK14 H3	WB, IF	Upstate Biotechnology
Rabbit polyclonal	AcK9 H3	WB, IF	Upstate Biotechnology
Rabbit polyclonal	AcK9,14 H3	WB, IF	Upstate Biotechnology
Rabbit polyclonal	AcK27 H3	WB, IF	Upstate Biotechnology
Rabbit polyclonal	Trimethyl K9 H3	WB, IF	Abcam
Rabbit polyclonal	Total H3	WB	Cell Signaling Technology
Rabbit polyclonal	PS6 HMGN1 S6	WB, IF	Upstate Biotechnology
Rabbit polyclonal	Total HMGN1	WB	Abcam
Mouse monoclonal	pS5 RNA pol II	IF	Upstate Biotechnology
Rabbit polyclonal	MSK1	IF	Sigma Chemical Company
Rabbit polyclonal	MSK2	IF	Zymed
Rabbit polyclonal	MSK2	IF	R and D

Table 2.1. Primary antibodies. Primary antibodies used in Western blot (WB) or indirect immunofluorescence (IF) experiments are shown with their commercial source and application. The type of antibody (monoclonal or polyclonal), species of origin, and epitope are listed.

Conjugate	Type	Company
Texas red	Donkey anti-rat	Jackson ImmunoResearch
FITC	Donkey anti-mouse	Jackson ImmunoResearch
Cy3	Sheep anti-rabbit	Sigma Chemical Company
FITC	Rabbit anti-rat	Sigma Chemical Company
HRP	Goat anti-rabbit	BIO-RAD
HRP	Rabbit anti-rat	Sigma Chemical Company

Table 2.2. Secondary Antibodies. Horse radish peroxidase (HRP)-conjugated antibodies used in Western blot experiments and FITC-, Cy3-, and texas red-conjugated antibodies used in indirect fluorescence experiments are listed with their commercial source and species of origin are listed.

Several factors must be taken into account when working with antibodies specific to modified histones. Lack of specificity to the desired epitope is common, as is epitope occlusion, which can occur if multiple residues have been modified in close range. For example, an antibody recognizing an epitope of H3 including phosphorylated serine 28 may not be able to bind H3 that has also been acetylated at lysine 27. Since multiple hisone modifications are known to take place on the same molecule, this can significantly complicate analysis. In recent years antisera recognizing different combinations of modifications on one histone have been produced, however antisera recognizing H3 phosphorylated at serine 28 in combination with other modifications are not yet available.

Manipulation of Cells with TPA, EGF, TSA, H89 and Colcemid

Phosphorylation of histone H3 occurs during mitosis and following stimulation of the MAPK pathway. In order to examine H3 phosphorylation in a group of cells undergoing mitosis, cells grown to approximately 65% confluence were treated with colcemid (Sigma, St. Louis, MO) at a concentration of 0.06 μg/ml for 16 hours before harvesting or fixation. Colcemid interferes with mitosis by inhibiting the formation of spindle microtubules; treatment with this agent increases the proportion of cells in mitosis. To confirm an increase in the number of cells undergoing mitosis, fluorescence activated cell sorting (FACS) was performed.

Epidermal growth factor (EGF) and 12-0-tetradeconylphorbol-13-acetate (TPA) were used to stimulate the MAPK pathway. In order to remove background H3 phosphorylation from cells undergoing mitosis, 10T1/2 and C3 cells were first grown to 100% and 80% confluence, respectively, and serum starved for periods of 24 hours or 48 hours, respectively. Cells were then left untreated, treated with 100 nM TPA (Sigma, St. Louis, MO) or treated with 50 ng/ml EGF (Sigma, St. Louis, MO) for periods of 7 to 90 minutes. In experiments using trichostatin A (TSA), cells were first treated with 100 nM TPA for 15 min, and then treated with a combination of 100 nM TPA and 500 ng/ml TSA for 15 min (Sigma, St. Louis, MO).

The kinase inhibitor H89 was used to inhibit specific elements of the MAPK pathway. H89 (Calbiochem) used at a concentration of 10 μM, inhibits MSK1 and MSK2. When required, cells were treated with 10 μM H89 for 30 min prior to TPA stimulation.

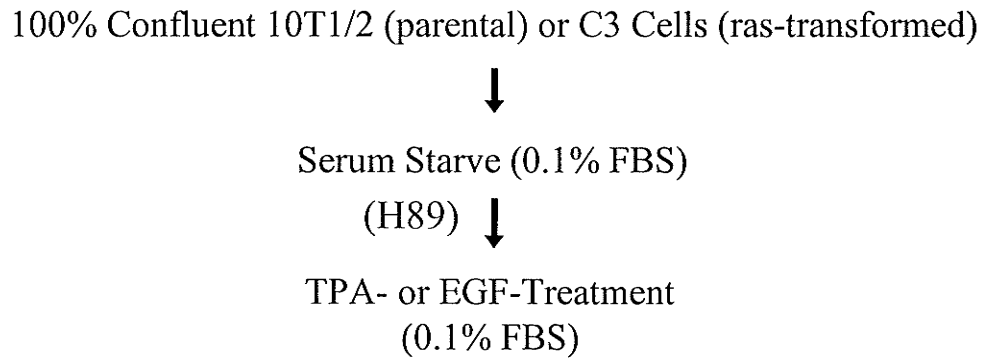

Figure 2-1. Flow diagram representing cell treatments. Parental 10T1/2 or ras-transformed C3 cells were grown to 100% confluence prior to serum starvation for 24 or 48 hours respectively. The MSK1/2 inhibitor H89 was added to media 30 min before the start of TPA/EGF treatment when required.

Flow Cytometric Analysis of Cell Cycle Distribution

To determine the cellular distribution in different phases of the cell cycle, flow cytometric analysis was performed on various treated and untreated cells. Cells harvested by trypsinization were washed twice with PBS (pH 7.5) before being spun down and resuspended in 2 ml PBS (pH 7.5). This suspension of cells was added to 4 ml ice-cold 95% ethanol in a drop-wise manner while mixing. The resulting suspension was incubated in the cold room (approximately 4°C) for a minimum of 20 min, maximum of 16 hours, after which 1 µl of a 10 µg/µl ethidium bromide stock was added to stain DNA. Tubes containing cell suspensions were then wrapped in aluminum foil and taken to Dr. Ed Rector for analysis.

Analysis was performed on a Beckman Coulter EPICS Altra Fluorescence Activated Cell Sorter (Missisauga, Ont) with EXPO32 MultiCOMP software version 1.2. Samples were

gated to avoid counting debris or cells that were stuck together. Excitation of fluorescent signal, via laser, took place at 488 nm, and the intensity of emitted fluorescence was then measured at 610nm.

Extraction of Histones and HMG Proteins

Total histone preparation was done as described previously [209]. To prepare samples of total histones, frozen pellets of cells were thawed on ice prior to resuspension in 1-5 ml NP-40 buffer (10mM Tris pH 7.6, 150 mM NaCl, 1.5 mM $MgCl_2$, 0.1% NP-40, 1mM PMSF, 1mM sodium orthovanadate, 1mM NaF, 25mM β-glycerophosphate, and 5mM sodium butyrate). For cells that were 100% confluent, approximately 0.5 ml NP-40 buffer was used per 140 mm (diameter) plate of confluent cells. When extracting histones from cycling cells, volumes were adjusted accordingly. After resuspension cells were homogenized 10 times and run through a 3 ml syringe with a 22-gauge needle three times. These steps were performed on ice.

At this point samples were placed in Sarstedt 15 ml tubes and centrifuged at 4000 rpm for five minutes at 4°C. The resulting supernatant was discarded and the pellet resuspended in RSB buffer (10mM Tris pH 7.6, 10mM NaCl, 3mM $MgCl_2$, 1mM PMSF, 1mM sodium orthovanadate, 1mM NaF, 25mM β glycerophosphate, and 5mM sodium butyrate). Approximately 0.25 ml RSB buffer was used per 140 mm plate of 100% confluent cells. Samples were then transferred to Eppendorf tubes and 4N H_2SO_4 was added to a final concentration of 0.4 N. After mixing by inverting the samples several times, they were incubated on ice for approximately 1 hour.

After this acid extraction, samples were centrifuged at 14 000 rpm in a microcentrifuge for 10 minutes in the cold room (approximately 4°C). Supernatants were transferred to new eppendorf tubes, to which 100% TCA (trichloroacetic acid) was added to a final concentration of 18% (v/v). Samples were then incubated on ice for approximately 45 minutes to allow proteins to precipitate. The samples were then centrifuged in the cold room for 10 minutes at 14 000 rpm in a benchtop microcentrifuge. The resulting supernatant was discarded, and the pellet washed as follows. First pellets were washed once with 1 ml of a solution containing 5 µl 12.1 M HCl for every 1 ml acetone. Upon addition of wash solution, eppendorf tubes were inverted several times before centrifugation at 13 000 rpm on a benchtop microcentrifuge at room temperature for 2 to 3 minutes. Pellets were then washed with 1 ml of acetone twice, centrifuging for 2 to 3 minutes in between washes. Following the final wash as much liquid as possible was removed from the tubes and the pellets were left to air dry at room temperature overnight. The next day dried pellets were resuspended in 50 to 150 µl of ddH_2O. This was done on ice, after which the samples were stored at -20°C.

Quantification of Histones

Prepared histones were quantified using the TCA precipitation assay performed as follows. Ten µl of each sample was placed in separate glass tubes. To each tube, 790 µl ddH_20 and 400 µl of 50% TCA (1:1 v/v TCA/ddH_20) was added. A blank was prepared by mixing 400 µl of 50% TCA (1:1 v/v TCA/ddH_20) and 800 µl ddH_20. Absorbance at 400 nm was then measured using a spectrophotometer (Ultraspec 3000 Pharmacia

Biotech) and the concentration of each sample calculated according to the following formula: Concentration (μg/μl) = A_{400} X 120/0.093 / 1000.

Two Dimensional Gel Electrophoresis

Acid-extracted histones were separated by two dimensional gel electrophoresis in which histones separated in acid-urea-triton polyacrylamide gels were run into SDS-PAGE gels. Acid-urea-triton polyacrylamide gels separate positively charged proteins based on size and hydrophobicity. Minor residue changes in H3.1, H3.2, and H3.3 cause these proteins to separate into distinct bands. Bands of separated histone variants are then compacted as they pass through the stacking portion of the second dimension SDS polyacrylamide gel. This allows for easier detection with stains such as 8-Anilino-1-naphthalene-sulfonic acid (ANS) and HRP-conjugated antibodies.

First dimension acid-urea-Triton (AUT) polyacrylamide gel: The following stock solutions were prepared for use in acid-urea-triton gels. TEMED/acetic acid stock (4% TEMED, 43.1% acetic acid), 30% acrylamide stock (29.2% acrylamide, 0.8% bis-acrylamide), 0.004% riboflavin stock, and 3M potassium acetate pH 4.0. Running buffer for acid-urea-triton gels was made by combining 948 ml of double distilled water with 562 ml glacial acetic acid.

To pour the separating portion of an acid-urea-triton gel, 4 g urea, 5 ml 30% acrylamide stock, 1.25 ml TEMED/acetic acid stock, 1 ml 0.004% riboflavin, 200 μl Triton X-100, 100 μl thiodiglcycol, and 2.45 ml double distilled water were combined in a beaker and mixed until the urea completely dissolved. An approximately 12 cm separating gel was

then poured in between thin glass plates with 0.75 mm spacers. Prior to polymerization, the gel solution was overlayed with 70% ethanol, after which the gel was placed in between two light boxes for 1 hour to polymerize.

A stacking gel, made by combining 3.2 g urea, 2 ml 30% acrylamide stock, 1 ml 3M potassium acetate, 800 µl 0.004% riboflavin, 160 µl Triton-X-100, 80 µl thiodiglycol, 80 µl TEMED and 680 µl double distilled water, was poured and a 10-well comb inserted before polymerizing the stacking gel in the same way as the separating gel. After polymerization the gel was wrapped in damp paper towels, covered with plastic wrap and placed in the cold room (approximately 4°C) overnight.

Sample preparation: Samples to be run were first combined with reducing mix, then double distilled water and AUT sample buffer just before loading. Samples were prepared on the day the gel was to be run as follows: 15 µg of each sample was placed in a clean eppendorf tube. For each 5µl of sample, 4µl of reducing mix (1/1/1/1 by volume: 2-mercaptoethanol, 20% (w/v) cysteamine, ddH_2O, 1 M Tris-HCl pH 8.8) was added, after which samples mixed with reducing mix were incubated at room temperature for 20 minutes. For every 5 µl of sample, 4.3 µl of double-distilled water and 6.7 µl of sample buffer (6 M urea, 5% acetic acid, 12.5 mg/ml protamine sulfate, 0.2% pyronin Y, 30% sucrose) was added just before loading gel. Protamine sulfate binds to free carboxyl groups in the gel matrix; this decreases the binding of histones and results in less smearing [273].

Running of AUT gel: Gels were run in the cold room at approximately 4°C. One half hour before the start of sample loading, the gel apparatus, complete with running buffer, was set up such that it was cold prior to the application of voltage. Samples prepared as

described above with 10 μg of each sample were run toward the cathode. Gels were run until the pyronin Y in the sample buffer ran off the bottom of the gel, which took approximately 4 hours at 250 V at 4°C.

AUT gel treatment: After sufficient separation of H3 variants was achieved, the AUT polyacrylamide gel was removed from the glass plates and rinsed once in double distilled water. Gels were then stained with 8-Anilino-1-naphthalene-sulfonic acid (ANS). To this end, gels were placed on a rocking platform in a container of freshly prepared staining solution of 90 μg/ml ANS (Eastman KODAK Company, Rochester, New York). Gels were stained for 30 minutes at room temperature, after which staining solution was removed and replaced with ddH_20. Gels were destained in double distilled H_2O over a period of 1 hour with several changes of wash solution.

Stained gels were then placed on a UV transilluminator to view the histone variant bands. After locating H3.1, H3.2, and H3.3, lanes were cut to encompass these bands for each sample. Sample lanes were then placed in small plastic dishes, to which 50 ml of 2D gel solution (5% β-mercaptoethanol, 2.3% SDS, 62.5 mM Tris pH 6.8) was added. The dishes were then covered and placed on a rocking platform for 30 minutes to prepare proteins to run into an SDS-gel.

Second dimension SDS-polyacrylamide gel: Slices of AUT polyacrylamide gels treated as described above were applied to the top of the stacking portion of SDS-polyacrylamide gels. For this type of analysis SDS gels were 15% polyacrylamide, poured as described previously with the use of 1.0 mm spacers. After application of the AUT gel slice, SDS-PAGE running buffer was added and the gels run for approximately 1.25 hours at 200V.

Transfer of Proteins to Nitrocellulose

Proteins, including histones, were transferred to nitrocellulose for immunoblot analysis. After running SDS-PAGE gel, the gel was carefully removed from between the glass plates and set up in a sandwich such that proteins could be transferred to a pre-soaked (in transfer buffer) piece of nitrocellulose. Transfer buffer contained 400 mM 3-(cyclohexylamino)-1-propanesulfonic acid (CAPS) and 20% methanol in ddH_20. Histone transfer was carried out overnight at 50 volts (V) or for 1 h at 100 V, always in the cold room. Transfer of other proteins was done overnight (approximately 16 h) at 50 V in the cold room.

Acid-Urea Polyacrylamide Gel Separation of Acid-Extracted Histones

Acid-urea polyacrylamide gels separate histones based on size and charge, such that one charge-altering modification results in a shift upward of one band. This type of gel was used to analyse the phosphorylation and acetylation of H3. The following stock solutions were made up and stored in brown bottles at 4°C for not longer than 2 months. TEMED/acetic acid stock (4% TEMED, 43.1% acetic acid), 30% acrylamide stock (29.2% acrylamide, 0.8% bis-acrylamide), 0.004% riboflavin stock, and 3M potassium acetate pH 4.0. Running buffer, consisting of 52 glacial acetic acid in 1L water, was made up just before use.

The separating gel was made by combining the following in a glass beaker: 7.20 g urea, 10.0 ml 30% acrylamide stock, 2.50 ml 4% TEMED/Acetic acid stock, 2 ml 0.004% riboflavin, 200 µl thiodiglycol, ddH_2O to 19.4 ml. The solution was mixed until all urea

dissolved, after which it was poured between glass plates (approximately 6 inches (height) by 8 inches), 70% ethanol placed on top, and the plates placed in between two light boxes for 3 to 4 hours. At this point the ethanol was poured off and the gel rinsed twice with water.

The stacking gel was made by combining 2.88 g urea, 1.6 ml 30% acrylamide stock, 2.33 ml 3M potassium acetate pH 4.0, 800 µl 0.004% riboflavin, 80 µl thiodiglycol, 80 µl TEMED with enough double-distilled water to make 8 ml. Stacking gel was then poured on top of the separating gel, a comb with 25 wells inserted, and the apparatus was again placed in between two light boxes for 3-4 hours. After polymerizing the gel was wrapped and stored at 4°C overnight before use.

The following day samples were prepared as follows: 15 µg of each sample was placed in a clean eppendorf tube. For each 5µl of sample, 4µl of reducing mix (1/1/1/1 by volume: 2-mercaptoethanol, 20% (w/v) cysteamine, ddH_2O, 1 M Tris-HCl pH 8.8) was added, after which samples mixed with reducing mix were incubated at room temperature for 20 minutes. For every 5 µl of pure sample, 4.3 µl of double-distilled water and 6.7 µl of sample buffer (6 M urea, 5% acetic acid, 12.5 mg/ml protamine sulfate, 0.2% pyronin Y, 30% sucrose) was added just before loading gel. Protamine sulphate was added to sample buffer to reduce smearing of the histones.

Gels were run on the large BIORAD setup, with a cooling core, at 250 V for 25 hours, in running buffer (3L: 156 ml glacial acetic acid plus 2844 ml double distilled water). Gels were then removed from the apparatus and histones transferred to polyvinylidene fluoride (PVDF) membrane as positive proteins.

Transfer of Histones to PVDF Membrane as Positive Proteins

Histones in acid-urea gels were transferred to PVDF membrane as described previously by Dimitrov and Wolffe [274]. This was accomplished by setting up the transfer apparatus as usual (see section on Western blots), then inversing the orientation of the sandwich with respect to the positive and negative electrodes. Transfer took place overnight at 50V in the cold room (approximately 4°C) in transfer buffer containing 0.7% acetic acid, 10% methanol.

Coommassie Blue Staining of Histones in SDS-Polyacrylamide, AU and AUT gels

Acid-extracted histone samples separated by SDS-PAGE or acid-urea-Triton gel or acid-urea gel were stained with Coommassie Blue. After running, gels were carefully removed from glass plates and placed in Coommassie Blue solution (45% (v/v) methanol, 9% (v/v) glacial acetic acid, 0.04% (w/v) Coommassie Brilliant Blue) and incubated at room temperature overnight.

Gels were destained the following day. Staining solution was removed and destaining solution (7% (v/v) glacial acetic acid, 5% (v/v) methanol) added, after which gels were placed on a rocking platform. Destaining solution was changed 4-5 times over a period of several hours.

Staining Histones with 8-Anilino-1-Napthalene-Sulfonic Acid (ANS)

Histones separated by acid-urea and acid-urea-triton were stained with ANS (Kodak). After running, gels approximately 7 inches long containing histones were removed from

between glass plates and rinsed in ddH_20. Gels were then placed in a container with freshly prepared staining solution (90 μg/ml ANS in ddH_2O). The dish containing gel and staining solution was incubated on a rocking platform for 30 minutes at room temperature to stain proteins, after which the staining solution was discarded and replaced with ddH_2O. Gel was washed with multiple changes of ddH_2O on the rocking platform for 1 hour, changing the water approximately every 10 minutes. Following washing the gel was illuminated on a UV (ultraviolet) light box and photographed.

Drying Gels

Stained gels were scanned with the Kodak Imager before drying. Gels were dried when necessary with the following procedure. Film (Hyperfilm, Amersham Biosciences) and gel were pre-soaked in soaking solution (10% glycerol, 20% ethanol) for approximately 30 minutes. Gel was then put in between 2 pieces of film such that no air bubbles were present and the setup secured with metal clips. Gels were allowed to dry at room temperature for 2 days.

Immunostaining Proteins on Membranes

Immunostaining of proteins on nitrocellulose membranes was carried out as per standard protocols. Dry membranes were baked at 65°C and blocked with solutions of PBS (phosphate buffered saline, pH7.5), PBST (PBS with 0.5% tween 20), TBS (tris buffered saline, pH 7.5), or TBST (TBS with 0.5% tween 20) containing 2-8% skim milk powder or 5% bovine serum albumin (BSA) for periods of 20 minutes to 1 hour. Membranes

were then incubated in primary antibody solution (1:200 to 1:3000 dilution of primary antibody in PBS, PBST, TBS or TBST containing 0 – 4% skim milk powder or BSA) for periods of 2 to 16 h. After this incubation membranes were removed from primary antibody solution and washed with washing solution (PBS, PBST, TBS or TBST) several times, 5 min each, before incubation in secondary antibody solution (secondary antibody 1:5000 to 1:10000 in PBS, PBST, TBS or TBST) for 20 minutes to 1 hour. Membranes were then washed several times before development with enhanced chemiluminescence (ECL) plus Western Blotting Detection Reagents (Amersham Biosciences) and exposure to film.

Staining Proteins with India Ink

Acid-extracted proteins present on dried nitrocellulose and PVDF membranes were stained with a solution of India Ink (diluted 1 to 300) in PBS for a period of no more than 3 minutes on a rocking platform. Staining solution was then discarded and membranes were rinsed with ddH_2O before beginning a procedure to immunostain proteins.

Stripping Immunostained Membranes

Membranes were stripped of commercial antibodies following exposure to film in the following manner. Membranes (nitrocellulose or PVDF) were washed four times for 5 minutes each in PBS, pH 7.5, and then incubated with stripping solution (62.5 mM Tris-Cl pH 6.8, 2% SDS, 100 mM β-mercaptoethanol) for 30 minutes at 50°C. Membranes were then washed in PBS three times, 5 minutes each, before they were developed with

ECL and re-exposed to film. An absence of signal on the film indicated that stripping was successful.

Indirect Immunofluorescence.

10T1/2 cells were grown on glass coverslips (Fisher Scientific) placed inside the wells of 24-well plates (Corning Incorporated, Corning, NY, USA) and grown to 100% confluence. Cells were then washed twice with PBS and placed in media supplemented with 0.1% FBS for 24 h. Half of the wells were then treated with 100 nM TPA for 15 min. Cells were then fixed in a 4% paraformaldehyde solution for 30 min on ice and immersed in 500 µl of quenching solution (75 mM NH_4Cl, 20 mM glycine in PBS) for 10 min. Cells were then incubated in permeabilizing solution (0.5% Triton X-100 in PBS) for 30 min on ice, after which the permeabilizing solution was removed by two washes with PBS and the cells incubated in blocking solution (0.02% saponin, 0.05% sodium azide, 1% bovine serum albumin, 0.1% fish skin gelatin and 4% normal goat serum) for 1 h in a moist chamber at room temperature. Cells were then incubated with dilutions of primary antibody in antibody dilution buffer (0.02% saponin, 0.05% sodium azide, 1% bovine serum albumin, 0.05% fish skin gelatin and 1% normal goat serum) overnight at 4°C in a moist chamber. Cells were then washed with PBS for 15 min, changing the PBS twice. After aspirating the PBS, secondary antibody diluted in antibody dilution buffer was added and allowed to sit for 1 h at room temperature in a moist chamber. Cells were then washed for 15 min with PBS and mounted onto slides with Vectashield mounting medium with DAPI (Vector Laboratories Inc., Burlingame,CA,USA). Pictures were taken at 0.25 µm increments with a Zeiss Axioplan 2 microscope and AxioCam HR CCD

(Zeiss). Images of nuclei or whole cells were deconvolved with Axiovision 3.1 software (constrained iterative).

Soft Agar Assay for Colony Formation

The soft agar assay for colony formation measures a cell's ability to grow in an anchorage independent fashion. Most normal cells require adherence to a solid surface to grow and divide. In this assay, cells are seeded in medium made semi-solid by the addition of agarose. Only cells able to grow without adhering onto a solid surface can grow and divide in semi-solid medium. Due to the semi-solid state of the media, cells do not move apart after cell division, creating colonies.

Base Agar Preparation: Cells are seeded into semi-solid media that is placed directly on top of a solid base containing media solidified by the addition of agarose. Plates can be prepared with base agar and kept at 4°C up to three days before cells are seeded. To prepare base agar, melted, sterile 1% agarose and 2X α-MEM (prepared by making α-MEM as per manufacturers instructions with the exception of halving the final volume, and adding twice the usual amount (per ml) of FBS and antibiotics) warmed in a 40°C waterbath were mixed 1:1 and poured into plates. Media was allowed to set for approximately 5 minutes.

Seeding cells in semi-solid media: Semi-solid media is made by mixing (1:1, v/v) sterile 0.7% agarose and 2X αMEM (including FBS and antimicrobials, antifungals). While sterile 0.7% agarose and 2X αMEM warmed in a waterbath at 40°C logarithmically growing 10T1/2 and C3 cells were harvested by trypsinization and counted using a

Coulter Counter. Semi-solid media was then mixed and approximately 5000 cells seeded per plate. Plates were left to set for 5 minutes so that the top layer became semi-solid and then placed in the tissue culture incubator (37°C, 5% CO_2).

Counting Colonies: After colonies grew, they were counted and photographed on a dissecting light microscope.

Spectral Karyotyping (SKY)

SKY analysis was performed on 10T1/2 cells with the SkyPaint Probe kit for mouse samples from Applied Spectral Imaging (Viste, CA) according to manufacturer's instructions.

Chapter Three: Results

I. *The Induction Pattern of H3 Phosphorylation at Serine 28 is Parallel to that at Serine 10*

Exposing 100% confluent, serum-starved fibroblasts to agents that stimulate the MAPK-pathway such as growth factors, phorbol esters and irradiation activates a series of kinases, including ERKs [275]. This treatment also results in the phosphorylation of histone H3 at serine 10 and HMGN1 at serines 6, 20 and 24 [180]. We extracted histones from sets of cells that were a) grown to 100% confluence, b) grown to 100% confluence and serum-starved for 24 hours, and c) grown to 100% confluence, serum-starved, and treated with 100 nM TPA for 15 minutes. Histones were separated by SDS-PAGE, transferred to nitrocellulose, and immunostained with antisera against H3 phosphorylated at serine 28 (pS28 H3). As expected, we were unable to detect pS28 H3 in cells that had been serum-starved for 24 hours, nor could we detect pS28 H3 in 100% confluent cells (Figure 3-1 A).

To determine if the temporal induction pattern of H3 phosphorylation at serine 28 is similar to that at serine 10, 100% confluent, serum-starved 10T1/2 mouse fibroblasts were treated with the phorbol ester TPA (100 nM) for varying lengths of time (Figure 3-1 B). Histones extracted from treated and untreated cells were separated by SDS-PAGE, transferred to nitrocellulose and phosphorylated H3 was detected with antisera specific to H3 phosphorylated at serine 10 (pS10 H3) or serine 28 (pS28 H3). Following detection blots were stripped and re-probed with antisera against total H3, which served as a loading control.

As shown in Figure 3-1 B, the induction pattern of H3 phosphorylation at serine 28 is very similar to that at serine 10. Phosphorylation of H3 at serine 28 is rapid and transient.

On both residues phosphorylation is induced such that levels are dramatically increased 15 minutes after the beginning of treatment, remain high 30 minutes into treatment, are decreased 60 minutes after treatment began, and are close to levels seen in untreated cells 90 minutes after the onset of exposure to TPA. Phosphoacetylated serine 10 lysine 14 H3 (pS10AcK14 H3) was also detected with specific antisera, revealing that the number of molecules of H3 with this combination of modifications also increases dramatically upon mitogen stimulation. The induction pattern of pS10AcK14 H3 was similar to that of pS10 H3 and pS28 H3, with levels of pS10AcK14 H3 rising rapidly at the start of stimulation and beginning to decrease more than 30 minutes later. This pattern is comparable to the transient activation of ERK following stimulation of the mitogen activated protein kinase pathway. Active ERKs can be detected in mouse 10T1/2 fibroblasts following a 15 min TPA treatment and reach a maximum at 30 minutes, after which they subside [275].

To determine the enzyme most likely responsible for the phosphorylation of H3 at serine 28, 100% confluent, serum-starved 10T 1/2 mouse fibroblasts were treated with 100 nM TPA for 15 minutes in the presence and absence of the kinase inhibitor H89 (Figure 3-1 C). At a concentration of 10 μM, H89 has been shown to significantly decrease the activity of several protein kinases including MSK1, MAPK-activated protein kinase 1b (MAPKAP-K1b), PKA, PKBα, p70 ribosomal protein S6 kinase (S6K1), Rho-dependent protein kinase II (ROCK-II) and AMP-activated protein kinase (AMPK) [276]. H89 was added to culture medium 30 minutes prior to the start of stimulation. Histones extracted from treated and untreated cells were separated by SDS-PAGE. Levels of H3 phosphorylated at serine 10 or at serine 28 were then detected with specific antisera. To

control for loading, nitrocellulose membranes containing histones were stained with India Ink (Figure 3-1 C, lowest panel). A thirty minute pre-treatment with H89 effectively prevented TPA-induced phosphorylation of H3 at serine 10 and at serine 28 (Figure 3-1 C). In a paper published in 2003, Soloaga *et al* [180] demonstrated that mitogen-induced phosphorylation is abrogated in knockouts of MSK1/2 (mouse embryonic fibroblasts), confirming our suspicion that MSKs mediate mitogen-induced H3 phosphorylation.

Following stimulation of the Ras-MAPK pathway, many small foci of H3 phosphorylated at serine 10 appear in the nucleus. These foci are excluded from pericentromeric heterochromatin [209]. Indirect immunofluorescence was performed to determine the subcellular localization of H3 modified by mitogen-induced phosphorylation at serine 28. H3 phosphorylated at serine 10 and at serine 28 was visualized in 100% confluent, serum-starved 10T1/2 mouse fibroblasts treated with 100 nM TPA for 15 minutes. Antisera specific to H3 phosphorylated at serine 10 or serine 28 stained numerous small foci of pH3 throughout the nucleus after 15 min TPA (Figure 3-2). Arrows point out regions of intense DAPI staining that correspond to AT-rich pericentromeric heterochromatin [209]. Like H3 phosphorylated at serine 10, H3 phosphorylated at serine 28 is excluded from regions of highly condensed pericentromeric heterochromatin in interphase cells. Thus this modification is occurring on potentially transcriptionally competent chromatin. We also observed mitotic chromosomes intensly stained with antisera against both pS10 H3 and pS28 H3 on slides of serum-starved cells, excluding differential antibody access to highly condensed chromatin as an explanation for our observed pattern of pS10 H3 and pS28 H3 in interphase cells (data not shown).

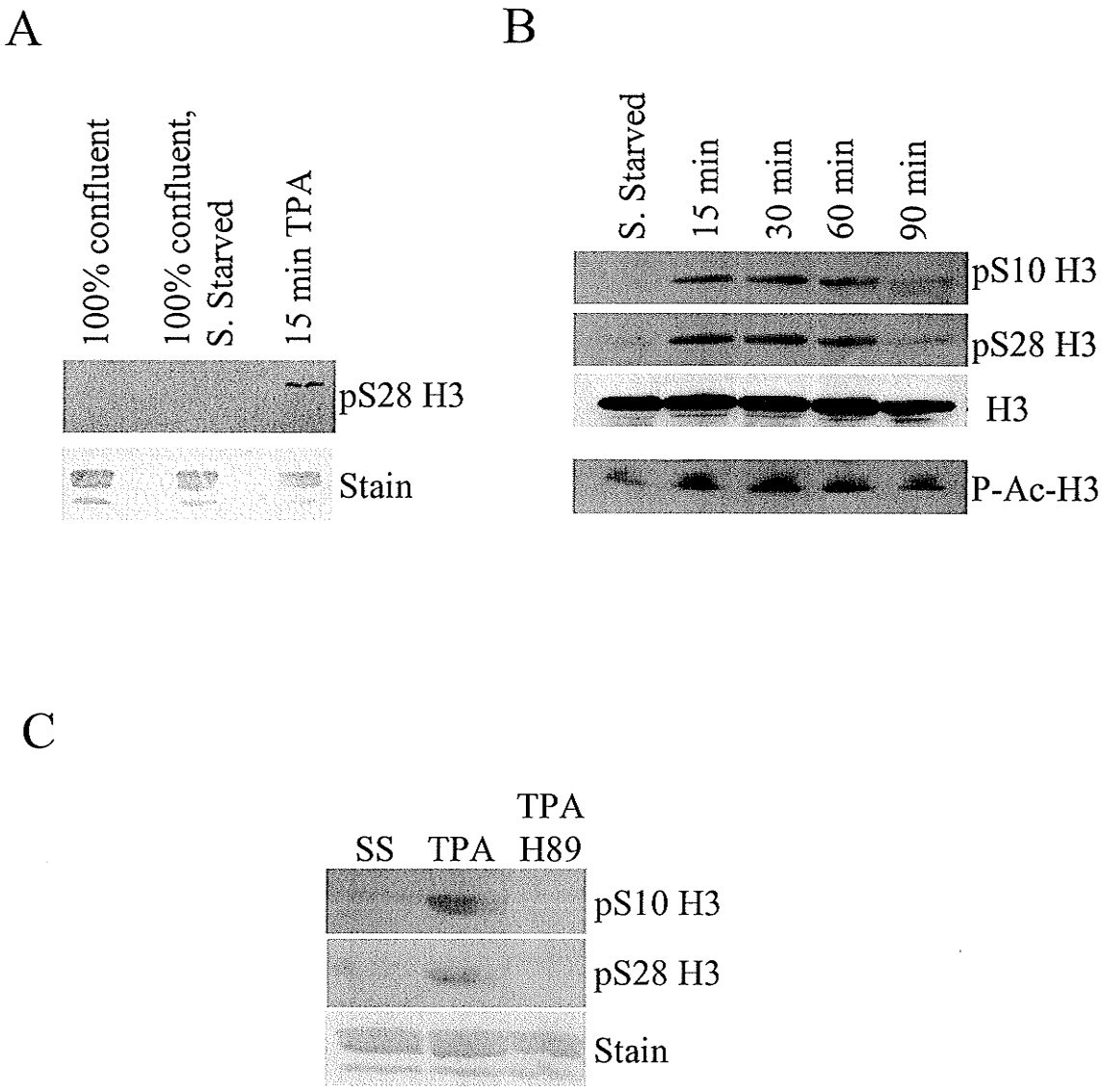

Figure 3-1. Phosphorylation of H3 at serine 28 is induced by stimulation of the Ras-MAPK pathway. A, B and C) Histones extracted from 100% confluent, 100% confluent and serum starved (SS or S. Starved) and TPA-treated 10T1/2 mouse fibroblasts were separated by SDS polyacrylamide gel electrophoresis prior to immunoblotting with antibodies specific for H3 phosphorylated on serine 10 (pS10 H3) or 28 (pS28 H3), total H3 and H3 phosphoacetylated at serine 10 lysine 14 (pS10AcK14 H3). A) H3 phosphorylated at serine 28 could not be detected in 100% confluent cells or cells that were serum-starved, but was found in TPA treated cells. India ink stain was used to confirm equal loading of samples. B) Timeline of H3 phosphorylation exhibits the temporal pattern of induction following stimulation of 100% confluent, serum-starved 10T1/2 fibroblasts with 100 nM TPA. C) The addition of the MSK1/2 inhibitor H89 to culture medium 30 min prior to a 15 min TPA treatment prevents H3 phosphorylation; India ink stain shows equal loading.

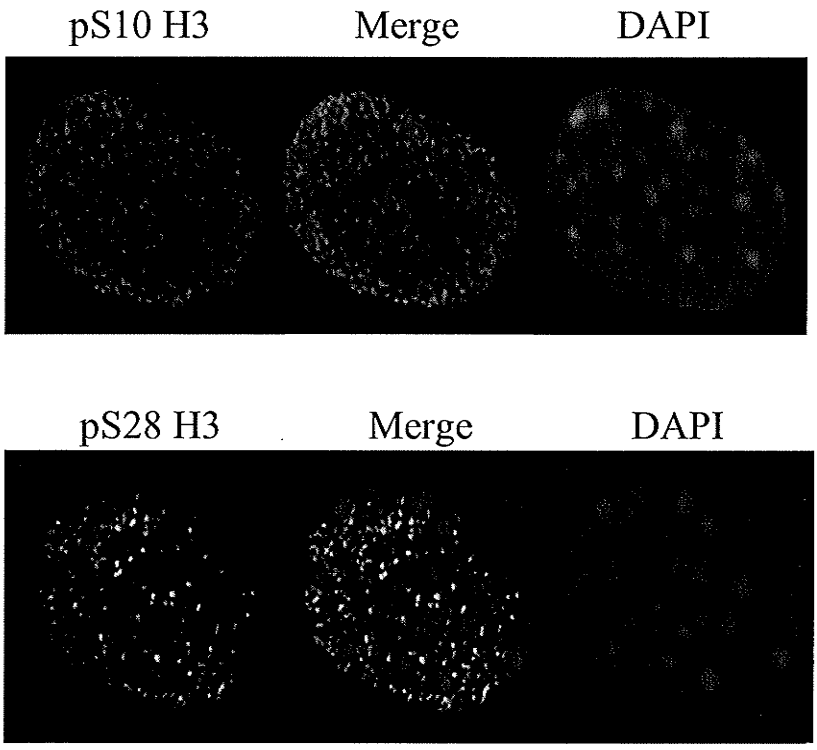

Figure 3-2. H3 phosphorylated at serine 10 or 28 is excluded from pericentromeric heterochromatin. Indirect immunofluorescence with antisera against phosphorylated H3 serine 28 (pS28 H3) or serine 10 (pS10 H3) was performed on interphase 10T1/2 cells. Cells were co-stained with DAPI. Digital optical sections of 0.25 μm were obtained and false-coloured green (pS28 H3), red (pS10 H3) or blue (DAPI). Images were deconvolved with Axiovision 3.1 software. Yellow arrows point at regions of pericentromeric heterochromatin.

II. Steady State Levels of Mitogen-Induced H3 Phosphorylation

Histone modifications are thought to act in combination with each other as part of a histone code that is interpreted by the cell and converted into specific biological outcomes [229]. Acetic acid-urea polyacrylamide gels (AU gels) resolve histones based on size and charge and were used to analyze the extent of charge-altering modifications present on the population of histone H3 participating in mitogen-induced phosphorylation at serine 10 and 28. Phosphorylation and acetylation reduce the net positive charge on H3, resulting in slower migration of the isoform according to the number of charge-altering modifications [208]. Thus a molecule of H3 having been modified by acetylation twice (di-acetylated) will run more slowly than a molecule of H3 having been modified by phosphorylation once (mono-phosphorylated). Modifications that do not alter the net charge of H3, such as methylation, do not alter migration in acid-urea polyacrylamide gels.

Histones extracted from serum-starved 10T1/2 cells that were either treated with 100 nM TPA for 15 min or left untreated were resolved in the AU gel shown in Figure 3-3 and stained with Coommassie Blue. Note that in both lanes of this gel the majority of H3 lies in the non-modified band, indicating that most of the H3 in the nucleus of these cells is unmodified, even after mitogen-stimulation. TPA-treatment results in the modification of only a small fraction of histones associated with the genome.

To determine the distribution of H3 modified isoforms participating in TPA-induced H3 phosphorylation histones extracted from the nuclei of untreated and TPA-treated (100 nM; 15 min) cells were separated in AU gels, transferred to PVDF membrane and immunostained with antisera specific for H3 phosphorylated at serine 10 (pS10 H3), H3

phosphorylated at serine 28 (pS28 H3), H3 phosphoacetylated serine 10 lysine 14 H3 (pS10AcK14 H3), and total H3.

As shown in Figure 3-4 A, H3 phosphorylated at serine 10 was present in mono-, di-, tri-modified forms of H3, with a small amount in tetra-modified forms. Density scans of the results in Figure 3-4 A indicate that fifteen minutes into TPA treatment H3 phosphorylated at serine 10 is present in the mono- and di-modified fractions of H3, and less so in the tri-modified fraction (Figure 3-4 B). Thirty and sixty minutes into TPA-treatment the majority of H3 modified by phosphorylation at serine 10 is present as a mono-modified isoform of H3 (Figure 3-4 A and B). Antisera specific to H3 modified by phosphorylation at serine 10 and acetylation at lysine 14 detected the presence of this combination of modifications mainly in di-modified isoforms of H3 (Figure 3-4 A).

The distribution of H3 phosphorylated at serine 28 among modified isoforms differed from that of H3 phosphorylated at serine 10. Antisera specific to H3 phosphorylated at serine 28 detected the presence of this modification in mono-, di-, and tri-modified isoforms (Figure 3-4 A). A small amount of H3 phosphorylated at serine 28 was detected in tetra-modified isoforms of H3 (Figure 3-4 A). In contrast to the results for H3 phosphorylation at serine 10, at fifteen and thirty minutes into TPA-treatment H3 phosphorylated at serine 28 is primarily present in a tri-modified isoform (Figure 3-4 A and B). Sixty minutes after the start of TPA stimulation of the Ras-MAPK pathway, H3 phosphorylated at serine 28 is most prominent in tri-modified isoforms of H3, followed by mono- and di-modified isoforms (Figure 3-4 B).

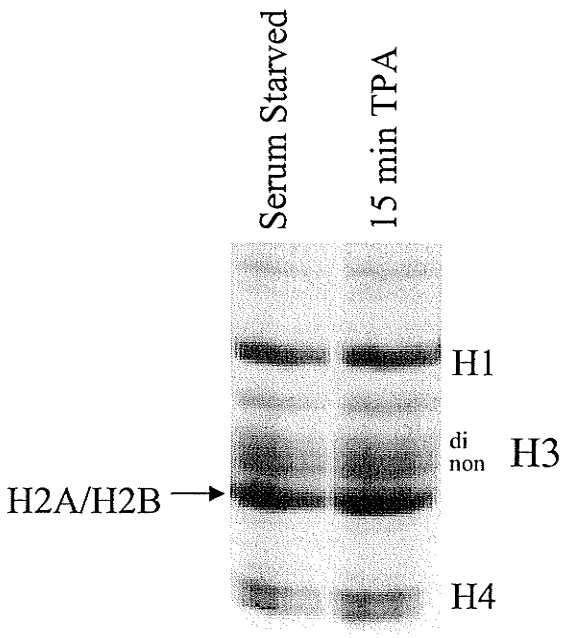

Figure 3-3. Acid-urea gel analysis of histones. Histones extracted from mouse fibroblasts were electrophoretically resolved in an acid-urea polyacrylamide gel. Bands were stained with Commassie Blue. Histones are labeled, with non, and di representing non-modified and di-modified H3 respectively.

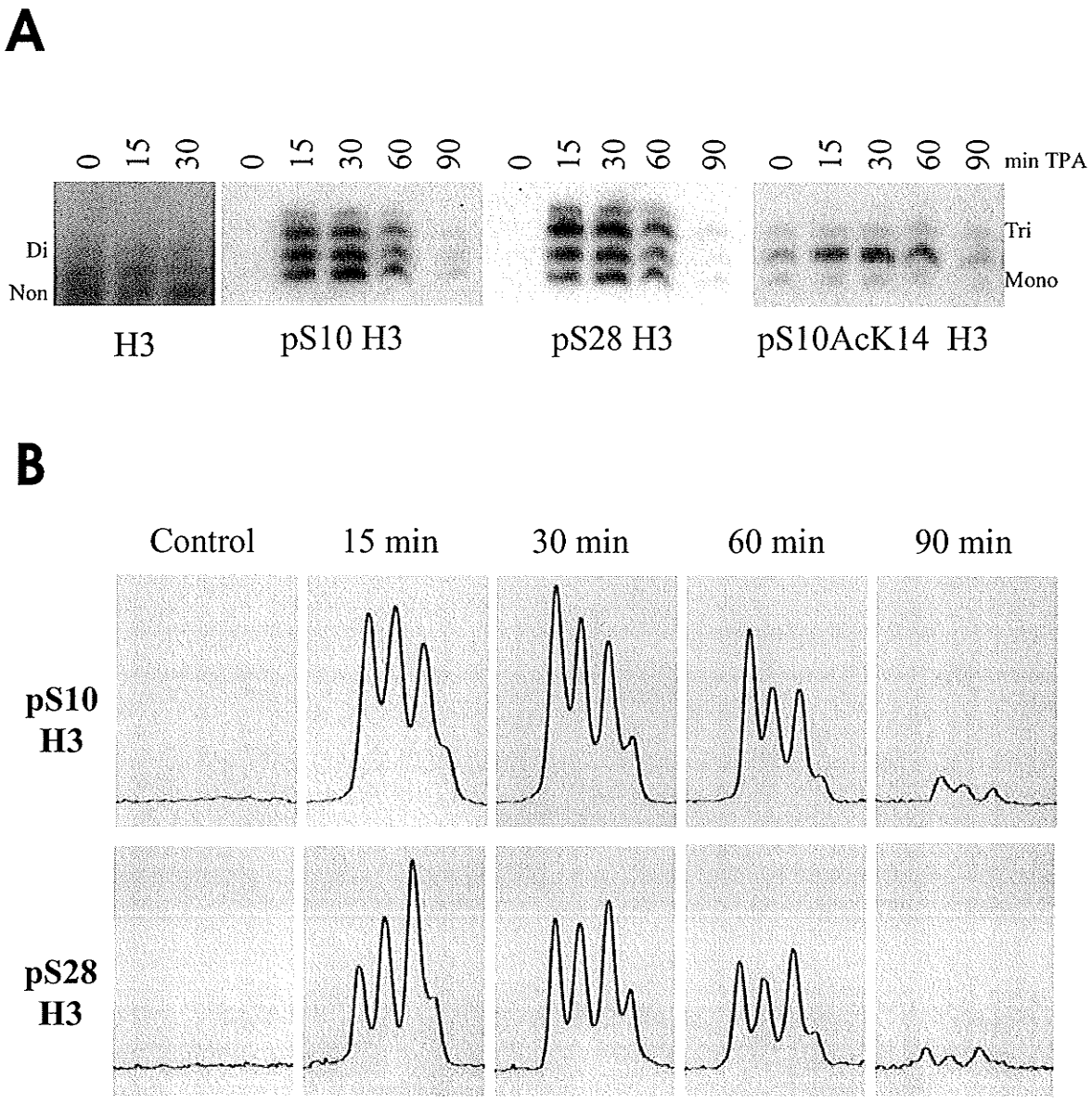

Figure 3-4. Steady-state distribution of H3 modified forms participating in TPA-induced phosphorylation. A and B) 100% confluent, serum-starved 10T1/2 fibroblasts were untreated or treated with 100 nM TPA for the times indicated at the top of each panel. A) Immunostaining of modified forms of H3 separated on an acetic acid–urea (AU) polyacrylamide gel with antibodies specific for total H3, phosphorylated H3 serine 10 (pS10 H3), phosphorylated H3 serine 28 (pS28 H3), and phosphorylated H3 Ser 10, acetylated Lys-14 H3 (pS10AcK14H3). Mono-, di-, tri-, and tetra- refer to the mono-, di-, tri-, and tetra-modified forms of H3, respectively. B) Relative abundance of modified states participating in TPA-induced H3 phosphorylation. Density of bands in (A) as determined by scanning the autoradiogram on a BioRad model 1650 scanning densitometer.

Histone hyperacetylation, mediated by the opposing activities of histone acetyltransferases and histone deacetylases, has long been associated with transcriptional activity. Levels of acetylated histone H3 present at immediate-early genes increase following mitogen or stress stimulation of the MAPK pathway [180,205]. Thus we sought to determine if the phosphorylation of H3 at serine 28 also occurs in regions where dynamic acetylation is taking place. To this end, 100% confluent, serum-starved cells were treated with a combination of the HDAC inhibitor trichostatin A (TSA) and TPA. TPA was added first for a period of fifteen minutes before TSA was added for an additional 15 minutes.

Histones extracted from treated and untreated cells were separated by SDS-PAGE, transferred to nitrocellulose and immunostained with antisera against H3 acetylated at lysines 9 and 14 (AcK9, 14 H3) (Figure 3-5 A). Loads were controlled for by staining membranes with India ink. The lanes containing TPA-treated and TPA, TSA-treated samples show increased loading compared to the serum-starved (SS) lane (lowest panel). The increased load in the TPA-treated lane accounts for the increased amount of AcK9, 14 H3 in this lane compared to the SS lane. The load in the TPA-treated lane is also up compared to that in the TPA, TSA-treated lane. However, the TPA, TSA-treated lane contains more AcK9, 14 H3 than both the SS lane and the TPA-treated lane. Thus the increased amount of AcK9, 14 H3 present in the TPA, TSA-treated lane can only be partially accounted for by the increased load (compared to SS), and must represent an increase in the amount of this histone modification in TPA,TSA-treated cells compared to serum-starved cells. Thus as expected treatment with TSA led to an increase in the

steady-state level of H3 acetylated at lysines 9 and 14 within 15 min of the start of treatment.

H3 phosphorylated at serine 10 was immunostained (Figure 3-5 B) on another blot and was elevated in both the TPA-treated and TPA, TSA-treated samples. Extracted histones were also separated on acid-urea gels, transferred to PVDF membrane, and immunostained for modified forms of H3 (pS10 H3, pS28 H3, pS10AcK14 H3). Total H3 was also stained as a loading control. As shown in Figure 3-5 C, following addition of TSA pS10 H3 and pS28 H3 modified forms of H3 are found in tri- and tetra-modified states. This result indicates that H3 phosphorylated at either serine 10 or serine 28 is in a region of chromatin undergoing dynamic acetylation.

Epitope occlusion has been noted for antibodies specific for modified histones. This phenomenon, in which the presence of additional modifications at sites within the antibody's epitope prevent antibody-antigen binding, limits the use of modification-specific antibodies. For example, an antibody to H3 phosphorylated at serine 10 described by Clayton *et al* [207], cannot recognize H3 phosphorylated at serine 10 if the molecule has also been acetylated at lysine 9. Other antibodies to H3 phosphorylated at serine 10 are able to recognize this modification even if acetylation at lysine 14 is present [208]. TSA-treatment leads to the formation of highly acetylated isoforms of H3. Possible sites of acetylation are lysines 4, 9, 14, 18, 23, and 27, all of which are in relatively close proximity to serine 10 and serine 28. Our antibodies for both H3 phosphorylated at serine 10 and H3 phosphorylated at serine 28 were able to detect highly acetylated isoforms of H3 (Figure 3-5 C), indicating that epitope occlusion due to acetylation was likely not a factor in our results. Other modifications, such as

methylation which can occur on H3 adjacent to serine 10 at lysine 9 and adjacent to serine 28 at lysine 27 could still be a factor in epitope recognition.

III. *Cells Containing a Constitutively Active Ras Display Anchorage-Independent Growth and Contain Increased Levels of Phosphorylated Chromatin Proteins*

Chromatin structure is often altered in transformed cells. Previous studies have shown that *ras*-transformed cells contain increased amounts of H3 phosphorylated at serine 10 [209]. We hypothesized that levels of H3 phosphorylated at serine 28 would also be increased in transformed cells. To compare histone modification levels, histones were extracted from sets of cell cycle matched parental 10T1/2 and *ras*-transformed C3 cells. Keeping the proportion of cells in each phase of the cell cycle approximately the same in each sample controlled for the extensive phosphorylation of H3 occurring in mitosis. Histones extracted from a set of cell cycle matched 10T1/2 and C3 cells were separated by SDS-PAGE, transferred to nitrocellulose, and immunostained with antisera specific to H3 phosphorylated at serine 28 or serine 10 and for total H3 to compare loading (Figure 3-6 A). Fluorescence activated cell sorting determined that the proportion of cells in the G2 and mitosis phases combined was 20% in 10T1/2 cells compared to 16% in C3 cells (refer to table in Figure 3-6 B). As expected, our *ras*-transformed C3 cells contained increased amounts of H3 phosphorylated at serine 10 (Figure 3-6 A). The level of H3 phosphorylated at serine 28 was more abundant in C3 cells even though the parental 10T1/2 cells had a slightly higher proportion of cells in the G2/M phase of the cell cycle. Immunoblots were stripped following detection of pS10 H3 and pS28 H3 and re-probed with antisera against total H3 to show equal loading of each sample.

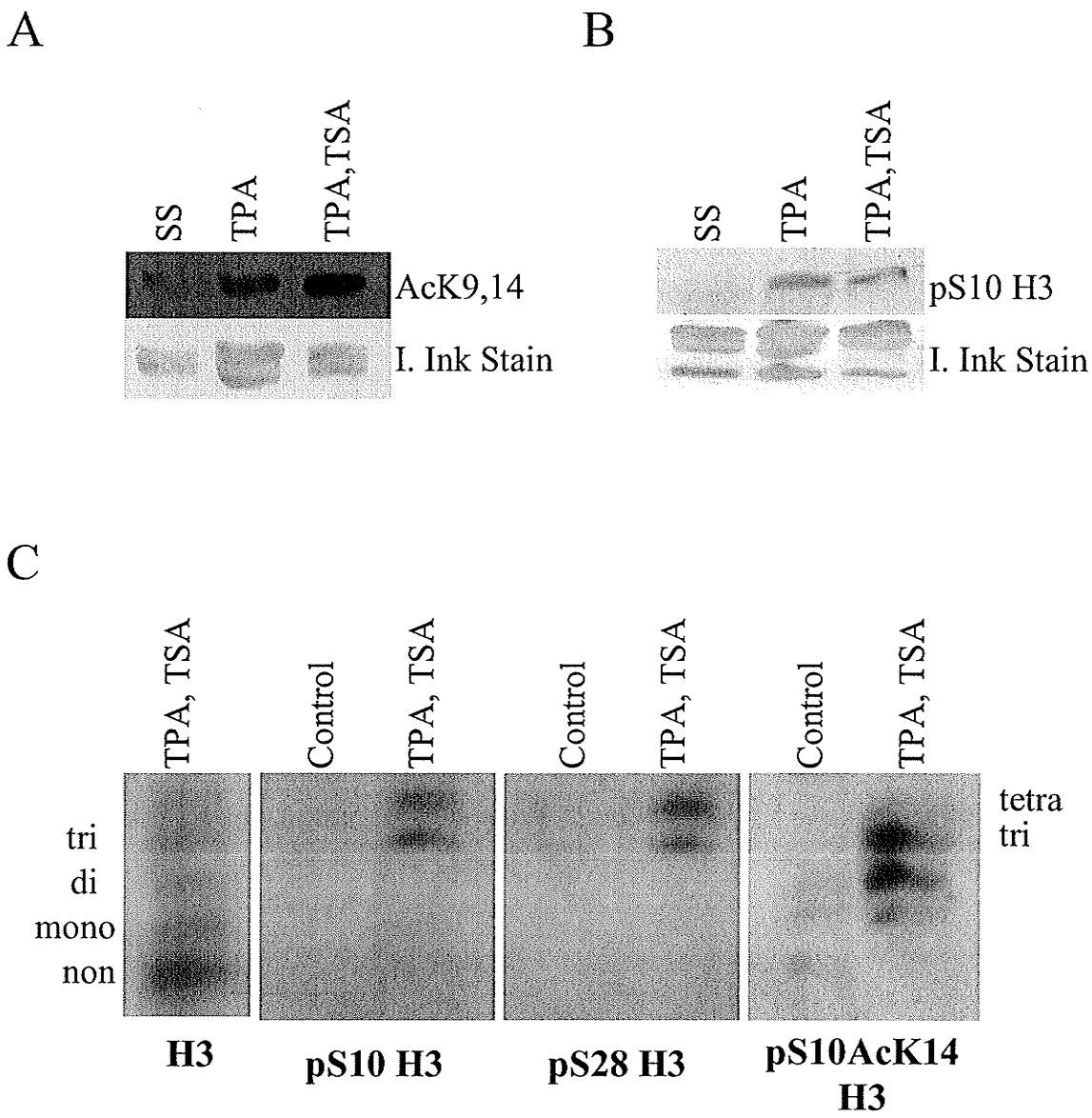

Figure 3-5. Mitogen-induced H3 phosphorylation occurs on chromatin undergoing dynamic acetylation. 100% confluent, serum-starved 10T1/2 fibroblasts were treated with 100 nM TPA for 15 min followed by a combination of 100 nM TPA and 500 ng/ml TSA for 15 min. A and B) Histones separated by SDS-PAGE were immunostained with antisera against H3 acetylated at lysines 9 and 14 (AcK9,14) and H3 phosphorylated at serine 10 (pS10 H3). India ink (I. Ink) was used to check for equal loading. C) Modified forms of H3 separated on an AU polyacrylamide gel and immunostained with antisera specific for H3 phosphorylated at serine 10 (pS10 H3), phosphorylated at serine 28 (pS28 H3), phosphoacetylated (pS10AcK14 H3) and total H3

A

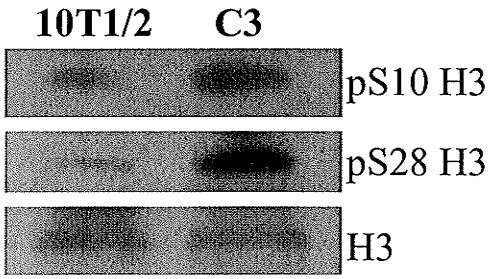

B

Cell Line	G1	S	G2/M
	cell cycle phase (% distribution)		
10T1/2	63	17	20
C3	60	24	16

Figure 3-6. *Ras*-transformed cells contain increased levels of H3 phosphorylated at serine 28. A) Histones extracted from a set of cell-cycle matched 10T1/2 and C3 cells were resolved in SDS-polyacrylamide gels, transferred to nitrocellulose and immunostained with antisera against H3 phosphorylated at serine 10 (pS10 H3), H3 phosphorylated at serine 28 (pS28 H3) and total H3. B) The percentage of cells determined by fluorescence activated cell sorting to be in G1 phase, S phase and G2/M phases combined are given for the samples in (A).

The structural chromatin protein HMGN1 is also targeted for MAPK pathway induced phosphorylation at serine residues 6, 20 and 24 [180]. Given that our *ras*-transformed cells display an altered chromatin structure [209] and increased levels of H3 phosphorylated at serines 10 and 28 (Figure 3-6), we hypothesized that these cells also contained increased amounts of phosphorylation on HMGN1 at serine 6, 20 and 24, and that this may contribute to their abnormal chromatin structure.

Like histone H3, HMGN1 becomes phosphorylated during mitosis. Recognizing this, we collected a set of parental 10T1/2 and transformed C3 cells with equal proportions of cells in G2/M phases. Acid-extracted material from one plate of 10T1/2 cells and 2 different plates of C3 cells were separated by SDS-PAGE and transferred to nitrocellulose. An antibody is commercially available against HMGN1 phosphorylated at serine 6, but not serine 20 or 24. Thus, blots were immunostained with antisera against HMGN1 phosphorylated at serine 6 (pS6 HMGN1), then stripped and re-probed with antisera against total HMGN1 as a control for loading (Figure 3-7 A).

The results of fluorescence activated cell sorting are shown in Figure 3-7 B. In all three samples 22% of cells were in mitosis or G2 phase, providing an approximately equal background of HMGN1 phosphorylation occurring during mitosis. Similar levels of pS6 HMGN1 were detected in both samples from C3 cells (C3 a and C3 b, Figure 3-7 A lanes 1 and 3). Approximately equal levels of total HMGN1 were detected in all three lanes. The level of pS6 HMGN1 in C3 cells was higher than in the parental 10T1/2 cells.

Abnormal nuclear morphology is a hallmark used to diagnose cancer. C3 cells, produced by transfecting parental 10T1/2 mouse fibroblasts with a constitutively active *Ha-ras* oncogene, also have this feature [249]. In addition, most normal cells require adherence

to a solid support in order to grow and divide. The loss of this phenomenon is a characteristic of transformed cells. In a paper published in 1987, C3 cells were shown to grow in an anchorage-independent manner [272]. As cells lines have a tendency towards genomic instability and change over time, we performed the colony formation assay to ascertain that our C3 cells were still able to grow in an anchorage-independent manner.

Equal numbers of 10T1/2 and C3 cells were seeded in semi-solid media and incubated at 37°C (5% CO_2) for periods of two to four weeks. As pictured in Figure 3-8, the parental 10T1/2 cells were not able to proliferate, while the *ras*-transformed C3 cells formed many colonies. The lower panel of pictures, taken at a relatively high magnification, provide a close-up view of the colonies. In a representative experiment, an average of 1265 colonies of C3 cells and 25 colonies of 10T1/2 cells were counted (refer to table in Figure 3-8 B). Thus the C3 cells used in these studies exhibit the hallmark ability of transformed cells to grow in an anchorage-independent manner.

A

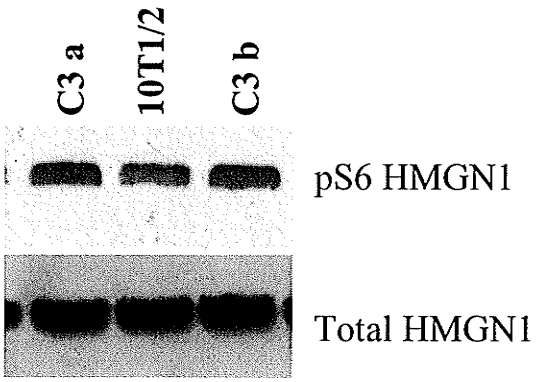

B

Cell Line	G1	S	G2/M
	cell cycle phase (% distribution)		
10T1/2	61	16	22
C3 a	55	23	22
C3 b	55	23	22

Figure 3-7. Increased amounts of HMGN1 phosphorylated at serine 6 are present in *ras*-transformed cells. A) Acid-extracted proteins from a set of cell-cycle matched 10T1/2 and C3 cells were resolved in SDS-polyacrylamide gels, transferred to nitrocellulose and immunostained with antisera against HMGN1 phosphorylated at serine 6 (pS6 HMGN1) and total HMGN1. B) The percentage of cells from (A) in each phase of the cell cycle as determined by fluorescence activated cell sorting. G1 represents G1 phase, S represents S phase and G2/M represents the G2 and M phases combined.

A

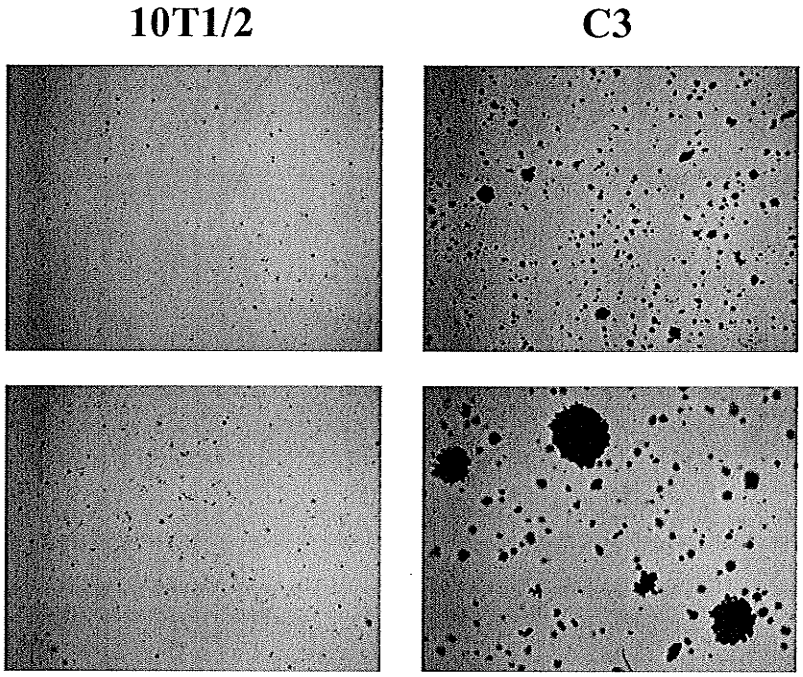

B

Cell Line	Number of Colonies
Parental 10T1/2	25
Ras-Transformed C3	1265

Figure 3-8. *Ras*-transformed cells grow in an anchorage-independent manner. Equal numbers of parental 10T1/2 mouse fibroblasts and *ras*-transformed C3 cells were seeded in semi-solid media in a soft agar assay for colony formation. A) Pictures taken after 14 days incubation at 37°C. The top panel shows cells at 12X magnification, the bottom at 19X magnification. B) The average number of colonies of 5 cells or more as counted under a light microscope.

IV. Characteristics of Mitogen-Induced H3 Phosphorylation in Ras-Transformed Cells

The pattern of mitogen-induced expression of the immediate-early *c-fos* gene in C3 cells differs from what is seen in the parental cells. When measured by Northern blot at 0, 15, 30, 60 and 90 minutes into TPA-stimulation, c-fos message levels were highest at 15 minutes in parental cells but at 30 minutes in the *ras*-transformed C3 cells [198]. To determine if the timing of the induction of H3 phosphorylation matches the temporal pattern of message induction, modified histones extracted from C3 cells treated with TPA for periods of 0, 15, 30, 60 and 90 minutes were separated by SDS-PAGE, transferred to nitrocellulose, and detected with the antisera against H3 phosphorylated at serine 10 and serine 28 (Figure 3-9). As seen in parental 10T1/2 cells, phosphorylation of H3 at serine 10 and at serine 28 is induced within fifteen minutes of the beginning of TPA-stimulation. In samples taken at 0, 15, 30, 60 and 90 minutes TPA-treatment, the highest levels of H3 phosphorylation at serine 10 or 28 was detected at thirty and sixty minutes in *ras*-transformed cells (Figure 3-9 lanes 3,4). As in parental 10T1/2 cells, phosphorylation at serines 10 and 28 was transient, decreasing substantially within 90 minutes of the start of stimulation. Overall, the temporal pattern of H3 phosphorylation in C3 cells is similar to that seen in the parental cells (Figure 3-1); however we detected the peak to be later in C3 cells. The maximal levels of H3 phosphorylation at serine 10 and serine 28 in mitogen-induced *ras*-transformed cells (Figure 3-9) matches the peak level of mitogen-induced *c-fos* message in these cells [198].

To determine if *ras*-transformation had an effect on the spatial localization of H3 phosphorylated at serines 10 or 28, we fixed cycling, untreated C3 cells and performed

indirect immunofluorescence with the antisera described above. The results, shown in Figure 3-10, indicate that like in parental 10T1/2 cells many foci of phosphorylated H3 are present in the interphase nucleus of C3 cells localized to regions of relatively relaxed chromatin.

In mouse fibroblasts, HMGN1 is rapidly phosphorylated by MSK1 and 2 at serines 6, 20 and 24 by MSK1/2 following stimulation of the Ras-MAPK pathway [180]. As HMGN1 -/- cells display increased levels of steady-state H3 phosphorylation at serine 10, it has been postulated that phosphorylation events on HMGN1 facilitate its dissociation from nucleosomes to allow increased phosphorylation of H3 [195]. We sought to determine if, like phosphorylation of H3, the temporal induction pattern of HMGN1 phosphorylation at serine 6 in response to Ras-MAPK pathway stimulation is altered in *ras*-transformed cells. To this end, acid-extracted proteins from 100% confluent, serum-starved 10T1/2 and C3 cells treated with 100 nM TPA for periods lasting between 0 and 90 min were resolved in SDS-polyacrylamide gels and analyzed by immunoblot with antisera against total HMGN1 and HMGN1 phosphorylated at serine 6 (pS6 HMGN1) (Figure 3-11). In parental 10T1/2 cells, a dramatic increase in the level of pS6 HMGN1 was observed 15 minutes after the start of TPA-treatment (Figure 3-11). Levels of pS6 HMGN1 remained high for the length of the study, dropping only slightly at 90 min TPA. In *ras*-transformed cells a similar pattern was observed (Figure 3-11). A substantial increase in the amount of pS6 HMGN1 was already present 7 minutes after the start of TPA-stimulation. A further increase was detected at 15 min, after which levels remained high until decreasing slightly in the 90 min sample. Total HMGN1 stained to act as a loading control detected similar amounts of total HMGN1 in all lanes of C3 samples.

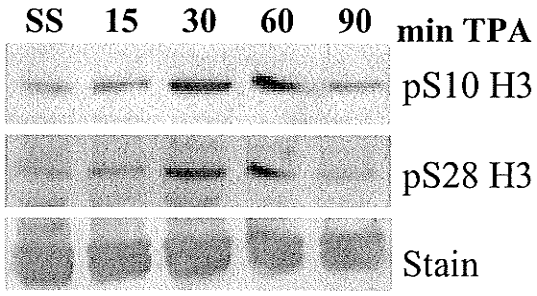

Figure 3-9. Phosphorylation of H3 on serine 28 is induced by stimulation of the Ras-MAPK pathway in *ras*-transformed cells. Histones extracted from TPA-stimulated, serum-starved (SS) C3 cells were resolved on SDS–15% polyacrylamide gels, transferred to nitrocellulose, and immunostained with antisera against H3 phosphorylated on serine 10 (pS10 H3) or 28 (pS28 H3). Membranes were stained with India Ink (stain) as a control for loading.

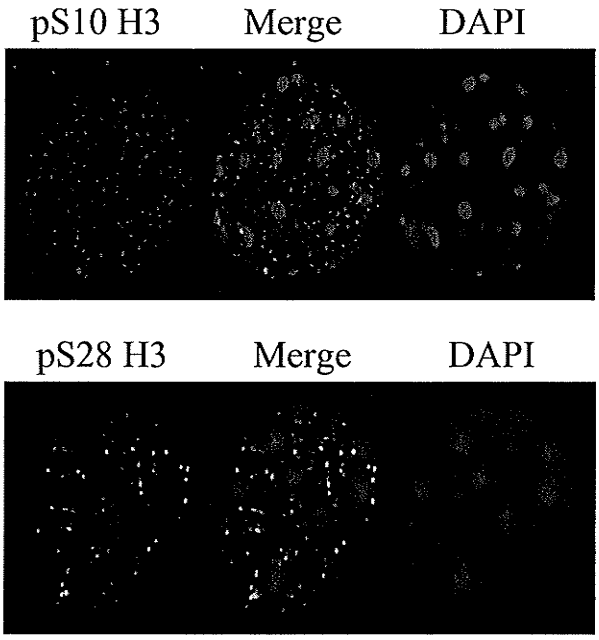

Figure 3-10. Phosphorylated H3 localizes to regions of relatively relaxed chromatin in interphase C3 cells. Indirect immunofluorescence to detect phosphorylated H3 serine 28 (pS28 H3) or serine 10 (pS10 H3) was performed on interphase, untreated C3 cells grown to approximately 70% confluence. Cells were co-stained with DAPI. Digital optical sections of 0.25 μm were obtained and false-coloured green (pS28 H3), red (pS10 H3) or blue (DAPI). Images of nuclei were deconvolved with Axiovision 3.1 software.

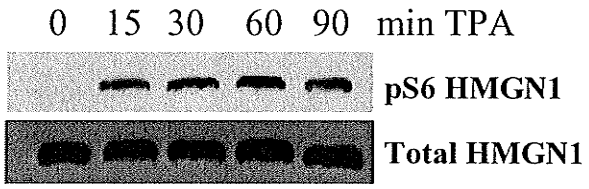

10T1/2

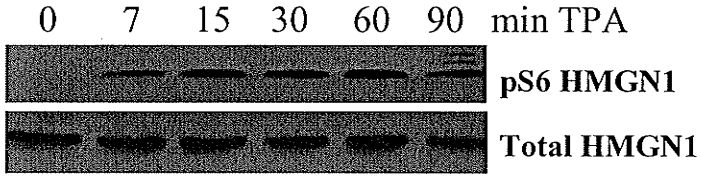

C3

Figure 3-11. Phosphorylation of HMGN1 following stimulation of the Ras-MAPK pathway. Acid extracted proteins from 100% confluent, serum-starved, TPA-treated 10T1/2 or C3 cells were resolved on SDS-polyacrylamide gels, transferred to nitrocellulose, and immunostained with antisera against total HMGN1 or HMGN1 phosphorylated at serine 6 (pS6 HMGN1).

The chromatin of *ras*-transformed fibroblasts is less condensed than that of parental cells [209] and contains increased levels of modifications to chromatin proteins (Figures 3-6, 3-7) relative to parental cells. C3 cells, transformed with *Ha-ras*, contain increased amounts of activated ERKs and higher levels of H3 kinase activity relative to parental cells, indicating that the Ras-MAPK pathway is constitutively active in these cells [262]. To determine if constitutive activation of the Ras-MAPK pathway results in a shift in the steady-state level of charge-altering modifications present on H3 phosphorylated at serine 10 or 28, we analysed histone samples extracted from C3 cells on acid-urea polyacrylamide gels. Included were regularly cycling cells, cells treated with the microtubule-interfering agent colcemid, and cells that were 100% confluent, serum-starved and TPA-treated for various lengths of time.

Despite constitutive activation of the Ras-MAPK pathway, the steady-state distribution of H3 modified forms participating in TPA-induced H3 phosphorylation is similar to what is seen in parental cells (Figure 3-12 A). At 30 min TPA treatment, pS10 H3 and pS28 H3 were detected in mono-, di-, tri-, and tetra-modified isoforms. As was found in parental 10T1/2 cells, H3 phosphorylated at serine 10 was most likely to be present in a population of H3 having only one or two residues whose charge had been altered by acetylation or phosphorylation (mono- or di-modified). In addition, H3 phosphorylated at serine 28 tended to be in higher modified isoforms than those seen for pS10 H3 (Figure 3-12 A).

C3 cells were also treated with a combination of TPA and the HDAC-inhibitor TSA. Histones extracted from cells which were treated with TPA/TSA for a period of 15 min following a 15 minute incubation with TPA were separated by SDS-PAGE, transferred to

nitrocellulose, and immunostained with antibodies to acetyl lysine 9, 14 H3 and H3 phosphorylated at serine 10. Results are shown in Figure 3-12 B, which indicate that TSA treatment led to an increase in the steady-state level of H3 acetylated at lysines 9 and 14. The sample, which had only been treated with TPA, did not show elevation of AcK9, 14 H3, while the sample treated only with TSA had levels approximately equal to that of samples treated with a combination of TPA/TSA. Staining with antisera to H3 phosphorylated at serine 10 demonstrated the expected induction in TPA-treated samples.

Samples were also separated in acid-urea polyacrylamide gels. In this case, treatment with TSA (Figure 3-12 C) resulted in a shift of pS10 H3 and pS28 H3 into higher modified states. As in the parental cells, pS10 H3 and pS28 H3 extracted from C3 cells treated with a combination of TPA and TSA were present in tri- and tetra-modified isoforms, indicating that these populations had two or three other charge-altering modifications. Antisera against H3 phosphoacetylated at serine 10 lysine 14 detected an increase in this combination of modifications in cells treated with a combination of TPA and TSA, with most species of pS10AcK14 H3 being in di- and tri-modified states. In parental 10T1/2 cells, H3 phosphoacetylated at serine 10 lysine 14 was predominantly in a di-modified state (Figure 3-12 C). Given that the acid-urea gel staining pattern of both H3 phosphorylated at serine 10 and H3 phosphorylated at serine 28 bears great similarity to that seen in samples from parental 10T1/2 cells, this result likely represents a shift of pS10AcK14 H3 into higher modified states.

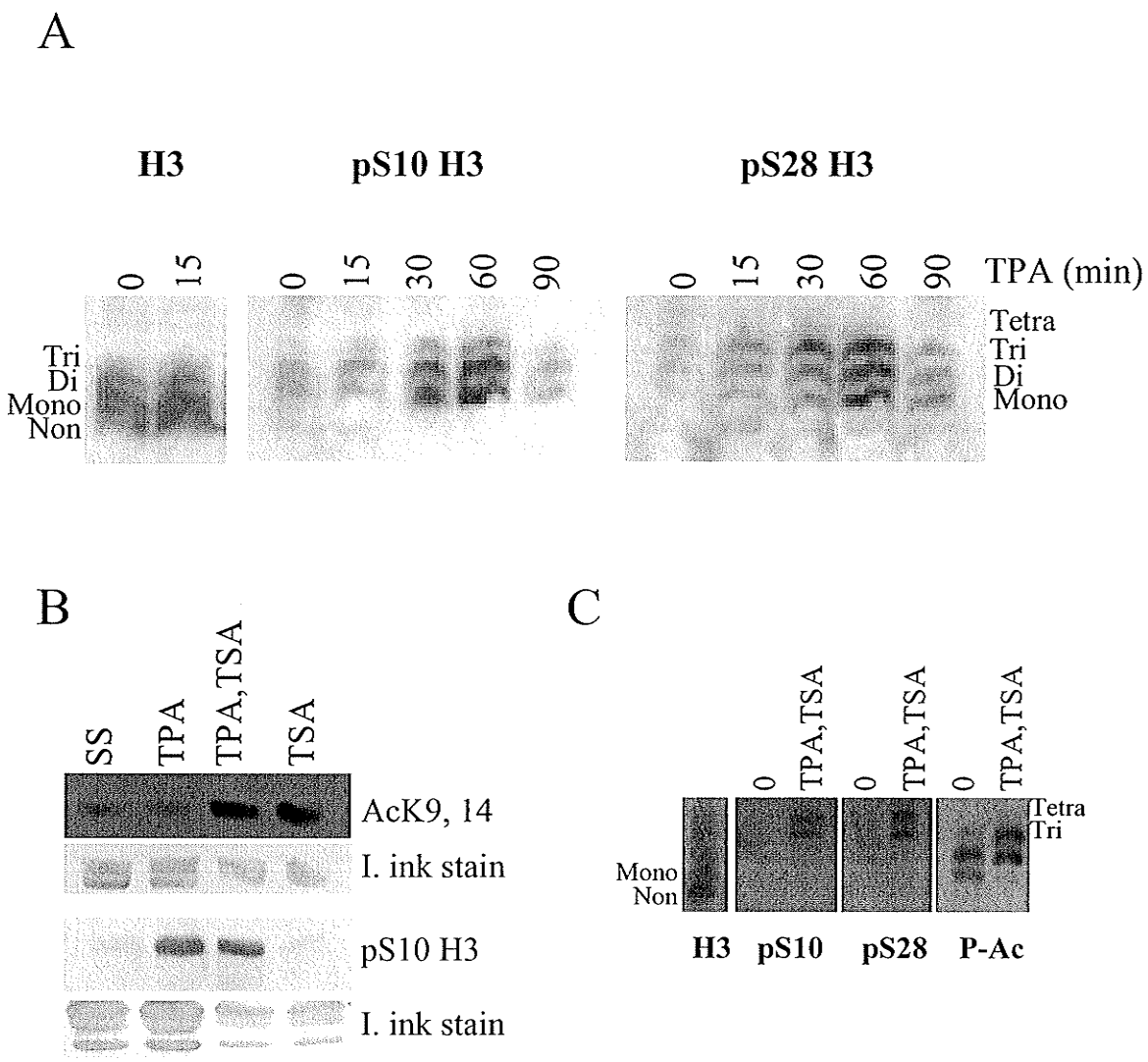

Figure 3-12. Steady-state levels of H3 modified forms participating in TPA-induced H3 phosphorylation in *ras*-transformed cells. A and C) Histones extracted from TPA-stimulated, serum-starved C3 cells were resolved on acid urea gels, transferred to PVDF membrane, and immunostained with antisera against H3 phosphorylated at serine 10 (pS10 H3), H3 phosphorylated at serine 28 (pS28 H3), H3 phosphoacetylated at serine 10 lysine 14 (P-Ac) and total H3. B and C) Histones were extracted from cells treated with a combination of 100 nM TPA for 15 min followed by 100 nM TPA and 500 ng/ml TSA for an additional 15 min. B) Samples were separated by SDS-PAGE, transferred to nitrocellulose and immunostained with antisera against H3 acetylated at lysine 9 and 14 (AcK9, 14) and H3 phosphorylated at serine 10 (pS10 H3). India ink was used to stain membranes as a loading control.

Unlike H3 phosphorylation following stimulation of the Ras-MAPK pathway, Aurora B-mediated phosphorylation of histone H3 at serine 10 and 28 during mitosis is widespread. The Aurora B-mediated H3 phosphorylation of chromatin in 10T1/2 cells during G2 and M phases is shown in Figure 3-13; cells were grown to approximately 60% confluence in complete medium, fixed and stained with the antisera described above. Phosphorylation of H3 begins in late G2 in regions of pericentromeric heterochromatin (Figure 3-13 B, top panel) and spreads in the pattern of chromosome condensation. In 10T1/2 cells, phosphorylation of H3 at serine 10 precedes that at serine 28 (Figure 3-13 A). By prophase, condensed chromosomes are highly phosphorylated at serine 10 and 28, and remain that way until late telophase (Figure 3-13 B).

To determine the number of charge-altering modifications present on H3 tails that are phosphorylated at serines 10 or 28 during mitosis, we extracted histones from cycling 10T1/2 and C3 cells and those treated with colcemid. FACS was performed to determine the percentage of cells in each phase of the cell cycle. Colcemid effectively prevented cells from completing mitosis, raising the proportion of cells in G2/M from 20 to 80% in treated cells (Figure 3-14 B). The expected increase in the level of phosphorylated H3 present in colcemid-treated cells was confirmed by separating extracted histone samples by SDS-PAGE, transferring to nitrocellulose and immunostaining with antibodies recognizing H3 phosphorylated at serine 10 and serine 28. The results of this Western blot are shown in Figure 3-14 A. When we compared the distribution of phosphorylated H3 isoforms taking part in TPA-induced phosphorylation to that in cycling and colcemid-treated cells, a striking difference was found. In the serum-starved, TPA-treated cells, H3 phosphorylated at serine 10 and 28 was present in mono-, di- and tri-modified

isoforms with minor amounts existing in tetra-modified states (Figures 3-4 and 3-12). H3 phosphorylated during mitosis in 10T1/2 cells was most prevalent in di-modified isoforms, with very little in mono- or tri-modified states (Figure 3-14 C). This was true for isoforms of H3 phosphorylated at serine 10 and at serine 28. In *ras*-transformed C3 cells, H3 phosphorylated during mitosis also tended to be in di-modified isoforms, however an increased proportion of isoforms phosphorylated at serine 28 were in a tri-modified state (Figure 3-14 C).

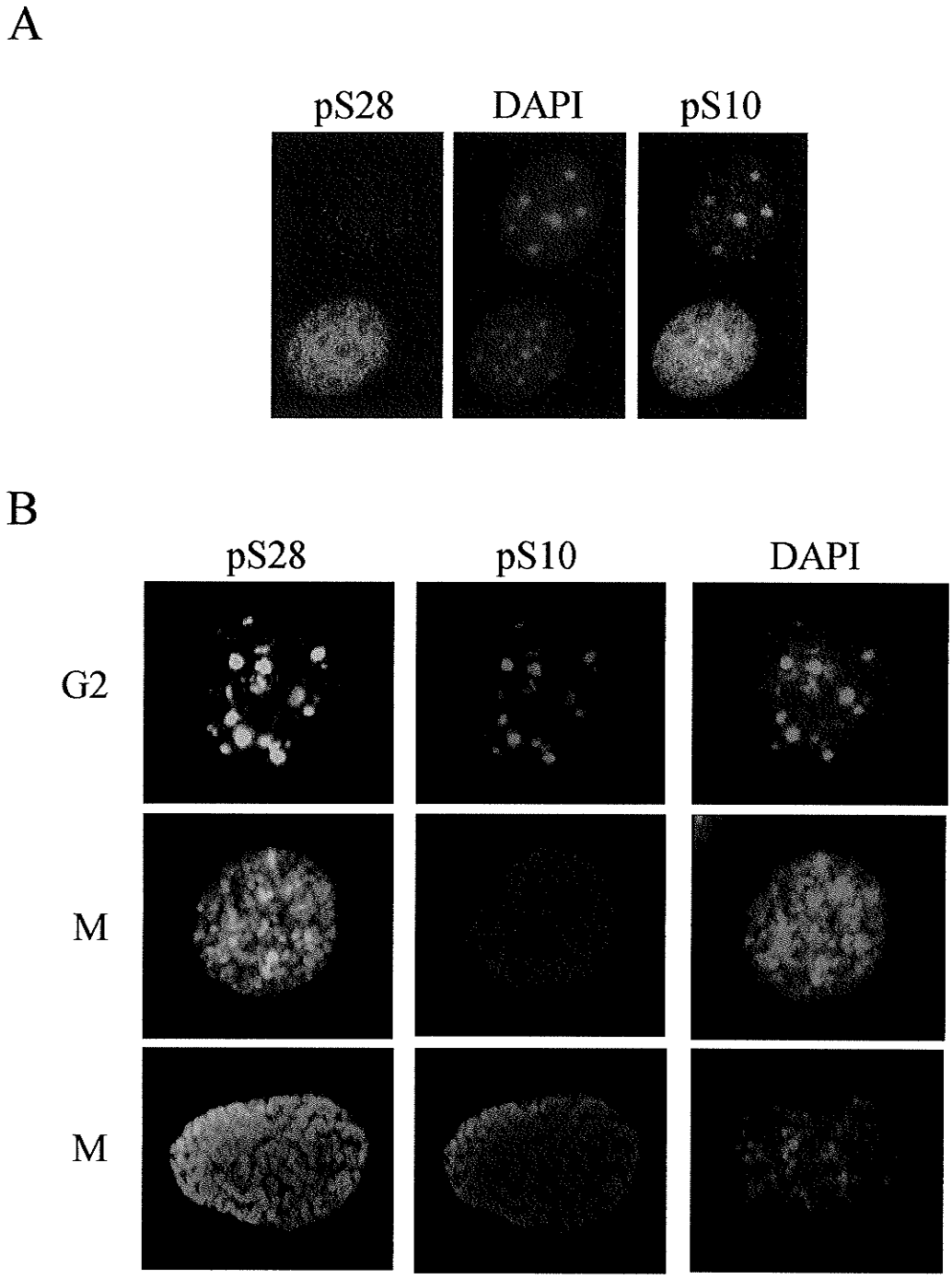

Figure 3-13. Phosphorylation of H3 at serine 10 and at serine 28 occurs on condensed chromosomes during mitosis. 10T1/2 cells were fixed and stained with antibodies recognizing H3 phosphorylated at serine 10 (pS10) and serine 28 (pS28). Cells were co-stained with DAPI. Digital optical sections of 0.25 or 0.3 μm were obtained and false-coloured green (pS28), red (pS10) or blue (DAPI). A) Phosphorylation of serine 10 in late G2 precedes that of serine 28. B) The cell cycle phase (M stands for Mitosis) is indicated on the left side of the panel.

A

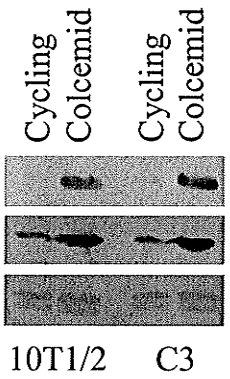

B

	G1	S	G2/M
	cell cycle phase (% distribution)		
10T1/2 cycling	63	17	20
10T1/2 colcemid	10	10	80

C

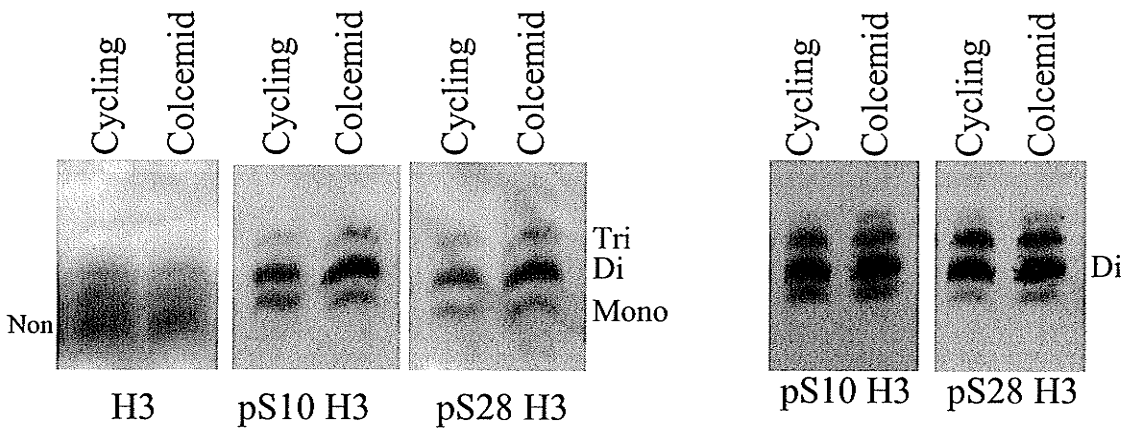

Figure 3-14. Steady-state distribution of H3 modified forms participating in mitotic H3 phosphorylation. A and C) Histones were extracted from 10T1/2 and C3 cells that were untreated or treated with 0.06 μg/ml colcemid for 16 hours. A) Increased H3 phosphorylation in samples from colcemid-treated cells. Modified histones resolved in SDS-polyacrylamide gels, transferred to nitrocellulose and detected with antisera against phosphorylated H3 serine 10 (pS10 H3) and phosphorylated H3 serine 28 (pS28 H3). India ink stain (lowest panel) was used to check loading. B) The percentage of cells from in each phase of the cell cycle as determined by fluorescence activated cell sorting (G1 phase, S phase, and G2/M phases combined). C) Immunostaining of modified forms of H3 separated on an acetic acid–urea (AU) polyacrylamide gel with antisera against total H3 in addition to the antisera described above.

V. *Analysis of H3 Variant Modification*

The process of transcription disrupts nucleosomes. As H3.3 is the only H3 variant to accumulate outside of S-phase [277], it will be incorporated into the disrupted nucleosomes associated with transcriptionally active genes as they are reconstituted in G0, G1 and G2 phases of the cell cycle. Enrichment of H3.3 at transcriptionally active loci is likely a consequence of this event [93,278-281]. Thus we surmised that G1-phase transcription of immediate-early genes would lead to the incorporation of H3.3 and an enrichment of this variant in immediate-early gene chromatin. We hypothesized that H3.3 is the major target of Ras-MAPK-pathway induced H3 phosphorylation.

To this end, we separated H3 variants extracted from 100% confluent serum-starved and TPA-stimulated (15 minutes) mouse 10T1/2 mouse fibroblasts by two dimensional electrophoresis. Histones were resolved electrophoretically in a first dimension acid-urea-triton (AUT) gel by size and hydrophobicity (Figure 3-15 A) followed by electrophoresis through a SDS-15% polyacrylamide gel. Separation of histones in an SDS 15%-polyacrylamide gel, shown in Figure 3-15 B, is generally by size. The resolution of mouse fibroblast histones after two dimensional gel electrophoresis in this manner is shown by the Coommassie Blue-stained two dimensional gel pattern in Figure 3-15 C. Histone H4 migrates the fastest through AUT and SDS-15% polyacrylamide gels. Differences in the hydrophobicity of H3.1, H3.2 and H3.3 separate bands of these variants in AUT gels. The bands become compacted during electrophoresis through the second dimension SDS polyacrylamide gel. Following two dimensional gel electrophoresis, histones were transferred to nitrocellulose and immunostained with

antisera against phosphorylated H3. India ink or staining with antisera against total H3 was used to visualize the location of histone variants on nitrocellulose blots.

The distribution of H3 variants phosphorylated at serine 10 or at serine 28 following TPA-stimulation of serum-starved cells is shown in Figure 3-16. No phosphorylation of H3 on serine 10 or 28 was found in serum-starved cells that had not been stimulated with TPA (Figure 3-16 A and data not shown). Following TPA-stimulation, phosphorylation of serine 10 and of serine 28 was detected on H3.2 and H3.3, and to a lesser extent H3.1 (Figure 3-16 B and C left panel). The low levels of phosphorylation on H3.1 appear to correlate with a lower abundance of this variant (Figure 3-16 B and C, lower left panel), however we detected greater levels of H3.1 phosphorylated on serine 10 than H3.1 phosphorylated on serine 28. Thus, contrary to our hypothesis H3.1, H3.2, and H3.3 are all targets for TPA-induced phosphorylation. The distribution of H3 variants phosphorylated at serine 10 and at serine 28 was also determined for samples taken from serum-starved, TPA-treated *ras*-transformed C3 cells. No phosphorylation was detected in serum-starved cells (data not shown). Similar to the parental fibroblasts, phosphorylation of serine 10 and serine 28 was observed on H3.1, H3.2, and H3.3 (Figure 3-16 B and C).

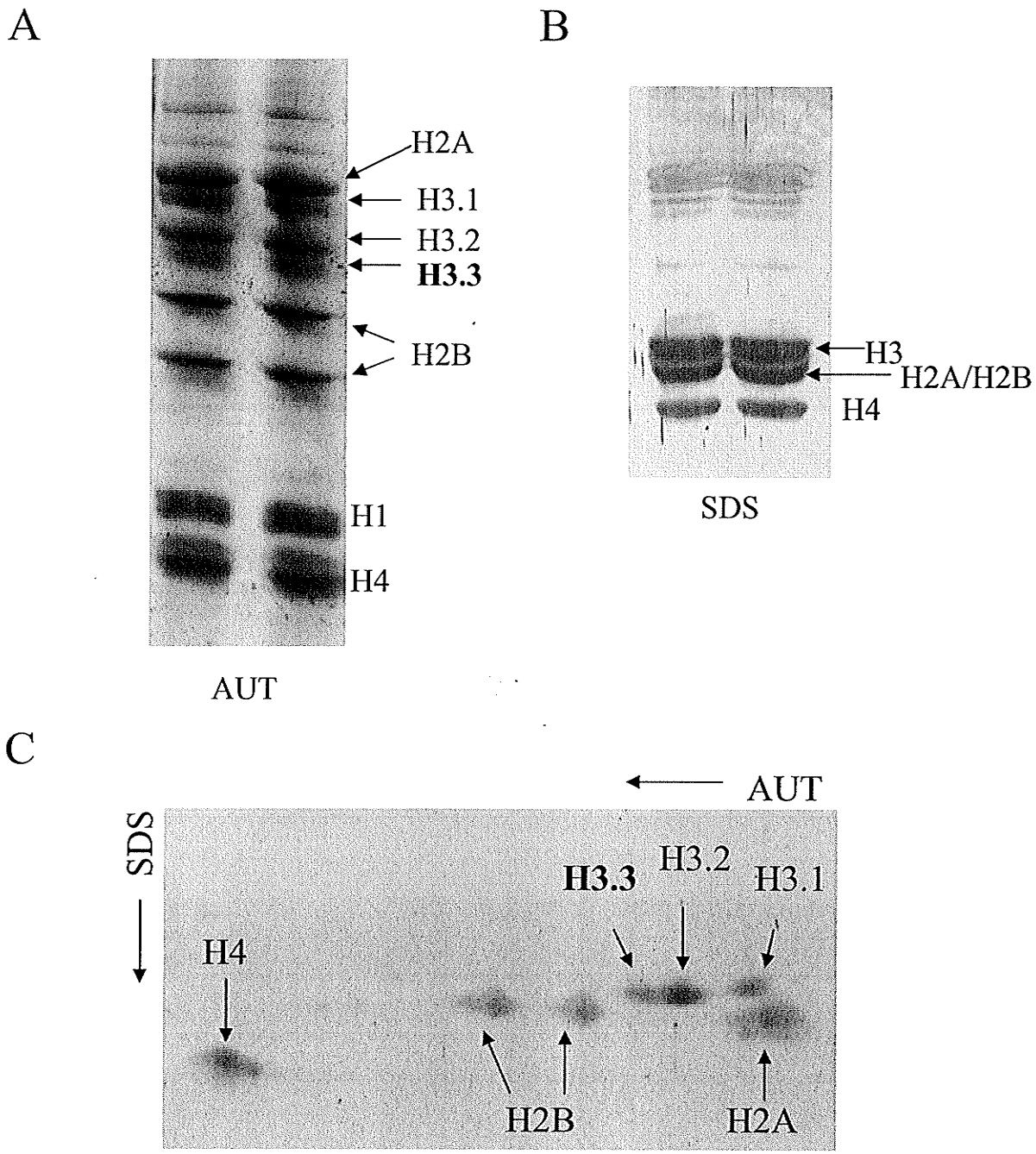

Figure 3-15. Resolution of mouse fibroblast histones by two-dimensional electrophoresis. A) Resolution of murine histones in AUT polyacrylamide gels. B) Resolution of histones in SDS 15%-polyacrylamide gels. C) Histones extracted from mouse fibroblasts were first electrophoretically resolved in an AUT polyacrylamide gel in the direction shown at the top of the panel, followed by electrophoresis through a second dimension SDS-15% polyacrylamide gel. A, B and C) The pattern of histones was revealed with Commassie Blue staining.

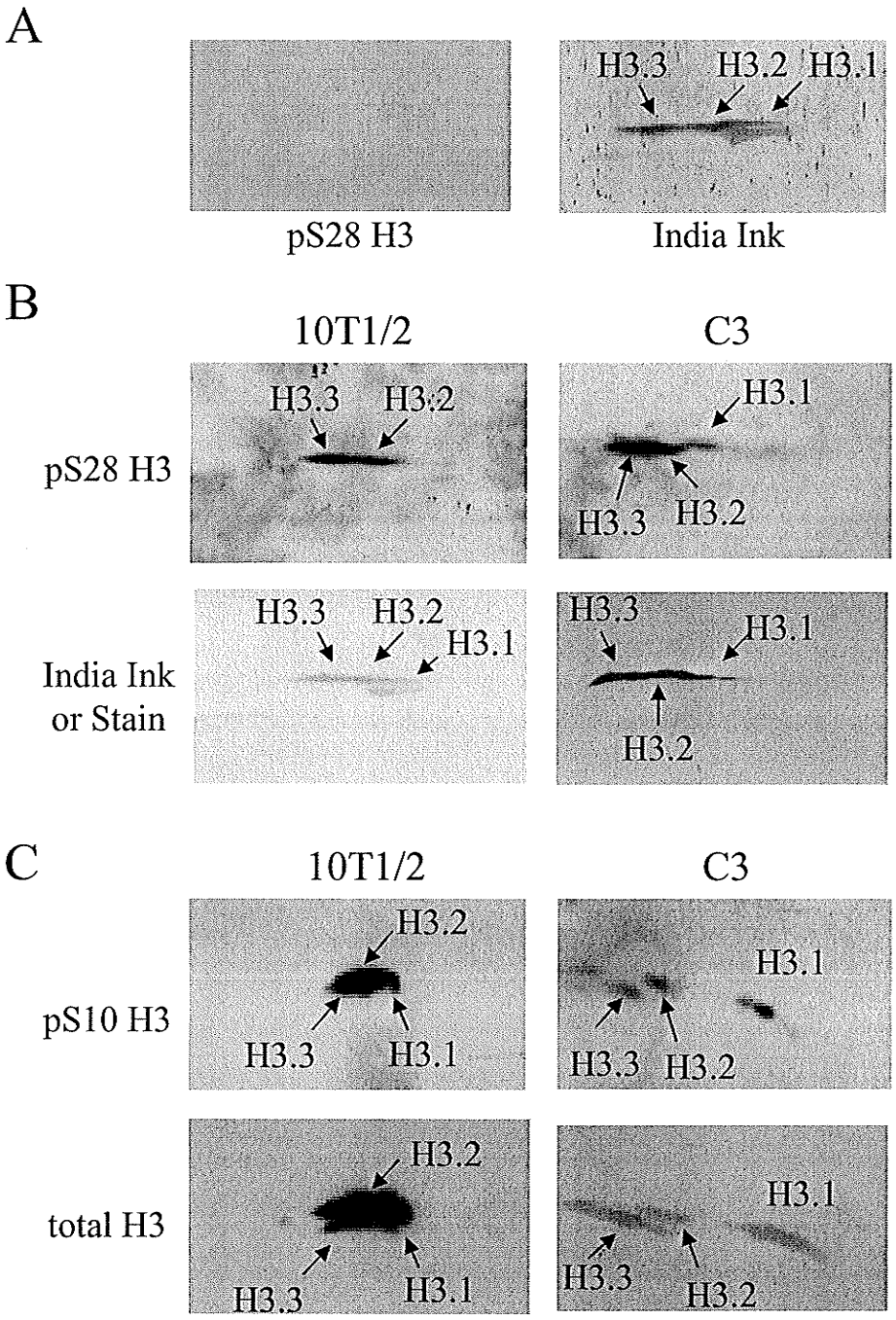

Figure 3-16. Identification of H3 variants participating in TPA-induced phosphorylation. A) Histones extracted from 100% confluent, serum-starved 10T1/2 cells separated by two-dimensional electrophoresis and immunostained for H3 phosphorylated on serine 28 (pS28 H3). The India Ink stained blot shown on the right indicates the loading of histone samples. B and C) Histones extracted from 10T1/2 or C3 cells treated with TPA for 15 min were separated by two-dimensional electrophoresis and immunostained for phosphorylated H3 serine 28 (pS28 H3) or phosphorylated H3 Ser-10 (pS10 H3) as indicated on the left hand side of panel. Corresponding India Ink-stained blots or blots immunostained for total H3 are shown in the lower panels.

The H3 variants phosphorylated by Aurora B during mitosis were also determined. Histones extracted from cycling and colcemid-treated cells were resolved in two-dimensional AUT-SDS polyacrylamide gels, transferred to nitrocellulose and modified histones detected with antisera against H3 phosphorylated at serine 10 (pS10 H3) or at serine 28 (pS28 H3). Due to the fact that H3 phosphorylation during interphase occurs only on a very small subset of genes, the overwhelming majority of H3 molecules phosphorylated at serine 10 or 28 in these samples will have come from a cell undergoing mitosis. The results of this experiment, shown in Figure 3-17, do not indicate a preference for any one of H3.1, H3.2 or H3.3. Phosphorylation of H3 on serine 10 and on serine 28 took place on all three non-centromeric variants of H3 in both parental (Figure 3-17, left panel) and C3 fibroblasts (right panel).

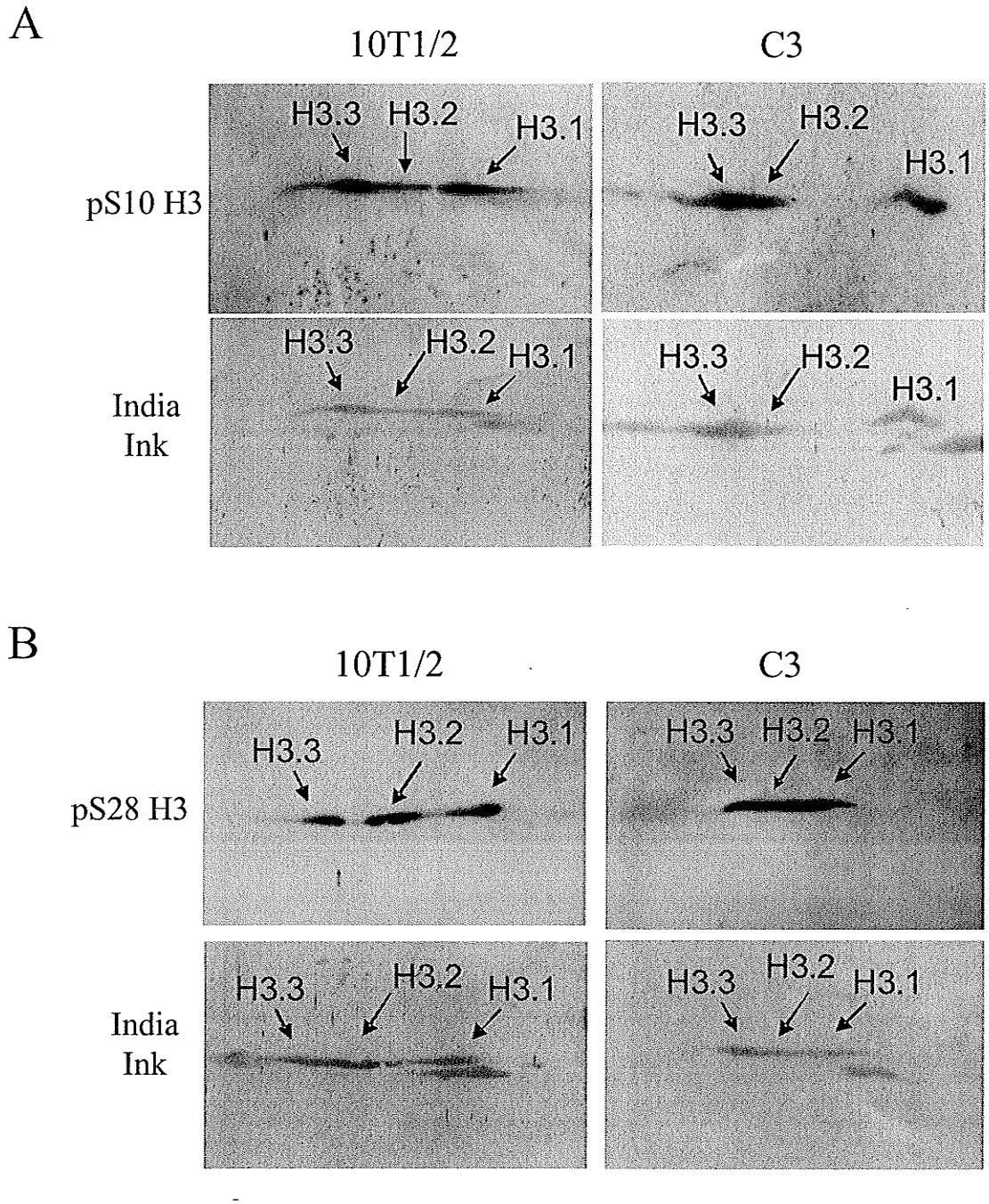

Figure 3-17. H3 variant phosphorylation during mitosis. A and B) Histone variants isolated from cycling and colcemid-treated 10T1/2 and C3 cells were resolved by two-dimensional electrophoresis and transferred onto nitrocellulose membranes. Blots were immunostained with antibodies recognizing H3 phosphorylated on serine 10 (pS10 H3) or serine 28 (pS28 H3). Loading of histone samples was determined by staining with India ink (lower part of panels).

VI. *Distinct Pools of Chromatin Become Phosphorylated at Serine 10 or at Serine 28 Following Stimulation of the MAPK Pathway*

We have found that H3 phosphorylation in response to stimulation of the Ras-MAPK pathway at serine 28 tends to take place on H3 tails that are modified by acetylation/phosphorylation to a greater extent than those tails on which H3 is phosphorylated at serine 10. The presence of significant amounts of H3 phosphorylated at serine 28 or serine 10 in the mono-modified isoform of H3 indicates that this phosphorylation event is not dependent on phosphorylation at serine 10 and *vice versa*. To establish if these modifications were occurring in the same areas of chromatin in 100% confluent, serum-starved, EGF- or TPA-treated fibroblasts the location of H3 phosphorylated at serine 28 was visualized by indirect immunofluorescence in combination with H3 phosphorylated at serine 10 and H3 phosphoacetylated at serine 10 lysine 14.

EGF predominantly stimulates the Ras-MAPK but also weakly stimulates the p38 MAPK pathway. Antisera against H3 phosphorylated at serine 10 and H3 phosphorylated at serine 28 recognized many foci in serum-starved cells treated with EGF for periods of 10, 15 and 30 minutes (Figure 3-18). All foci were excluded from pericentromeric heterochromatin, and most foci of H3 phosphorylated at serine 28 did not overlap foci of H3 phosphorylated at serine 10. TPA does not stimulate the p38 MAPK pathway. We compared the phosphorylation pattern induced by EGF to that induced by TPA. Following stimulation of the Ras-MAPK pathway with EGF or TPA, maximal levels of phosphorylation are observed approximately 15 minutes after the start of treatment. At this timepoint, antisera against H3 phosphorylated at serine 10 and H3 phosphorylated at

serine 28 recognized many foci in each TPA-stimulated cell (Figure 3-19). As was seen in EGF-treated cells, foci were located in regions of relatively relaxed chromatin, and most of the numerous foci of H3 phosphorylated at serine 10 present in each cell did not colocalize with foci of H3 phosphorylated at serine 28 (Figure 3-19 A). We estimate that approximately 83% of foci of H3 phosphorylated at serine 28 do not overlap foci of H3 phosphorylated at serine 10, in serum-starved cells treated with TPA for a period of 15 min. A linescan through an imaged nucleus using metamorph software to measure the intensity of each signal (Figure 3-19 B) indicated that most peaks of pS28 H3 do not correspond to peaks of pS10 H3. Some peaks, however, do overlap (see arrow, Figure 3-19 B), perhaps indicating that some foci are targeted for H3 phosphorylation at both residues following MAPK-pathway stimulation.

Furthermore, most foci of phosphoacetylated (serine 10 lysine 14) H3, a combination of modifications found at immediate-early genes following stimulation of the MAPK pathway [207], did not colocalize with H3 phosphorylated at serine 28 (Figure 3-20 A). In a linescan of these data several peaks of pS28 H3 overlap peaks of pS10AcK14 H3, however almost none line up exactly (Figure 3-20 B). Thus these results indicate that for the most part phosphorylation of H3 at serine 28 occurs independently of phosphorylation at serine 10 on distinct regions of chromatin.

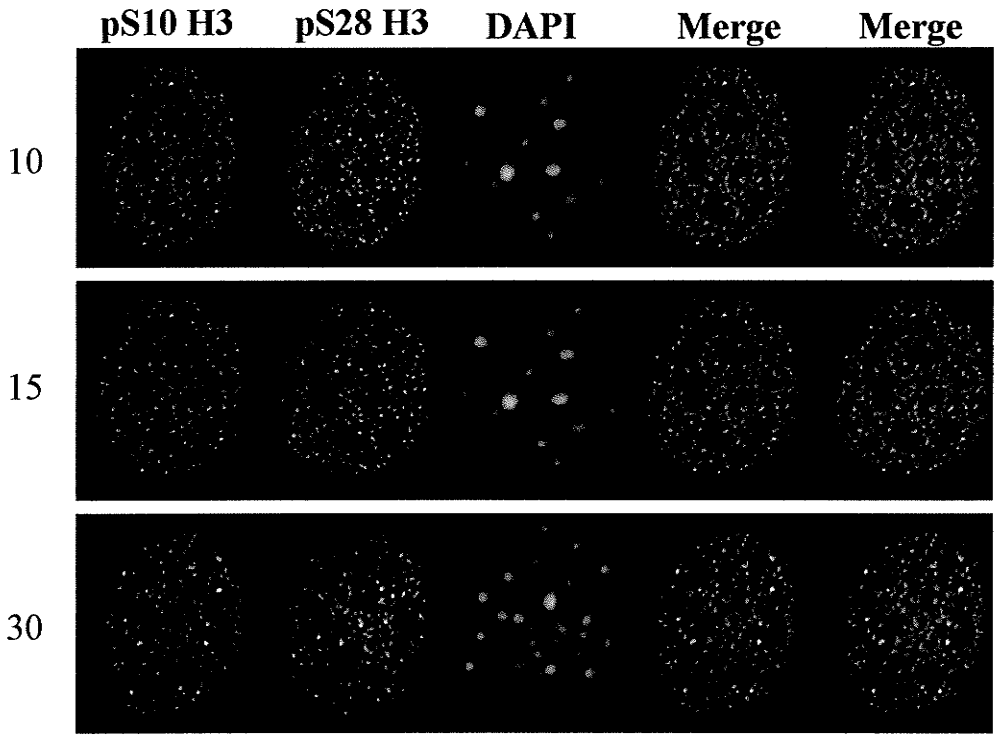

Figure 3-18. Independent pools of chromatin are phosphorylated on H3 at serine 10 and at serine 28 following EGF stimulation. 100% confluent, serum-starved 10T1/2 cells were treated with 50 ng/ml EGF for 10, 15 or 30 minutes before cells were fixed and immunostained with antisera recognizing H3 phosphorylated at serine 10 or serine 28. Digital optical sections were obtained and false coloured red (pS28 H3), green (pS10 H3) or blue (DAPI). Images were deconvolved using Axiovision 3.1 software.

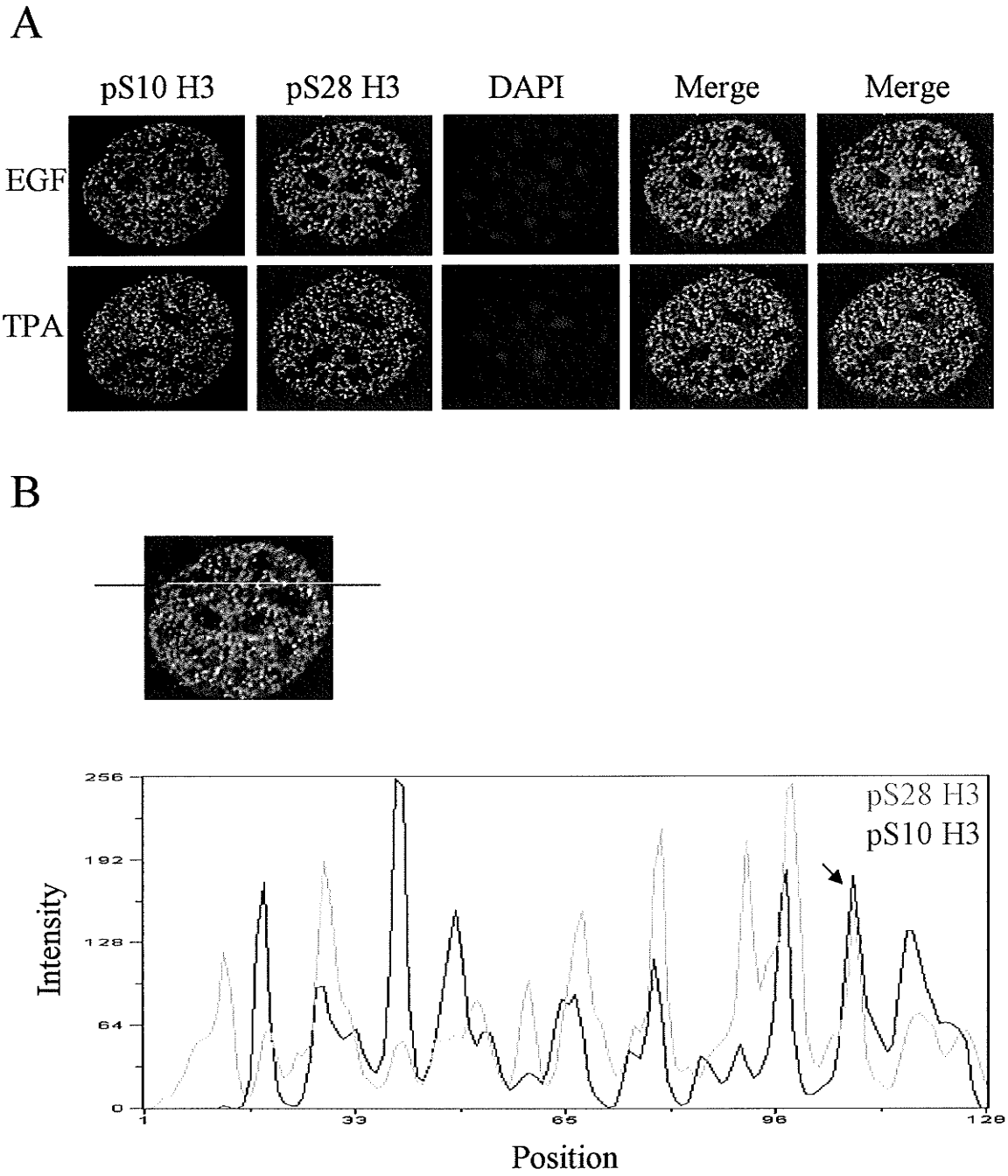

Figure 3-19. Foci of H3 phosphorylated at serine 10 or serine 28 are distinct at the time of maximal phosphorylation following Ras-MAPK pathway stimulation. 100% confluent, serum-starved 10T1/2 cells were treated with 100 nM TPA or 50 ng/ml EGF for 15 minutes before cells were fixed and immunostained with antisera recognizing H3 phosphorylated at serine 10 (pS10 H3) or serine 28 (pS28 H3). A) Digital optical sections were obtained and false coloured red (pS10 H3), green (pS28 H3) or blue (DAPI). B) Metamorph software was used on a deconvolved image of a TPA-treated cell to obtain a linescan along the blue line shown in the upper panel. Intensity values for pS10 H3 and pS28 H3 can be seen in the linescan in the lower panel. The black arrow indicates two overlapping peaks.

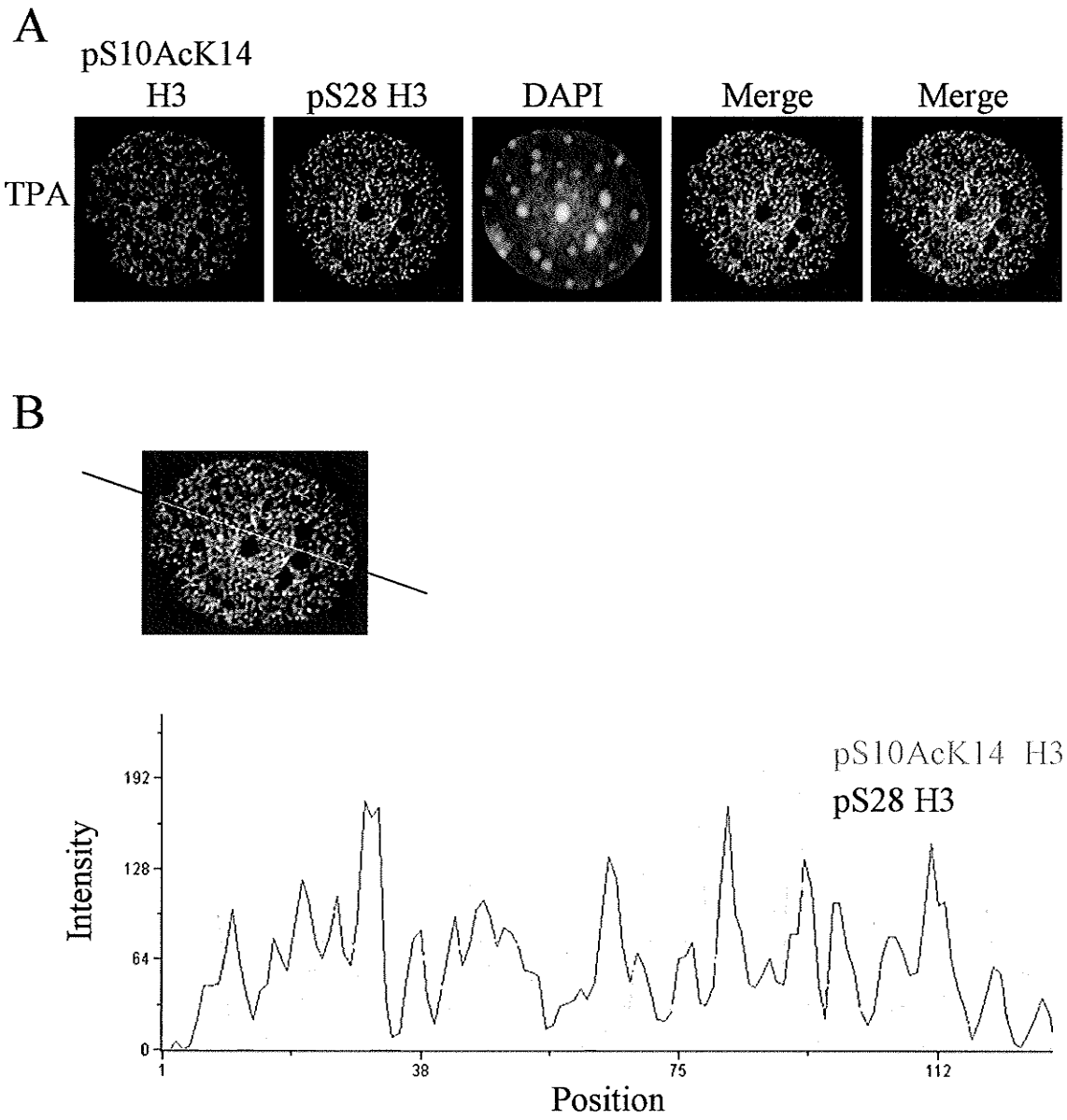

Figure 3-20. Regions of chromatin phosphorylated at serine 28 following TPA stimulation are distinct from those phosphoacetylated at serine 10 lysine 14. A) 100% confluent, serum-starved 10T1/2 cells were treated with 100 nM TPA for 15 minutes before cells were fixed and immunostained with antisera recognizing H3 phosphorylated at serine 28 or phosphoacetylated at serine 10 lysine 14. Digital optical sections were obtained and false coloured red (pS10AcK14 H3), green (pS28 H3) or blue (DAPI). B) Metamorph software was used on a deconvolved image of a TPA-treated cell to obtain a linescan along the blue line shown in the upper panel. Intensity values for pS10AcK14 H3 and pS28 H3 can be seen in the linescan in the lower panel.

Phosphorylation of HMGN1 following mitogen-stimulation is postulated to cause its release from nucleosomes and allow for increased H3 phosphorylation at serines 10 and 28. We visualized pS6 HMGN1 in 100% confluent, serum-starved, TPA-treated 10T1/2 cells by indirect immunofluorescence and found that following MAPK pathway stimulation numerous foci of pS6 HMGN1 are present that do not colocalize with foci of H3 phosphorylated at serine 28 (Figure 3-21 A). A linescan of this data revealed little overlap between peaks of pS6 HMGN1 and pS28 H3 (Figure 3-21 B).

Constitutive activation of the Ras-MAPK pathway in C3 cells leads to elevated levels of pS10 H3 and pS28 H3. This could be achieved in one of two ways; (1) an increased number of residues are being phosphorylated at the normal targets of mitogen-induced H3 phosphorylation or (2) there is aberrant targeting of the H3 kinases leading to H3 phosphorylation at inappropriate foci. Aberrant targeting could cause foci that should only be phosphorylated at one residue, perhaps serine 28, to become phosphorylated at both. To determine if pools of chromatin targeted for phosphorylation at serine 10 or serine 28 remain separate in cells containing a constitutively active Ras-MAPK pathway, we performed indirect immunofluorescence of cycling C3 cells.

Figure 3-22 shows the presence of numerous foci of H3 phosphorylated at serine 10 and serine 28 in the interphase nucleus of *ras*-transformed cells. Detection of pS10 H3 and pS28 H3 in the same nucleus determined that even in *ras*-transformed cells, when the Ras-MAPK pathway is constitutively active, foci of pS10 H3 remain separate from foci of pS28 H3.

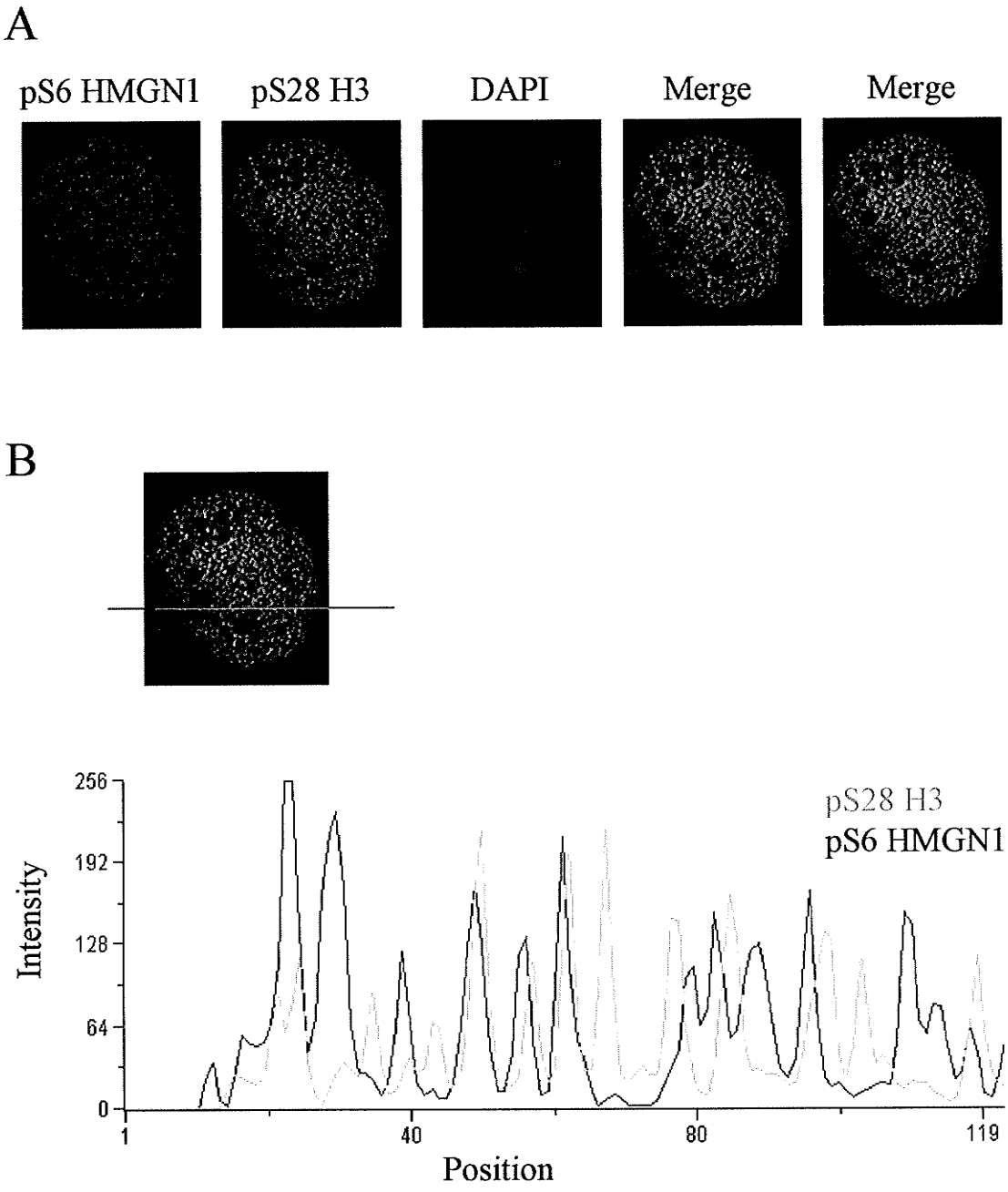

Figure 3-21. Following TPA stimulation foci of phosphorylated HMGN1 do not colocalize with regions of H3 phosphorylated at serine 28. A) 100% confluent, serum-starved 10T1/2 cells were treated with 100 nM TPA for 15 minutes before cells were fixed and immunostained with antisera recognizing H3 phosphorylated at serine 28 (pS28 H3) and HMGN1 phosphorylated at serine 6 (pS6 HMGN1) Digital optical sections were obtained and false coloured red (pS6 HMGN1), green (pS28 H3) or blue (DAPI). Images were deconvolved with Axiovision 4.4 software. B) Metamorph software was used on a deconvolved image of a TPA-treated cell to obtain a linescan along the blue line shown in the upper panel. The intensity of pS28 H3 and pS6 HMGN1 are shown in the lower panel.

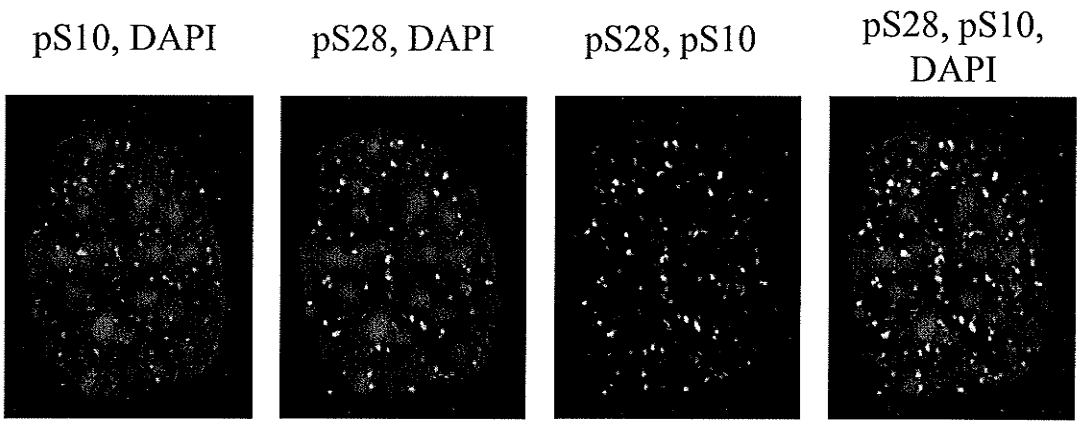

Figure 3-22. Phosphorylation of H3 at serine 28 remains distinct from that at serine 10 in *ras*-transformed cells. Indirect immunofluorescence was performed on interphase C3 cells. H3 phosphorylated at serine 28 (pS28) and H3 phosphorylated at serine 10 (pS10) were detected in a single cell with specific antisera. Cells were co-stained with DAPI. Digital optical sections of 0.25 μm were obtained and false-coloured green (pS28), red (pS10) or blue (DAPI). Images were deconvolved with Axiovision 3.1 software.

VII. Foci of RNA Polymerase II, MSK1 and MSK2 Associate with Regions of H3 Phosphorylated at Serine 10 and Serine 28 in Mitogen-Induced Fibroblasts

Phosphorylation of H3 at serine 10 is known to occur at immediate-early genes such as *c-jun*, *c-myc*, and *c-fos* following stimulation of the Ras-MAPK pathway [180,209]. H3 phosphorylation is thought to facilitate activation of these genes. The targets for H3 phosphorylation at serine 28 have not yet been identified. We hypothesize that targets for mitogen-induced H3 phosphorylation at serine 28 are also immediate early genes.

Before progression to transcriptional elongation, RNA polymerase II is phosphorylated at serine 5. We used indirect immunofluorescence to visualize the subcellular location of RNA polymerase II phosphorylated at serine 5 (pS5 RNA pol II) and pS10 H3 or pS28 H3 in serum-starved, TPA-treated (100 nM) 10T1/2 cells. Many foci of pS5 RNA pol II were present in the TPA-treated nuclei, each potentially representing a site of transcription. In a timeline monitoring the induction of H3 phosphorylation, many foci of H3 phosphorylated at serine 10 (Figure 3-23) or serine 28 (Figure 3-24) overlap foci of pS5 RNA pol II. The greatest amount of colocalization is seen at the timepoints showing the highest levels of H3 phosphorylation, those being 10, 15 and 30 min TPA. These data are consistent with the presence of pS10 H3 and pS28 H3 at sites of mitogen-induced transcription.

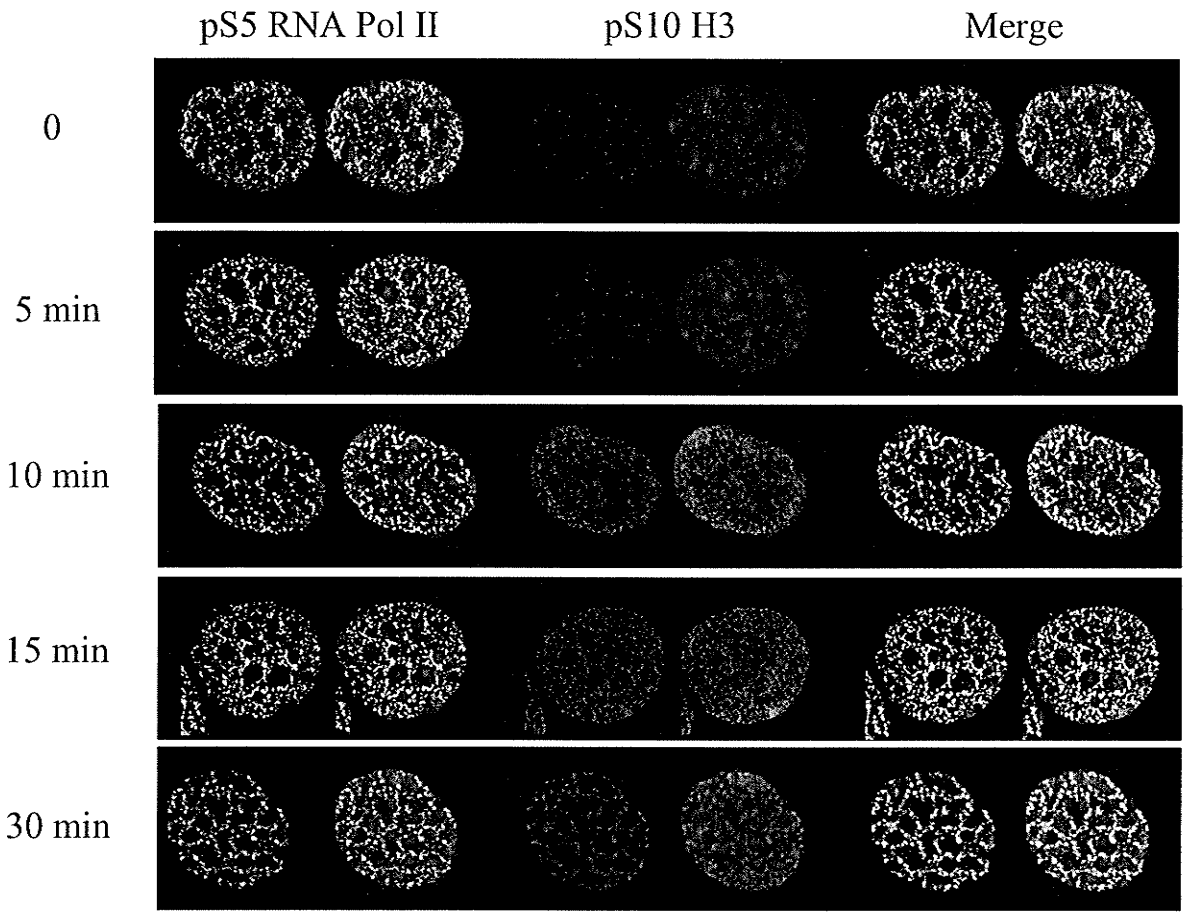

Figure 3-23. Temporal localization of mitogen-induced H3 phosphorylation at serine 10 and pS5 RNA pol II. 100% confluent, serum-starved 10T1/2 cells were treated with 100 nM TPA before cells were fixed and immunostained with antisera recognizing H3 phosphorylated at serine 10 and RNA pol II phosphorylated at serine 5. Digital optical sections were obtained and false coloured green (pS5 RNA pol II), red (pS10 H3) or blue (DAPI). Images were deconvolved with Axiovision 4.4 software.

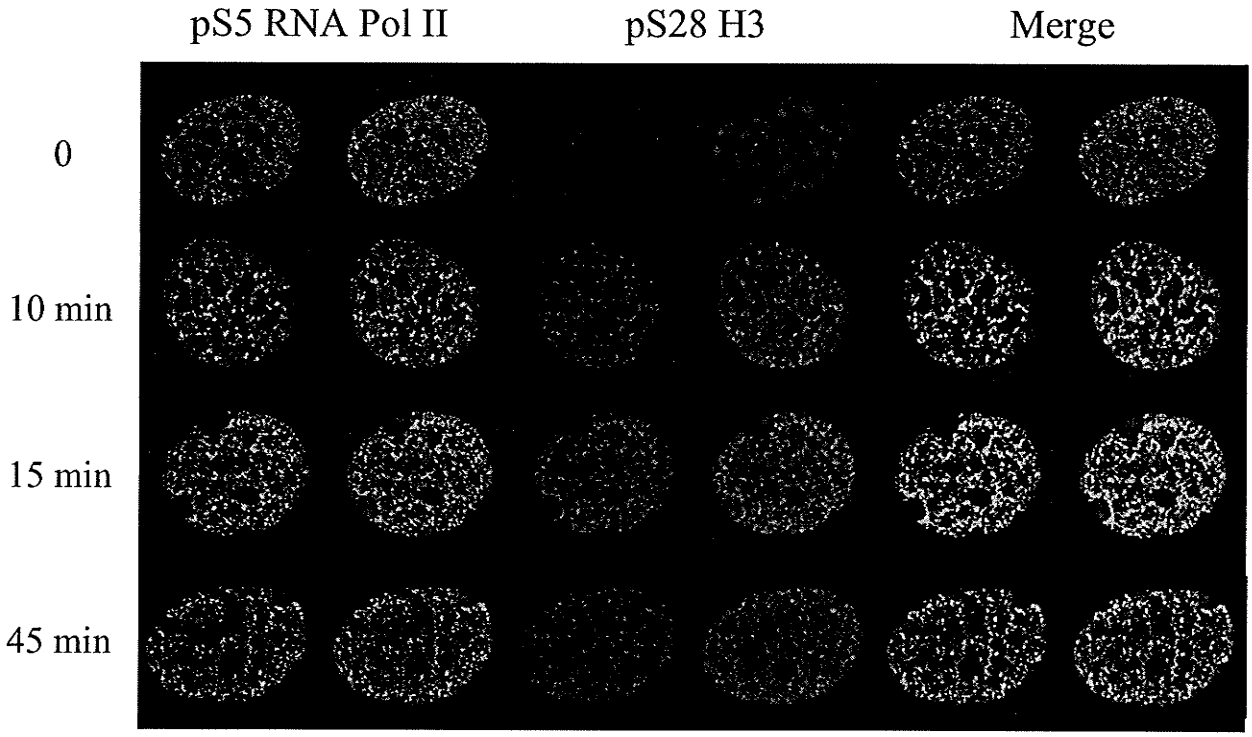

Figure 3-24. Temporal localization of mitogen-induced H3 phosphorylation at serine 28 and pS5 RNA pol II. 100% confluent, serum-starved 10T1/2 cells were treated with 100 nM TPA before cells were fixed and immunostained with antisera recognizing H3 phosphorylated at serine 28 and RNA pol II phosphorylated at serine 5. Digital optical sections were obtained and false coloured green (pS5 RNA pol II), red (pS28 H3) or blue (DAPI). Images were deconvolved with Axiovision 4.4 software.

To further analyze the relationship between mitogen-induced foci of phosphorylated H3 and pS5 RNA pol II, the images were analyzed with Metamorph software. Linescans were performed on images of serum-starved and TPA-treated (10 minutes) fibroblasts. In untreated cells (Figures 3-25 and 3-26 A, upper panels) signal from pS10 H3 and pS28 H3 is low, and very few peaks of pS10H3 and pS28 H3 are at the same position, or very near to the same position, as peaks of pS5 RNA pol II. The number of peaks of pS5 RNA pol II that coincide with peaks of pS10 H3 and pS28 H3 is significantly increased in TPA-treated cells (Figures 3-25 and 3-26, lower panels), although many foci of pS10 H3 and pS28 H3 do not overlap foci of pS5 RNA pol II. This is likely due to the fact that not all genes induced by TPA and EGF follow the same temporal pattern of induction; at this timepoint some genes will be transcribing, some will not yet be initiated, and some will have finished transcribing. We used indirect immunofluorescence to visualise the location of H3 phosphorylated at serine 10, H3 phosphorylated at serine 28, and pS5 RNA pol II in confluent, serum-starved C3 cells that had been exposed to TPA for 30 minutes. Antisera to pS10 H3 and pS28 H3 recognized numerous foci of modified H3 throughout regions of relatively relaxed chromatin (Figure 3-27) including many that overlapped foci of pS5 RNA pol II.

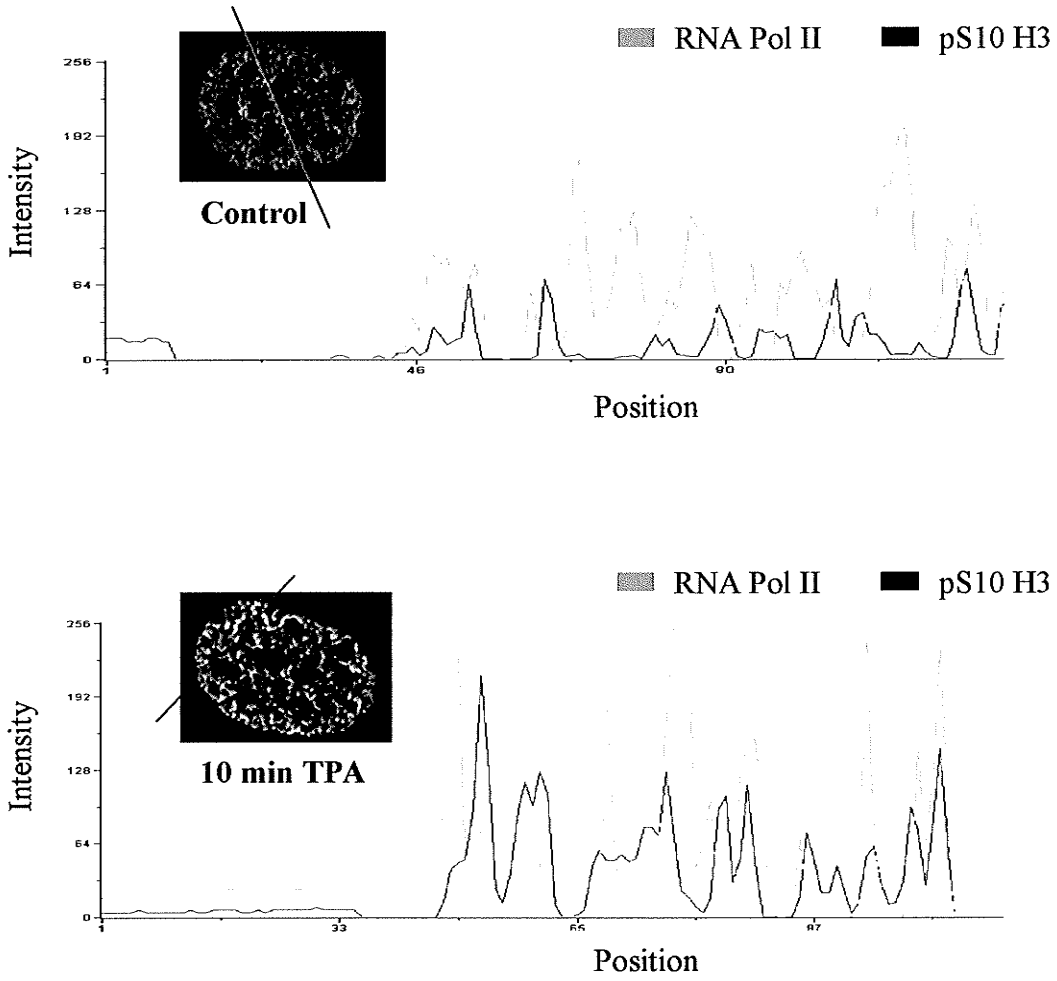

Figure 3-25. Image analysis of foci of pS5 RNA pol II and mitogen-induced foci of H3 phosphorylated at serine 10. Metamorph software was used on deconvolved images of control (upper panel) and TPA-treated (100 nM for 10 min; lower panel) cells to produce linescans. The intensity of H3 phosphorylated at serine 10 (pS10 H3) and RNA pol II phosphorylated at serine 5 (pS5 RNA pol II) are shown.

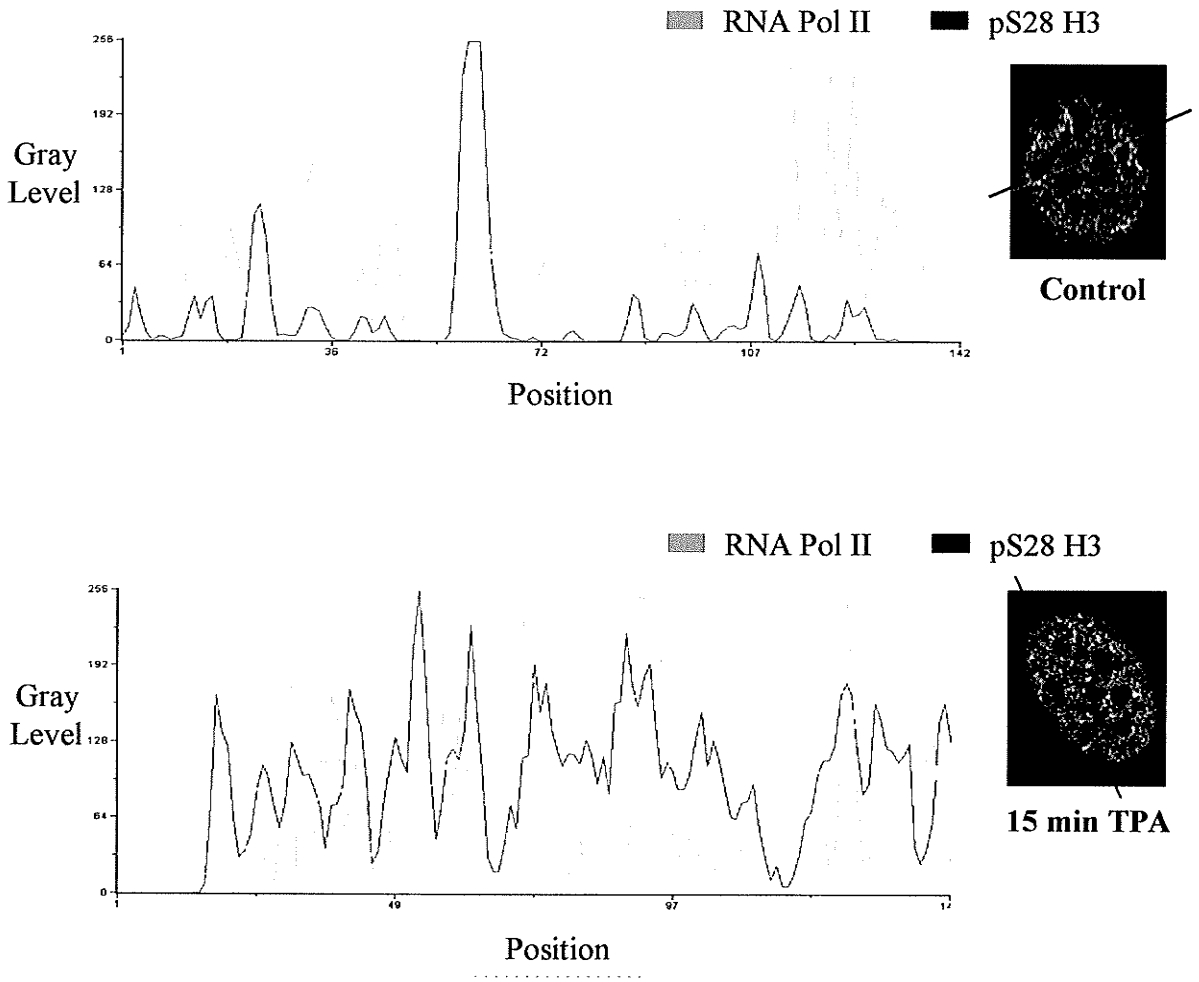

Figure 3-26. Image analysis of foci of pS5 RNA pol II and mitogen-induced foci of H3 phosphorylated at serine 28. Metamorph software was used on deconvolved images of control (upper panel) and TPA-treated (100 nM for 10 min; lower panel) cells to produce linescans. The intensity of H3 phosphorylated at serine 28 (pS28 H3) and RNA pol II phosphorylated at serine 5 (pS5 RNA pol II) are shown.

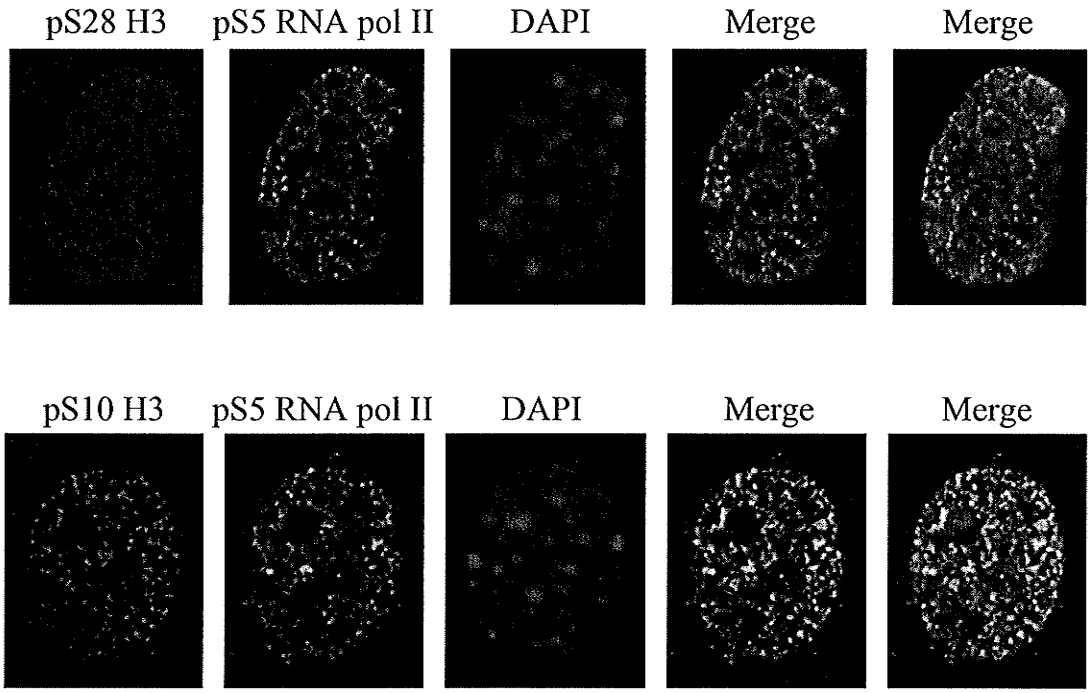

Figure 3-27. Foci of phosphorylated H3 colocalize with foci of pS5 RNA pol II in *ras*-transformed cells. *Ras*-transformed, serum-starved C3 cells were TPA-treated for 30 min before fixation and indirect immunofluorescence with antisera specific for phosphorylated H3 serine 28 (pS28 H3) or serine 10 (pS10 H3) and RNA polymerase II phosphorylated at serine 5 (pS5 RNA pol II). Cells were co-stained with DAPI. Digital optical sections of 0.25 μm were obtained and false-coloured green (pS5 RNA pol II), red (pS10 H3 or pS28 H3) or blue (DAPI). Images of nuclei were deconvolved with Axiovision 4.4 software.

The way in which MSK1 and MSK2 are targeted to regions of chromatin following stimulation of the MAPK pathway has not been elucidated, but these enzymes are most likely recruited by a transcription factor or associate with the RNA pol II complex. The majority of foci of pS10 H3 do not overlap with foci of pS28 H3 in serum-starved, TPA-treated cells. Thus these two modifications are targeted separately and may be phosphorylated by different enzymes. Although *in vitro* MSK1 and MSK2 phosphorylate serine 10 and serine 28 of H3, it is possible that *in vivo* MSK1 phosphorylates one residue of H3 and MSK2 phosphorylates the other. If MSK1/2 are tethered to specific genes by transcription factors or are associated with the pol II complex, they may remain at the site of H3 phosphorylation during transcription. We thus visualized MSK1 and MSK2 along with pS28 in serum-starved, TPA-treated 10T1/2 cells. We observed a portion of MSK1 and MSK2 present in the cytoplasm of both serum-starved and TPA-treated cells. 15 min into TPA stimulation, foci of pS28 H3 colocalize with a significant number of foci of MSK1 and a significant number of foci of MSK2 (Figure 3-28). We cannot make definite conclusions, but from these results it appears that both MSK1 and MSK2 target serine 28 for phosphorylation.

A

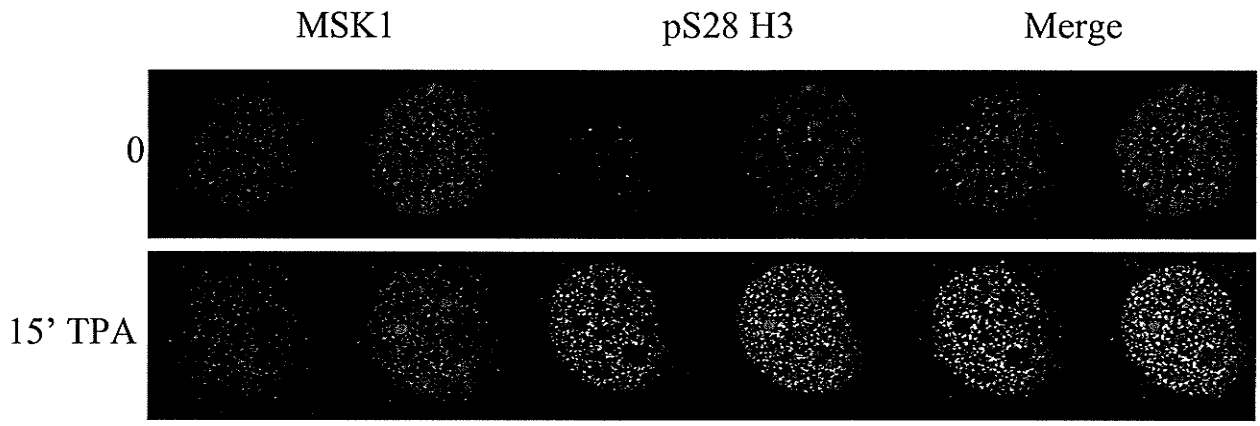

B

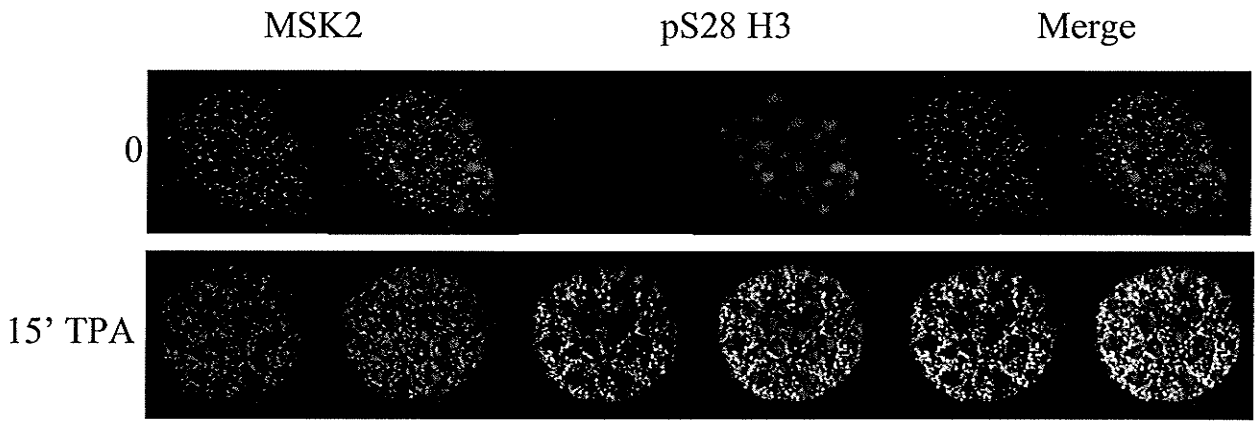

Figure 3-28. Localization of MSK1 and MSK2 with mitogen-induced foci of H3 phosphorylated at serine 28. 100% confluent, serum-starved 10T1/2 cells were treated with 100 nM TPA for 15 minutes before cells were fixed and immunostained with antisera recognizing H3 phosphorylated at serine 28 (pS28 H3), MSK1 (A) and MSK2 (B). Digital optical sections were obtained and false coloured red (MSK1/2), green (pS28 H3) or blue (DAPI). Images of nuclei were deconvolved with Axiovision 4.4 software.

VIII. Mitogen-Stimulation of Serum-Starved Cells Produces Various Amounts of Phosphorylated H3

Phosphorylation of H3 following TPA or EGF stimulation of the Ras-MAPK pathway was visualized by indirect immunofluorescence as described previously. Pictures taken with a Zeiss Axioplan 2 microscope reveal that stimulation produces cells with varying amounts of pS10 H3 and pS28 H3. While some cells contain very high levels of pS10 H3 and pS28 H3 (Figure 3-29 A, see white arrows), the level of pS10 H3 or pS28 H3 is very low in others (see yellow arrows). Additionally, even some unstimulated cells contain relatively high levels of H3 phosphorylated at serine 10 or at serine 28 (see white arrow in upper panel). Cells containing high levels of H3 phosphorylated at serine 10 also contained high levels of H3 phosphorylated at serine 28. Cells were also stained for pS28 H3 in combination with phosphoacetylated (S10K14) H3 (pS10AcK14 H3). A wide variety in levels of pS10AcK14 H3 was observed in the stimulated cells (Figure 3-29 B), and like pS10 H3, cells with high levels of pS10AcK14 H3 also contained high levels of pS28 H3.

Like histone H3, HMGN1 is also a target for MSK1/2 mediated phosphorylation after stimulation of the MAPK pathway. We determined that similar to pS10 H3 and pS28 H3, the level of pS6 HMGN1 in any given cell was highly variable post mitogen stimulation (Figure 3-30). To determine if the variety in levels of pS10 H3 and pS28 H3 could be due to differences in the amount of the H3 kinases present in each cell, we co-stained pS28 H3 with MSK1 or MSK2 (Figure 3-31). The detected amount of MSK1 or MSK2 present in each cell also varied though not as widely as pS10 H3 and pS28 H3. Levels of pS28 H3 did not correspond to levels of MSK1 or MSK2. Cells with relatively

high amounts of pS28 H3 did not have relatively high amounts of MSK1 and MSK2 (refer to white arrows Figure 3-31). These two kinases show complete activation, meaning that all MSK1/2 in the cell is activated upon stimulation of the MAPK pathway [282], therefore all of the MSK1/2 detected by our antibodies should be active MSK1/2. Thus one would predict that differences in the level of TPA- or EGF-induced pS10 H3 and pS28 H3 are due to an increased or decreased number of targets in any given cell.

To explore this possibility, SKY analysis was performed by Dr. Sabine Mai and Susan Pritchard. The results showed that the mouse 10T1/2 fibroblast cell line contains numerous cells with abnormal genomes (data not shown). Many chromosomal abnormalities were detected including losses and extra chromosomes, which could account for an increased/decreased number of targets for H3 phosphorylation following stimulation of the MAPK pathway.

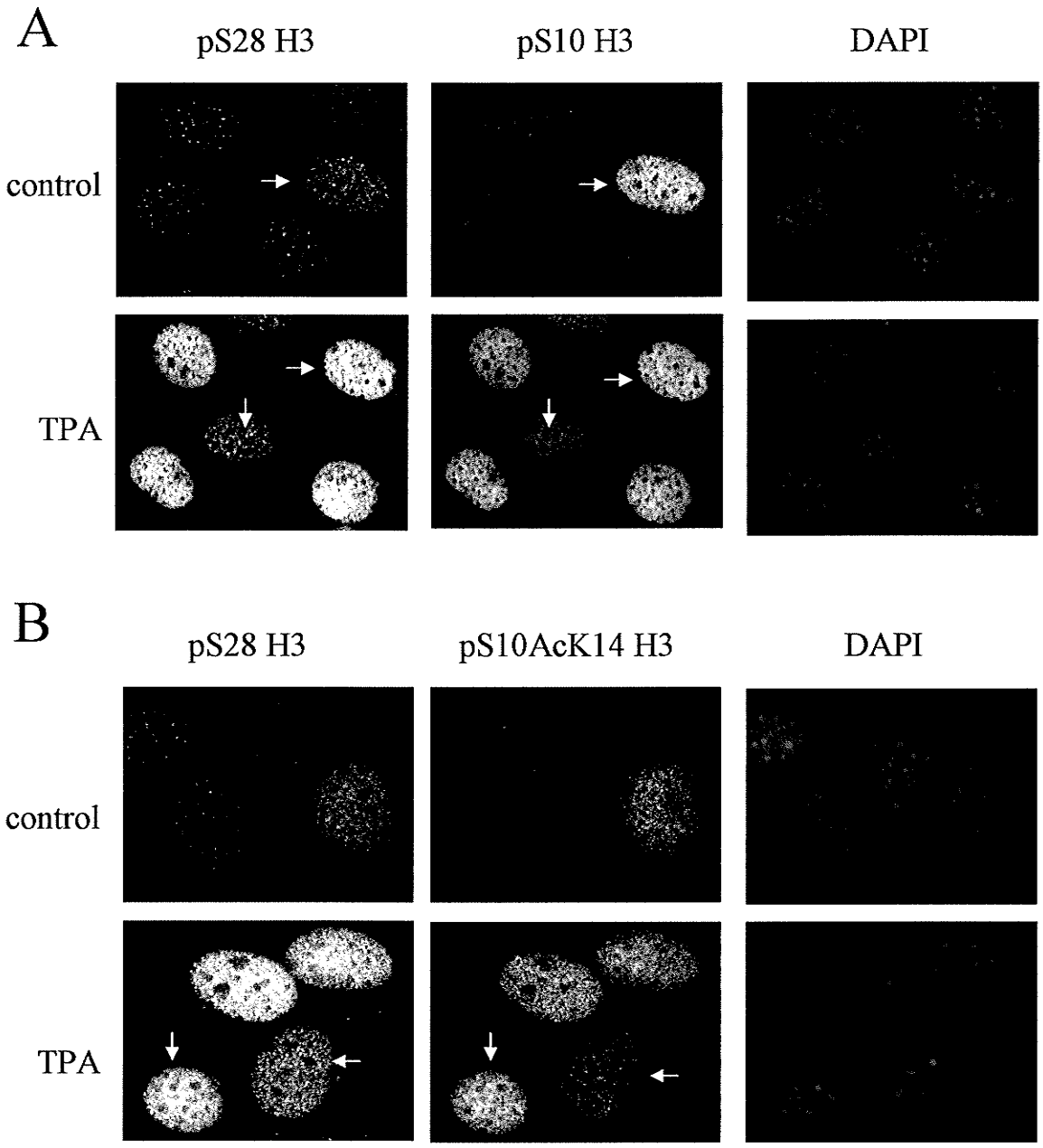

Figure 3-29. Levels of phosphorylated H3 vary in TPA-stimulated cells. Serum-starved 10T1/2 cells were treated with TPA for 15 min or untreated before fixation. Indirect immunofluorescence was performed with antisera against H3 phosphorylated at serine 10 (pS10 H3), at serine 28 (PS28 H3) and phosphoacetylated at serine 10 lysine 14 (pS10AcK14 H3). Cells were co-stained with DAPI. Digital optical sections of 0.3 μm were obtained and false-coloured blue (DAPI), red (pS10 H3 and pS10AcK14 H3) and green (pS28 H3). Yellow arrows indicate cells with low levels of pS28 H3, pS10 H3 and pS10AcK14 H3. White arrows indicate cells with high levels of pS10 H3, pS28 H3 and pS10AcK14 H3.

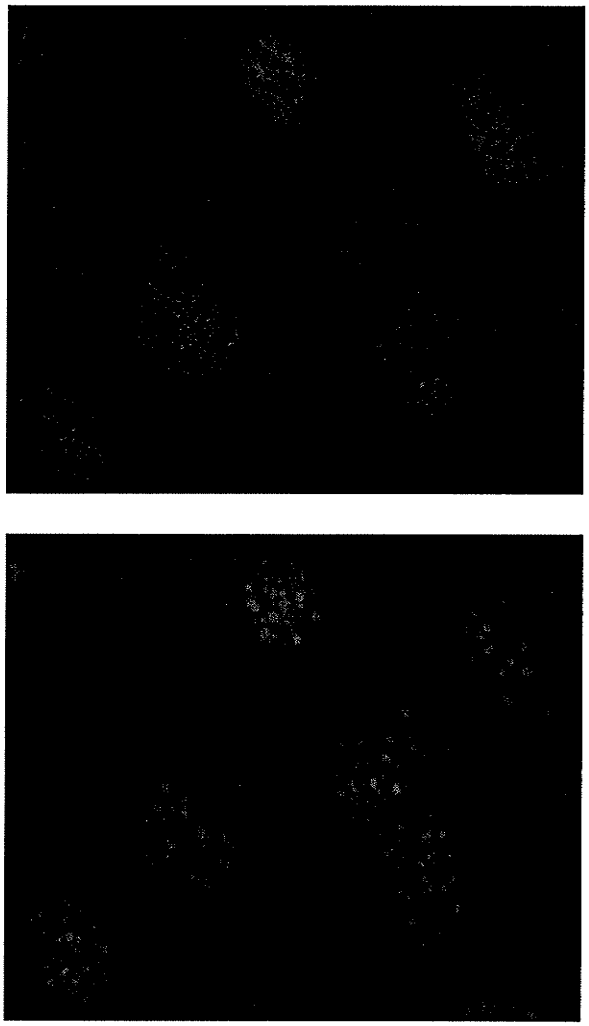

Figure 3-30. TPA-stimulation results in cells with variable amounts of phosphorylated HMGN1. Indirect immunofluorescence with antisera against HMGN1 phosphorylated at serine 6 (pS6 HMGN1) was performed on serum-starved, TPA-treated 10T1/2 cells. Cells were co-stained with DAPI. Digital optical sections of 0.3 μm were obtained and false-coloured blue (DAPI) and red (pS6 HMGN1). A yellow arrow points out a cell with very low levels of pS6 HMGN1. A white arrow indicates a cell with relatively high levels of pS6 HMGN1.

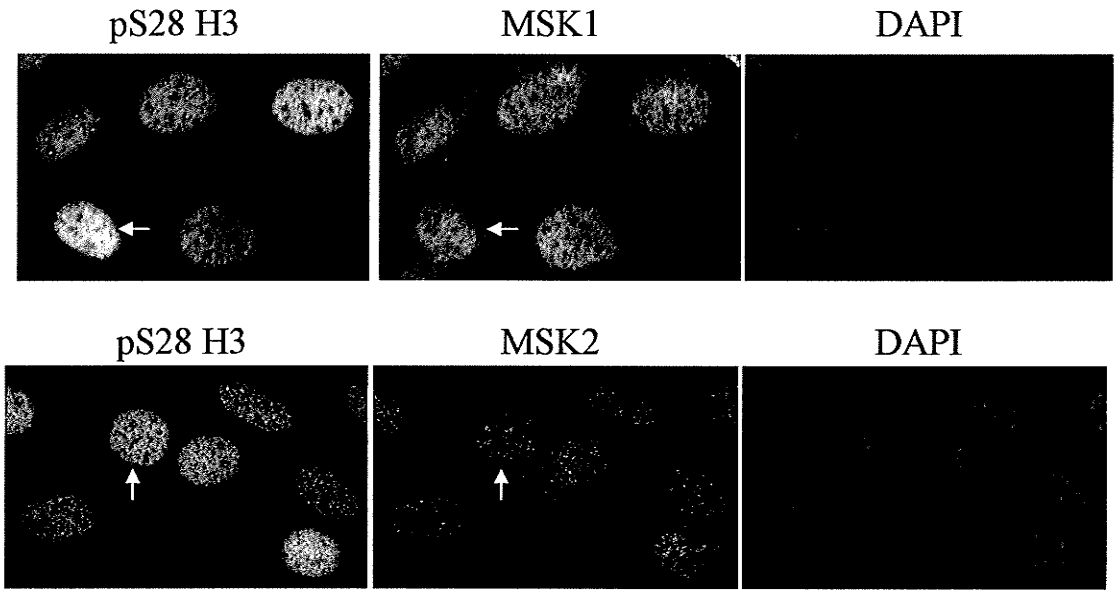

Figure 3-31. Levels of the H3 kinases MSK1 and MSK2 do not correlate with the level of H3 phosphorylation at serine 28. 10T1/2 cells serum-starved and treated with TPA for 15 minutes were fixed and stained with antisera against H3 phosphorylated at serine 28 (pS28 H3), MSK1, and MSK2. Cells were co-stained with DAPI before digital optical sections of 0.3 μm were captured and false-coloured green (pS28 H3), red (MSK1 and MSK2) or blue (DAPI). White arrows point out cells with relatively high amounts of pS28 H3.

Chapter Four: Conclusions and Discussion

MAJOR FINDINGS

The pattern of mitogen-induced H3 phosphorylation at serine 28 is similar to that at serine 10 in several ways. Mitogen-induced H3 phosphorylation may take place in regions of chromatin marked for transcription.

1) The timing of induction and loss of TPA- or EGF-induced phosphorylation at serine 28 following the start of mitogen stimulation is similar to that at serine 10.

2) As is seen for H3 phosphorylated at serine 10, mitogen-induction leads to the appearance of numerous foci of H3 phosphorylated at serine 28 in regions of relatively relaxed chromatin that are undergoing dynamic acetylation.

3) All non-centromeric variants of H3 (H3.1, H3.2, and H3.3) become phosphorylated at serine 10 and serine 28.

4) A fraction of the mitogen-induced foci of serine10-phosphorylated H3, as well as a fraction of the mitogen-induced foci of serine 28-phosphorylated H3, colocalize with serine 5-phosphorylated RNA polymerase II.

Many of the above mentioned characteristics of mitogen-induced H3 phosphorylation remain unchanged in *ras*-transformed cells despite continual stimulation of the pathway and increased amounts of phosphorylation on chromatin proteins:

1) Levels of H3 phosphorylated at serine 10, H3 phosphorylated at serine 28, and HMGN1 phosphorylated at serine 6 are elevated in *ras*-transformed cells.

2) As demonstrated in parental cells, mitogen induction of *ras*-transformed cells leads to the appearance of numerous foci of H3 phosphorylated at serines 10 or 28 that are excluded from pericentromeric heterochromatin. H3 phosphorylation takes place on dynamically acetylated chromatin, and H3.1, H3.2, and H3.3 participate in TPA-induced H3 phosphorylation at serine 10 and 28.

3) The distribution of modified forms of H3 participating in TPA-induced H3 phosphorylation at serines 10 and 28 is similar to that in parental cells.

In response to a stimulated Ras-MAPK pathway, phosphorylation of H3 at serine 28 occurs independently of phosphorylation at serine 10, and important aspects of H3 phosphorylation at serine 28 differ from that at serine 10:

1) Acid-urea gel analysis indicates that a portion of pS10 H3 and pS28 H3 have only been modified by one charge-altering event. Thus phosphorylation of serine 28 does not require prior phosphorylation of serine 10 (and vice versa), and phosphorylation at one residue does not necessarily lead to the phosphorylation of the other.

2) Following mitogen stimulation, H3 tails that become phosphorylated at serine 28 tend to be acetylated to a greater extent than those tails that are phosphorylated at serine 10.

3) Analyses by indirect immunofluorescence indicate that upon mitogen stimulation, phosphorylation of H3 at serine 28 is targeted to a different pool of chromatin than phosphorylation of H3 at serine 10. This remains true in *ras*-transformed cells despite

elevated levels of interphase H3 phosphorylation and continual activation of the Ras-MAPK pathway.

Much of this work was published in *Dunn KL and Davie JR. Stimulation of the Ras-MAPK pathway leads to independent phosphorylation of histone H3 on serines 10 and 28. Oncogene 2005. 24(21):3492-502.*

A second manuscript will be submitted to *Cancer Research*: *Dunn KL and Davie JR. Characteristics of Ras-MAPK pathway induced H3 phosphorylation at serine 28 in ras-transformed cells.*

Discussion

Stimulation of the Ras-MAPK pathway in mouse fibroblasts by growth factors or phorbol esters (TPA) results in the transient increase in phosphorylated active ERKs [275]. The TPA induced phosphorylation of H3 parallels the temporal stimulation of the ERKs, with phosphorylated ERK and phosphorylated H3 levels being maximal at 30 min [275,283]. Previous studies demonstrated that inhibition of the Ras-MAPK with the MEK inhibitors PD98059 or UO126 prevented the TPA-induced phosphorylation of H3 at serine 10 or serine 28, demonstrating that TPA-induced H3 phosphorylation was a consequence of stimulation of the Ras-MAPK pathway [180,198]. Constitutive stimulation of the Ras-MAPK pathway in oncogene (*ras*)-transformed cells results in an increased steady state of phosphorylated active ERKs [262] and of serine 10- and serine 28-phosphorylated H3 (this study). In mouse fibroblasts, the major H3 kinase responsive to a TPA or oncogene activated Ras-MAPK pathway is the mitogen and stress activated protein kinase (MSK1/2) [262]. Inhibition of MSK1/2 activity with H89 prevents H3 phosphorylation in TPA induced serum-starved 10T1/2 and C3 cells.

We observed many similarities in the phosphorylation of H3 at serine 10 and serine 28. Both modifications are induced by the same stimuli, disappear within the same time frame, and are located within relatively relaxed chromatin conformations. Further, the *ras*-transformed cells contain increased amounts of H3 phosphorylated at serine 10 and serine 28. These observations suggest that these two modifications work together. However, AU gel analyses determined that a significant portion of H3 phosphorylated at serine 28 and H3 phosphorylated at serine 10 exist on an H3 that has not been otherwise phosphorylated (the mono-modified form), suggesting that the two modifications do not

function in a cooperative manner. Furthermore, this mono-modified form was present in significant amounts 15 and 30 min after stimulation of the pathway began, the time when we observe phosphorylation to be at a maximum. Thus, phosphorylation of serine 28 is not dependent upon the phosphorylation of serine 10 or vice versa. Further, although MSK1/2, the kinase mediating mitogen induced phosphorylation of H3, is capable of phosphorylating H3 on either residue [178,195], our results suggest that the enzyme selects either serine 10 or serine 28 but not both sites for phosphorylation.

Following TPA stimulation of 10T1/2 mouse fibroblasts, the distribution of pS10 H3 among the modified H3 isoforms is quite distinct from that of pS28 H3. H3 molecules phosphorylated at serine 10 tend to reside in poorly modified isoforms (primarily mono-modified at 30 and 60 min post-TPA addition), while H3 phosphorylated at serine 28 is present in highly modified isoforms (primarily tri-modified). A combination of H3 (serine 10) phosphorylation and acetylation has been detected on immediate-early genes with the chromatin immunoprecipitation assay [207,208], providing evidence that a sub-population of H3 phosphorylated at serine 10 in the di-modified band is also modified by acetylation on Lys-14. Our results with an antibody against H3 phosphoacetylated at serine 10 lysine 14 detected the vast majority of H3 tails modified by this combination of acetylation and phosphorylation in the di-modified band, in agreement with a previous report [208]. It is thus possible that the di-modified form containing H3 phosphorylated at serine 10 is phosphoacetylated rather than being di-phosphorylated at serines 10 and 28. Conversely, the di- and tri-modified isoforms containing H3 phosphorylated at serine 28 may represent mono-phosphorylated and mono-acetylated or di-acetylated forms, respectively.

This striking difference suggests that TPA-induced H3 phosphorylation at serine 28 occurs in chromatin domains that have a higher steady-state level of acetylation than those regions undergoing phosphorylation of H3 at serine 10. This result also implies that the balance of HAT and HDAC activity present at loci targeted for H3 phosphorylation at serine 10 differs from that at those loci containing pS28 H3.

However, H3 phosphorylated at either serine 10 or serine 28 is localized in dynamically acetylated chromatin regions, which can be driven into highly acetylated states when the histone deacetylase activity is inhibited with trichostatin A. It has been demonstrated directly that TPA-induced pS10 H3 is associated with immediate early genes *c-fos*, *c-myc* and *c-jun* [207,209]. The observations that mitogen-induced serine 28-phosphorylated H3 is engaged in dynamic acetylation typically linked to transcribed chromatin [284] and that a portion of pS28 H3 colocalizes with pS5 RNA pol II suggests that this phosphorylated form of H3 is also associated with genes responding to a stimulated Ras-MAPK pathway. However, our results suggest that the genes associated with H3 phosphorylated at serine 10 will differ from those bound to H3 phosphorylated at serine 28.

Serine 28 is targeted for phosphorylation separately from serine 10 after stimulation of the Ras-MAPK pathway: Indirect immunofluorescence allowed us to observe the location of various modified forms of H3 after stimulation of the Ras-MAPK pathway. The numerous foci that appeared upon TPA treatment were excluded from pericentromeric heterochromatin and were present in regions of more relaxed chromatin, a finding that supports the involvement of H3 phosphorylated at serine 28 in the

transcriptional process. In agreement with previous findings that H3 phosphorylated at serine 10 and H3 phosphoacetylated at serine 10 lysine 14 are involved in gene expression, foci of these modified forms of H3 were also found in regions of relatively decondensed chromatin after TPA stimulation. Surprisingly, many foci of H3 phosphorylated at serine 28 were found in areas where H3 phosphorylated at serine 10 was absent, indicating that some form of regulation exists that allows these two modifications to be targeted separately. Since we published these data Dyson *et al* have published results similar to ours [282]. They demonstrated that treatment of serum-starved mouse fibroblasts with anisomycin, which stimulates the p38 stress pathway, results in distinct foci of pS10 H3 and pS28 H3 [282]. Also consistent with our results, immunodepletion of cross-linked chromatin preparations with antisera against pS10 H3 did not result in co-depletion of pS28 H3 [282]. We estimate that 83% of H3 phosphorylated at serine 10 or serine 28 did not co-localize in our images of serum-starved cells treated with TPA. Areas of pS28 H3 were also located outside of regions where H3 was modified by a combination of phosphorylation at serine 10 and acetylation at lysine 14. Thus, the modification events associated with H3 phosphorylation at serine 10 are distinct from those of H3 phosphorylation at serine 28, a large percentage of the time. Therefore the di- and tri-modified bands of H3 modified by phosphorylation at serine 28 are unlikely to be di-phosphorylated, but rather mono- or di-acetylated and mono-phosphorylated (refer to Figure 4-1).

We should note that the resolution of this type of imaging will not allow us to decipher if each foci contains only one gene target, or if several genes targeted for phosphorylation are located in close proximity to each other. Furthermore, it is also possible that either

serine 10 or serine 28 is preferentially rather than exclusively targeted. This would result in dramatically higher levels of phosphorylation on one residue, and minimal levels on the other. This would concur with what we visualized through indirect immunofluorescence. Acid urea polyacrylamide gel analysis determined that many molecules of H3 participating in TPA-induced phosphorylation at serine 10 and at serine 28 have only one charge-altering modification, which would be consistent with preferential phosphorylation at one residue.

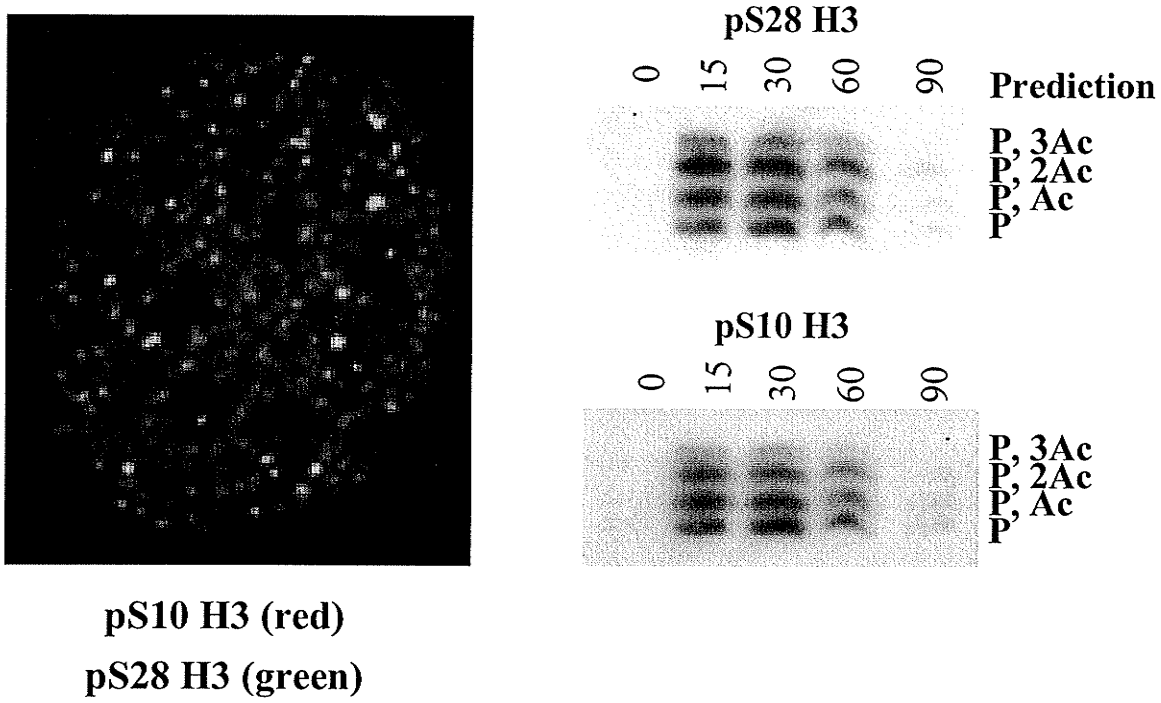

Figure 4-1. Predicted modification status of H3 phosphorylated in response to mitogen stimulation. Left panel: TPA-treated parental mouse fibroblast fixed and immunostained with antisera against pS10 H3 and pS28 H3. Right panel: Histones extracted from TPA-treated fibroblasts separated on an acid-urea polyacrylamide gel and immunostained with antisera against pS10 H3 and pS28 H3. The predicted modification status of each immunostained band is given on the right.

Targeting of MSK1/2 for specific phosphorylation of serine 10 or serine 28: The mechanism by which this occurs is unclear and there are several possible explanations; 1) MSK1 and MSK2 each target only one residue, and are recruited to different genes. Substrate specificity of MSK1/2 could be influenced by interacting proteins. 2) The promoter architecture surrounding genes targeted for mitogen-induced H3 phosphorylation favours the phosphorylation of one residue over the other. This could be influenced by bound transcription factors. 3) A histone code present at genes prior to induction dictates phosphorylation at serine 10 or 28.

It is possible that MSKs are pre-positioned within reach of the nucleosomes to be altered; we have found that MSK1 can be cross-linked to DNA with formaldehyde before and after TPA stimulation [210]. MSK1 bound to the trefoil factor 1 gene in MCF-7 breast cancer cells is increased by treatment with estradiol or TPA [285]. In a differing scenario, chromatin immunoprecipitation assays indicate that MSK1 only becomes associated with the IL-6 promoter following TNF stimulation [286]. Furthermore, inhibitors of the MAPK pathway including PD 98059, SB 203580 and H89 prevent TNF-induced MSK1 recruitment to the IL-6 promoter [286]. Formaldehyde used in these studies cross-links proteins to each other as well as to DNA, thus it is not apparent if MSK1 is bound directly to DNA. MSKs may be recruited to DNA through interactions with transcription factors or in complex with other chromatin modifiers or chromatin remodelling complexes. These interactions may influence target genes and determine which residue of H3 becomes phosphorylated.

All evidence to date, including knockouts and *in vitro* assays, indicates that MSK1 and MSK2 phosphorylate histone H3 at both serine residues [180,282]. We have determined

through indirect immunofluorescence that following TPA-stimulation a fraction of H3 phosphorylated at serine 28 colocalizes with foci of MSK1, and that a fraction of pS28 H3 foci colocalizes with MSK2. This would support the notion that both MSK1 and MSK2 phosphorylate histone H3 at serine 10 and at serine 28, and that other factors, most likely transcription factors or the promoter architecture, define substrate specificity.

Stimulation of the Ras-MAPK pathway increases the steady-state level of histone acetylation at immediate-early genes [205,208]. Treatment with TSA, which does not induce the expression of immediate-early genes, results in enhanced acetylation in specific regions of *c-fos* and *c-jun* [287]. Levels of acetylation post-TSA treatment were related to levels pre-treatment; acetylation was not enhanced in regions where acetylation was not detected pre-treatment, and was higher in regions having relatively high levels of acetylation before treatment. These results strongly suggest that specific regions of these two immediate-early genes are targeted for acetylation and that the enzymes responsible for this are located near these regions prior to the start of treatment [287]. In support of this, ChIP analysis of quiescent cells with antisera against HDACs 1, 3, 4 and 6 found these proteins to be associated with chromatin along various parts of the *c-fos* and *c-jun* coding region [287]. Constitutive targeting of HATs and HDACs to immediate-early genes likely results in the formation of a distinct pattern, consisting of histones modified at particular lysine residues, across these genes that could influence future modification events through the histone code. Further, a similar situation may exist at genes targeted for mitogen-induced phosphorylation of H3 at serine 28. In this possibility, differences in the pattern of histone modifications present at genes targeted for pS10 H3 and pS28 H3

would result in a preference for MSK1/2 to phosphorylate serine 10 or serine 28 respectively.

A recent study has determined that in mouse fibroblasts, all H3 tri-methylated at lysine 4 is hypersensitive to TSA, indicating that most or all molecules of tri-methyl lysine 4 H3 are undergoing dynamic acetylation [287]. H3 methylated at lysine 9, which is often associated with heterochromatin [288,289], did not exhibit this sensitivity. Methylation of H3 at lysine 4 is now known to be present at the immediate-early genes *c-jun* and *c-fos*, both of which are targets for mitogen-induced H3 phosphorylation at serine 10 [207,208,287]. ChIP analysis detected tri-methyl lysine 4 H3 at *c-jun* and *c-fos* before and after MAPK pathway stimulation [287]. Further, ChIP analysis of *c-fos* and *c-jun* with antisera against H3 methylated at lysine 4 and acetylated H3 revealed that regions hypersensitive to TSA contain H3 trimethylated at lysine 4 [287]. Thus it is possible that lysine 4 methylation when in combination with the acetylation of H3 lysine residues acts as the mark that separates sites of mitogen-induced H3 phosphorylation at serine 10 from sites of mitogen induced H3 phosphorylation at serine 28. A constitutive mark of acetylated, lysine 4-trimethylated H3 could potentially sterically hinder phosphorylation at serine 28, or could orient the MSK1/2 enzyme in such a way that phosphorylation at serine 10 occurs preferentially. Alternatively, the presence of this mark at loci targeted for serine 10 phosphorylation following MAPK pathway stimulation may alter the binding site of any number of nuclear factors, which could then result in differences in transcription factor/complex binding at these loci. Any factor bound to chromatin can influence the availability of histone tails, and could therefore promote the phosphorylation of one residue instead of the other.

Mitotic H3 phosphorylation: During G2–M phase of the cell cycle, H3 is extensively phosphorylated by the kinase Aurora B at serine 10 and serine 28. Mass spectrometric analysis has revealed a very complex pattern of post-translational modification of H3 variants during mitosis in mammalian cells [290]. The maximal phosphorylation of H3 and the participation of all H3 variants during this period in the cell cycle provided a reference for H3 phosphorylation events occurring during TPA-induced H3 phosphorylation of serum-starved G1 phase 10T1/2 mouse fibroblasts and C3 cells. In analyses of the distribution of the modified H3 isoforms having been modified by phosphorylation at serine 10 or serine 28, we observed that mitotic H3 phosphorylated on serine 10 or serine 28 was found mainly on an H3 tail that is modified by one other charge-altering event (the di-modified form). During mitosis the amount of hyperacetylated H3 diminishes although lower levels of acetylation persist [291]. Given the widespread nature of mitotic H3 phosphorylation, we suggest that a portion of the di-modified forms of phosphorylated H3 are most likely di-phosphorylated. A di-phosphorylated (Thr-3, Ser-10) peptide corresponding to a region within the amino-terminal portion of H3 has been detected by mass spectrometry, thus this combination of modifications is one possible identity for di-modified molecules we detected with antisera to pS10 H3.

By immunoblot, we detected mitotic phosphorylation of serine 10 and of serine 28 on H3.1, H3.2 and H3.3 in parental and *ras*-transformed cells. This result has been confirmed in human cells arrested in mitosis by Garcia *et al*, who used mass spectrometry to detect serine 10 and serine 28 phosphorylation on all three non-centromeric H3 variants [290]. In this study several discrepancies between the combinations of

modifications present on different variants were found, suggesting that variants have specialized functions during mitosis. For example, H3.1 and H3.2 showed higher amounts of methylation at lysine 27 in combination with phosphorylation at serine 28 than H3.3 [290].

H3 variant phosphorylation: Recent reports in the literature have linked histone variant H3.3 with transcriptional activity [93,94,281]. Chromatin immunoprecipitation assays have found H3 phosphorylated on serine 10 in the chromatin associated with immediate-early genes during transcription [205,207,209]. Therefore, if the chromatin associated with immediate-early genes is enriched in H3.3, we would expect induction of the Ras-MAPK pathway to result in a disproportionate increase in the amount of H3.3 phosphorylated on serine 10 as compared to the other H3 variants. The same would be expected of phosphorylation on serine 28 if this modification is occurring at genes expressed following stimulation of the Ras-MAPK pathway. In contrast to our expectations, we observed that H3.2, H3.3 and to a lesser extent H3.1 was phosphorylated at serine 28 and that all three H3 variants participated in TPA-induced phosphorylation at serine 10 in TPA-stimulated, serum-starved 10T1/2 mouse fibroblasts and C3 cells. Differing levels of phosphorylation of H3.1 at serine 10 versus serine 28 further supports our result that H3 phosphorylated at serine 10 is located in different chromatin regions from that of H3 phosphorylated at serine 28.

H3.3 is thought to be incorporated into regions of transcriptional activity after nucleosomes are disrupted by the passage of transcription machinery. This would lead to an accumulation of H3.3 within the coding regions of active genes. However, a recent

study has found that H3.3 tends to be present mainly in the promoters of these genes, and that it persists through mitosis to "mark" transcriptionally active genes [96]. Other studies imply that incorporation of H3.3 is not restricted to transcribed regions and varies from one gene to another in its inclusion in upstream regulatory regions and coding regions [292]. Following stimulation of the Ras-MAPK pathway, pS10 H3 can be detected in the promoters and coding regions of several immediate-early genes. Thus our observation that H3.3 was not selectively phosphorylated at serine 10 or serine 28 following induction of the Ras-MAPK pathway is consistent with the results of Chow *et al [96]*; if nucleosomes throughout the coding region have an H3 variant composition similar to that of bulk chromatin they will outnumber the nucleosomes modified within the promoter. Further, H3 phosphorylation may exceed the confines of the transcription unit and occur throughout a chromatin domain in a manner similar to that observed for acetylated H3 and H3 methylated at lysine 4 [293].

H3 phosphorylation in ras-transformed cells: Mitogen-induced H3 phosphorylation at serines 10 and 28 was slightly delayed in C3 cells; we detected maximum levels of pS10 H3 and pS28 H3 at 30 minutes in C3 cells versus 15 minutes in parental fibroblasts. This correlates with the delayed induction of certain immediate early genes [198], and may be due to changes in the parameters of the Ras-MAPK pathway brought on by oncogenic Ras. Cells may respond to a continuously active pathway by altering levels of mediators such that the pathway responds differently. In addition, oncogenic Ras may cause increased genomic instability which in turn leads to chromatin that is more or less sensitive to mitogenic stimuli.

In addition to the increase in H3 phosphorylated at serine 10, oncogene-transformed cells often display defects in nuclear architecture including irregular nuclear matrix profiles [250] and abnormal nuclear morphologies [294]. We have determined that *ras*-transformed cells also contain elevated levels of H3 phosphorylated at serine 28. Increased levels of H3 phosphorylated at serine 28 in *ras*-transformed cells may contribute, along with these defects, to the relaxed chromatin structure and aberrant gene expression observed in these cells. Elucidation of the mechanism by which phosphorylation at serine 10 is distinct from phosphorylation on serine 28 and determination of the specific subsets of genes affected by these modifications may provide new targets for therapeutic agents in cancer therapy.

C3 cells also contain increased amounts of phosphorylation on the structural chromatin protein HMGN1. This protein regulates the accessibility of DNA for factor binding and modulates modification of histone H3. Phosphorylation of HMGN1 at serine 6, as seen following mitogen-stimulation, causes its release from nucleosomes potentially resulting in an opportunity for nuclear factors to bind. Thus increased phosphorylation of this protein could result in significant changes to the structure of chromatin, altered modification profiles for the histones, and aberrant gene expression.

MSKs phosphorylated chromatin in a selective manner. Despite constitutive activation of the Ras-MAPK pathway in C3 cells, the distribution of H3 modified forms participating in TPA-induced phosphorylation is remarkably similar to that in the parental cells. In addition, sites of H3 phosphorylation at serine 10 are kept separate from sites of H3 phosphorylation at serine 28. Stimulation of the MAPK pathway with TPA or EGF in C3H 10T1/2 mouse fibroblasts results in stoichiometric (complete) activation of MSK1,

meaning that all molecules of MSK1 become phosphorylated and activated [282]. Although *ras*-transformed C3 cells do not have elevated levels of MSKs, H3 kinase activity in stimulated C3 cells is increased relative to stimulated parental 10T1/2 cells [262]. This increased H3 kinase activity is likely responsible for the increased amounts of H3 phosphorylated at serine 10 and at serine 28. Increased phosphorylation levels of histone H3 mean one of two things: either there is an increase in the number of residues undergoing steady-state phosphorylation at each targeted foci, or there is an increase in the number of foci. Given the exquisite targeting exhibited by the Ras-MAPK pathway, evidenced by the separation of most foci of pS10 H3 from foci of pS28 H3, it seems more likely that there are an increased number of phosphorylated residues at each targeted foci.

The rheostat model, in which differing levels of stimulation produce different biological outcomes, may be of relevance here. Cells containing constitutively active Ras also contain elevated levels of pS10 H3 and pS28 H3, but not nearly as much as stimulated cells, suggesting that stimulation by activated Ras is not just an on/off switch. The high level of stimulation provided by 100 nM TPA results in similar phosphorylation of H3 in both parental and *ras*-transformed cell, as evidenced by similar locations and patterns on acid-urea polyacrylamide gels. It may be that TPA stimulation results in H3 phosphorylation at a different set of genes than those targeted constitutively in *H-ras* transformed cells.

pS10 H3 and pS28 H3 are involved in transcription: In addition to demonstrating that mitogen-induced phosphorylation of H3 at serines 10 and 28 occurs on dynamically acetylated chromatin, we have shown that following stimulation of the Ras-MAPK

pathway, a portion of the many foci of pS10 H3 colocalize with RNA pol II that has been phosphorylated at serine 5. This would be the expected result if those foci associated with pS5 RNA pol II were undergoing transcription; only a fraction would be colocalized and undergoing transcription in accordance with the transcriptional program initiated by Ras-MAPK pathway stimulation [171]. We found a very similar result for pS28 H3, adding to the evidence that phosphorylation of this residue also plays a role in gene expression.

The mechanism by which mitogen-induced H3 phosphorylation, at serine 10 or 28, contributes to gene expression is not well understood. When we visualized the nuclear location of pS28 H3 and pS6 HMGN1 in TPA- and EGF-stimulated cells, they did not colocalize. This result is in agreement with the current model of mitogen-induced phosphorylation of chromatin proteins, which states that phosphorylation of HMGN1 causes its dissociation from chromatin and gives kinases better access to phosphorylate serine 10 and 28 of H3 [195].

Higher order chromatin structure is an impediment to transcription. Phosphorylation of histone H3 at serine 10 does not disrupt chromatin folding, nor does triacetylation of the H3 amino-terminal tail [295,296]. However, acetylation of histone H4 at lysine 4 interferes with the formation of cross-fiber interactions within chromatin and prevents the formation of 30 nm-type fibers [295]; therefore certain modifications, and combinations thereof, can dramatically affect the compaction state of chromatin. H3 phosphoacetylated at serine 10 lysine 14 and serine 10 lysine 9 is associated with immediate-early genes during mitogen-induced transcription, and mitogen-induced phosphorylation of H3 at serine 28 tends to occur on H3 tails that undergo a higher steady-state level of acetylation

than those undergoing phosphorylation at serine 10. The effect of a combination of modifications on the amino-terminus of H3, namely acetylation and phosphorylation, has not been determined and may be of significant consequence in the formation of higher order chromatin structures.

It is likely that H3 phosphorylation contributes to gene expression through mediating proteins. 14-3-3 isoforms have been identified as proteins that specifically bind H3 phosphorylated at serine 10 in a manner that is not disrupted by acetylation of H3 at lysine 9 or 14 [297]. Isoforms of 14-3-3 bind *c-jun* and *c-fos*, making them potential mediators of the effects of histone H3 phosphorylation at immediate-early genes [297].

Future Directions and a Current Model of Mitogen-Induced H3 Phosphorylation

A current model of H3 phosphorylation following stimulation of the Ras-MAPK pathway is shown in Figure 4-2. In this model, stimulation of the Ras-MAPK pathway by growth factors such as EGF or phorbol esters like TPA results in phosphorylation of H3 at serine 10 on a specific set of immediate-early genes. Chromatin at these genes is also undergoing dynamic acetylation to a limited extent, including at lysines 9 and 14. At another set of genes, H3 is being rapidly phosphorylated at serine 28 on chromatin containing a higher steady-state level of H3 acetylation. Chromatin remodellers (SWI/SNF), HATs (p300), and HDACs work in conjunction with MSKs near the site of the pre-initiation complex (PIC) to facilitate transcription. These factors, and additional proteins necessary for their proper functioning, may or may not associate in a complex with MSK1 or MSK2.

Our model does not address the mechanism by which MSK1/2 phosphorylates only one residue, either serine 10 or serine 28, at each loci. This is likely to vary, and may rely upon components of the MSK1/2 complex. Some genes targeted for phosphorylation at serine 10 are likely marked with trimethyl lysine 4, acetylated H3. Determining the components found in MSK1/2 complexes, including transcription factors, chromatin modifiers and remodellers, will be an important step to understanding the pathway that generates rapid transcription of immediate-early genes following mitogen stimulation.

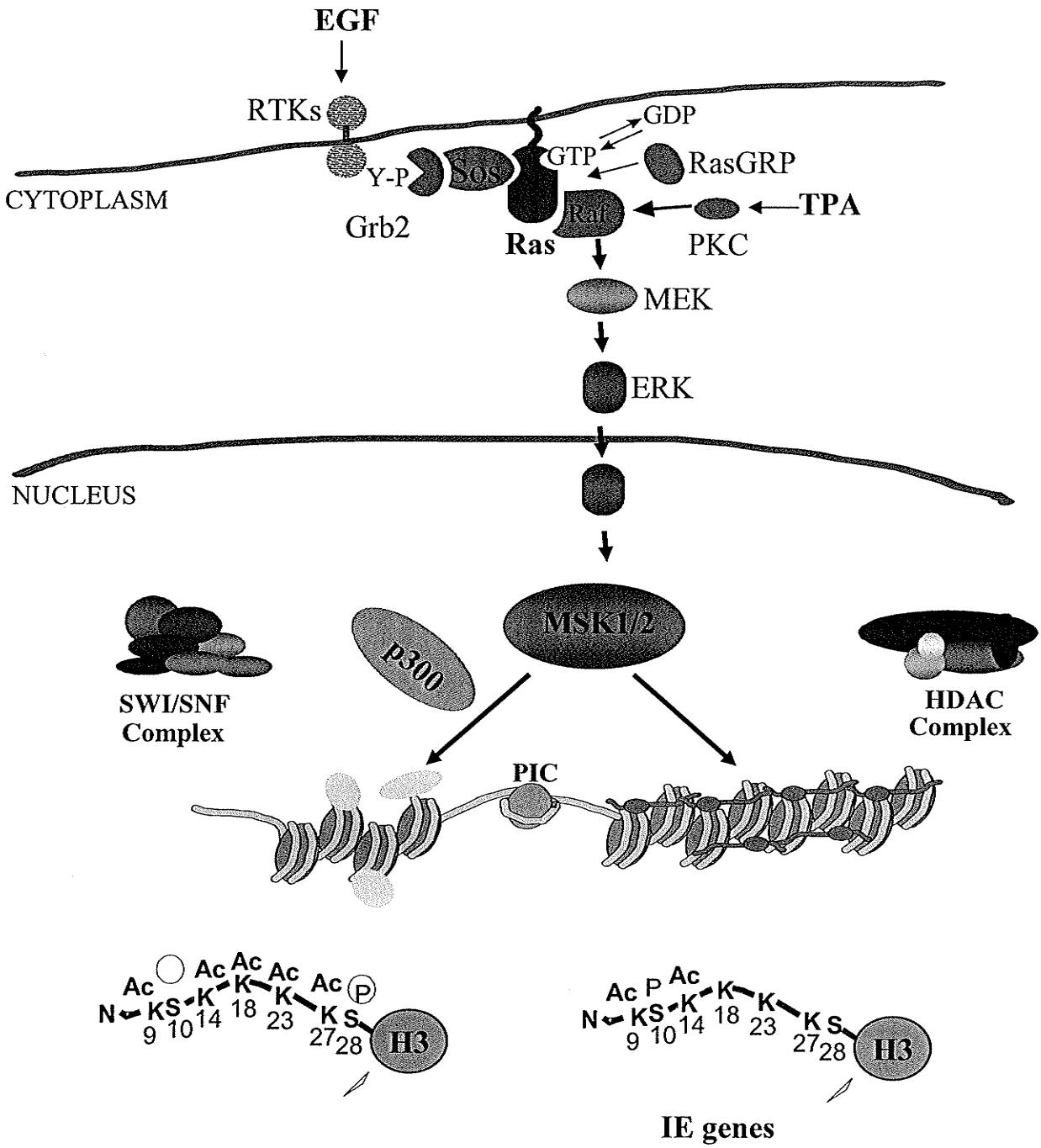

Figure 4-2. Model of mitogen-induced H3 phosphorylation. Stimulation of the Ras-MAPK pathway by growth factors such as EGF or phorbol esters such as TPA results in the activation of a series of kinases including the chromatin modifying enzymes MSK1 and MSK2. At specific immediate-early genes, histone H3 is rapidly phosphorylated at serine 10. In the same timeframe, other unidentified loci having higher steady state levels of acetylation on H3 are phosphorylated at serine 28. MSK1/2 work in conjunction with HATs (e.g. p300) and chromatin remodellers to facilitate transcription.

Although we can stipulate that mitogen-induced pS10 H3 is present at certain immediate-early genes, TPA-stimulation of serum-starved fibroblasts leads to the appearance of numerous foci of phosphorylated H3. Thus many targets of mitogen-induced phosphorylation of H3 at serine 10 remain to be identified. Each of the foci appearing following the start of mitogen stimulation is predicted to be a site of gene transcription, a portion of which are immediate-early genes that transcribe at induced levels within 15 minutes of the start of stimulation. Following serum-stimulation of human fibroblasts the transcription of various others genes is induced 30 minutes to several hours after stimulation began; this includes many involved in inflammation, tissue remodeling, coagulation and hemostasis [171]. Targets of mitogen-induced H3 phosphorylation at serine 28 are unknown. Like foci of pS10 H3, foci of pS28 H3 are numerous following TPA- or EGF-stimulation of serum-starved fibroblasts. Chromatin immunoprecipitation experiments with an antibody that specifically recognizes H3 phosphorylated at serine 28 will provide valuable information on the placement, extent and purpose of mitogen-induced phosphorylation of H3 at serine 28. Using this method, DNA could be isolated from immunoprecipitated chromatin and hybridized to a CpG island microarray containing the promoters and/or coding regions of many immediate-early genes. The inclusion of non-immediate-early genes on the array could also identify other targets. Parallel experiments done with antibodies recognizing H3 phosphorylated at serine 10 could also be done for the same purpose, as to date only a fraction of the genes associated with pS10 H3 have been discovered.

The increased H3 phosphorylation at serines 10 and 28 present in *ras*-transformed cells is either the result of an increase in the average number of residues phosphorylated at each

target gene or an increase in the number of target genes. A ChIP (chromatin immunoprecipitation) on chip (CpG island array) may be used to identify targets of mitogen-induced H3 phosphorylation in *ras*-transformed cells. A comparison of the gene targets in parental and *ras*-transformed cells may yield new targets for the production of anti-cancer drugs.

Part of this discussion was originally published in Dunn KL and Davie JR. Stimulation of the ras-MAPK pathway leads to independent phosphorylation of histone H3 on serines 10 and 28. Oncogene 2005. 24(21):3492-502.

Appendix A:

The Nuclear Matrix, the Insulator-Binding Protein CTCF, and Functional Domains of Chromatin

Background

Enhancers are sequences of DNA that bind transcription factors and enhance the transcription of particular genes. Enhancers may be located up to 1 megabase away from their target gene, and studies have shown that most are not specific, meaning that they are capable of enhancing transcription at many genes [130,131]. Enhancers act through one of two mechanisms. The first involves direct contact between the enhancer and target gene in which factors bound to the enhancer allow for easier formation of the RNA pol II complex at the target gene promoter. The second does not involve direct contact and instead relies upon the procession of a signal down the strand of DNA from enhancer to promoter.

Insulators act as another level of gene regulation; they are DNA elements teamed with associated proteins that block inappropriate activation by enhancers and/or silencing by the spread of heterochromatin (refer to Figure A-1). The latter function is referred to as boundary formation or barrier activity. Not all insulators are capable of both barrier and enhancer-blocking activity. Even at insulators capable of both boundary formation and enhancer-blocking, the two activities can be separated. Insulators can be turned on or off, and must be placed along the strand of DNA intervening the enhancer and heterologous promoter or heterochromatin. Combinations of several insulators in close proximity to each other have been observed at several loci.

Two assays have been developed to functionally define insulators. In the enhancer blocking assay, a construct is created that contains a strong enhancer, a neomycin resistance gene and the proposed insulator. A second insulator, known to prevent the

spread of heterochromatin, is placed upstream of all other elements to protect against position effect variegation [298]. The proposed insulator is interspersed between the promoter and enhancer. After stable transfection into an erythroleukemia cell line, constructs containing insulators will produce significantly fewer G418-resistant colonies than those without insulators. To test for the ability to block heterochromatin formation and the effects on position effect variegation another assay has been developed. In this case, the proposed insulator is not placed in between enhancer and promoter, but instead lies upstream of both. If the proposed insulator is capable of protecting genes from position effects it will result in an increased number of G418-resistant colonies as compared to a control containing no insulator [298].

Figure A-1. Insulators prevent the activation of promoters by heterologous enhancers. The enhancer in the above figure could activate transcription from promoters 1 (P1) and 2 (P2) if not for the presence of the intervening insulator. Transcription is enhanced at P1, but not P2.

The Insulator-Binding Protein CTCF

CCCTC-binding factor (CTCF) is a vertebrate insulator binding protein that mediates enhancer blocking [299]. It is a highly conserved, ubiquitously expressed nuclear protein that interacts with target sequences approximately 50 bp in length [300]. At 727

amino acids, the full length, major form of CTCF has a molecular mass of 82 kDa [301], but due to sequences in its amino- and carboxyl-termini it runs at approximately 130 kDa in SDS-PAGE polyacrylamide gels [302]. Several studies have detected the major form of CTCF migrating at 140 kDa [299,302,303]. A minor isoform of CTCF, in which the carboxyl-terminus has been lost, migrates at approximately 70 kDa [302]. The central domain in CTCF, 100% identical in chicken and human, makes use of different combinations of the 11 zinc fingers to bind extremely divergent sites, including promoters, silencers, and enhancers (refer to Figure A-2). In addition to its role in mediating insulator activity, CTCF participates in transcriptional activation, silencing, imprinting genetic information and X-chromosome inactivation.

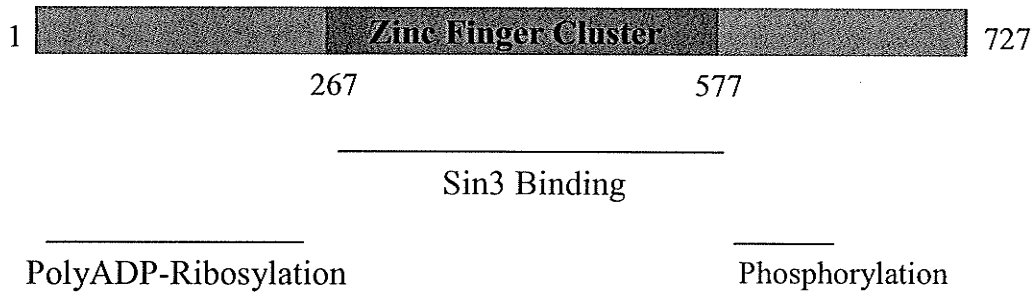

Figure A-2. Diagrammatic representation of vertebrate CTCF. The DNA-binding zinc finger cluster of the 728 amino acid CCCTC-binding factor is shown along with regions for Sin3 binding and post-translational modification by phosphorylation and polyADP-ribosylation.

The DNA Binding Capacity of CTCF

CTCF binds to a wide variety of DNA sequences and has many target sites throughout the genome including promoters, silencers and insulators. Although CTCF appears to prefer CG-rich sequences, no single consensus sequence can encompass all binding sites. Several are relatively high in CG content, including sites within the coding regions of human and mouse *c-myc* genes and in between the Igf2 and H19 genes [304-307]. A sequence of three direct repeats of CCCTC upstream of the chicken *c-myc* promoter interacts with CTCF [300]. In contrast, the second module of the chicken lysozyme silencer is AT rich, does not contain a CCCTC motif, and interacts with CTCF [306]. Different combinations of the 11 zinc fingers are used to bind DNA [299,301,306,308,309]. For example, binding to the human *c-myc* P2 promoter utilizes zinc fingers 4 through 11, while either 1 to 8 or 5 to 11 are used to bind at the F1 element of the chicken lysozyme silencer [306].

CTCF Confers Enhancer-Blocking Activity

Lower eukaryotes may employ several different mechanisms to impart insulator activity. Five proteins are known to mediate insulator function in *Drosophila*: suppressor of hairy wing (Su(Hw)), boundary element associated factor 32 (BEAF32), Zw5, GAGA factor, and *Drosophila* CTCF (dCTCF) [310-314]. Recently discovered, dCTCF has a similar domain structure and displays comparable DNA binding capacity to vertebrate CTCF. Also like vertebrate CTCF, dCTCF can specifically repress transcription and mediates enhancer blocking at the Fab-8 insulator [315]. Enhancer blocking activity of the *Drosophila* gypsy insulator, mediated by Su(Hw) and a cofactor Mod(mdg4) [314],

appears to involve attachment to the nuclear envelope [316]. In yeast, the formation of heterochromatin at active genes can be prevented by tethering insulator elements to components of the nuclear pore complex (NPC) [317]. This evidence strongly suggests that insulator activity in lower eukaryotes involves attachment to nuclear substructures, a property which has not yet been observed in vertebrates.

Vertebrate CTCF binds insulators including Fab-8, sites within the human and mouse beta-globin locus, the chicken HS4 element, the imprinting control region of the Igf2/H19 locus, and near the promoter of the *Tsix* gene at the mouse X-inactivation center [304,305,315,318-320] . Several CTCF-binding insulators that block enhancer activity do not act as barriers to the spread of heterochromatin [321]. A CTCF binding site in the chicken HS4 element located at the 5' end of the chicken β-globin locus is required to produce enhancer-blocking activity in this element [321]. In fact, until recently it was thought that CTCF conferred enhancer-blocking activity to all known vertebrate insulators [299,305,322-326]. The mechanism by which CTCF imparts enhancer-blocking activity is unclear; evidence to date suggests that it involves the creation of distinct, functional domains of chromatin regulated by covalent modification of CTCF binding sites. For example, different methylation patterns are present on paternal and maternal alleles at several loci containing CTCF binding sites [319,327-330] including the imprinting control region between the Igf2 and H19 genes [331]. DNA methylation at this loci prevents CTCF binding and insulator activity [304,305,332], creating a functional domain of chromatin at the paternal allele that is different from that at the maternal allele [333].

Models of Insulator Activity

1) *Tethering*: Insulators may tether DNA to fixed nuclear structures to create loops of chromatin in which genes are regulated together. This could involve one or more substructures such as nuclear pores or the nuclear envelope. Since heterochromatin is self-propagating from a focal point, attachment to a subnuclear structure will result in steric hindrance to the spread of condensed chromatin structure. In a similar mechanism, tethering could block the procession of a signal travelling from an enhancer to a promoter, or prevent chromatin from taking on a conformation that would allow direct (protein-mediated) contact between enhancers and heterologous promoters.

The mechanism by which insulators impart their enhancer-blocking and barrier activities may be specific to each insulator. For example, although silencing of the yeast HML locus can be controlled by tethering it to the NPC, this is not so for the yeast HMR locus [334]. Control of insulator function at the yeast HMR locus must be by alternate means, which is also likely the case for vertebrate insulators as none have been identified to associate with the NPC or nuclear envelope. Chromatin domains could also result from interactions with the nuclear matrix [335]. In this scenario, the nuclear matrix would act as an anchor point to define domains for structural and functional regulation [335]. In support of this hypothesis, several insulators are found beside matrix attachment regions (MARs) [336] and it has been determined that a region mediating insulator activity 5' of the chicken lysozyme promoter is also a matrix attachment region (MAR) [337].

2) *The Barrier Model*: Similar to the tethering model, a large DNA-bound complex at the insulator could physically block the propagation of chromatin structure or a signal on route to a promoter.

3) *Nucleosome Positioning and Availability*: Insulators in conjunction with the proteins that bind them can alter the regular spacing of nucleosomes to create a nucleosome gap, which could disrupt the self-propagation of condensed chromatin [338]. Additionally, insulator-binding proteins may interact with histones to mask nucleosomes [114], creating a situation in which proteins needed to propagate heterochromatin compete for binding with those proteins bound to the insulator.

4) *Histone Code Manipulation:* The *Drosophila* gypsy insulator localizes to regions interspersed between condensed and decondensed chromatin structure [339,340] and CTCF has been shown to bind insulators that separate regions with low levels of histone acetylation from regions enriched in acetylated H3 [341]. Localization of insulators to regions of transition in chromatin structure raises the possibility that these elements modulate chromatin to achieve enhancer-blocking or barrier activity. In yeast, tethering a histone acetyltransferase to regions of chromatin creates a substantial domain of acetylated histones through which condensed chromatin cannot pass [342]. Manipulation of the histone code by insulators or insulator-associated factors could create or destroy binding sites for various proteins, including those necessary for the propagation of heterochromatin or maintenance of euchromatin.

Regulation of DNA Binding Capacity and Enhancer-Blocking Activity of CTCF

The functional roles of CTCF associated with its DNA binding ability are regulated by several means. Differential methylation of DNA at CTCF binding sites was the first of these mechanisms to be discovered. DNA is methylated at the H19 imprinting control region in only one allele; CTCF will not bind to methylated sites, leading to the inactivity

of this insulator on one allele only [304,305,332,333]. In addition, two post-translational modifications to CTCF have been identified: phosphorylation by CK2 (casein kinase II) and polyADP-ribosylation by PARP-1 (poly(ADP-ribose) polymerase) (refer to Figure A-2) [343,344]. Both modifications play important functional roles. While phosphorylation takes place on several residues in the C-terminus, of which serine 612 appears to be particularly important, polyADP-ribosylation occurs in the N-terminal portion of CTCF. Phosphorylation may affect its DNA binding capacity and alter its role in transcriptional activation and or repression on a gene-by-gene basis [343,344]. Unlike other transcription factors including YY1 [345], the DNA binding capacity of CTCF does not seem to be altered by polyADP-ribosylation [344]. Chromatin immunoprecipitation analysis found CTCF bound to more than 140 target sites, many of which were also bound by a polyADP-ribosylated protein. Furthermore, inhibition of PARP activity prevents activity of the insulator located within the imprinting control region of H19 and may prevent the function of CTCF-bound insulators on a much wider scale [344].

Other transcription factors also influence the enhancer-blocking activity of CTCF. A recent study found an interaction between CTCF and the POZ- (pox virus and zinc finger) zinc finger transcription factor Kaiso, which has a consensus binding site near to the site of CTCF binding at the 5' β-globin insulator. When intact, this site inhibits enhancer-blocking by CTCF [346].

CTCF is involved in Transcriptional Activation and Repression

CTCF can act as a transcriptional activator or repressor. For example, studies indicate that CTCF is involved in transcriptional activation of the amyloid β-protein precursor

(APP), which is cleaved to produce amyloid β-protein [301,347]. Characteristics of Alzheimer's disease and Down's syndrome include extracellular deposition of this protein [348-350]. The first 100 bp upstream of the APP transcription start site are adequate to achieve high levels of APP transcription [351,352]. This region contains the sequence GCCGCTAGGGGT located 82 to 93 bp upstream of the transcription start site. APBβ, a nuclear factor binding site, is the major activation site within this region [353] and binds CTCF [309]. Experiments indicate CTCF binding to the APBβ domain is needed to reach optimal transcriptional activity [309] and that CTCF may be involved in upregulating transcription at the APP gene in response to TGFβ [354]. Deletion of a 248 amino acid region in the amino-terminus of CTCF destroys its ability to activate transcription [301,309].

CTCF is involved in transcriptional repression at the *c-myc* gene, when bound to the second module (F1) of the chicken lysozyme silencer [300,306,308,355,356], and at the hTERT (human telomerase reverse transcriptase) gene [357]. The location of CTCF binding at the chicken *c-myc* gene is different from that at the human *c-myc* gene. As well, the target sequences are quite divergent. In both cases CTCF acts as a transcriptional repressor, indicating that this function for CTCF has been conserved throughout vertebrate evolution [308]. Repression can be regulated by post-translational phosphorylation of four serine residues within the carboxyl-terminus of CTCF, which results in an increased expression of the human and chicken *c-myc* genes [358]. The presence of thyroid hormone can also abrogate repression through CTCF binding sites and nearby thyroid hormone response elements through a mechanism that does not remove bound CTCF [325]. This result suggests that CTCF is not recruited during

repression but bound to this site constitutively. Steady-state levels of acetylation on histone H4 near CTCF binding sites increases in the presence of thyroid hormone, suggesting that targeted modulation of chromatin structure is involved [359]. Analysis of the CTCF-binding site in the proximal exonic region of hTERT revealed that the effectiveness of this element in repressing transcription can be modulated by the distance between it and the hTERT promoter, indicating that nucleosome positioning is a factor in this case of CTCF-mediated transcriptional repression [357].

In vitro studies indicate the presence of tissue-specific repressive domains in CTCF. Regions within the zinc finger domain, N-terminal region and C-terminal regions were able to repress transcription of a reporter gene in chicken erythroblasts, while only portions of the zinc finger domain and C-terminal region functioned as repressors in African Green Monkey kidney cells (COS-1 and CV-1 cells) [360]. Other *in vitro* studies found that GST-CTCF co-immunoprecipitates with Sin3A. This protein is part of the Sin3A co-repressor complex that contains HDAC1 and HDAC2, and additional studies indicated the presence of HDAC activity in material immunoprecipitated with antisera against GST-CTCF [360]. Association of CTCF with chromatin modifying enzymes further suggests that CTCF mediates its various effects through a mechanism including the modulation of chromatin structure [360].

CTCF is Involved in Imprinting Genetic Information

A small number of mammalian genes, generally found in clusters, undergo genomic imprinting [361]. During this process maternal and paternal alleles inherit epigenetic marks, resulting in the expression of one allele as determined by its parent of origin.

Although the mechanism is not well understood, it is associated with the differential methylation of DNA and various histone modifications.

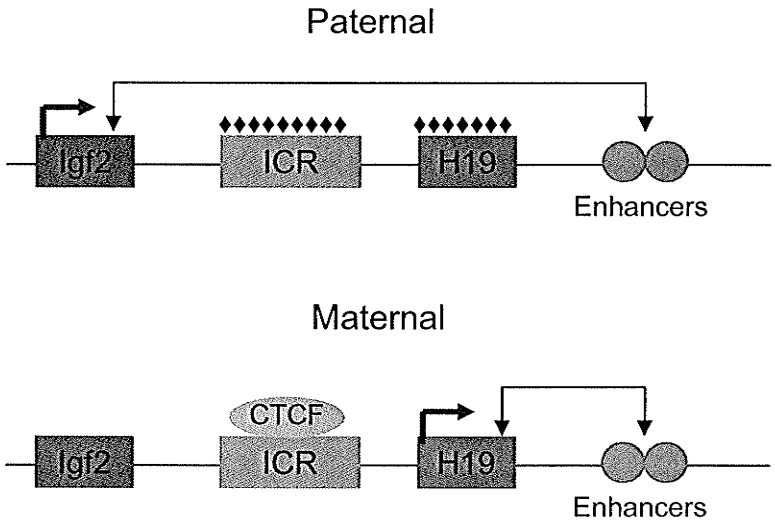

Figure A-3. Genomic imprinting controls expression of the Igf2 and H19 genes. The imprinting control region (green box) interspersed between Igf2 (blue box) and H19 (red box) is methylated on the paternal allele (black diamonds). On the paternal allele, upstream enhancers (grey circles) are able to communicate with the Igf2 gene; transcription, represented by a red arrow, takes place. On the maternal allele transcription of H19 occurs, but CTCF binding to the imprinting control region prevents enhancer-mediated activation of the Igf2 gene.

CTCF binds several loci, which exhibit different methylation patterns on paternal and maternal alleles [319,327-330], the best characterized being the imprinting control region (ICR) between the Igf2 and H19 genes [331]. These genes located approximately 80 kb apart are reciprocally imprinted and share a set of enhancers downstream of H19 (refer to Figure A-3) [362-365]. The imprinting control region interspersed between the two contains four CTCF binding sites [304,305,322,323]. DNA methylation on the paternal allele prevents CTCF binding and insulator activity [304,305,332], such that transcription

of the Igf2 gene is enhanced while H19 is repressed [366]. On the maternal allele CTCF binds the ICR, preventing contact between Igf2 and its upstream enhancers but allowing activation of the H19 gene [367].

The CTCF Protein Family

CTCF is part of the BORIS–CTCF protein family of proteins that share their 11 zinc-finger DNA binding domain [368]. BORIS, the brother of the regulator of imprinted sites, contains distinct N- and C-termini. Expression patterns of CTCF and BORIS are mutually exclusive during male germline development [368,369]. Genome-wide demethylation takes place during BORIS expression and later reappears concomitantly with the onset of CTCF expression in postmeiotic spermatocytes, leading to suggestions that BORIS associates with demethylases as a way to regulate CTCF binding at insulators including that between the Igf2 and H19 genes [368].

CTCF is a Putative Tumour Suppressor

Mutation or deletion of tumour suppressor genes is a key factor in the formation of human malignancies [370,371]. Tumour suppressor genes are defined as those whose function actively prevents the one or more of the series of events leading to tumour formation. These genes tend to code for proteins playing roles in cell division, regulation of transcription, and DNA repair. Mutations to tumour suppressor genes cause deregulation of important cellular processes.

Several findings led to the proposal that CTCF is a tumour suppressor gene.

Rearrangements of the CTCF gene have been observed in breast carcinoma cell lines, and rearrangements of the exons encoding the zinc finger DNA-binding domain of CTCF were detected in a fresh breast tumour sample [372]. Moreover, four common missense mutations in the exons coding for the zinc finger DNA-binding domain of CTCF are found in breast, prostate and Wilm's tumours [373]. Selective loss of DNA binding was observed in the resulting mutant CTCF, which decreased binding to the proliferation-related genes myc and Igf2 but not to other loci including the APP promoter, lysozyme silencer, or β-globin insulator [373]. These findings led researchers to hypothesize that change-of-function mutations to CTCF contribute to the development of human malignancies [373], which is supported by a study of invasive breast carcinoma samples, cytoplasmic expression of CTCF associated with increased tumour size and vascular invasion [374].

Several studies indicate that alterations to chromatin structure by chromatin modifying enzymes have a role in the genesis of cancer [375-377]. Evidence suggests that CTCF associates with complexes able to modulate chromatin structure [360], and thus may be involved in maintaining appropriate chromatin conformations. Changes in the ability of CTCF to bind specific sequences of DNA could lead to altered recruitment of chromatin modifiers and abnormal chromatin structure, thereby producing aberrant gene expression leading to malignancy [378].

Rational and Hypothesis

CTCF has been shown to bind insulators that separate regions with low levels of histone acetylation from regions enriched in acetylated H3 [341]. Other studies have found evidence that CTCF associates with chromatin-modifying histone deacetylases. Co-immunoprecipitation studies of a GST-CTCF construct indicate that the zinc finger domain of CTCF associates with the Sin3A co-repressor complex [360]. This study also determined that material immunoprecipitating with GST-CTCF contained histone deacetylase activity, but did not identify specific HDACs [360]. Several insulators are found beside matrix attachment regions (MARs) [336] and it has been determined that a region mediating insulator activity 5' of the chicken lysozyme promoter is also a matrix attachment region (MAR) [337]. HDAC1 and HDAC2 associate with the nuclear matrix and are part of the Sin3A co-repressor complex. Binding of CTCF to the base of chromatin loops could create a situation where the enhancer-blocking activity of CTCF is regulated by a functional association with the HDACs found on the nuclear matrix. We therefore hypothesize that CTCF associates with the nuclear matrix and histone deacetylases to impart its enhancer-blocking activity

Hypothesis:

CTCF confers enhancer-blocking activity to insulators through an association with the nuclear matrix and nuclear matrix associated proteins HDAC1 and HDAC2.

Our objectives were to answer the following questions:

1. Does CTCF associate with the nuclear matrix?
2. Does CTCF bind MARs? In other words, is CTCF at the base of chromatin loops?
3. Does CTCF function in association with the nuclear-matrix bound chromatin modifiers HDAC1 and HDAC2? If so, does this association occur on the nuclear matrix?

Cell Lines and Tissue Culture

MCF-7(T5) breast cancer cells were cultured in Dulbecco's Modified Eagle Medium (DMEM) (Gibco, NY, USA), prepared as per manufacturers instructions. Powdered medium was added to a volume of ddH_2O measuring 5% less than the required final volume of media with gentle stirring. To this, 3.7g of sodium bicarbonate ($NaHCO_3$) was added per liter of media. The media was then diluted to its final volume and stirred gently until all particulates were fully dissolved. The pH was adjusted to 7.5 with 1N HCl or 1N NaOH and the media sterilized by filtration (Corning bottle top filter, 0.22 μm, Corning, NY). Media was stored in this condition at 4°C for no longer than two weeks before use.

Supplements were added to DMEM just before use to such that it contained 100 units/ml penicillin, 100 μg/ml streptomycin sulfate, 6.3% FBS, 0.3% glucose and 2 mM L-glutamine. Cells were cultured in plastic tissue culture flasks or plates (Nunc, VWR International, Mississauga, ON) in a humidified environment, at 37°C with 5%CO_2. Cells were grown to 60 – 80% confluence, at which point they were removed from dishes by trypsinization and one fifth of the cells added to a new tissue culture dish. Procedures for trypsinization, preparation for storage in a liquid nitrogen tank, and starting up frozen cells were as described for 10T1/2 and C3 cells.

Preparation of Cell Lysates

Cell lysates were prepared as previously described [379]. Briefly, media covering cells grown on 140 mm plates was aspirated and the cells washed with PBS, pH 7.5. Approximately 1 X 10^6 MCF-7 (T5) cells were then collected in 500 µl of IGEPAL buffer [1% (v/v) IGEPAL, 150 mM NaCl, 50 mM Tris-Cl, pH 8.0, 1 mM PMSF, and 1 X protease inhibitor cocktail from Roche]. While on ice, the cell suspension was passed through a 25-gauge syringe four times and sonicated at 40% output for 15 seconds twice. After centrifugation the supernatant (cell lysate) was collected and stored at -20°C. Protein concentration was determined using the Bio-Rad Protein Assay (Bio-Rad Laboratories).

Cellular Fractionation with Triton X-100

Cellular fractionation with Triton X-100 was performed as described previously [20]. MCF7 (T5) cells were grown to 80% confluence in a 140 mm plate. Media was aspirated and the cells were washed twice with PBS, pH 7.5. Cells were then scraped into 1.5 ml PBS and pelleted by centrifugation at 1000 rpm for 3 min at 4°C. The PBS was then aspirated and the cells resuspended in TNM buffer (300 mM sucrose, 100 mM NaCl, 10 mM Tris-Cl, pH 8.0, 2 mM $MgCl_2$, 1% thiodiglycol, 1 mM PMSF, 1 X protease inhibitor cocktail from Roche). One drop of this fraction was placed on a slide, and 100 µl of this cellular fraction was saved. The suspension was then passed through a 22-gauge needle five times, after which one drop was placed on the slide and compared to the cellular

fraction. The suspension was centrifuged and the cytosol and nuclei separated. Nuclei were checked under a light microscope before resuspension in TNM buffer containing 0.5 % Triton X-100. The sample was then placed on ice for 5 min before centrifugation at maximum speed in a microfuge at 4°C for 10 minutes. The resulting Triton-soluble fraction (supernatant) and Triton-insoluble fraction (pellet) were stored at -20°C for future use.

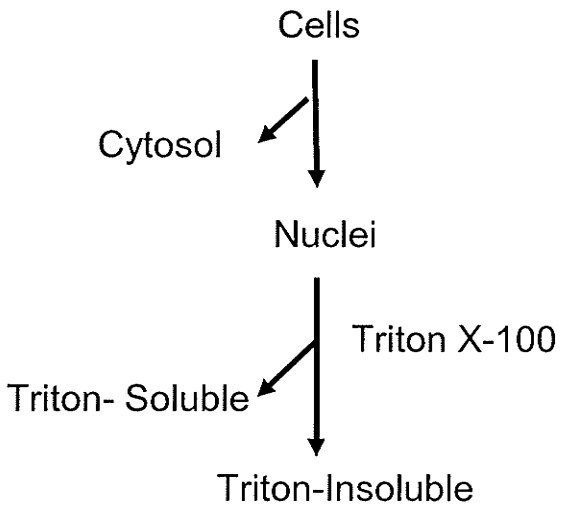

Figure A-4. Cellular Fractionation by Triton Extraction. Nuclei are isolated and extracted with a solution containing 0.5% Triton X-100. This results in the formation of a Triton-Soluble fraction (supernatant) and a Triton-Insoluble fraction (pellet).

Isolation of Proteins Cross-Linked to DNA by Cisplatin in Situ.

Proteins were cross-linked to DNA with cisplatin in MCF-7 breast cancer cells as described previously [18]. Cell pellets (1×10^6 cells/ml) were incubated with 1 mM

cisplatin for 2 h at 37°C. Lysis buffer (5 M urea, 2 M guanidine hydrochloride, 2 M NaCl, 0.2 M potassium phosphate, pH 7.5) was then added to the cells followed by hydroxylapatite (Bio-Rad Laboratories, Hercules, CA). RNA and proteins not cross-linked to DNA were removed from the resin by three washes with lysis buffer. The protein-DNA cross-links were reversed by adding 1 M thiourea.

Isolation of Nuclear Matrix Proteins

Nuclear matrices were isolated as described previously [380]. MCF7 (T5) cells grown to 80% confluence were washed with PBS, pH 7.5. Approximately 1 X 10^7 cells were resuspended in 5 ml cold TNM buffer (300 mM sucrose, 100 mM NaCl, 10 mM Tris-Cl, pH 8.0, 2 mM $MgCl_2$, 1% (v/v) thiodiglycol, 1 mM PMSF, 10μg/ml aprotinin and 1 μg/ml leupeptin) to which Triton X-100 was added to a final concentration of 0.25% (v/v). Suspended cells were passed through a 22-gauge syringe five times. Nuclei (20 A_{260}/ml) isolated through centrifugation were digested with 100 μg/ml DNAse 1 (Sigma, St. Louis, MO) for two hours at room temperature in DIG buffer [50 mM NaCl, 300 mM sucrose, 10 mM Tris–Cl, pH 7.4, 3 mM MgCl2, 1% (v/v) thiodiglycol, and 0.5% (v/v) Triton X-100] with 1 mM PMSF, 10 μg/ml aprotinin, and 1 μg/ml leupeptin. The removal of chromatin was then facilitated by the addition of ammonium sulfate (ICN Biomedicals, Aurora, OH) slowly, while mixing, to a final concentration of 0.25 M. Samples were then centrifuged at 9600*g* for 10 min at 4°C after which the supernatant, termed the S3 fraction, was saved. The pellet, termed the NM1-IF fraction, contained the

nuclear matrix and associated intermediate filaments. It was resuspended in 8 M urea and stored at -20°C.

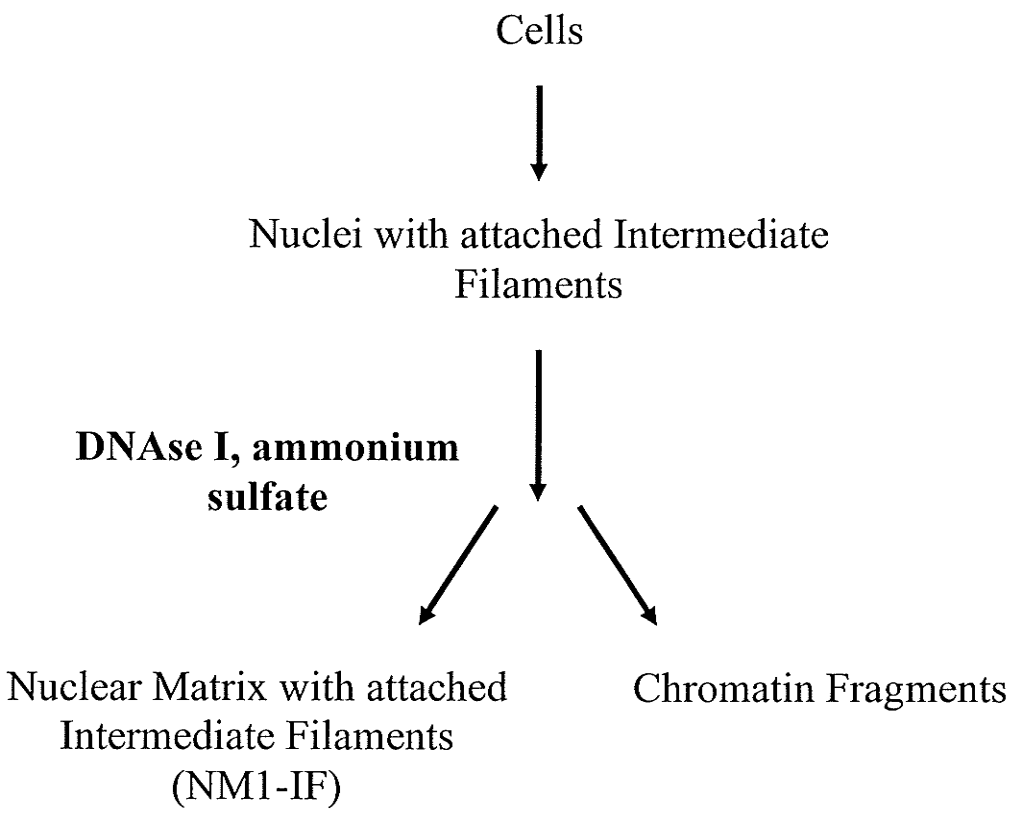

Figure A-5. Flow diagram of nuclear matrix preparation. To prepare nuclear matrices, nuclei are first isolated with intermediate filaments still attached. Nuclei are then treated with DNAse 1 and ammonium sulfate to remove chromatin fragments.

Immunoprecipitation of HDAC1 and HDAC2

Antibodies specific to human HDAC1 and human HDAC2 were used to immunoprecipitate these proteins from MCF-7 (T5) cell lysates. MCF-7 (T5) cell lysate

(500 µg of total protein) prepared as described above was added to immunoprecipitation (IP) buffer (50 mM Tris-Cl pH 8.0, 150 mM NaCl, 0.5% IGEPAL, 50 mM NaF, 1mM EDTA, 1X proteinase inhibitor cocktail from Roche) to give a final volume of 1 ml. Cell lysate was pre-cleared with 50 µl of a 1:1 slurry of Protein A Sepharose (Pierce) (in IP buffer) for 30 min at 4 °C. Five µg of polyclonal antibody specific for HDAC1 (ABR: Affinity Bioreagents Inc.) or HDAC2 (ABR) was incubated with the pre-cleared sample overnight at 4°C with rotation. A negative control was done in which no antibody was added. A polyclonal antibody specific for ubiquitinated proteins was used as a non-specific control. After incubation with polyclonal antibody, 50 µl of Protein A Sepharose (Pierce) was added and the samples were incubated for 2 h at 4°C with rotation. Beads were washed 3 times with 1 ml of IP buffer and resuspended in SDS PAGE loading buffer.

Separation of Protein Samples by SDS-PAGE

At times protein samples, including cell lysates, immunoprecipitated material and samples resulting from various types of extractions (Triton, NM1-IF, etc) were separated by SDS-PAGE. The procedure for this separation was as described above for histone separation with the following modifications. Ten percent polyacrylamide gels were used. The separating portion of these gels was prepared by combining 4.2 ml ddH_20, 2.5 ml 4X Tris-Cl/SDS pH 8.8, 3.3 ml 30% acrylamide stock, 33.3 µl 10% APS, and 6.7 µl TEMED. The stacking portion was prepared as described above. Ten percent polyacrylamide gels were poured between glass plates with spacers of 1.0 or 1.5 mm. These gels were run at 175 V for 1.5 h to 2 h.

Transfer of Proteins to Nitrocellulose

Proteins, including histones, were transferred to nitrocellulose for immunoblot analysis. After running SDS-PAGE gel, the gel was carefully removed from between the glass plates and set up in a sandwich such that protein will be transferred to a pre-soaked (in transfer buffer) piece of nitrocellulose. Transfer buffer contained 400 mM 3-(Cyclohexylamino)-1-propanesulfonic acid (CAPS) and 20% methanol in ddH_20. Transfer was done overnight (approximately 16 h) at 50 V in the cold room.

Immunoblot Analyses

Proteins from the various fractions were separated by SDS 10% PAGE and analysed by immunoblotting with antibodies specific for the C-terminal 570-727 residues of CTCF in a protocol similar to that described above (Upstate Biotechnology, Inc.; Lake Placid, NY, USA), HDAC1 (Affinity Bioreagents; Golden, CO, USA) and HDAC2 (Affinity Bioreagents).

RESULTS

CTCF is a Nuclear Matrix Protein

The subcellular distribution of CTCF was determined in MCF-7 (T5) breast cancer cells. MCF-7 (T5) breast cancer cells were fractionated in TNM buffer and the nuclei extracted with 0.5% Triton X-100. The resulting fractions were a Triton-soluble fraction containing components loosely bound in the nucleus, and a Triton-insoluble fraction containing components tightly bound to structures in the nucleus.

Immunoblot analysis was used to detect CTCF in these fractions as well as cellular, cytosolic and nuclear fractions. This analysis detected isoforms of CTCF migrating at 155 kDa and 90 kDa (Figure A-6). The major 150 kDa isoform was detected in the nuclear and Triton-insoluble fraction, indicating that CTCF is tightly bound to a nuclear structure (Figure A-6). The nuclear matrix and DNA are both possible structures that could be retaining CTCF in the nucleus through Triton extraction.

Nuclear matrices were isolated from MCF-7 (T5) breast cancer cells to determine if the CTCF present in the Triton-insoluble fraction was associated with the nuclear matrix. In this procedure, isolated nuclei are treated with DNAse to remove chromatin. The resulting fractions, including nuclei before and after DNAse treatment, were separated on SDS-polyacrylamide gels, transferred to nitrocellulose, and analysed by immunoblot. CTCF was detected in all fractions except the cytoplasm: cellular, nuclei before and after DNAse treatment, nucleoplasm and the nuclear matrix (NM1-IF) (Figure A-7 A). A significant amount of the 155 kDa major isoform of CTCF was present in the nuclear matrix fraction.

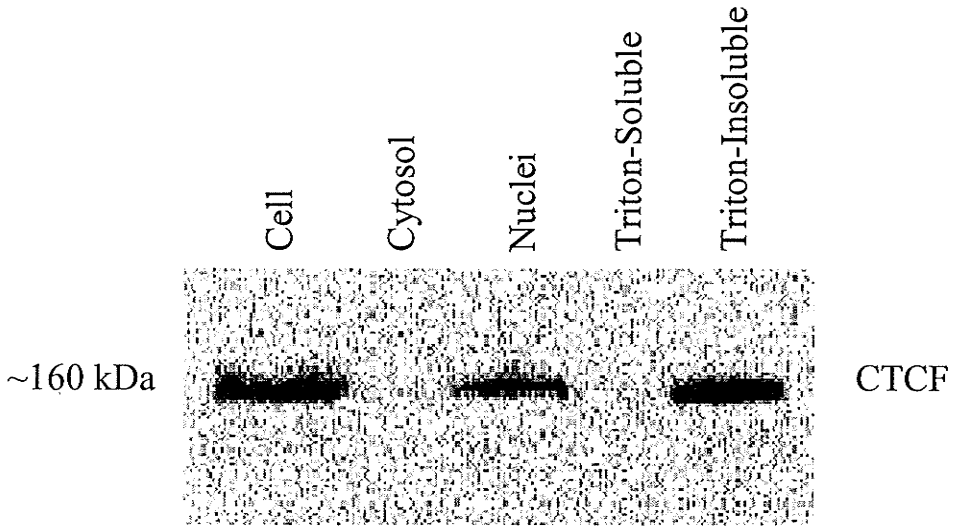

Figure A-6. CTCF is tightly bound in the nucleus. Nuclei isolated from MCF-7 (T5) breast cancer cells were extracted with 0.5% Triton X-100. Equal volumes of cell fractions, cell lysate (lane 1), cytoplasm (lane 2), nuclei (lane 3), Triton-soluble (lane 4), and Triton-insoluble (lane 5), were run on SDS 10% polyacrylamide gels and transferred to nitrocellulose membrane. An anti-CTCF antibody immunochemically stained membrane is shown. CTCF was detected in the cell lysate, nuclear, and Triton-insoluble fractions (lanes 1, 3, and 5).

A standard curve was generated by running increasing volumes of a known concentration of NM1-IF on an SDS–PAGE gel, immunoblotting, and scanning the blot into the Image Station 440CF (Kodak Digital Science). The net intensity of the CTCF band, as determined using 1D Image Analysis Software (Kodak Digital Science), was plotted against the volume loaded to obtain the best trendline (Microsoft Excel). The intensity of the CTCF band in cellular and NM1-IF fractions was then used with the equation for the trendline to determine the relative amounts of CTCF in cellular and NM1-IF fractions. This analysis indicated that at least 21% of the major CTCF isoform was associated with the nuclear matrix. The minor isoform of CTCF detected in these experiments, migrating at 90 kDa, was found in the chromatin-released fraction, but not in the nuclear matrix fraction (NM1-IF) (Figure A-7 A). Fractions were also analysed by immunoblot with an antibody specific for human HDAC1, which is known to associate with the nuclear matrix [20]. This test gave the expected results, with HDAC excluded from the cytosol but present in all other fractions, including the NM1-IF, demonstrating that our fractionation was performed correctly. As can be seen in Figure A-7, DNAse I digestion done at room temperature subjected the 155 kDa isoform of CTCF to proteolysis, but did not have a similar effect on HDAC1. The 90 kDa isoform of CTCF was not detected in fractions before DNAse digestion, suggesting that it is, in fact, a product of proteolysis occurring during the DNAse digestion. This band also appears in other fractions that were not digested with DNAse, thus the proteolysis in not likely due to a protease present in the DNAse I preparation.

The above mentioned nuclear matrix preparation was done in the presence of protease inhibitors, and precautions were taken to keep samples on ice at all times. Figure A-7 B

shows a nuclear matrix preparation that was performed without protease inhibitors at a higher average temperature. Under these conditions, extensive proteolysis of CTCF is evident in the nuclear fraction collected after DNAse 1 digestion, the nucleoplasm and the nuclear matrix (NM1-IF).

Cisplatin is a cross-linking agent that preferentially cross-links nuclear matrix proteins to MAR DNA [381-383]. We used this technique to determine if the nuclear matrix associated isoform of CTCF was bound to DNA *in situ*. MCF-7 (T5) breast cancer cells were incubated with cisplatin to cross-link proteins to DNA, after which the cross-linked proteins were separated by SDS-PAGE and analysed by immunoblot along with cell lysate (Figure A-8). Both the major (155 kDa) and minor (90 kDa) isoforms were present in the cell lysate. The major isoform was also detected in both cisplatin cross-linked protein samples, indicating that CTCF is potentially a MAR binding protein. Also detected in the cross-linked samples were isoforms migrating at 135, 120 and 75 kDa. These were reproducibly detected in cisplatin cross-linked samples; however the 90 kDa isoform was not present.

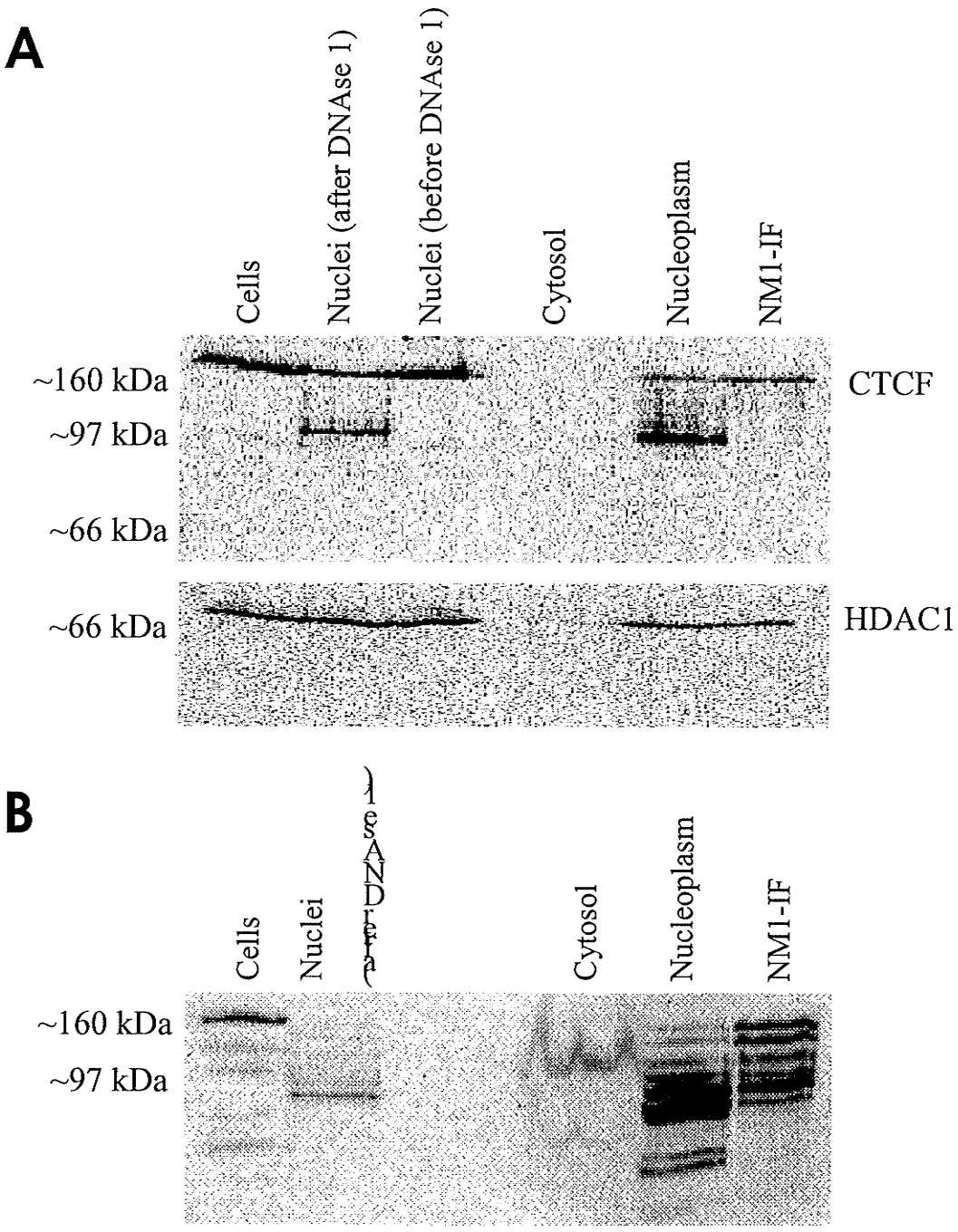

Figure A-7. CTCF associates with the nuclear matrix. The nuclear matrix was isolated from MCF-7 (T5) breast cancer cells. A) Aliquots of whole cells (lane 1), nuclei before and after DNAse 1 digestion (lane 3 and 2), cytosol (lane 4), and nucleoplasm (lane 5) were saved. Samples including the nuclear matrix fraction (NM1-IF) (lane 6) were analyzed by SDS 10% PAGE. Immunoblot analyses were performed with antibodies specific for CTCF and HDAC1. B) Degradation of CTCF is more extensive in samples isolated at higher temperatures without protease inhibitors.

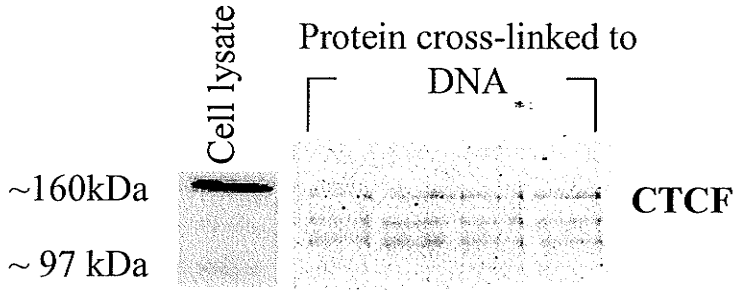

Fig. A-8. Cisplatin cross-links CTCF to DNA in situ. MCF-7 breast cancer cells were incubated with 1 mM cisplatin and the proteins cross-linked to DNA isolated. Samples of cisplatin cross-linked proteins (20 μg) and 40 μg of MCF-7 cell lysate (lane 1) were separated by SDS 10% PAGE and transferred to nitrocellulose membrane. The membrane was immunochemically stained with antibodies specific for CTCF.

CTCF does not Associate with HDAC1 or HDAC2

Previous *in vitro* studies had implied that CTCF may associate with histone deacetylases to mediate its many activities in the nucleus. In these studies, a pull-down assay was employed to determine that a GST-CTCF construct co-immunoprecipitated with Sin3A, part of the Sin3A HDAC complex [360]. The immunoprecipitated material also contained HDAC activity, further suggesting that CTCF interacts with the Sin3A HDAC complex [360].

The Sin3A HDAC complex contains HDACs 1 and 2. We therefore attempted to more directly show an interaction between CTCF and HDAC1 and HDAC2 through co-immunoprecipitation experiments. These experiments were done under low stringency conditions, such that protein-protein interactions were not destroyed. To control for specificity of the antibody-antigen interaction, we included an isotype-matched antibody against ubiquitin-conjugated proteins. As an additional control we left primary antibody out of one sample.

Fractions of bound and unbound material were saved for each immunoprecipitation condition, as well as a fraction of the material used for immunoprecipitation (input). These samples were separated on SDS-polyacrylamide gels, transferred to nitrocellulose, and immunostained with antibodies specific for CTCF, HDAC1, and HDAC2 (Figure A-9). We did not detect CTCF in fractions immunoprecipitated with antibodies recognizing HDAC1 or antibodies recognizing HDAC2. CTCF was present in the unbound fractions, indicating that the majority of CTCF does not interact with HDAC1 or HDAC2. The conditions used during immunoprecipitation experiments have the potential to disrupt interactions between proteins. To determine if protein-protein interactions were disrupted

under our immunoprecipitation conditions, we also stained material immunoprecipitated with antibodies recognizing HDAC2 for HDAC1. As shown in Figure A-10, HDAC1 was found in fractions immunoprecipitated with antibodies for HDAC2 (lane 4). A larger amount of HDAC1 was in the unbound fraction (lane7), indicating that a proportion, but not all, of cellular HDAC1 is in complex with HDAC2. Therefore our immunoprecipitation protocol did not destroy protein complexes.

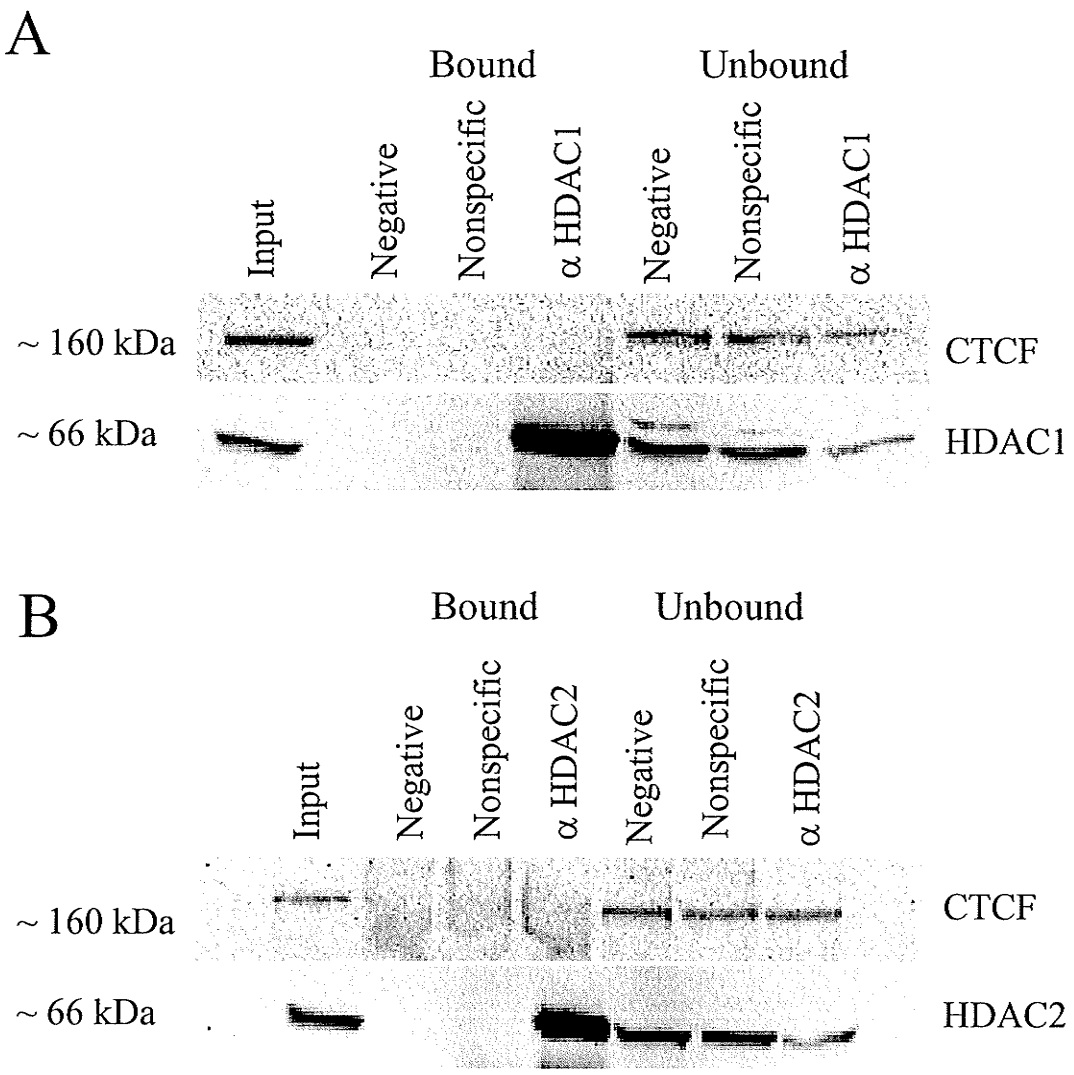

Figure A-9. CTCF does not associate with HDAC1 or HDAC2. Five hundred micrograms of MCF-7 (T5) breast cancer cell lysate was incubated with 5 μg anti-HDAC1 polyclonal antibody or 5 μg anti-HDAC2 polyclonal antibody. The immunoprecipitated (bound) and immunodepleted (unbound) fractions were collected. A negative control to which no antibody was added was also included. Five hundred micrograms of MCF-7 (T5) breast cancer cell lysate was also incubated with a polyclonal antibody specific for ubiquitinated proteins to check the specificity of binding (nonspecific). (A) Samples of the HDAC1 immunoprecipitation were separated by SDS 10% PAGE and analyzed by immunoblot analyses. The efficiency of immunoprecipitation was confirmed by immunoblot analyses with an HDAC1-specific antibody (see lanes 4 and 7). The presence of CTCF in unbound fractions (lanes 5–7) was determined by immunoblot analyses with an antibody specific for CTCF. (B) HDAC2 was immunoprecipitated from MCF-7 (T5) breast cancer cell lysate. Samples were separated by SDS 10% PAGE. The efficiency of immunoprecipitation was confirmed by immunoblot analyses with an HDAC2-specific antibody (see lanes 4 and 7). The presence of CTCF in unbound fractions (lanes 5–7) was determined by immunoblot analyses with an antibody specific for CTCF.

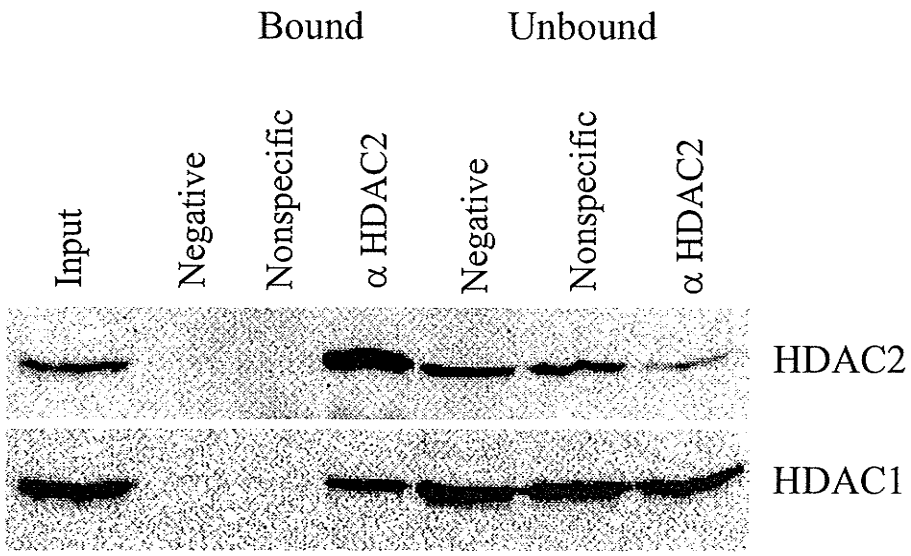

Figure A-10. HDAC1 co-immunoprecipitates with HDAC2. Five hundred micrograms of MCF-7 (T5) breast cancer cell lysate was incubated with 5 μg anti-HDAC2 polyclonal antibody. A negative control to which no antibody was added was also included, as well as an antibody to ubiquinated proteins to check specificity of binding (nonspecific). Immunoprecipitated (bound) and immunodepleted (unbound) fractions were collected. Samples were separated by SDS 10% PAGE and analyzed by immunoblot analyses. The efficiency of immunoprecipitation was confirmed by immunoblot analyses with antibodies recognizing HDAC2 and HDAC1.

MAJOR FINDINGS:

- We were the first to identify CTCF as a nuclear-matrix associated protein. This has important structural implications for the organization of chromatin as well as the mechanism by which insulators protect genes from inappropriate activation.

- Nuclear matrix proteins are preferentially cross-linked to MARs *in situ* in a procedure employing cisplatin. Using this procedure, we found that CTCF can be cross-linked to DNA by cisplatin, indicating that it is bound to MARs *in situ*.

- We determined that CTCF does not function in a complex with HDAC1 or HDAC2, both components of the Sin3A co-repressor complex, implying that these two enzymes are not recruited to CTCF-bound insulators as had previously been postulated.

Much of this work was published in Dunn KL, Zhao H, and Davie JR. The insulator binding protein CTCF associates with the nuclear matrix. Exp. Cell Res. 2003. 288(1):218-223.

Conclusions and Discussion

MARs are located next to several insulators [336]. Certain insulators, for example a region 5' of the chicken lysozyme promoter, are known to attach to the nuclear matrix [337]. We have found that at least 21% of the 155 kDa major form of the insulator-binding protein CTCF is associated with the nuclear matrix (Figure A-7). The actual percentage is most likely higher than this, as the nuclear matrix isolation procedure often results in the loss of some true nuclear matrix proteins. As well, we have found that the major 155 kDa form of CTCF was highly susceptible to degradation. Several attempts to prevent this degradation, including the addition of protease inhibitors and lowering of incubation temperatures were unsuccessful, which leads us to speculate that a CTCF-specific protease may be present in our cells.

The 90 kDa minor form of CTCF was not detected in all samples. In cell lysates containing this minor form, only small quantities were found (Figure A-6, Figure A-7 A lane 1, Figure A-8 lysate); increased amounts were detected in samples that were manipulated at room temperature (Figure A-7 B). Furthermore, many isoforms of CTCF were present in samples of proteins cross-linked to DNA by cisplatin (Figure A-8), suggesting that these and the 90 kDa minor form of CTCF are the product of protease digestion. We did not detect the proteolytic 90 kDa minor form of CTCF in nuclear matrix samples (Figure A-7 A). The antisera against CTCF recognized the C-terminal region of the protein, thus this result indicates that the N-terminal portion of CTCF contains a nuclear matrix targeting domain.

A CTCF binding site at the 5' boundary of the human apolipoprotein B gene is found interposed between a DNAse 1-sensitive region containing upstream regulatory elements and a region of condensed chromatin downstream [336]. Similarly, the 3'HS insulator proposed to insulate the α-globin LCR from downstream olfactory gene enhancers is marked by a DNAse 1 hypersensitive site [303]. The placement of insulators at points of transition from condensed chromatin structure to a more open conformation suggests that CTCF employs chromatin modulation as a mechanism to mediate insulator function. It is plausible that proteins bound to insulators work to manipulate the histone code. This could be through innate histone-modifying capabilities or recruitment of chromatin modifying enzymes and would result in the modulation of chromatin structure and the formation and/or removal of DNA binding sites. For example, the binding of co-repressor complexes to histones may be prevented [114]. The transcription factor USF (upstream stimulatory factor) is proposed to recruit histone modifiers to the HS4 element and mediate insulator barrier activity by means of the chain terminator model [114,384]. In this model histone modifications present at the insulator act as a barrier to the propagation of condensed chromatin [114]. For example, H3 acetylated at K9 would block the heterochromatin-associated methylation of this residue [384].

The nuclear matrix-associated, MAR-binding protein SATB1 associates with the HDAC-containing NuRD complex [385]. *In vitro* immunoprecipitation data provides evidence with a GST-CTCF construct that CTCF recruits the Sin3A HDAC complex [360]. In spite of this our studies failed to find an association between CTCF and HDACs 1 and 2, demonstrating that neither Sin3A nor NuRD HDAC complexes are recruited by CTCF. Other studies, published after ours, were also unable to detect an interaction between

CTCF and Sin3 [386], nor an interaction between CTCF and YB-1, as had been previously reported [387].

Two predominant themes have emerged in models to explain the enhancer-blocking activity of insulators. In one, communication between enhancer and promoter via a processive signal travelling down the strand of DNA is blocked by the presence of a large protein complex bound to an insulator [388]. Although plausible, this model is disputed by the finding that two tandem copies of the *Drosophila* Su(Hw) insulator placed in between enhancer and promoter are not capable of blocking enhancer activity [389,390]. The other predominant theme involves formation of independently regulated chromatin loop domains. Theoretically, this would increase the distance between promoter and enhancer, or could make it sterically impossible for them to interact, thereby preventing enhancer activity that requires direct enhancer-promoter contact [388]. The structure of the protein-DNA complex at the base of the loop would stop any processive signals moving from enhancer to promoter. In support of this model, two copies of Su(Hw) flanking an enhancer block enhancer activity more effectively than a single insulator interposed between enhancer and promoter [389].

The formation of chromatin loops via insulators has been found associated with the enhancer-blocking and barrier activity of yeast insulators [316,317,391]. Through mediating proteins, the *Drosophila* gypsy insulator forms clusters that are tethered to the nuclear periphery [316]. Later studies determined that the mediating proteins, Su(Hw) and Mod(mdg4), associate with the nuclear matrix [392], which has components from the nuclear envelope and the nucleolus as well as DNA binding proteins. Identification of CTCF as a nuclear matrix-associated protein and a MAR-binding protein provides

another possible mechanism for the formation of independently regulated chromatin loops in vertebrates. This nuclear substructure could serve as a docking point with CTCF providing the functional connection with insulator DNA elements [393]. Our finding that CTCF associates with the nuclear matrix has been repeated in another study which also determined that CTCF-bound insulators are associated with the nuclear matrix (MARs), and that this association is dependent on the presence of an intact CTCF-binding site [394]. Given that CTCF binding sites are also required for enhancer-blocking activity, this result provides strong evidence for our model that an interaction between CTCF and the nuclear matrix is critical to the proper functioning of vertebrate insulators.

Although no vertebrate insulators have been identified that are tethered to nuclear pores as is seen in yeast, it has now been established that a portion of CTCF localizes to the nucleolar periphery, potentially through an interaction with nucleophosmin [386]. Furthermore, both CTCF and the CTCF-associated factor nucleophosmin are able to oligomerise, and a CTCF- mediated interaction between chromosomes 7 and 11 has been observed [394,395]. These data suggest that CTCF mediates enhancer-blocking through a tethering mechanism with several possible means for chromatin loop formation: association with the nuclear matrix, association with nucleoli, and association with other insulators. The separation of chromatin into distinct functional domains is shown in Figure A-11. Tethering by any of these measures could prevent promoter-enhancer interactions or stop a processive signal traveling from enhancer to promoter. In this case the components of nucleoli, nuclear matrix or insulator-bound protein complex would serve as structural barriers to the propagation of a signal traversing a strand of DNA from enhancer to promoter (234).

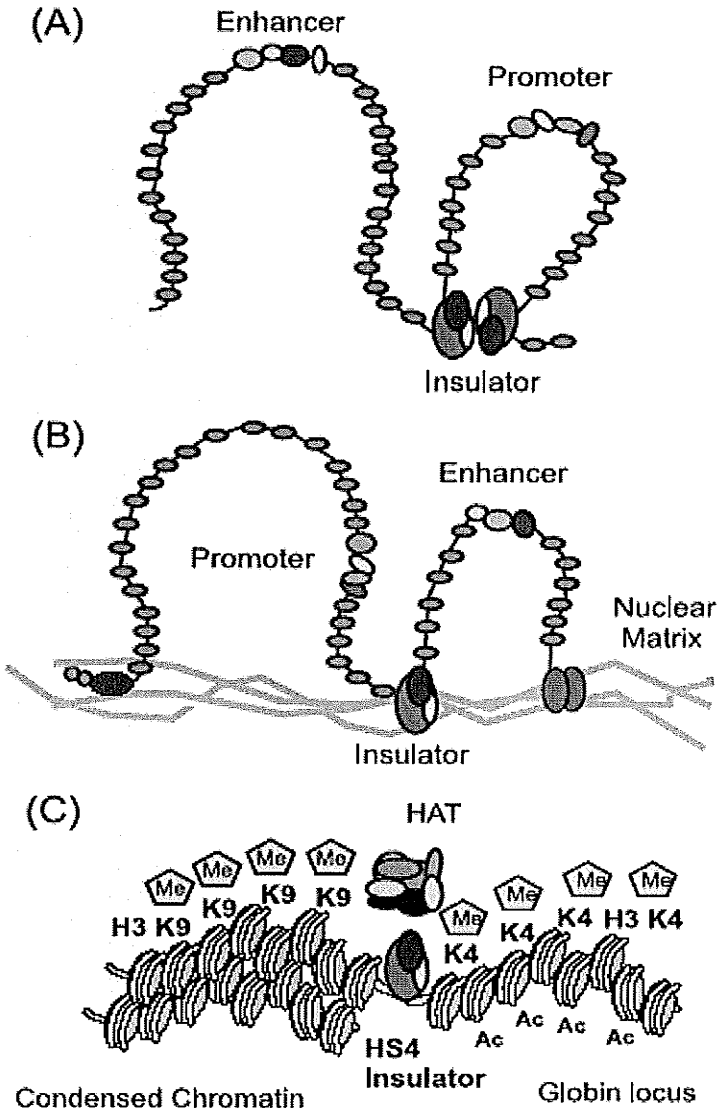

Figure A-11. Models of Insulator Enhancer-Blocking and Barrier Activity. A and B. Nucleosomes are represented by orange ovals along the strand of DNA. At the enhancer and promoter, bound transcription factors are represented by green, yellow, blue, pink, and purple ovals. A. Two insulators bound by CTCF containing complexes interact with each other. B. CTCF bound insulators associate with the nuclear matrix to create functionally distinct chromatin domains. C. Barrier activity achieved by modulation of chromatin structure. The chicken 5′ HS4 insulator lies in between a region of condensed, H3 K9-methylated chromatin (yellow pentagons) and a region of H3 K4-methylated chromatin (blue pentagons). Proteins bound to this insulator recruit complexes containing HATs to maintain acetylation of H3 K9, thereby preventing methylation of this residue.

Insulators may be tethered to specific nuclear locations in accordance with the factors required for their function. A recent study produced results that imply ADP-ribosylation of CTCF, or the extension of it, occurs after CTCF is bound to DNA [344]. PARP, the enzyme responsible for ADP-ribosylation of CTCF, is enriched in nucleoli. Several chromatin modifiers including HDACs associate with the nuclear matrix.

Two proteins that bind and confer activity to insulators in *Drosophila*, GAGA factor and Mod(mgd4), interact and appear to promote interactions between insulators that allow distal enhancers to bypass intervening insulators. [396]. This would explain the fact that the tandem placement of two insulators in the enhancer-blocking assay prevents their function. Further, the BTB/POZ domain present in both Mod(mgd4) and CP190, another *Drosophila* enhancer-blocking insulator-binding protein, can interact with itself to promote the formation of multimers [339]. As well, CTCF is also capable of interacting with itself to form multimers [394]. Modifications to the binding sites for these proteins, for example in the way that CTCF binding is regulated by DNA methylation, could serve as additional level of regulation. This points to a complex method of insulator regulation in which some loop formations confer insulator enhancer-blocking activity while others actually allow insulator "blocking".

Despite findings that might lead one to suggest that insulators in vertebrates and lower eukaryotes share a common mechanism of enhancer-blocking, key differences are present. For example, while Su(Hw) and Mod(mgd4) appear to be a typical nuclear matrix associated proteins, CTCF is not [394]. The association of CTCF with the matrix is much more stable, being resistant to higher salt conditions and is not dependent upon intact RNA [394]. In addition, no vertebrate insulators have been found to associate with

nuclear pores, as is seen in yeast. Further, tethering to the nuclear matrix in vertebrate cells is dependent on an intact CTCF-binding site while insulator tethering to the nuclear envelope in *Drosophila* requires DNA in addition to that which binds Su(Hw) [397]. The CTCF binding to HS4 occurs in regions that are relatively GC-rich [394], contrary to the AT-rich nature of many MARs, while sequences surrounding Su(Hw) binding sites in the *Drosophila* gypsy insulator are MAR-like [394,398,399]. These differences point out a fundamental difference in the way a vertebrate insulator-mediating protein interacts with the matrix as opposed to those in *Drosophila*, and may be indicative of a divergence in the mechanism by which insulator enhancer-blocking is achieved.

The *Drosophila* Topors (topoisomerase I-interacting arginine/serine rich) protein, which interacts with the Su(Hw) insulator protein complex, associates with nuclear lamina [400]. We did not identify the proteins connecting CTCF with the nuclear matrix. However, studies published after ours point towards nucleophosmin, a protein enriched in the granular portion of nucleoli and associated with the nuclear matrix, as a CTCF-associated factor [5,386]. Thus CTCF may be recruited to the nuclear matrix through its interaction with nucleophosmin [386]. Further, ChIP experiments have identified both CTCF and nucleophosmin as proteins bound to insulators *in vivo*, suggesting that the interaction between CTCF and nucleophosmin recruits the HS4 insulator to the nuclear matrix [394]. Although there is considerable data to support the hypothesis that functional interactions with the nuclear matrix via CTCF control insulator function, it is still not known what percentage of insulators are actually MARs. It is most likely that many insulators have yet to be clearly defined and there is evidence that some, such as

the CTCF-binding sites in the mouse Igf2/H19 imprinted control region, do not associate with the nuclear matrix at all [134].

Several studies indicate that alterations to chromatin structure by chromatin modifying enzymes have a role in the genesis of cancer [375-377]. Proteins required for the proper organization of chromatin within the nucleus may also be involved in the modification of chromatin structure during transformation. The evidence presented here indicates that CTCF binds to MAR DNA at the base of chromatin loops and is therefore involved in spatially and functionally organizing chromatin by anchoring it to the nuclear matrix. Furthermore, CTCF has been identified as the mediator of a specific, functional interaction between chromosomes 7 and 11 that influences gene expression [395]. These discoveries imply roles for CTCF in organizing nuclear DNA that could explain why mutations in the DNA binding domain of CTCF are seen in breast, prostrate, and Wilms' tumours [373].

Future Directions

In the last several years great strides have been made to elucidate the mechanism by which insulators achieve enhancer-blocking and barrier activity. In vertebrates, one additional protein capable of mediating enhancer-blocking activity has been found, and several enhancer-blocking insulators that do not contain binding sites for CTCF have been identified [401]. Maps of histone modifications, attachment sites to the nuclear matrix, and bound proteins have all contributed a great deal to our understanding of these elements. However, many aspects remain unclear, including the relationship between histone modifications and insulator activity.

Enhancer blocking appears to involve tethering of insulators to nuclear substructures and the modulation of chromatin structure. Detailed mapping of the positions of modified histones and chromatin modifying enzymes along regions of insulator activity by chromatin immunoprecipitation assay would further elucidate our understanding of insulator function, and may provide clues as to the binding partners of CTCF. Although CTCF has been established as a required element of many enhancer-blocking insulators, it is not known whether co-factors exist. It would certainly seem likely that other proteins are required to produce what appears to be a modulation of chromatin structure observed around several insulator elements. This raises the additional question as to the source of any co-factors, which could be recruited by CTCF or to a specific location in the nucleus (e.g. matrix).

At some sites of insulation, several insulators separate an enhancer from a heterologous promoter. Although the recent discovery of an interaction and possible "looping out" mechanism to by-pass the enhancer-blocking activity of distal insulators in *Drosophila* lays the groundwork for the purpose of multiple insulators in this type of situation, there is much left to understand about insulators placed in this fashion. Detailed examination of histone modifications, the methylation status of DNA, and the modification status of bound proteins may provide evidence as to the regulation of elements spaced in this way.

Part of this discussion was originally published in: Dunn KL, Zhao H, Davie JR. The insulator binding protein CTCF associates with the nuclear matrix. Exp. Cell Res. 2003. 288(1):218-223.

Appendix B: Reference List

Reference List

1. Trieschmann, L., Martin, B., and Bustin, M. (1998). The chromatin unfolding domain of chromosomal protein HMG-14 targets the N-terminal tail of histone H3 in nucleosomes. *Proc.Natl.Acad.Sci.USA* **95**, 5468-5473.

2. Nickerson, J. A. (2001). Experimental observations of a nuclear matrix. *J.Cell Sci.* **114**, 463-474.

3. Misteli, T. and Spector, D. L. (1998). The cellular organization of gene expression. *Curr.Opin.Cell Biol.* **10**, 323-331.

4. Schul, W., de Jong, L., and van Driel, R. (1998). Nuclear neighbours: the spatial and functional organization of genes and nuclear domains. *J.Cell Biochem.* **70**, 159-171.

5. Mattern, K. A., Humbel, B. M., Muijsers, A. O., de Jong, L., and van Driel, R. (1996). HnRNP proteins and B23 are the major proteins of the internal nuclear matrix of HeLa S3 cells. *J.Cell.Biochem.* **62**, 275-289.

6. Nickerson, J. A., Blencowe, B. J., and Penman, S. (1995). The architectural organization of nuclear metabolism. *Int.Rev.Cytol.* **162A**, 67-123.

7. Davie, J. R., Samuel, S. K., Spencer, V. A., Holth, L. T., Chadee, D. N., Peltier, C. P., Sun, J.-M., Chen, H. Y., and Wright, J. A. (1999). Organization of chromatin in cancer cells:role of signalling pathways. *Biochem.Cell Biol.* **77**, 265-275.

8. Gerner, C., Holzmann, K., Meissner, M., Gotzmann, J., Grimm, R., and Sauermann, G. (1999). Reassembling proteins and chaperones in human nuclear matrix protein fractions. *J.Cell Biochem.* **74**, 145-151.

9. He, D. C., Nickerson, J. A., and Penman, S. (1990). Core filaments of the nuclear matrix. *J.Cell Biol.* **110**, 569-580.

10. Nickerson, J. A., Krockmalnic, G., Wan, K. M., and Penman, S. (1997). The nuclear matrix revealed by eluting chromatin from a cross- linked nucleus. *Proc.Natl.Acad.Sci.U.S.A.* **94**, 4446-4450.

11. Hendzel, M. J., Delcuve, G. P., and Davie, J. R. (1991). Histone deacetylase is a component of the internal nuclear matrix. *J.Biol.Chem.* **266**, 21936-21942.

12. Delcuve, G. P. and Davie, J. R. (1989). Chromatin structure of erythroid-specific genes of immature and mature chicken erythrocytes. *Biochem.J.* **263**, 179-186.

13. Jackson, D. A. and Cook, P. R. (1985). Transcription occurs at a nucleoskeleton. *EMBO J.* **4**, 919-925.

14. Hentzen, P. C., Rho, J. H., and Bekhor, I. (1984). Nuclear matrix DNA from chicken erythrocytes contains beta- globin gene sequences. *Proc.Natl.Acad.Sci.U.S.A.* **81**, 304-307.

15. Thorburn, A., Moore, R., and Knowland, J. (1988). Attachment of transcriptionally active DNA sequences to the nucleoskeleton under isotonic conditions. *Nucleic Acids Res.* **16**, 7183.

16. Hendzel, M. J., Sun, J.-M., Chen, H. Y., Rattner, J. B., and Davie, J. R. (1994). Histone acetyltransferase is associated with the nuclear matrix. *J.Biol.Chem.* **269**, 22894-22901.

17. Reyes, J. C., Muchardt, C., and Yaniv, M. (1997). Components of the human SWI/SNF complex are enriched in active chromatin and are associated with the nuclear matrix. *J.Cell Biol.* **137**, 263-274.

18. Kimura, H., Tao, Y., Roeder, R. G., and Cook, P. R. (1999). Quantitation of RNA polymerase II and its transcription factors in an HeLa cell: little soluble holoenzyme but significant amounts of polymerases attached to the nuclear substructure. *Mol.Cell Biol.* **19**, 5383-5392.

19. Davie, J. R. (1995). The nuclear matrix and the regulation of chromatin organization and function. *In* "Structural and functional organization of the nuclear matrix" (R. Berezney and K. W. Jeon, Eds.), Academic Press, Orlando, Florida.

20. Sun, J.-M., Chen, H. Y., and Davie, J. R. (2001). Effect of estradiol on histone acetylation dynamics in human breast cancer cells. *J.Biol.Chem.* **276**, 49435-49442.

21. Gilbert, N., Gilchrist, S., and Bickmore, W. A. (2005). Chromatin organization in the mammalian nucleus. *Int.Rev.Cytol.* **242**, 283-336.

22. Hansen, J. C. (2002). Conformational dynamics of the chromatin fiber in solution: determinants, mechanisms, and functions. *Annu.Rev.Biophys.Biomol.Struct.* **31**, 361-392.

23. Finch, J. T., Lutter, L. C., Rhodes, D., Brown, R. S., Rushton, B., Levitt, M., and Klug, A. (1977). Structure of nucleosome core particles of chromatin. *Nature* **269**, 29-36.

24. Richmond, T. J., Finch, J. T., Rushton, B., Rhodes, D., and Klug, A. (1984). Structure of the nucleosome core particle at 7 A resolution. *Nature* **311**, 532-537.

25. Struck, M. M., Klug, A., and Richmond, T. J. (1992). Comparison of X-ray structures of the nucleosome core particle in two different hydration states. *J.Mol.Biol.* **224**, 253-264.

26. Van Holde, K. E. (1988). "Chromatin," 1 ed., Springer-Verlag, New York.

27. Wolffe, A. P. (2001). Transcriptional regulation in the context of chromatin structure. *Essays Biochem.* **37**, 45-57.

28. Luger, K., Mader, A. W., Richmond, R. K., Sargent, D. F., and Richmond, T. J. (1997). Crystal structure of the nucleosome core particle at 2.8 A resolution. *Nature* **389**, 251-260.

29. Spencer, V. A. and Davie, J. R. (1999). Role of covalent modifications of histones in regulating gene expression. *Gene* **240**, 1-12.

30. Arents, G., Burlingame, R. W., Wang, B. C., Love, W. E., and Moudrianakis, E. N. (1991). The nucleosomal core histone octamer at 3.1 A resolution: a tripartite protein assembly and a left-handed superhelix. *Proc.Natl.Acad.Sci.U.S.A.* **88**, 10148-10152.

31. Yager, T. D., McMurray, C. T., and Van Holde, K. E. (1989). Salt-induced release of DNA from nucleosome core particles. *Biochemistry* **28**, 2271-2281.

32. Zhou, Y. B., Gerchman, S. E., Ramakrishnan, V., Travers, A., and Muyldermans, S. (1998). Position and orientation of the globular domain of linker histone H5 on the nucleosome. *Nature* **395**, 402-405.

33. Lever, M. A., Th'ng, J. P., Sun, X., and Hendzel, M. J. (2000). Rapid exchange of histone H1.1 on chromatin in living human cells. *Nature* **408**, 873-876.

34. Misteli, T., Gunjan, A., Hock, R., Bustin, M., and Brown, D. T. (2000). Dynamic binding of histone H1 to chromatin in living cells. *Nature* **408**, 877-881.

35. Lu., M. J., Mpoke, S. S., Dadd, C. A., and Allis, C. D. (1995). Phosphorylated and dephosphorylated linker histone H1 reside in distinct chromatin domains in Tetrahymena macronuclei. *Mol.Biol.Cell* **6**, 1077-1087.

36. Dou, Y., Mizzen, C. A., Abrams, M., Allis, C. D., and Gorovsky, M. A. (1999). Phosphorylation of linker histone H1 regulates gene expression in vivo by mimicking H1 removal. *Mol.Cell* **4**, 641-647.

37. Davie, J. R. (1997). Nuclear matrix, dynamic histone acetylation and transcriptionally active chromatin. *Mol.Biol.Rep.* **24**, 197-207.

38. Leuba, S. H., Bustamante, C., Van Holde, K., and Zlatanova, J. (1998). Linker histone tails and N-tails of histone H3 are redundant: scanning force microscopy studies of reconstituted fibers. *Biophys.J.* **74**, 2830-2839.

39. Zlatanova, J., Leuba, S. H., and Van Holde, K. (1998). Chromatin fiber structure: morphology, molecular determinants, structural transitions. *Biophys.J.* **74**, 2554-2566.

40. Spotswood, H. T. and Turner, B. M. (2002). An increasingly complex code. *J.Clin.Invest* **110**, 577-582.

41. Camporeale, G., Shubert, E. E., Sarath, G., Cerny, R., and Zempleni, J. (2004). K8 and K12 are biotinylated in human histone H4. *Eur.J.Biochem.* **271**, 2257-2263.

42. Davie, J. R. (2004). Histone modifications. *In* "Chromatin structure and dynamics: state-of-the-art" (J. Zlatanova and S. Leuba, Eds.), Elsevier, Amsterdam.

43. Freitas, M. A., Sklenar, A. R., and Parthun, M. R. (2004). Application of mass spectrometry to the identification and quantification of histone post-translational modifications. *J.Cell Biochem.* **92**, 691-700.

44. Zhang, L., Eugeni, E. E., Parthun, M. R., and Freitas, M. A. (2003). Identification of novel histone post-translational modifications by peptide mass fingerprinting. *Chromosoma* **112**, 77-86.

45. Hebbes, T. R., Thorne, A. W., and Crane Robinson, C. (1988). A direct link between core histone acetylation and transcriptionally active chromatin. *EMBO J.* **7**, 1395-1402.

46. Hebbes, T. R., Thorne, A. W., Clayton, A. L., and Crane Robinson, C. (1992). Histone acetylation and globin gene switching. *Nucleic Acids Res.* **20**, 1017-1022.

47. Ip, Y. T., Jackson, V., Meier, J., and Chalkley, R. (1988). The separation of transcriptionally engaged genes. *J.Biol.Chem.* **263**, 14044-14052.

48. Sterner, D. E. and Berger, S. L. (2000). Acetylation of histones and transcription-related factors. *Microbiol.Mol.Biol.Rev.* **64**, 435-459.

49. Grant, P. A., Eberharter, A., John, S., Cook, R. G., Turner, B. M., and Workman, J. L. (1999). Expanded lysine acetylation specificity of Gcn5 in native complexes. *J.Biol.Chem.* **274**, 5895-5900.

50. Dhalluin, C., Carlson, J. E., Zeng, L., He, C., Aggarwal, A. K., and Zhou, M. M. (1999). Structure and ligand of a histone acetyltransferase bromodomain. *Nature* **399**, 491-496.

51. Ornaghi, P., Ballario, P., Lena, A. M., Gonzalez, A., and Filetici, P. (1999). The bromodomain of Gcn5p interacts in vitro with specific residues in the N terminus of histone H4. *J.Mol.Biol.* **287**, 1-7.

52. Marmorstein, R. (2001). Structure and function of histone acetyltransferases. *Cell Mol.Life Sci.* **58**, 693-703.

53. John, S., Howe, L., Tafrov, S. T., Grant, P. A., Sternglanz, R., and Workman, J. L. (2000). The something about silencing protein, Sas3, is the catalytic subunit of NuA3, a yTAF(II)30-containing HAT complex that interacts with the Spt16 subunit of the yeast CP (Cdc68/Pob3)-FACT complex. *Genes Dev.* **14**, 1196-1208.

54. Vogelauer, M., Wu, J., Suka, N., and Grunstein, M. (2000). Global histone acetylation and deacetylation in yeast. *Nature* **408**, 495-498.

55. Collingwood, T. N., Urnov, F. D., and Wolffe, A. P. (1999). Nuclear receptors: coactivators, corepressors and chromatin remodeling in the control of transcription. *J.Mol.Endocrinol.* **23**, 255-275.

56. Peterson, C. L. and Laniel, M. A. (2004). Histones and histone modifications. *Curr.Biol.* **14**, R546-R551.

57. Martin, C. and Zhang, Y. (2005). The diverse functions of histone lysine methylation. *Nat.Rev.Mol.Cell Biol.* **6**, 838-849.

58. Peters, A. H., Kubicek, S., Mechtler, K., O'Sullivan, R. J., Derijck, A. A., Perez-Burgos, L., Kohlmaier, A., Opravil, S., Tachibana, M., Shinkai, Y., Martens, J. H., and Jenuwein, T. (2003). Partitioning and plasticity of repressive histone methylation states in mammalian chromatin. *Mol.Cell* **12**, 1577-1589.

59. Rice, J. C., Briggs, S. D., Ueberheide, B., Barber, C. M., Shabanowitz, J., Hunt, D. F., Shinkai, Y., and Allis, C. D. (2003). Histone methyltransferases direct different degrees of methylation to define distinct chromatin domains. *Mol.Cell* **12**, 1591-1598.

60. Cao, R. and Zhang, Y. (2004). The functions of E(Z)/EZH2-mediated methylation of lysine 27 in histone H3. *Curr.Opin.Genet.Dev.* **14**, 155-164.

61. Bannister, A. J., Zegerman, P., Partridge, J. F., Miska, E. A., Thomas, J. O., Allshire, R. C., and Kouzarides, T. (2001). Selective recognition of methylated lysine 9 on histone H3 by the HP1 chromo domain. *Nature* **410**, 120-124.

62. Fischle, W., Wang, Y., Jacobs, S. A., Kim, Y., Allis, C. D., and Khorasanizadeh, S. (2003). Molecular basis for the discrimination of repressive methyl-lysine marks in histone H3 by Polycomb and HP1 chromodomains. *Genes Dev.* **17**, 1870-1881.

63. Huyen, Y., Zgheib, O., Ditullio, R. A., Jr., Gorgoulis, V. G., Zacharatos, P., Petty, T. J., Sheston, E. A., Mellert, H. S., Stavridi, E. S., and Halazonetis, T. D. (2004). Methylated lysine 79 of histone H3 targets 53BP1 to DNA double-strand breaks. *Nature* **432**, 406-411.

64. Pray-Grant, M. G., Daniel, J. A., Schieltz, D., Yates, J. R., III, and Grant, P. A. (2005). Chd1 chromodomain links histone H3 methylation with SAGA- and SLIK-dependent acetylation. *Nature* **433**, 434-438.

65. Wysocka, J., Swigut, T., Milne, T. A., Dou, Y., Zhang, X., Burlingame, A. L., Roeder, R. G., Brivanlou, A. H., and Allis, C. D. (2005). WDR5 associates with histone H3 methylated at K4 and is essential for H3 K4 methylation and vertebrate development. *Cell* **121**, 859-872.

66. Birger, Y., Ito, Y., West, K. L., Landsman, D., and Bustin, M. (2001). HMGN4, a newly discovered nucleosome-binding protein encoded by an intronless gene. *DNA Cell Biol.* **20**, 257-264.

67. West, K. L., Ito, Y., Birger, Y., Postnikov, Y., Shirakawa, H., and Bustin, M. (2001). HMGN3a and HMGN3b, two protein isoforms with a tissue-specific expression pattern, expand the cellular repertoire of nucleosome-binding proteins. *J Biol.Chem.* **276**, 25959-25969.

68. Shirakawa, H., Landsman, D., Postnikov, Y. V., and Bustin, M. (2000). NBP-45, a novel nucleosomal binding protein with a tissue-specific and developmentally regulated expression. *J Biol.Chem.* **275**, 6368-6374.

69. Catez, F., Lim, J. H., Hock, R., Postnikov, Y. V., and Bustin, M. (2003). HMGN dynamics and chromatin function. *Biochem.Cell Biol.* **81**, 113-122.

70. Bustin, M. (2001). Chromatin unfolding and activation by HMGN(*) chromosomal proteins. *Trends Biochem.Sci.* **26**, 431-437.

71. Alfonso, P. J., Crippa, M. P., Hayes, J. J., and Bustin, M. (1994). The footprint of chromosomal proteins HMG-14 and HMG-17 on chromatin subunits. *J.Mol.Biol.* **236**, 189-198.

72. Hock, R., Wilde, F., Scheer, U., and Bustin, M. (1998). Dynamic relocation of chromosomal protein HMG-17 in the nucleus is dependent on transcriptional activity. *EMBO J* **17**, 6992-7001.

73. Catez, F., Brown, D. T., Misteli, T., and Bustin, M. (2002). Competition between histone H1 and HMGN proteins for chromatin binding sites. *EMBO Rep.* **3**, 760-766.

74. Birger, Y., West, K. L., Postnikov, Y. V., Lim, J. H., Furusawa, T., Wagner, J. P., Laufer, C. S., Kraemer, K. H., and Bustin, M. (2003). Chromosomal protein HMGN1 enhances the rate of DNA repair in chromatin. *EMBO J* **22**, 1665-1675.

75. Rubinstein, Y. R., Furusawa, T., Lim, J. H., Postnikov, Y. V., West, K. L., Birger, Y., Lee, S., Nguyen, P., Trepel, J. B., and Bustin, M. (2005).

Chromosomal protein HMGN1 modulates the expression of N-cadherin. *FEBS J* **272**, 5853-5863.

76. Furusawa, T., Lim, J. H., Catez, F., Birger, Y., Mackem, S., and Bustin, M. (2006). Down-regulation of nucleosomal binding protein HMGN1 expression during embryogenesis modulates Sox9 expression in chondrocytes. *Mol.Cell Biol.* **26**, 592-604.

77. Birger, Y., Catez, F., Furusawa, T., Lim, J. H., Prymakowska-Bosak, M., West, K. L., Postnikov, Y. V., Haines, D. C., and Bustin, M. (2005). Increased tumorigenicity and sensitivity to ionizing radiation upon loss of chromosomal protein HMGN1. *Cancer Res.* **65**, 6711-6718.

78. Rogakou, E. P., Pilch, D. R., Orr, A. H., Ivanova, V. S., and Bonner, W. M. (1998). DNA double-stranded breaks induce histone H2AX phosphorylation on serine 139. *J.Biol.Chem.* **273**, 5858-5868.

79. Al Rashid, S. T., Dellaire, G., Cuddihy, A., Jalali, F., Vaid, M., Coackley, C., Folkard, M., Xu, Y., Chen, B. P., Chen, D. J., Lilge, L., Prise, K. M., Bazett Jones, D. P., and Bristow, R. G. (2005). Evidence for the direct binding of phosphorylated p53 to sites of DNA breaks in vivo. *Cancer Res.* **65**, 10810-10821.

80. Rogakou, E. P., Boon, C., Redon, C., and Bonner, W. M. (1999). Megabase chromatin domains involved in DNA double-strand breaks in vivo. *J.Cell Biol.* **146**, 905-916.

81. Li, A., Eirin-Lopez, J. M., and Ausio, J. (2005). H2AX: tailoring histone H2A for chromatin-dependent genomic integrity. *Biochem.Cell Biol.* **83**, 505-515.

82. Pehrson, J. R. and Fried, V. A. (1992). MacroH2A, a core histone containing a large nonhistone region. *Science* **257**, 1398-1400.

83. Csankovszki, G., Panning, B., Bates, B., Pehrson, J. R., and Jaenisch, R. (1999). Conditional deletion of Xist disrupts histone macroH2A localization but not maintenance of X inactivation [letter]. *Nat.Genet.* **22**, 323-324.

84. Gilbert, S. L., Pehrson, J. R., and Sharp, P. A. (2000). XIST RNA associates with specific regions of the inactive X chromatin. *J.Biol.Chem.* **275**, 36491-36494.

85. Dryhurst, D., Thambirajah, A. A., and Ausio, J. (2004). New twists on H2A.Z: a histone variant with a controversial structural and functional past. *Biochem.Cell Biol.* **82**, 490-497.

86. Thambirajah, A. A., Dryhurst, D. D., Ishibashi, T., Li, A., Maffey, A. H., and Ausio, J. (2006). H2A.Z stabilizes chromatin in a way that is dependant on core histone acetylation. *J Biol.Chem.*

87. Millar CB, Xu F, Zhang K, and Grunstein M (2006). Acetylation of H2AZ Lys 14 is associated with genome-wide gene activity in yeast. *Genes Dev.* **20**, 711-722.

88. Chadwick, B. P. and Willard, H. F. (2001). A novel chromatin protein, distantly related to histone H2A, is largely excluded from the inactive X chromosome. *J.Cell Biol.* **152**, 375-384.

89. Li, W., Nagaraja, S., Delcuve, G. P., Hendzel, M. J., and Davie, J. R. (1993). Effects of histone acetylation, ubiquitination and variants on nucleosome stability. *Biochem.J.* **296**, 737-744.

90. Leonardson, K. E. and Levy, S. B. (1989). Chromatin reorganization during emergence of malignant Friend tumors: early changes in H2A and H2B variants and nucleosome repeat length. *Exp.Cell Res.* **180**, 209-219.

91. Hake, S. B. and Allis, C. D. (2006). Histone H3 variants and their potential role in indexing mammalian genomes: The "H3 barcode hypothesis". *Proc.Natl.Acad.Sci.U.S.A* **103**, 6428-6435.

92. Ausio, J., Abbott, D. W., Wang, X., and Moore, S. C. (2001). Histone variants and histone modifications: a structural perspective. *Biochem.Cell Biol.* **79**, 693-708.

93. Ahmad, K. and Henikoff, S. (2002). Histone H3 variants specify modes of chromatin assembly. *Proc.Natl.Acad.Sci.U.S.A* **99**, 16477-16484.

94. McKittrick, E., Gafken, P. R., Ahmad, K., and Henikoff, S. (2004). Histone H3.3 is enriched in covalent modifications associated with active chromatin. *Proc.Natl.Acad.Sci.U.S.A* **101**, 1525-1530.

95. Johnson, L., Mollah, S., Garcia, B., Muratore, T., Shabanowitz, J., Hunt, D., and Jacobsen, S. (2004). Mass spectrometry analysis of Arabidopsis histone H3 reveals distinct combinations of post-translational modifications. *Nucleic Acids Res.* **32**, 6511-6518.

96. Chow, C. M., Georgiou, A., Szutorisz, H., Maia, E. S. A., Pombo, A., Barahona, I., Dargelos, E., Canzonetta, C., and Dillon, N. (2005). Variant histone H3.3 marks promoters of transcriptionally active genes during mammalian cell division. *EMBO Rep.* **6**, 354-360.

97. Hake, S., arcia, B., enjamin A.Garcia, auer, M., ellaire, G., habanowitz, J., azett-Jones, D., llis, D., and unt, D. (2006). Expression patterns and post-translational modifications associated with mammalian histone H3 variants. *J.Biol.Chem.* **281**, 559-568.

98. Hake, S. B., Garcia, B. A., Kauer, M., Baker, S. P., Shabanowitz, J., Hunt, D. F., and Allis, C. D. (2005). Serine 31 phosphorylation of histone variant H3.3 is

specific to regions bordering centromeres in metaphase chromosomes. *Proc.Natl.Acad.Sci.U.S.A* **102**, 6344-6349.

99. Jin, J., Cai, Y., Li, B., Conaway, R. C., Workman, J. L., Conaway, J. W., and Kusch, T. (2005). In and out: histone variant exchange in chromatin. *Trends Biochem.Sci.* **30**, 680-687.

100. Loyola, A. and Almouzni, G. (2004). Histone chaperones, a supporting role in the limelight. *Biochim.Biophys.Acta* **1677**, 3-11.

101. Turner, B. M. (2000). Histone acetylation and an epigenetic code. *BioEssays* **22**, 836-845.

102. Stancheva, I. (2005). Caught in conspiracy: cooperation between DNA methylation and histone H3K9 methylation in the establishment and maintenance of heterochromatin. *Biochem.Cell Biol.* **83**, 385-395.

103. Wallace, J. A. and Orr-Weaver, T. L. (2005). Replication of heterochromatin: insights into mechanisms of epigenetic inheritance. *Chromosoma* **114**, 389-402.

104. Fahrner, J. A., Eguchi, S., Herman, J. G., and Baylin, S. B. (2002). Dependence of histone modifications and gene expression on DNA hypermethylation in cancer. *Cancer Res.* **62**, 7213-7218.

105. Lehnertz, B., Ueda, Y., Derijck, A. A., Braunschweig, U., Perez-Burgos, L., Kubicek, S., Chen, T., Li, E., Jenuwein, T., and Peters, A. H. (2003). Suv39h-mediated histone H3 lysine 9 methylation directs DNA methylation to major satellite repeats at pericentric heterochromatin. *Curr.Biol.* **13**, 1192-1200.

106. Tariq, M., Saze, H., Probst, A. V., Lichota, J., Habu, Y., and Paszkowski, J. (2003). Erasure of CpG methylation in Arabidopsis alters patterns of histone H3 methylation in heterochromatin. *Proc.Natl.Acad.Sci.U.S.A* **100**, 8823-8827.

107. Dillon, N. and Festenstein, R. (2002). Unravelling heterochromatin: competition between positive and negative factors regulates accessibility. *Trends Genet.* **18**, 252-258.

108. Lachner, M., O'Carroll, D., Rea, S., Mechtler, K., and Jenuwein, T. (2001). Methylation of histone H3 lysine 9 creates a binding site for HP1 proteins. *Nature* **410**, 116-120.

109. Verschure, P. J., van, D. K., I, Manders, E. M., Hoogstraten, D., Houtsmuller, A. B., and van Driel, R. (2003). Condensed chromatin domains in the mammalian nucleus are accessible to large macromolecules. *EMBO Rep.* **4**, 861-866.

110. Sekinger, E. A. and Gross, D. S. (2001). Silenced chromatin is permissive to activator binding and PIC recruitment. *Cell* **105**, 403-414.

111. Cheng, T. H. and Gartenberg, M. R. (2000). Yeast heterochromatin is a dynamic structure that requires silencers continuously. *Genes Dev.* **14**, 452-463.

112. Festenstein, R., Pagakis, S. N., Hiragami, K., Lyon, D., Verreault, A., Sekkali, B., and Kioussis, D. (2003). Modulation of heterochromatin protein 1 dynamics in primary Mammalian cells. *Science* **299**, 719-721.

113. Grewal, S. I. and Moazed, D. (2003). Heterochromatin and epigenetic control of gene expression. *Science* **301**, 798-802.

114. West, A. G. and Fraser, P. (2005). Remote control of gene transcription. *Hum.Mol.Genet.* **12**, R101-R111.

115. Hennig, W. (1999). Heterochromatin. *Chromosoma* **108**, 1-9.

116. Saha, A., Wittmeyer, J., and Cairns, B. R. (2006). Chromatin remodelling: the industrial revolution of DNA around histones. *Nat.Rev.Mol.Cell Biol.* **7**, 437-447.

117. Corona, D. F. and Tamkun, J. W. (2004). Multiple roles for ISWI in transcription, chromosome organization and DNA replication. *Biochim.Biophys.Acta* **1677**, 113-119.

118. Deuring, R., Fanti, L., Armstrong, J. A., Sarte, M., Papoulas, O., Prestel, M., Daubresse, G., Verardo, M., Moseley, S. L., Berloco, M., Tsukiyama, T., Wu, C., Pimpinelli, S., and Tamkun, J. W. (2000). The ISWI chromatin-remodeling protein is required for gene expression and the maintenance of higher order chromatin structure in vivo. *Mol.Cell* **5**, 355-365.

119. Goldmark, J. P., Fazzio, T. G., Estep, P. W., Church, G. M., and Tsukiyama, T. (2000). The Isw2 chromatin remodeling complex represses early meiotic genes upon recruitment by Ume6p. *Cell* **103**, 423-433.

120. Morillon, A., Karabetsou, N., O'Sullivan, J., Kent, N., Proudfoot, N., and Mellor, J. (2003). Isw1 chromatin remodeling ATPase coordinates transcription elongation and termination by RNA polymerase II. *Cell* **115**, 425-435.

121. Martens, J. A. and Winston, F. (2003). Recent advances in understanding chromatin remodeling by Swi/Snf complexes. *Curr.Opin.Genet.Dev.* **13**, 136-142.

122. Martens, J. A. and Winston, F. (2002). Evidence that Swi/Snf directly represses transcription in S. cerevisiae. *Genes Dev.* **16**, 2231-2236.

123. Bazett-Jones, D. P., Mendez, E., Czarnota, G. J., Ottensmeyer, F. P., and Allfrey, V. G. (1996). Visualization and analysis of unfolded nucleosomes associated with transcribing chromatin. *Nucleic Acids Res.* **24**, 321-329.

124. Prior, C. P., Cantor, C. R., Johnson, E. M., Littau, V. C., and Allfrey, V. G. (1983). Reversible changes in nucleosome structure and histone H3 accessibility in transcriptionally active and inactive states of rDNA chromatin. *Cell* **34**, 1033-1042.

125. Nacheva, G. A., Guschin, D. Y., Preobrazhenskaya, O. V., Karpov, V. L., Ebralidse, K. K., and Mirzabekov, A. D. (1989). Change in the pattern of histone binding to DNA upon transcriptional activation. *Cell* **58**, 27-36.

126. Kireeva, M. L., Walter, W., Tchernajenko, V., Bondarenko, V., Kashlev, M., and Studitsky, V. M. (2002). Nucleosome remodeling induced by RNA polymerase II. Loss of the H2A/H2B dimer during transcription. *Mol.Cell* **9**, 541-552.

127. Van Holde, K. E., Lohr, D. E., and Robert, C. (1992). What happens to nucleosomes during transcription? *J.Biol.Chem.* **267**, 2837-2840.

128. Walia, H., Chen, H. Y., Sun, J.-M., Holth, L. T., and Davie, J. R. (1998). Histone acetylation is required to maintain the unfolded nucleosome structure associated with transcribing DNA. *J.Biol.Chem.* **273**, 14516-24522.

129. Wittschieben, B. O., Otero, G., de Bizemont, T., Fellows, J., Erdjument-Bromage, H., Ohba, R., Li, Y., Allis, C. D., Tempst, P., and Svejstrup, J. Q. (1999). A novel histone acetyltransferase is an integral subunit of elongating RNA polymerase II holoenzyme. *Mol.Cell* **4**, 123-128.

130. Butler, J. E. and Kadonaga, J. T. (2001). Enhancer-promoter specificity mediated by DPE or TATA core promoter motifs. *Genes Dev.* **15**, 2515-2519.

131. Calhoun, V. C., Stathopoulos, A., and Levine, M. (2002). Promoter-proximal tethering elements regulate enhancer-promoter specificity in the Drosophila Antennapedia complex. *Proc.Natl.Acad.Sci.* **99**, 9243-9247.

132. Lopes, S., Lewis, A., Hajkova, P., Dean, W., Oswald, J., Forne, T., Murrell, A., Constancia, M., Bartolomei, M., Walter, J., and Reik, W. (2003). Epigenetic modifications in an imprinting cluster are controlled by a hierarchy of DMRs suggesting long-range chromatin interactions. *Hum.Mol.Genet.* **12**, 295-305.

133. Sasaki, H., Ishihara, K., and Kato, R. (2000). Mechanisms of Igf2/H19 imprinting: DNA methylation, chromatin and long-distance gene regulation. *J Biochem.(Tokyo)* **127**, 711-715.

134. Weber, M., Hagege, H., Murrell, A., Brunel, C., Reik, W., Cathala, G., and Forne, T. (2003). Genomic imprinting controls matrix attachment regions in the Igf2 gene. *Mol.Cell Biol.* **23**, 8953-8959.

135. Fourel, G., Lebrun, E., and Gilson, E. (2002). Protosilencers as building blocks for heterochromatin. *BioEssays* **24**, 828-835.

136. Hall, I. M., Shankaranarayana, G. D., Noma, K., Ayoub, N., Cohen, A., and Grewal, S. I. (2002). Establishment and maintenance of a heterochromatin domain. *Science* **297**, 2232-2237.

137. Fourel, G., Magdinier, F., and Gilson, E. (2004). Insulator dynamics and the setting of chromatin domains. *BioEssays* **26**, 523-532.

138. Wei, Y., Mizzen, C. A., Cook, R. G., Gorovsky, M. A., and Allis, C. D. (1998). Phosphorylation of histone H3 at serine 10 is correlated with chromosome condensation during mitosis and meiosis in Tetrahymena. *Proc.Natl.Acad.Sci.* **95**, 7480-7484.

139. Gurley, L. R., D'Anna, J. A., Barham, S. S., Deaven, L. L., and Tobey, R. A. (1978). Histone phosphorylation and chromatin structure during mitosis in Chinese hamster cells. *Eur.J.Biochem.* **84**, 1-15.

140. Van Hooser, A., Goodrich, D. W., Allis, C. D., Brinkley, B. R., and Mancini, M. A. (1998). Histone H3 phosphorylation is required for the initiation, but not maintenance, of mammalian chromosome condensation. *J.Cell Sci.* **111**, 3497-3506.

141. Hsu, J. Y., Sun, Z. W., Li, X., Reuben, M., Tatchell, K., Bishop, D. K., Grushcow, J. M., Brame, C. J., Caldwell, J. A., Hunt, D. F., Lin, R., Smith, M. M., and Allis, C. D. (2000). Mitotic phosphorylation of histone H3 is governed by Ipl1/aurora kinase and Glc7/PP1 phosphatase in budding yeast and nematodes. *Cell* **102**, 279-291.

142. Goto, H., Tomono, Y., Ajiro, K., Kosako, H., Fujita, M., Sakurai, M., Okawa, K., Iwamatsu, A., Okigaki, T., Takahashi, T., and Inagaki, M. (1999). Identification of a novel phosphorylation site on histone H3 coupled with mitotic chromosome condensation. *J.Biol.Chem.* **274**, 25543-25549.

143. Preuss U, Landsberg G, and Scheidtmann KH (2003). Novel mitosis-specific phosphorylation of histone H3 at Thr11 mediated by Dlk/ZIP kinase. *Nucleic Acids Res.* **31**, 878-885.

144. Hendzel, M. J., Wei, Y., Mancini, M. A., Van Hooser, A., Ranalli, T., Brinkely, B. R., Bazett-Jones, D. P., and Allis, C. D. (1997). Mitosis-specific phosphorylation of histone H3 initiates primarily within pericentromeric heterochromatin durning G2 and spreads in an ordered fashion coincident with chromosome condensation. *Chromosoma* **106**, 348-360.

145. Wei, Y., Yu, L., Bowen, J., Gorovsky, M. A., and Allis, C. D. (1999). Phosphorylation of histone H3 is required for proper chromosome condensation and segregation. *Cell* **97**, 99-109.

146. Terada, Y., Tatsuka, M., Suzuki, F., Yasuda, Y., Fujita, S., and Otsu, M. (1998). AIM-1: a mammalian midbody-associated protein required for cytokinesis. *EMBO* **17**, 667-676.

147. de la Barre, A. E., Gerson, V., Gout, S., Creaven, M., Allis, C. D., and Dimitrov, S. (2000). Core histone N-termini play an essential role in mitotic chromosome condensation. *EMBO J.* **19**, 379-391.

148. De Souza, C. P., Osmani, A. H., Wu, L. P., Spotts, J. L., and Osmani, S. A. (2000). Mitotic histone H3 phosphorylation by the NIMA kinase in Aspergillus nidulans. *Cell* **102**, 293-302.

149. Giet, R. and Glover, D. M. (2001). Drosophila aurora B kinase is required for histone H3 phosphorylation and condensin recruitment during chromosome condensation and to organize the central spindle during cytokinesis. *J.Cell Biol.* **152**, 669-682.

150. Hsu JY, S. Z. L. X. R. M. T. K. B. D. G. J. B. C. C. J. H. D. L. R. S. M. A. CD. (2000). Mitotic phosphorylation of histone H3 is governed by Ipl1/aurora kinase and Glc7/PP1 phosphatase in budding yeast and nematodes. *Cell* **102**, 279-291.

151. Murnion, M. E., Adams, R. R., Callister, D. M., Allis, C. D., Earnshaw, W. C., and Swedlow, J. R. (2001). Chromatin-associated protein phosphatase 1 regulates aurora-B and histone H3 phosphorylation. *J.Biol.Chem.* **276**, 26656-26665.

152. Hans, F. and Dimitrov, S. (2001). Histone H3 phosphorylation and cell division. *Oncogene* **20**, 3021-3027.

153. Andrews, P. D., Knatko, E., Moore, W. J., and Swedlow, J. R. (2003). Mitotic Mechanics: the auroras come into view. *Curr.Opin.Cell Biol.* **15**, 672-683.

154. Tatsuka, M., Katayama, H., Ota, T., Tanaka, T., Odashima, S., Suzuki, F., and Terada, Y. (1998). Multinuclearity and increased ploidy caused by overexpression of the aurora- and Ipl1-like midbody-associated protein mitotic kinase in human cancer cells. *Cancer Res.* 4811-4816.

155. Vagnarelli, P. and Earnshaw, W. C. (2004). Chromosomal passengers: the four-dimensional regulation of mitotic events. *Chromosoma* **113**, 211-222.

156. Chen, J., Jin, S., Tahir, S. K., Zhang, H., Liu, X., Sarthy, A. V., McGonigal, T. P., Liu, Z., Rosenburg, S. H., and Ng, S. C. (2003). Survivin enhances Aurora B kinase activity and localizes Aurora B in human cells. *J Biol.Chem.* **278**, 486-490.

157. Dai, J., Sultan, S., Taylor, S. S., and Higgins, J. M. (2005). The kinase haspin is required for mitotic histone H3 Thr 3 phosphorylation and normal metaphase chromosome alignment. *Genes Dev.* **19**, 472-488.

158. Dai, J. and Higgins, J. M. (2005). Haspin: a mitotic histone kinase required for metaphase chromosome alignment. *Cell Cycle* **4**, 665-668.

159. Kogel, D., Plottner, O., Landsberg, G., Christian, S., and Scheidtmann, K. H. (1998). Cloning and characterization of Dlk, a novel serine/threonine kinase that is tightly associated with chromatin and phosphorylates core histones. *Oncogene* **17**, 2645-2654.

160. Deiss, L. P., Feinstein, E., Berissi, H., Cohen, O., and Kimchi, A. (1995). Identification of a novel serine/threonine kinase and a novel 15-kD protein as potential mediators of the gamma interferon-induced cell death. *Genes Dev.* **9**, 15-30.

161. Inbal, B., Cohen, O., Polak-Charcon, S., Kopolovic, J., Vadai, E., Eisenbach, L., and Kimchi, A. (1997). DAP kinase links the control of apoptosis to metastasis. *Nature* **390**, 180-184.

162. Cohen, O., Inbal, B., Kissil, J. L., Raveh, T., Berissi, H., Spivak-Kroizaman, T., Feinstein, E., and Kimchi, A. (1999). DAP-kinase participates in TNF-alpha- and Fas-induced apoptosis and its function requires the death domain. *J Cell Biol.* **146**, 141-148.

163. Kawai, T., Matsumoto, M., Takeda, K., Sanjo, H., and Akira, S. (1998). ZIP kinase, a novel serine/threonine kinase which mediates apoptosis. *Mol.Cell Biol.* **18**, 1642-1651.

164. Page, G., Lodige, I., Kogel, D., and Scheidtmann, K. H. (1999). AATF, a novel transcription factor that interacts with Dlk/ZIP kinase and interferes with apoptosis. *FEBS Lett.* **462**, 187-191.

165. Engemann, H., Heinzel, V., Page, G., Preuss, U., and Scheidtmann, K. H. (2002). DAP-like kinase interacts with the rat homolog of Schizosaccharomyces pombe CDC5 protein, a factor involved in pre-mRNA splicing and required for G2/M phase transition. *Nucleic Acids Res.* **30**, 1408-1417.

166. Prymakowska-Bosak, M., Misteli, T., Herrera, J. E., Shirakawa, H., Birger, Y., Garfield, S., and Bustin, M. (2001). Mitotic phosphorylation prevents the binding of HMGN proteins to chromatin. *Mol.Cell Biol.* **21**, 5169-5178.

167. Prymakowska-Bosak, M., Hock, R., Catez, F., Lim, J. H., Birger, Y., Shirakawa, H., Lee, K., and Bustin, M. (2002). Mitotic phosphorylation of chromosomal protein HMGN1 inhibits nuclear import and promotes interaction with 14.3.3 proteins. *Mol.Cell Biol.* **22**, 6809-6819.

168. Kunitoku, N., Sasayama, T., Marumoto, T., Zhang, D., Honda, S., Kobayashi, O., Hatakeyama, K., Ushio, Y., Saya, H., and Hirota, T. (2003). CENP-A phosphorylation by Aurora-A in prophase is required for enrichment of Aurora-B at inner centromeres and for kinetochore function. *Dev.Cell* **5**, 853-864.

169. Barber, C. M., Turner, F. B., Wang, Y., Hagstrom, K., Taverna, S. D., Mollah, S., Ueberheide, B., Meyer, B. J., Hunt, D. F., Cheung, P., and Allis, C. D. (2004). The enhancement of histone H4 and H2A serine 1 phosphorylation during mitosis and S-phase is evolutionarily conserved. *Chromosoma* **112**, 360-371.

170. Swank, R. A., Th'ng, J. P., Guo, X. W., Valdez, J., Bradbury, E. M., and Gurley, L. R. (1997). Four distinct cyclin-dependent kinases phosphorylate histone H1 at all of its growth-related phosphorylation sites. *Biochemistry* **36**, 13761-13768.

171. Iyer, V. R., Eisen, M. B., Ross, D. T., Schuler, G., Moore, T., Lee, J. C. F., Trent, J. M., Staudt, L. M., Hudson, J., Jr., Boguski, M. S., Lashkari, D., Shalon, D., Botstein, D., and Brown, P. O. (1999). The transcriptional program in the response of human fibroblasts to serum. *Science* **283**, 83-87.

172. Roux, P. P. and Blenis, J. (2004). ERK and p38 MAPK-activated protein kinases: a family of protein kinases with diverse biological functions. *Microbiol.Mol.Biol.Rev.* **68**, 320-344.

173. Edmunds, J. W. and Mahadevan, L. C. (2004). MAP kinases as structural adaptors and enzymatic activators in transcription complexes. *J.Cell Sci.* **117**, 3715-3723.

174. Kyriakis, J. M. and Avruch, J. (2001). Mammalian mitogen-activated protein kinase signal transduction pathways activated by stress and inflammation. *Physiol Rev.* **81**, 807-869.

175. Brose, N. and Rosenmund, C. (2002). Move over protein kinase C, you've got company: alternative cellular effectors of diacylglycerol and phorbol esters. *J.Cell Sci.* **115**, 4399-4411.

176. Kazanietz, M. G. (2000). Eyes wide shut: protein kinase C isozymes are not the only receptors for the phorbol ester tumor promoters. *Mol.Carcinog.* **28**, 5-11.

177. Chang, F., Steelman, L. S., Lee, J. T., Shelton, J. G., Navolanic, P. M., Blalock, W. L., Franklin, R. A., and McCubrey, J. A. (2003). Signal transduction mediated by the Ras/Raf/MEK/ERK pathway from cytokine receptors to transcription factors: potential targeting for therapeutic intervention. *Leukemia* **17**, 1263-1293.

178. Davie, J. R. (2003). MSK1 and MSK2 mediate mitogen- and stress-induced phosphorylation of histone H3: a controversy resolved. *Sci.STKE.* **2003**, E33.

179. Wiggin, G. R., Soloaga, A., Foster, J. M., Murray-Tait, V., Cohen, P., and Arthur, J. S. (2002). MSK1 and MSK2 are required for the mitogen- and stress-induced phosphorylation of CREB and ATF1 in fibroblasts. *Mol.Cell Biol.* **22**, 2871-2881.

180. Soloaga, A., Thomson, S., Wiggin, G. R., Rampersaud, N., Dyson, M. H., Hazzalin, C. A., Mahadevan, L. C., and Arthur, J. S. (2003). MSK2 and MSK1 mediate the mitogen- and stress-induced phosphorylation of histone H3 and HMG-14. *EMBO J.* **22**, 2788-2797.

181. Bode, A. M. and Dong, Z. (2005). Inducible covalent posttranslational modification of histone H3. *Sci.STKE.* **2005**, re4.

182. Gotoh, I., Adachi, M., and Nishida, E. (2001). Identification and characterization of a novel MAP kinase kinase kinase, MLTK. *J Biol.Chem.* **276**, 4276-4286.

183. Choi, H. S., Choi, B. Y., Cho, Y. Y., Zhu, F., Bode, A. M., and Dong, Z. (2005). Phosphorylation of Ser28 in histone H3 mediated by mixed lineage kinase-like mitogen-activated protein triple kinase alpha. *J.Biol.Chem.* **280**, 13545-13553.

184. Anest, V., Cogswell, P. C., and Baldwin, A. S., Jr. (2004). IkappaB kinase alpha and p65/RelA contribute to optimal epidermal growth factor-induced c-fos gene expression independent of IkappaBalpha degradation. *J.Biol Chem.* **279**, 31183-31189.

185. Anest, V., Hanson, J. L., Cogswell, P. C., Steinbrecher, K. A., Strahl, B. D., and Baldwin, A. S. (2003). A nucleosomal function for IkappaB kinase-alpha in NF-kappaB-dependent gene expression. *Nature* **423**, 659-663.

186. Yamamoto, Y., Verma, U. N., Prajapati, S., Kwak, Y. T., and Gaynor, R. B. (2003). Histone H3 phosphorylation by IKK-alpha is critical for cytokine-induced gene expression. *Nature* **423**, 655-659.

187. He, Z., Cho, Y. Y., Ma, W. Y., Choi, H. S., Bode, A. M., and Dong, Z. (2005). Regulation of ultraviolet B-induced phosphorylation of histone H3 at serine 10 by Fyn kinase. *J.Biol.Chem.* **280**, 2446-2454.

188. He, Z., Ma, W. Y., Liu, G., Zhang, Y., Bode, A. M., and Dong, Z. (2003). Arsenite-induced phosphorylation of histone H3 at serine 10 is mediated by Akt1, extracellular signal-regulated kinase 2, and p90 ribosomal S6 kinase 2 but not mitogen- and stress-activated protein kinase 1. *J Biol.Chem.* **278**, 10588-10593.

189. Huang, W., Mishra, V., Batra, S., Dillon, I., and Mehta, K. D. (2004). Phorbol ester promotes histone H3-Ser10 phosphorylation at the LDL receptor promoter in a protein kinase C-dependent manner. *J Lipid Res.* **45**, 1519-1527.

190. DeManno, D. A., Cottom, J. E., Kline, M. P., Peters, C. A., Maizels, E. T., and Hunzicker-Dunn, M. (1999). Follicle-stimulating hormone promotes histone H3 phosphorylation on serine-10. *Mol.Endocrinol.* **13**, 91-105.

191. Salvador, L. M., Park, Y., Cottom, J., Maizels, E. T., Jones, J. C., Schillace, R. V., Carr, D. W., Cheung, P., Allis, C. D., Jameson, J. L., and Hunzicker-Dunn, M. (2001). Follicle stimulating hormone stimulates protein kinase A mediated histone H3 phosphorylation and acetylation leading to select gene activation in ovarian granulosa cells. *J.Biol.Chem.* **276**, 40146-40155.

192. Taylor, S. S. (1982). The in vitro phosphorylation of chromatin by the catalytic subunit of cAMP-dependent protein kinase. *J Biol.Chem.* **257**, 6056-6063.

193. Mishra, S., Saleh, A., Espino, P. S., Davie, J. R., and Murphy, L. J. (2006). Phosphorylation of histones by tissue transglutaminase. *J Biol.Chem.* **281**, 5532-5538.

194. Mishra, S. and Murphy, L. J. (2004). Tissue transglutaminase has intrinsic kinase activity: identification of transglutaminase 2 as an insulin-like growth factor-binding protein-3 kinase. *J Biol.Chem.* **279**, 23863-23868.

195. Lim, J. H., Catez, F., Birger, Y., West, K. L., Prymakowska-Bosak, M., Postnikov, Y. V., and Bustin, M. (2004). Chromosomal protein HMGN1 modulates histone H3 phosphorylation. *Mol.Cell* **15**, 573-584.

196. Trivier, E., De Cesare, D., Jacquot, S., Pannetier, S., Zackai, E., Young, I., Mandel, J. L., Sassone-Corsi, P., and Hanauer, A. (1996). Mutations in the kinase Rsk-2 associated with Coffin-Lowry syndrome. *Nature* **384**, 567-570.

197. Sassone-Corsi, P., Mizzen, C. A., Cheung, P., Crosio, C., Monaco, L., Jacquot, S., Hanauer, A., and Allis, C. D. (1999). Requirement of Rsk-2 for epidermal growth factor-activated phosphorylation of histone H3. *Science* **285**, 886-891.

198. Strelkov, I. S. and Davie, J. R. (2002). Ser-10 phosphorylation of histone H3 and immediate early gene expression in oncogene-transformed mouse fibroblasts. *Cancer Res.* **62**, 75-78.

199. Bode, A. M. and Dong, Z. (2005). Inducible covalent posttranslational modification of histone H3. *Sci.STKE.* **2005**, re4.

200. Zhong, S., Jansen, C., She, Q. B., Goto, H., Inagaki, M., Bode, A. M., Ma, W. Y., and Dong, Z. (2001). Ultraviolet B-induced phosphorylation of histone H3 at serine 28 is mediated by MSK1. *J.Biol.Chem.* **276**, 33213-33219.

201. Clayton, A. L. and Mahadevan, L. C. (2003). MAP kinase-mediated phosphoacetylation of histone H3 and inducible gene regulation. *FEBS Lett.* **546**, 51-58.

202. Mahadevan, L. C., Willis, A. C., and Barratt, M. J. (1991). Rapid histone H3 phosphorylation in response to growth factors, phorbol esters, okadaic acid, and protein synthesis inhibitors. *Cell* **65**, 775-783.

203. Zhong, S., Zhang, Y., Jansen, C., Goto, H., Inagaki, M., and Dong, Z. (2001). MAP kinases mediate UVB-induced phosphorylation of histone H3 at serine 28. *J.Biol.Chem.* **276**, 12932-12937.

204. Barratt, M. J., Hazzalin, C. A., Zhelev, N., and Mahadevan, L. C. (1994). A mitogen- and anisomycin-stimulated kinase phosphorylates HMG-14 in its basic amino-terminal domain in vivo and on isolated mononucleosomes. *EMBO J.* **13**, 4524-4535.

205. Thomson, S., Clayton, A. L., and Mahadevan, L. C. (2001). Independent dynamic regulation of histone phosphorylation and acetylation during immediate-early gene induction. *Mol.Cell* **8**, 1231-1241.

206. Thomson, S., Hollis, A., Hazzalin, C. A., and Mahadevan, L. C. (2004). Distinct stimulus-specific histone modifications at hsp70 chromatin targeted by the transcription factor heat shock factor-1. *Mol.Cell* **15**, 585-594.

207. Clayton, A. L., Rose, S., Barratt, M. J., and Mahadevan, L. C. (2000). Phosphoacetylation of histone H3 on c-fos- and c-jun-associated nucleosomes upon gene activation. *EMBO J.* **19**, 3714-3726.

208. Cheung, P., Tanner, K. G., Cheung, W. L., Sassone-Corsi, P., Denu, J. M., and Allis, C. D. (2000). Synergistic coupling of histone H3 phosphorylation and acetylation in response to epidermal growth factor stimulation. *Mol.Cell* **5**, 905-915.

209. Chadee, D. N., Hendzel, M. J., Tylipski, C. P., Allis, C. D., Bazett-Jones, D. P., Wright, J. A., and Davie, J. R. (1999). Increased Ser-10 phosphorylation of histone H3 in mitogen-stimulated and oncogene-transformed mouse fibroblasts. *J.Biol.Chem.* **274**, 24914-24920.

210. Dunn, K. L., Espino, P., Drobic, B., He, S., and Davie, J. R. (2005). The Ras-MAPK signal transduction pathway, cancer and chromatin remodeling. *Biochem.Cell Biol.* **83**, 1-14.

211. Barratt, M. J., Hazzalin, C. A., Cano, E., and Mahadevan, L. C. (1994). Mitogen-stimulated phosphorylation of histone H3 is targeted to a small hyperacetylation-sensitive fraction. *Proc.Natl.Acad.Sci.USA* **91**, 4781-4785.

212. Deak, M., Clifton, A. D., Lucocq, L. M., and Alessi, D. R. (1998). Mitogen- and stress-activated protein kinase-1 (MSK1) is directly activated by MAPK and SAPK2/p38, and may mediate activation of CREB. *EMBO J.* **17**, 4426-4441.

213. Dalby, K. N., Morrice, N., Caudwell, F. B., Avruch, J., and Cohen, P. (1998). Identification of regulatory phosphorylation sites in mitogen-activated protein kinase (MAPK)-activated protein kinase-1a/p90rsk that are inducible by MAPK. *J.Biol.Chem.* **273**, 1496-1505.

214. Vik, T. A. and Ryder, J. W. (1997). Identification of serine 380 as the major site of autophosphorylation of Xenopus pp90rsk. *Biochem.Biophys.Res.Commun.* **235**, 398-402.

215. McCoy, C. E., Campbell, D. G., Deak, M., Bloomberg, G. B., and Arthur, J. S. (2005). MSK1 activity is controlled by multiple phosphorylation sites. *Biochem.J.* **387**, 507-517.

216. Arthur, J. S. and Cohen, P. (2000). MSK1 is required for CREB phosphorylation in response to mitogens in mouse embryonic stem cells. *FEBS Lett.* **482**, 44-48.

217. Janknecht, R. (2003). Regulation of the ER81 transcription factor and its coactivators by mitogen- and stress-activated protein kinase 1 (MSK1). *Oncogene* **22**, 746-755.

218. Nomura, M., Kaji, A., Ma, W. Y., Zhong, S., Liu, G., Bowden, G. T., Miyamoto, K. I., and Dong, Z. (2001). Mitogen- and stress-activated protein kinase 1 mediates activation of Akt by ultraviolet B irradiation. *J.Biol.Chem.* **276**, 25558-25567.

219. She, Q. B., Ma, W. Y., Zhong, S., and Dong, Z. (2002). Activation of JNK1, RSK2, and MSK1 is involved in serine 112 phosphorylation of Bad by ultraviolet B radiation. *J.Biol.Chem.* **277**, 24039-24048.

220. Zhang, Y., Liu, G., and Dong, Z. (2001). MSK1 and JNKs mediate phosphorylation of STAT3 in UVA-irradiated mouse epidermal JB6 cells. *J.Biol.Chem.* **276**, 42534-42542.

221. Wierenga, A. T., Vogelzang, I., Eggen, B. J., and Vellenga, E. (2003). Erythropoietin-induced serine 727 phosphorylation of STAT3 in erythroid cells is mediated by a MEK-, ERK-, and MSK1-dependent pathway. *Exp.Hematol.* **31**, 398-405.

222. Liu, G., Zhang, Y., Bode, A. M., Ma, W. Y., and Dong, Z. (2002). Phosphorylation of 4E-BP1 is mediated by the p38/MSK1 pathway in response to UVB irradiation. *J.Biol.Chem.* **277**, 8810-8816.

223. Thomson, S., Clayton, A. L., Hazzalin, C. A., Rose, S., Barratt, M. J., and Mahadevan, L. C. (1999). The nucleosomal response associated with immediate-early gene induction is mediated via alternative MAP kinase cascades: MSK1 as a potential histone H3/HMG-14 kinase. *EMBO J.* **18**, 4779-4793.

224. Ueda, T., Postnikov, Y. V., and Bustin, M. (2006). Distinct domains in high mobility group N variants modulate specific chromatin modifications. *J Biol.Chem.* **281**, 10182-10187.

225. Lim, J. H., West, K. L., Rubinstein, Y., Bergel, M., Postnikov, Y. V., and Bustin, M. (2005). Chromosomal protein HMGN1 enhances the acetylation of lysine 14 in histone H3. *EMBO J* **24**, 3038-3048.

226. Cosgrove, M. S., Boeke, J. D., and Wolberger, C. (2004). Regulated nucleosome mobility and the histone code. *Nat.Struct.Mol.Biol.* **11**, 1037-1043.

227. Huang, W., Batra, S., Atkins, B. A., Mishra, V., and Mehta, K. D. (2005). Increases in intracellular calcium dephosphorylate histone H3 at serine 10 in human hepatoma cells: potential role of protein phosphatase 2A-protein kinase CbetaII complex. *J.Cell Physiol* **205**, 37-46.

228. Nowak, S. J., Pai, C. Y., and Corces, V. G. (2003). Protein phosphatase 2A activity affects histone H3 phosphorylation and transcription in Drosophila melanogaster. *Mol.Cell Biol.* **23**, 6129-6138.

229. Nowak, S. J. and Corces, V. G. (2004). Phosphorylation of histone H3: a balancing act between chromosome condensation and transcriptional activation. *Trends Genet.* **20**, 214-220.

230. de, l. C., X, Lois, S., Sanchez-Molina, S., and Martinez-Balbas, M. A. (2005). Do protein motifs read the histone code? *BioEssays* **27**, 164-175.

231. Winston, F. and Allis, C. D. (1999). The bromodomain: a chromatin-targeting module? *Nat.Struct.Biol.* **6**, 601-604.

232. Kasten, M., Szerlong, H., Erdjument-Bromage, H., Tempst, P., Werner, M., and Cairns, B. R. (2004). Tandem bromodomains in the chromatin remodeler RSC recognize acetylated histone H3 Lys14. *EMBO J.* **23**, 1348-1359.

233. Bos, J. L. (1989). ras oncogenes in human cancer: a review. *Cancer Res.* **49**, 4682-4689.

234. Barbacid, M. (1987). ras genes. *Annu.Rev.Biochem.* **56**, 779-827.

235. Andreyev, H. J., Norman, A. R., Cunningham, D., Oates, J. R., and Clarke, P. A. (1998). Kirsten ras mutations in patients with colorectal cancer: the multicenter "RASCAL" study. *J.Natl.Cancer Inst.* **90**, 675-684.

236. Campbell, P. M. and Der, C. J. (2004). Oncogenic Ras and its role in tumor cell invasion and metastasis. *Semin.Cancer Biol.* **14**, 105-114.

237. Choi, H. S., Choi, B. Y., Cho, Y. Y., Mizuno, H., Kang, B. S., Bode, A. M., and Dong, Z. (2005). Phosphorylation of histone H3 at serine 10 is indispensable for neoplastic cell transformation. *Cancer Res.* **65**, 5818-5827.

238. Mizuno, H., Cho, Y. Y., Ma, W. Y., Bode, A. M., and Dong, Z. (2006). Effects of MAP kinase inhibitors on epidermal growth factor-induced neoplastic transformation of human keratinocytes. *Mol.Carcinog.* **45**, 1-9.

239. Hoshino, R., Chatani, Y., Yamori, T., Tsuruo, T., Oka, H., Yoshida, O., Shimada, Y., Ari-i S, Wada, H., Fujimoto, J., and Kohno, M. (1999). Constitutive activation of the 41-/43-kDa mitogen-activated protein kinase signaling pathway in human tumors. *Oncogene* **18**, 813-822.

240. Calipel, A., Lefevre, G., Pouponnot, C., Mouriaux, F., Eychene, A., and Mascarelli, F. (2003). Mutation of B-Raf in human choroidal melanoma cells mediates cell proliferation and transformation through the MEK/ERK pathway. *J.Biol.Chem.* **278**, 42409-42418.

241. Lechner, S., Muller-Ladner, U., Renke, B., Scholmerich, J., Ruschoff, J., and Kullmann, F. (2003). Gene expression pattern of laser microdissected colonic crypts of adenomas with low grade dysplasia. *Gut* **52**, 1148-1153.

242. Fearon, E. R. and Vogelstein, B. (1990). A genetic model for colorectal tumorigenesis. *Cell* **61**, 759-767.

243. Shih, C. and Weinberg, R. A. (1982). Isolation of a transforming sequence from a human bladder carcinoma cell line. *Cell* **29**, 161-169.

244. Hancock, J. F., Magee, A. I., Childs, J. E., and Marshall, C. J. (1989). All Ras proteins are polyisoprenylated but only some are palmitoylated. *Cell* **57**, 1177.

245. Cox, A. D., Hisaka, M. M., Buss, J. E., and Der, C. J. (1992). Specific isoprenoid modification is required for function of normal, but not oncogenic, Ras protein. *Mol.Cell Biol.* **12**, 2606-2615.

246. Schafer, W. R. and Rine J. (1992). Protein prenylation: genes, enzymes, targets, and functions. *Annu.Rev.Genet.* **26**, 209-237.

247. Macaluso M, Russo G, Cinti C, Bazan V, Gebbia N, and Russo A (2002). Ras family genes: an interesting link between cell cycle and cancer. *Journal of Cellular Physiology* **192**, 125-130.

248. Zink, D., Fische, A. H., and Nickerson, J. A. (2004). Nuclear structure in cancer cells. *Nat.Rev.Cancer* **4**, 677-687.

249. Fischer, A. H., Chadee, D. N., Wright, J. A., Gansler, T. S., and Davie, J. R. (1998). Ras-associated nuclear structural change appears functionally significant and independent of the mitotic signaling pathway. *J.Cell.Biochem.* **70**, 130-140.

250. Samuel, S. K., Minish, T. M., and Davie, J. R. (1997). Altered nuclear matrix protein profiles in oncogene transformed fibroblasts exhibiting high metastatic potential. *Cancer Res.* **57**, 147-151.

251. Muschel, R. J., Williams, J. E., Lowy, D. R., and Liotta, L. A. (1985). Harvey ras induction of metastatic potential depends upon oncogene activation and the type of recipient cell. *Am.J.Pathol.* **121**, 1-8.

252. Tuck, A. B., Wilson, S. M., and Chambers, A. F. (1990). ras transfection and expression does not induce progression from tumorigenicity to metastatic ability in mouse LTA cells. *Clin.Exp.Metastasis* **8**, 417-431.

253. Feldman, M. and Eisenbach, L. (1988). Genes controlling the metastatic phenotype. *Cancer Surv.* **7**, 555-572.

254. Price, J. E., Aukerman, S. L., Ananthaswamy, H. N., McIntyre, B. W., Schackert, G., Schackert, H. K., and Fidler, I. J. (1989). Metastatic potential of cloned murine melanoma cells transfected with activated c-Ha-ras. *Cancer Res.* **49**, 4274-4281.

255. Baisch, H., Collard, J., Zywietz, F., and Jung, H. (1990). No acquisition of metastatic capacity of R1H rhabdomyosarcoma upon transfection with c-Ha-ras oncogene. *Invasion Metastasis* **10**, 193-207.

256. Tsunokawa, Y., Esumi, H., Sasaki, M. S., Mori, M., Sakamoto, H., Terada, M., and Sugimura, T. (1984). Integration of v-rasH does not necessarily transform an immortalized murine cell line. *Gann* **75**, 732-736.

257. Tuck, A. B., Wilson, S. M., Khokha, R., and Chambers, A. F. (1991). Different patterns of gene expression in ras-resistant and ras- sensitive cells. *J.Natl.Cancer Inst.* **83**, 485-491.

258. Laitinen, J., Sistonen, L., Alitalo, K., and Holtta, E. (1990). c-Ha-ras (val 12) oncogene-transformed NIH-3T3 fibroblasts display more decondensed nucleosomal organization than normal fibroblasts. *J.Cell.Biol.* **111**, 9-17.

259. Laitinen, J., Saris, P., and Holtta, E. (1995). DNA methylation is not involved in the structural alterations of ornithine decarboxylase or total chromatin of c-Ha-rasVal 12 oncogene-transformed NIH-3T3 fibroblasts. *J.Cell Biochem.* **57**, 670-679.

260. Chadee, D. N., Taylor, W. R., Hurta, R. A. R., Allis, C. D., Wright, J. A., and Davie, J. R. (1995). Increased phosphorylation of histone H1 in mouse fibroblasts transformed with oncogenes or constitutively active mitogen-activated protein kinase kinase. *J.Biol.Chem.* **270**, 20098-20105.

261. Taylor, W. R., Chadee, D. N., Allis, C. D., Wright, J. A., and Davie, J. R. (1995). Fibroblasts transformed by combinations of *ras*, *myc* and mutant p53 exhibit increased phosphorylation of histone H1 that is independent of metastatic potential. *FEBS Lett.* **377**, 51-53.

262. Drobic, B., Espino, P. S., and Davie, J. R. (2004). MSK1 activity and histone H3 phosphorylation in oncogene-transformed mouse fibroblasts. *Cancer Res.* **64**, 9076-9079.

263. Chadee, D. N., Allis, C. D., Wright, J. A., and Davie, J. R. (1997). Histone H1b phosphorylation is dependent upon ongoing transcription and replication in normal and *ras*-transformed mouse fibroblasts. *J.Biol.Chem.* **272**, 8113-8116.

264. Herrera, R. E., Chen, F., and Weinberg, R. A. (1996). Increased histone H1 phosphorylation and relaxed chromatin structure in *Rb*-deficient fibroblasts. *Proc.Natl.Acad.Sci.USA* **93**, 11510-11515.

265. Chadee, D. N., Peltier, C. P., and Davie, J. R. (2002). Histone H1(S)-3 phosphorylation in Ha-ras oncogene-transformed mouse fibroblasts. *Oncogene* **21**, 8397-8403.

266. Dou, Y. and Gorovsky, M. A. (2002). Regulation of transcription by H1 phosphorylation in Tetrahymena is position independent and requires clustered sites. *Proc.Natl.Acad.Sci.U.S.A* **99**, 6142-6146.

267. Horn, P. J., Carruthers, L. M., Logie, C., Hill, D. A., Solomon, M. J., Wade, P. A., Imbalzano, A. N., Hansen, J. C., and Peterson, C. L. (2002). Phosphorylation of linker histones regulates ATP-dependent chromatin remodeling enzymes. *Nat.Struct.Biol.* **9**, 263-267.

268. Kaplan, L. J., Bauer, R., Morrison, E., Langan, T. A., and Fasman, G. D. (1984). The structure of chromatin reconstituted with phosphorylated H1. Circular dichroism and thermal denaturation studies. *J.Biol.Chem.* **259**, 8777-8785.

269. Hill, C. S., Rimmer, J. M., Green, B. N., Finch, J. T., and Thomas, J. O. (1991). Histone-DNA interactions and their modulation by phosphorylation of -Ser-Pro-X-Lys/Arg- motifs. *EMBO J.* **10**, 1939-1948.

270. Roth, S. Y. and Allis, C. D. (1992). Chromatin condensation: does histone H1 dephosphorylation play a role? *Trends Biochem.Sci.* **17**, 93-98.

271. Davie, J. R. and Chadee, D. N. (1998). Regulation and regulatory parameters of histone modifications. *J.Cell.Biochem.* **30/31**, 203-213.

272. Egan, S. E., McClarty, G. A., Jarolim, L., Wright, J. A., Spiro, I., Hager, G., and Greenberg, A. H. (1987). Expression of H-ras correlates with metastatic potential: evidence for direct regulation of the metastatic phenotype in 10T1/2 and NIH 3T3 cells. *Mol.Cell Biol.* **7**, 830-837.

273. Lennox, R. W. and Cohen, L. H. (1989). Analysis of histone subtypes and their modified forms by polyacrylamide gel electrophoresis. *Methods Enzymol.* **170**, 532-549.

274. Dimitrov, S. I. and Wolffe, A. P. (1997). Fine resolution of histones by two-dimensional polyacrylamide gel electrophoresis: developmental implications. *Methods* **12**, 57-61.

275. Espino, P. S., Drobic, B., Dunn, K. L., and Davie, J. R. (2005). Histone modifications as a platform for cancer therapy. *J.Cell Biochem.* **94**, 1088-1102.

276. Davies, S. P., Reddy, H., Caivano, M., and Cohen, P. (2000). Specificity and mechanism of action of some commonly used protein kinase inhibitors. *Biochem.J.* **351**, 95-105.

277. Tagami, H., Ray-Gallet, D., Almouzni, G., and Nakatani, Y. (2004). Histone H3.1 and H3.3 complexes mediate nucleosome assembly pathways dependent or independent of DNA synthesis. *Cell* **116**, 51-61.

278. Ridsdale, J. A. and Davie, J. R. (1987). Chicken erythrocyte polynucleosomes which are soluble at physiological ionic strength and contain linker histones are highly enriched in β-globin gene sequences. *Nucleic Acids Res.* **15**, 1081-1096.

279. Waterborg, J. H. (1993). Histone synthesis and turnover in alfalfa. Fast loss of highly acetylated replacement histone variant H3.2. *J.Biol.Chem.* **268**, 4912-4917.

280. Henikoff, S., Furuyama, T., and Ahmad, K. (2004). Histone variants, nucleosome assembly and epigenetic inheritance. *Trends Genet.* **20**, 320-326.

281. Workman, J. L. and Abmayr, S. M. (2004). Histone H3 variants and modifications on transcribed genes. *Proc.Natl.Acad.Sci.U.S.A* **101**, 1429-1430.

282. Dyson, M. H., Thomson, S., Inagaki, M., Goto, H., Arthur, S. J., Nightingale, K., Iborra, F. J., and Mahadevan, L. C. (2005). MAP kinase-mediated phosphorylation of distinct pools of histone H3 at S10 or S28 via mitogen- and stress-activated kinase 1/2. *J.Cell Sci.* **118**, 2247-2259.

283. Dunn, K. L. and Davie, J. R. (2005). Stimulation of the Ras-MAPK pathway leads to independent phosphorylation of histone H3 on serine 10 and 28. *Oncogene* **24**, 3492-3502.

284. Schubeler, D., MacAlpine, D. M., Scalzo, D., Wirbelauer, C., Kooperberg, C., van Leeuwen, F., Gottschling, D. E., O'Neill, L. P., Turner, B. M., Delrow, J., Bell, S. P., and Groudine, M. (2004). The histone modification pattern of active genes revealed through genome-wide chromatin analysis of a higher eukaryote. *Genes Dev.* **18**, 1263-1271.

285. Espino, P. S., Li, L., He, S., Yu, J., and Davie, J. R. (2005). Involvement of Ras-MAPK pathway in the transcriptional activation of the trefoil factor 1 gene. *Cancer Res.* **66**, 4610-4616.

286. Vermeulen, L., De Wilde, G., Van Damme, P., Vanden Berghe, W., and Haegeman, G. (2003). Transcriptional activation of the NF-kappaB p65 subunit by mitogen- and stress-activated protein kinase-1 (MSK1). *EMBO J.* **22**, 1313-1324.

287. Hazzalin, C. A. and Mahadevan, L. C. (2005). Dynamic acetylation of all lysine 4-methylated histone H3 in the mouse nucleus: analysis at c-fos and c-jun. *PLoS.Biol.* **3**, e393.

288. Nakayama, J., Rice, J. C., Strahl, B. D., Allis, C. D., and Grewal, S. I. (2001). Role of histone H3 lysine 9 methylation in epigenetic control of heterochromatin assembly. *Science* **292**, 110-113.

289. Rea, S., Eisenhaber, F., O'Carroll, D., Strahl, B. D., Sun, Z. W., Schmid, M., Opravil, S., Mechtler, K., Ponting, C. P., Allis, C. D., and Jenuwein, T. (2000). Regulation of chromatin structure by site-specific histone H3 methyltransferases. *Nature* **406**, 593-599.

290. Garcia, B. A., Barber, C. M., Hake, S. B., Ptak, C., Turner, F. B., Busby, S. A., Shabanowitz, J., Moran, R. G., Allis, C. D., and Hunt, D. F. (2005). Modifications of human histone H3 variants during mitosis. *Biochemistry* **44**, 13202-13213.

291. Kruhlak, M. J., Hendzel, M. J., Fischle, W., Bertos, N. R., Hameed, S., Yang, X. J., Verdin, E., and Bazett-Jones, D. P. (2001). Regulation of global acetylation in mitosis through loss of histone acetyltransferases and deacetylases from chromatin. *J.Biol.Chem.* **276**, 38307-38319.

292. Jin, C. and Felsenfeld, G. (2006). Distribution of histone H3.3 in hematopoietic cell lineages. *Proc.Natl.Acad.Sci.U.S.A* **103**, 574-579.

293. Litt, M. D., Simpson, M., Gaszner, M., Allis, C. D., and Felsenfeld, G. (2001). Correlation between histone lysine methylation and developmental changes at the chicken {beta}-globin locus. *Science* **293**, 2453-2455.

294. Fischer, A. H., West, P., and Shilkitus, W. W. (1992). A mutated H-ras alters nuclear morphology in a rat fibroblast cell line. *Patologia* **25**, 219.

295. Shogren-Knaak, M., Ishii, H., Sun, J. M., Pazin, M. J., Davie, J. R., and Peterson, C. L. (2006). Histone H4-K16 acetylation controls chromatin structure and protein interactions. *Science* **311**, 844-847.

296. Fry, C. J., Shogren-Knaak, M. A., and Peterson, C. L. (2004). Histone H3 amino-terminal tail phosphorylation and acetylation: synergistic or independent transcriptional regulatory marks? *Cold Spring Harb.Symp.Quant.Biol.* **69**, 219-226.

297. Macdonald, N., Welburn, J. P., Noble, M. E., Nguyen, A., Yaffe, M. B., Clynes, D., Moggs, J. G., Orphanides, G., Thomson, S., Edmunds, J. W., Clayton, A. L., Endicott, J. A., and Mahadevan, L. C. (2005). Molecular basis for the recognition of phosphorylated and phosphoacetylated histone h3 by 14-3-3. *Mol.Cell* **20**, 199-211.

298. Filippova, G. N., Cheng, M. K., Moore, J. M., Truong, J. P., Hu, Y. J., Nguyen, D. K., Tsuchiya, K. D., and Disteche, C. M. (2005). Boundaries between chromosomal domains of X inactivation and escape bind CTCF and lack CpG methylation during early development. *Dev.Cell* **8**, 31-42.

299. Bell, A. C., West, A. G., and Felsenfeld, G. (1999). The protein CTCF is required for the enhancer blocking activity of vertebrate insulators. *Cell* **98**, 387-396.

300. Lobanenkov, V. V., Nicolas, R. H., Adler, V. V., Paterson, H., Klenova, E. M., Polotskaja, A. V., and Goodwin, G. H. (1990). A novel sequence-specific DNA binding protein which interacts with three regularly spaced direct repeats of the CCCTC-motif in the 5'-flanking sequence of the chicken c-myc gene. *Oncogene* **5**, 1743-1753.

301. Vostrov, A. A., Taheny, M. J., and Quitschke, W. W. (2002). A region to the N-terminal side of the CTCF zinc finger domain is essential for activating transcription from the amyloid precursor protein promoter. *J.Biol.Chem.* **277**, 1619-1627.

302. Klenova, E. M., Nicolas, R. H., U S, Carne, A. F., Lee, R. E., Lobanenkov, V. V., and Goodwin, G. H. (1997). Molecular weight abnormalities of the CTCF transcription factor: CTCF migrates aberrantly in SDS-PAGE and the size of the expressed protein is affected by the UTRs and sequences within the coding region of the CTCF gene. *Nucleic Acids Res.* **25**, 466-474.

303. Saitoh, N., Bell, A. C., Recillas-Targa, F., West, A. G., Simpson, M., Pikaart, M., and Felsenfeld, G. (2000). Structural and functional conservation at the boundaries of the chicken beta-globin domain. *EMBO J.* **19**, 2315-2322.

304. Bell, A. C. and Felsenfeld, G. (2000). Methylation of a CTCF-dependent boundary controls imprinted expression of the Igf2 gene. *Nature* **405**, 482-485.

305. Hark, A. T., Schoenherr, C. J., Katz, D. J., Ingram, R. S., Levorse, J. M., and Tilghman, S. M. (2000). CTCF mediates methylation-sensitive enhancer-blocking activity at the H19/Igf2 locus. *Nature* **405**, 486-489.

306. Burcin, M., Arnold, R., Lutz, M., Kaiser, B., Runge, D., Lottspeich, F., Filippova, G. N., Lobanenkov, V. V., and Renkawitz, R. (1997). Negative protein 1, which is required for function of the chicken lysozyme gene silencer in conjunction with hormone receptors, is identical to the multivalent zinc finger repressor CTCF. *Mol.Cell Biol.* **17**, 1281-1288.

307. Kanduri, C., Holmgren, C., Pilartz, M., Franklin, G., Kanduri, M., Liu, L., Ginjala, V., Ulleras, E., Mattsson, R., and Ohlsson, R. (2000). The 5' flank of mouse H19 in an unusual chromatin conformation unidirectionally blocks enhancer-promoter communication. *Curr.Biol.* **10**, 449-457.

308. Filippova, G. N., Fagerlie, S., Klenova, E. M., Myers, C., Dehner, Y., Goodwin, G., Neiman, P. E., Collins, S. J., and Lobanenkov, V. V. (1996). An exceptionally conserved transcriptional repressor, CTCF, employs different combinations of zinc fingers to bind diverged promoter sequences of avian and mammalian c-myc oncogenes. *Mol.Cell Biol.* **16**, 2802-2813.

309. Vostrov, A. A. and Quitschke, W. W. (1997). The zinc finger protein CTCF binds to the APBbeta domain of the amyloid beta-protein precursor promoter. Evidence for a role in transcriptional activation. *J.Biol.Chem.* **272**, 33353-33359.

310. Zhao, K., Hart, C. M., and Laemmli, U. K. (1995). Visualization of chromosomal domains with boundary element-associated factor BEAF-32. *Cell* **81**, 879-889.

311. Gaszner, M., Vazquez, J., and Schedl, P. (1999). The Zw5 protein, a component of the scs chromatin domain boundary, is able to block enhancer-promoter interaction. *Genes Dev.* **13**, 2098-2107.

312. Ohtsuki, S. and Levine, M. (1998). GAGA mediates the enhancer blocking activity of the eve promoter in the Drosophila embryo. *Genes Dev.* **12**, 3325-3330.

313. Belozerov, V. E., Majumder, P., Shen, P., and Cai, H. N. (2003). A novel boundary element may facilitate independent gene refulation in the Antennapedia complex of Drosophila. *EMBO J.* **22**, 3113-3121.

314. Gerasimova, T. I., Gdula, D. A., Gerasimov, D. V., Simonova, O., and Corces, V. G. (1995). A Drosophila protein that imparts directionality on a chromatin insulator is an enhancer of position-effect variegation. *Cell* **82**, 587-597.

315. Moon, H., Filippova, G., Loukinov, D., Pugacheva, E., Chen, Q., Smith, S. T., Munhall, A., Grewe, B., Bartkuhn, M., Arnold, R., Burke, L. J., Renkawitz-Pohl, R., Ohlsson, R., Zhou, J., Renkawitz, R., and Lobanenkov, V. (2005). CTCF is conserved from Drosophila to humans and confers enhancer blocking of the Fab-8 insulator. *EMBO Rep.* **6**, 165-170.

316. Gerasimova, T. I., Byrd, K., and Corces, V. G. (2000). A chromatin insulator determines the nuclear localization of DNA. *Mol.Cell* **6**, 1025-1035.

317. Ishii, K., Arib, G., Lin, C., Van Houwe, G., and Laemmli, U. K. (2002). Chromatin boundaries in budding yeast: the nuclear pore connection. *Cell* **109**, 551-562.

318. Farrell, C. M., West, A. G., and Felsenfeld, G. (2002). Conserved CTCF insulator elements flank the mouse and human beta-globin loci. *Mol.Cell Biol.* **22**, 3820-3831.

319. Chao, W., Huynh, K. D., Spencer, R. J., Davidow, L. S., and Lee, J. T. (2002). CTCF, a candidate trans-acting factor for X-inactivation choice. *Science* **295**, 345-347.

320. Chung, J. H., Whiteley, M., and Felsenfeld, G. (1993). A 5' element of the chicken beta-globin domain serves as an insulator in human erythroid cells and protects against position effect in Drosophila. *Cell* **74**, 505-514.

321. Recillas-Targa, F., Pikaart, M. J., Burgess-Beusse, B., Bell, A. C., Litt, M. D., West, A. G., Gaszner, M., and Felsenfeld, G. (2002). Position-effect protection and enhacer blocking by the chicken beta-globin insulator are separable activities. *Proc.Natl.Acad.Sci.* **99**, 6883-6888.

322. Kanduri, C., Pant, V., Loukinov, D., Pugacheva, E., Qi, C. F., Wolffe, A., Ohlsson, R., and Lobanenkov, V. V. (2000). Functional association of CTCF with the insulator upstream of the H19 gene is parent of origin-specific and methylation-sensitive. *Curr.Biol.* **10**, 853-856.

323. Szabo, P., Tang, S. H., Rentsendorj, A., Pfeifer, G. P., and Mann, J. R. (2000). Maternal-specific footprints at putative CTCF sites in the H19 imprinting control region give evidence for insulator function. *Curr.Biol.* **10**, 607-610.

324. Filippova, G. N., Thienes, C. P., Penn, B. H., Cho, D. H., Hu, Y. J., Moore, J. M., Klesert, T. R., Lobanenkov, V. V., and Tapscott, S. J. (2001). CTCF-binding sites flank CTG/CAG repeats and form a methylation-sensitive insulator at the DM1 locus. *Nat.Genet.* **28**, 335-343.

325. Lutz, M., Burke, L. J., LeFevre, P., Myers, F. A., Thorne, A. W., Crane-Robinson, C., Bonifer, C., Filippova, G. N., Lobanenkov, V., and Renkawitz, R. (2003). Thyroid hormone-regulated enhancer blocking: cooperation of CTCF and thyroid hormone receptor. *EMBO J.* **22**, 1579-1587.

326. Tanimoto, K., Sugiura, A., Omori, A., Felsenfeld, G., Engel, J. D., and Fukamizu, A. (2003). Human beta-globin locus control region HS5 contains CTCF- and developmental stage-dependent enhancer-blocking activity in erythroid cells. *Mol.Cell Biol.* **23**, 8946-8952.

327. Ohta, T., Gray, T. A., Rogan, P. K., Buiting, K., Gabriel, J. M., Saitoh, S., Muralidhar, B., Bilienska, B., Krajewska-Walasek, M., Driscoll, D. J., Horsthemke, B., Butler, M. G., and Nicholls, R. D. (1999). Imprinting-mutation mechanisms in Prader-Willi syndrome. *Am.J.Hum.Genet.* **64**, 397-413.

328. Wylie, A. A., Murphy, S. K., Orton, T. C., and Jirtle, R. L. (2000). Novel imprinted DLK1/GTL2 domain on human chromosome 14 contains motifs that mimic those implicated in IGF2/H19 regulation. *Genome Res.* **10**, 1711-1718.

329. Paulsen, M., Takada, S., Youngson, N. A., Benchaib, M., Charlier, C., Segers, K., Georges, M., and Ferguson-Smith, A. C. (2001). Comparative sequence analysis of the imprinted Dlk1-Gtl2 locus in three mammalian species reveals highly conserved genomic elements and refines comparison with the Igf2-H19 region. *Genome Res.* **11**, 2085-2094.

330. Kanduri, C., Fitzpatrick, G., Mukhopadhyay, R., Kanduri, M., Lobanenkov, V., Higgins, M., and Ohlsson, R. (2002). A differentially methylated imprinting control region within the Kcnq1 locus harbors a methylation-sensitive chromatin insulator. *J.Biol.Chem.* **277**, 18106-18110.

331. Elson, D. A. and Bartolomei, M. S. (1997). A 5' differentially methylated sequence and the 3'-flanking region are necessary for H19 transgene imprinting. *Mol.Cell Biol.* **17**, 309-317.

332. Holmgren, C., Kanduri, C., Dell, G., Ward, A., Mukhopadhya, R., Kanduri, M., Lobanenkov, V., and Ohlsson, R. (2001). CpG methylation regulates the Igf2/H19 insulator. *Curr.Biol.* **11**, 1128-1130.

333. Wolffe, A. P. (2000). Transcriptional control: imprinting insulation. *Curr.Biol.* **10**, R463-R465.

334. Oki, M., Valenzuela, L., Chiba, T., Ito, T., and Kamakaka, R. T. (2004). Barrier proteins remodel and modify chromatin to restrict silenced domains. *Mol.Cell.Biol.* **24**, 1956-1967.

335. Bonifer, C., Hecht, A., Saueressig, H., Winter, D. M., and Sippel, A. E. (1991). Dynamic chromatin: the regulatory domain organization of eukaryotic gene loci. *J.Cell Biochem.* **47**, 99-108.

336. Antes, T. J., Namciu, S. J., Fournier, R. E., and Levy-Wilson, B. (2001). The 5' boundary of the human apolipoprotein B chromatin domain in intestinal cells. *Biochemistry* **40**, 6731-6742.

337. Phi-Van, L. and Stratling, W. H. (1996). Dissection of the ability of the chicken lysozyme gene 5' matrix attachment region to stimulate transgene expression and to dampen position effects. *Biochemistry* **35**, 10735-10742.

338. Bi, X. and Broach, J. R. (2001). Chromosomal boundaries in S.cerevisiae. *Curr.Opin.Genet.Dev.* **11**, 199-204.

339. Pai, C. Y., Lei, E. P., Ghosh, D., and Corces, V. G. (2004). The centrosomal protein CP190 is a component of the gypsy chromatin insulator. *Mol.Cell* **16**, 737-748.

340. Labrador, M. and Corces, V. G. (2002). Setting the boundaries of chromatin domains and nuclear organization. *Cell* **111**, 151-154.

341. Recillas-Targa, F., Bell, A. C., and Felsenfeld, G. (1999). Positional enhancer-blocking activity of the chicken beta-globin insulator in transiently transfected cells. *Proc.Natl.Acad.Sci.U.S.A* **96**, 14354-14359.

342. Chiu, Y. H., Yu, Q., Sandmeier, J. J., and Bi, X. (2003). A targeted histone acetyltransferase can create a sizable region of hyperactylated chromatin and counteract the propagation of transcriptionally silent chromatin. *Genetics* **165**, 115-125.

343. El-Kady, A. and Klenova, E. (2005). Regulation of the transcription factor, CTCF, by phosphorylation with protein kinase CK2. *FEBS Lett.* **579**, 1424-1434.

344. Yu, W., Ginjala, V., Pant, V., Chernukhin, I., Whitehead, J., Docquier, F., Farrar, D., Tavoosidana, G., Mukhopadhyay, R., Kanduri, C., Oshimura, M., Feinberg, A. P., Lobanenkov, V., Klenova, E., and Ohlsson, R. (2004). Poly(ADP-ribosyl)ation regulates CTCF-dependent chromatin insulation. *Nat.Genet.* **36**, 1105-1110.

345. Smith, S. (2001). The world according to PARP. *Trends Biochem.Sci.* **26**, 174-179.

346. Defossez, P. A., Kelly, K. F., Filion, G. J., Perez-Torrado, R., Magdinier, F., Menoni, H., Nordgaard, C. L., Daniel, J. M., and Gilson, E. (2005). The human enhancer blocker CTC-binding factor interacts with the transcription factor Kaiso. *J Biol.Chem.* **280**, 43017-43023.

347. Kang, J., Lemaire, H. G., Unterbeck, A., Salbaum, J. M., Masters, C. L., Grzeschik, K. H., Multhaup, G., Beyreuther, K., and Muller-Hill, B. (1987). The precursor of Alzheimer's disease amyloid A4 protein resembles a cell-surface receptor. *Nature* **325**, 733-736.

348. Glenner, G. G. and Wong, C. W. (1984). Alzheimer's disease and Down's syndrome: sharing of a unique cerebrovascular amyloid fibril protein. *Biochem.Biophys.Res.Commun.* **122**, 1131-1135.

349. Mann, D. M., Jones, D., Prinja, D., and Purkiss, M. S. (1990). The prevalence of amyloid (A4) protein deposits within the cerebral and cerebellar cortex in Down's syndrome and Alzheimer's disease. *Acta Neuropathol.(Berl)* **80**, 318-327.

350. Masters, C. L., Simms, G., Weinman, N. A., Multhaup, G., McDonald, B. L., and Beyreuther, K. (1985). Amyloid plaque core protein in Alzheimer disease and Down syndrome. *Proc.Natl.Acad.Sci.U.S.A* **82**, 4245-4249.

351. Chernak, J. M. (1993). Structural features of the 5' upstream regulatory region of the gene encoding rat amyloid precursor protein. *Gene* **133**, 255-260.

352. Izumi, R., Yamada, T., Yoshikai, S., Sasaki, H., Hattori, M., and Sakaki, Y. (1992). Positive and negative regulatory elements for the expression of the Alzheimer's disease amyloid precursor-encoding gene in mouse. *Gene* **112**, 189-195.

353. Quitschke, W. W. (1994). Two nuclear factor binding domains activate expression from the human amyloid beta-protein precursor promoter. *J.Biol.Chem.* **269**, 21229-21233.

354. Burton, T., Liang, B., Dibrov, A., and Amara, F. (2002). Transforming growth factor-beta-induced transcription of the Alzheimer beta-amyloid precursor protein gene involves interaction between the CTCF-complex and Smads. *Biochem.Biophys.Res.Commun.* **295**, 713-723.

355. Baniahmad, A., Steiner, C., Kohne, A. C., and Renkawitz, R. (1990). Modular structure of a chicken lysozyme silencer: involvement of an unusual thyroid hormone receptor binding site. *Cell* **61**, 505-514.

356. Kohne, A. C., Baniahmad, A., and Renkawitz, R. (1993). NeP1. A ubiquitous transcription factor synergizes with v-ERBA in transcriptional silencing. *J.Mol.Biol.* **232**, 747-755.

357. Renaud, S., Loukinov, D., Bosman, F. T., Lobanenkov, V., and Benhattar, J. (2005). CTCF binds the proximal exonic region of hTERT and inhibits its transcription. *Nucleic Acids Res.* **33**, 6850-6860.

358. Klenova, E. M., Chernukhin, I. V., El Kady, A., Lee, R. E., Pugacheva, E. M., Loukinov, D. I., Goodwin, G. H., Delgado, D., Filippova, G. N., Leon, J., Morse, H. C., III, Neiman, P. E., and Lobanenkov, V. V. (2001). Functional phosphorylation sites in the C-terminal region of the multivalent multifunctional transcriptional factor CTCF. *Mol.Cell Biol.* **21**, 2221-2234.

359. Litt, M. D., Simpson, M., Recillas-Targa, F., Prioleau, M. N., and Felsenfeld, G. (2001). Transitions in histone acetylation reveal boundaries of three separately regulated neighboring loci. *EMBO J.* **20**, 2224-2235.

360. Lutz, M., Burke, L. J., Barreto, G., Goeman, F., Greb, H., Arnold, R., Schultheiss, H., Brehm, A., Kouzarides, T., Lobanenkov, V., and Renkawitz, R. (2000). Transcriptional repression by the insulator protein CTCF involves histone deacetylases. *Nucleic Acids Res.* **28**, 1707-1713.

361. Verona, R. I., Mann, M. R., and Bartolomei, M. S. (2003). Genomic imprinting: intricacies of epigenetic regulation in clusters. *Annu.Rev.Cell Dev.Biol.* **19**, 237-259.

362. Ainscough, J. F., Dandolo, L., and Surani, M. A. (2000). Appropriate expression of the mouse H19 gene utilises three or more distinct enhancer regions spread over more than 130 kb. *Mech.Dev.* **91**, 365-368.

363. Leighton, P. A., Saam, J. R., Ingram, R. S., Stewart, C. L., and Tilghman, S. M. (1995). An enhancer deletion affects both H19 and Igf2 expression. *Genes Dev.* **9**, 2079-2089.

364. Thorvaldsen, J. L., Duran, K. L., and Bartolomei, M. S. (1998). Deletion of the H19 differentially methylated domain results in loss of imprinted expression of H19 and Igf2. *Genes Dev.* **12**, 3693-3702.

365. DeChiara, T. M., Efstratiadis, A., and Robertson, E. J. (1990). A growth-deficiency phenotype in heterozygous mice carrying an insulin-like growth factor II gene disrupted by targeting. *Nature* **345**, 78-80.

366. Li, E., Beard, C., and Jaenisch, R. (1993). Role for DNA methylation in genomic imprinting. *Nature* **366**, 362-365.

367. Engel, N., West, A. G., Felsenfeld, G., and Bartolomei, M. S. (2004). Antagonism between DNA hypermethylation and enhancer-blocking activity at the H19 DMD is uncovered by CpG mutations. *Nat.Genet.* **36**, 883-888.

368. Loukinov, D. I., Pugacheva, E., Vatolin, S., Pack, S. D., Moon, H., Chernukhin, I., Mannan, P., Larsson, E., Kanduri, C., Vostrov, A. A., Cui, H., Niemitz, E. L., Rasko, J. E., Docquier, F. M., Kistler, M., Breen, J. J., Zhuang, Z., Quitschke, W. W., Renkawitz, R., Klenova, E. M., Feinberg, A. P., Ohlsson, R., Morse, H. C., III, and Lobanenkov, V. V. (2002). BORIS, a novel male germ-line-specific protein associated with epigenetic reprogramming events, shares the same 11-zinc-finger domain with CTCF, the insulator protein involved in reading imprinting marks in the soma. *Proc.Natl.Acad.Sci.U.S.A* **99**, 6806-6811.

369. Klenova, E. M., Morse, H. C., III, Ohlsson, R., and Lobanenkov, V. V. (2002). The novel BORIS + CTCF gene family is uniquely involved in the epigenetics of normal biology and cancer. *Semin.Cancer Biol.* **12**, 399-414.

370. Weinberg, R. (1993). Tumor suppressor genes. *Neuron* **11**, 191-196.

371. Levine, A. J. (1993). The tumor suppressor genes. *Annu.Rev.Biochem.* **62**, 623-651.

372. Filippova, G. N., Lindblom, A., Meincke, L. J., Klenova, E. M., Neiman, P. E., Collins, S. J., Doggett, N. A., and Lobanenkov, V. V. (1998). A widely expressed transcription factor with multiple DNA sequence specificity, CTCF, is localized at chromosome segment 16q22.1 within one of the smallest regions of overlap for common deletions in breast and prostate cancers. *Genes Chromosomes.Cancer* **22**, 26-36.

373. Filippova, G. N., Qi, C. F., Ulmer, J. E., Moore, J. M., Ward, M. D., Hu, Y. J., Loukinov, D. I., Pugacheva, E. M., Klenova, E. M., Grundy, P. E., Feinberg, A. P., Cleton-Jansen, A. M., Moerland, E. W., Cornelisse, C. J., Suzuki, H., Komiya, A., Lindblom, A., Dorion-Bonnet, F., Neiman, P. E., Morse, H. C., III, Collins, S. J., and Lobanenkov, V. V. (2002). Tumor-associated zinc finger mutations in the CTCF transcription factor selectively alter tts DNA-binding specificity. *Cancer Res.* **62**, 48-52.

374. Rakha, E. A., Pinder, S. E., Paish, C. E., and Ellis, I. O. (2004). Expression of the transcription factor CTCF in invasive breast cancer: a candidate gene located at 16q22.1. *Br.J.Cancer* **91**, 1591-1596.

375. Alland, L., Muhle, R., Hou Jr., H., Potes, J., Chin, L., Schreiber-Agus, N., and DePinho, R. A. (1997). Role of N-CoR and histone deacetylase in Sin3-mediated transcriptional repression. *Nature* **387**, 49-55.

376. DePinho, R. A. (1998). Transcriptional repression. The cancer-chromatin connection. *Nature* **391**, 533-536.

377. Yang, X. J., Ogryzko, V. V., Nishikawa, J., Howard, B. H., and Nakatani, Y. (1996). A p300/CBP-associated factor that competes with the adenoviral oncoprotein E1A. *Nature* **382**, 319-324.

378. Dunn, K. L. and Davie, J. R. (2003). The many roles of the transcriptional regulator CTCF. *Biochem.Cell Biol.* **81**, 161-167.

379. Sun, J. M., Chen, H. Y., Moniwa, M., Litchfield, D. W., Seto, E., and Davie, J. R. (2002). The transcriptional repressor Sp3 is associated with CK2 phosphorylated histone deacetylase 2. *J.Biol.Chem.* **277**, 35783-35786.

380. Samuel, S. K., Minish, M. M., and Davie, J. R. (1997). Nuclear matrix proteins in well and poorly differentiated human breast cancer cell lines. *J.Cell.Biochem.* **66**, 9-15.

381. Holth, L. T., Chadee, D. N., Spencer, V. A., Samuel, S. K., Safneck, J. R., and Davie, J. R. (1998). Chromatin, nuclear matrix and the cytoskeleton: role of cell structure in neoplastic transformation. *Int.J.Oncol.* **13**, 827-837.

382. Samuel, S. K., Spencer, V. A., Bajno, L., Sun, J.-M., Holth, L. T., Oesterreich, S., and Davie, J. R. (1998). *In situ* cross-linking by cisplatin of nuclear matrix-bound transcription factors to nuclear DNA of human breast cancer cells. *Cancer Res.* **58**, 3004-3008.

383. Baiker, A., Maercker, C., Piechaczek, C., Schmidt, S. B., Bode, J., Benham, C., and Lipps, H. J. (2000). Mitotic stability of an episomal vector containing a human scaffold/matrix-attached region is provided by association with nuclear matrix. *Nat.Cell Biol.* **2**, 182-184.

384. West, A. G., Huang, S., Gaszner, M., Litt, M. D., and Felsenfeld, G. (2004). Recruitment of histone modifications by USF proteins at a vertebrate barrier element. *Mol.Cell* **16**, 453-463.

385. Yasui, D., Miyano, M., Cai, S., Varga-Weisz, P., and Kohwi-Shigematsu, T. (2002). SATB1 targets chromatin remodelling to regulate genes over long distances. *Nature* **419**, 641-645.

386. Yusufzai, T. M., Tagami, H., Nakatani, Y., and Felsenfeld, G. (2004). CTCF tethers an insulator to subnuclear sites, suggesting shared insulator mechanisms across species. *Mol.Cell* **13**, 291-298.

387. Chernukhin, I. V., Shamsuddin, S., Robinson, A. F., Carne, A. F., Paul, A., El-Kady, A. I., Lobanenkov, V. V., and Klenova, E. M. (2000). Physical and functional interaction between two pluripotent proteins, the Y-box DNA/RNA-binding factor, YB-1, and the multivalent zinc finger factor, CTCF. *J Biol.Chem.* **275**, 29915-29921.

388. Bell, A. C. and Felsenfeld, G. (1999). Stopped at the border: boundaries and insulators. *Curr.Opin.Genet.Dev.* **9**, 191-198.

389. Cai, H. N. and Shen, P. (2001). Effects of cis arrangement of chromatin insulators on enhancer-blocking activity. *Science* **291**, 493-495.

390. Muravyova, E., Golovnin, A., Gracheva, E., Parshikov, A., Belenkaya, T., Pirrotta, V., and Georgiev, P. (2001). Loss of insulator activity by paired Su(Hw) chromatin insulators. *Science* **291**, 495-498.

391. Ishii, K. and Laemmli, U. K. (2003). Structural and dynamic functions establish chromatin domains. *Mol.Cell* **11**, 237-248.

392. Byrd, K. and Corces, V. G. (2003). Visualization of chromatin domains created by the gypsy insulator of Drosophila. *J.Cell Biol.* **162**, 565-574.

393. Dunn, K. L., Zhao, H., and Davie, J. R. (2003). The insulator binding protein CTCF associates with the nuclear matrix. *Exp.Cell Res.* **288**, 218-223.

394. Yusufzai, T. M. and Felsenfeld, G. (2004). The 5'HS4 chicken beta-globin insulator is a CTCF-dependent nuclear matrix associated element. *Proc.Natl.Acad.Sci.* **101**, 8629-8624.

395. Ling, J. Q., Li, T., Hu, J. F., Vu, T. H., Chen, H. L., Qiu, X. W., Cherry, A. M., and Hoffman, A. R. (2006). CTCF mediates interchromosomal colocalization between Igf2/H19 and Wsb1/Nf1. *Science* **312**, 269-272.

396. Melnikova, L., Juge, F., Gruzdeva, N., Mazur, A., Cavalli, G., and Georgiev, P. (2004). Interaction between the GAGA factor and Mod(mdg4) proteins

promotes insulator bypass in Drosophila. *Proc.Natl.Acad.Sci.U.S.A* **101**, 14806-14811.

397. Xu, Q., Li, M., Adams, J., and Cai, H. N. (2004). Nuclear location of a chromatin insulator in Drosophila melanogaster. *J.Cell Sci.* **117**, 1025-1032.

398. Nabirochkin, S., Ossokina, M., and Heidmann, T. (1998). A nuclear matrix/scaffold attachment region co-localizes with the gypsy retrotransposon insulator sequence. *J.Biol.Chem.* **273**, 2473-2479.

399. Scott, K. C., Taubman, A. D., and Geyer, P. K. (1999). Enhancer blocking by the Drosophila gypsy insulator depends upon insulator anatomy and enhancer strength. *Genetics* **153**, 787-798.

400. Capelson, M. and Corces, V. G. (2005). The ubiquitin ligase dTopors directs the nuclear organization of a chromatin insulator. *Mol.Cell* **20**, 105-116.

401. Magdinier, F., Yusufzai, T. M., and Felsenfeld, G. (2004). Both CTCF-dependent and -independent insulators are found between the mouse T cell receptor alpha and Dad1 genes. *J.Biol.Chem.* **279**, 25381-25389.